Development of Mechanistic Mathematical Models for Gene-mediated Drug-drug Interactions

A thesis submitted to the University of Manchester for the degree of

PhD in the Faculty of Biology, Medicine and Health

2016

Hajar K. Alavi

School of Health Sciences

Manchester School of Pharmacy

List of Contents

Word count: 44,699

List of Tables

List of Figures

Abbreviations

ADR	: Adverse drug reactions
AF	: Activation function
AF-1	: Activation function 1
AF-2	: Activation function 2
Ah	: Aromatic hydrocarbon
AhR	: Aryl hydrocarbon receptor
AmR	: Amphiregulin
AP1	: Activator protein 1
AR	: Androgen receptor
CAR	: Constitutive androstane receptor
CDK	: Cyclin-dependent kinase
CLEM4	: Constitutive liver enhancer module
COUP-TF	: Chicken ovalbumin upstream promoter transcription factor
CTE	: C-terminal extension
CYP	: Cytochrome P450
Cyt C.	: Cytochrome C
DAX-1	: Dosage-sensitive sex reversal-adrenal hypoplasia congenital critical region on the X chromosome protein 1
DBD	: DNA binding domain
DCF	: Dichlorofluorescein
Dex	: Dexamethasone
DDIs	: Drug-drug interactions
DMEM	: Dulbecco's modified Eagles's medium
DR*n*	: Direct repeat with *n* base pairs spacing
EAR	: ErbA-related protein
ECACC	: European collection of cell culture
ER	: Endoplasmic reticulum or Estrogen receptor
ER*n*	: Everted repeat with *n* base pairs spacing
ERK	: Extracellular-regulated kinase

ERR : Estrogen-related receptor
FACS : Fluorescence-activated cell sorting
FAD : Flavin adenine dinucleotide
FAO : Fatty acid radical
FAOOH : Fatty acid hydroperoxide
FBS : Foetal bovine serum
F-dex : Fluorescin-labelled Dex
FDX : Ferrodoxin
FDXR : Ferrodoxin reductase
FMN : Flavin mononucleotide
FXR : Farnesoid X receptor
GCNF : Germ cell nuclear factor
GCs : Glucocorticoids
GI : Gastro-intestinal
GSK-3 : Glycogen synthase kinase-3
GR : Glucocorticoid receptor
GRE : Glucocorticoid response element
GST : Glutathione S-transferase
HNF4α : Hepatocyte nuclear factor 4α
HPA : Hypothalamic-pituitary-adrenal
HPF-1 : HepG2-specific P450 2C factor-1
HPLC : High performance liquid chromatography
HSP : Heat shock protein
HSP90 : Heat shock protein 90
ICAM1 : Intracellular adhesion molecule 1
IDR : Indirect response
IL : Interleukin
IR*n* : Inverted repeat with *n* base pairs spacing
JNK : c-Jun N-terminal kinase
Keto : Ketoconazole
LBD : Ligand binding domain
LC-MS : Liquid chromatography–mass spectrometry
LDR : Luciferin detection reagent

LRH	: Liver receptor homolog
LXR	: Liver X receptor
MAPK	: Mitogen protein kinases
MDR	: Multi-drug resistance
MI	: Metabolic Intermediate
MMO	: Microsomal monooxygenase system
MMP2	: Matrix metalloprotease 2
MR	: Mineralocorticoid receptor
mRNA	: Messenger ribonucleic acid
NCBI	: National Centre for Biotechnology Information, USA
NF1	: Nuclear factor 1
NOR	: Neuron-derived orphan receptor
NGFI-B	: Nerve growth factor-induced clone B
NR	: Nuclear receptor
NRCOA	: Nuclear receptor coactivator
NSAID	: Non-steroidal anti-inflammatory drug
NFkB	: Nuclear factor kappa B
ODE	: Ordinary differential equation
PAGE	: Polyacrylamide gel electrophoresis
PAH	: Phenylalanine hydroxylase
PBS	: Phosphate-buffered saline
PDGF	: Platelet derived growth factor
PGC-1α	: Peroxisome proliferators-activated receptor γ co-activator 1α
P-gp	: P-glycoprotein
PK-PD	: Pharmacokinetic-pharmacodynamic
PNR	: Photoreceptor-specific nuclear receptor
PPAR	: Peroxisome proliferator-activated receptor
POR	: P450 oxidoreductase
PR	: Progesterone receptor
PT	: Prothrombin time
PXR	: Pregnane-X Receptor
PXRE	: PXR response element

QT interval	: Measurement of the heart's electrical cycle
RAR	: Retinoic acid receptor
ROR	: Retinoic acid related orphan nuclear receptor
ROS	: Reactive Oxygen Species
RPL19	: Ribosomal protein 19
RXRα	: Retinoid X receptor alpha
S211	: Serine 211
SF1	: Steroidogenic factor 1
SHP	: Small heterodimer partner
SPZ	: Sulfaphenazole
SRC-1	: Steroid receptor coactivator-1
TLL	: Tailless-like receptor
TR	: Thyroid receptor
US FDA	: United States' Food and Drug Administration
VEGF	: Vascular endothelial growth factor
XREM	: Xenobiotic responsive enhancer module

Abstract

The University of Manchester
Submitted by: Hajar K. Alavi
Degree title: Doctor of Philosophy (PhD)
Thesis title: Development of mechanistic mathematical models for gene-mediated drug-drug interactions
Date of submission: 02.11.2016

The glucocorticoid receptor (GR) is a member of the nuclear hormone receptors family and has been shown to exert significant effects on the induction of cytochrome P450 (CYP) enzymes responsible for the metabolism of many xenobiotics. CYP3A4/5 and CYP2C9 are important CYP enzymes which metabolise more that 60% of drugs. Induction or inhibition of the enzymatic activity and the levels of these enzymes can have significant effects on drug metabolism. Understanding the role of GR and other nuclear receptors, pregnane X receptor (PXR) and the constitutive androstane receptor (CAR), in the mechanisms effecting CYP3A4/5 and CYP2C9 levels and activity can aid in the development of *in vitro* and *in vivo* models which have become a target for scientists in the clinic and the industry. The commonly prescribed synthetic glucocorticoid (GC) drug, dexamethasone (Dex), can induce GR, PXR and CAR and was used in this study to analyse its effects on the CYP enzymes studied.

The hypothesis of this project was that changes in CYP3A4/5 and CYP2C9 gene expression affect drug metabolism and changes in gene expression of these CYP enzymes was under GR, PXR and CAR control, thus affecting the concentration and therapeutic activity of drugs metabolized by these enzymes during chronic use of GCs in conditions such as rheumatoid arthritis and asthma. This study aimed to measure mRNA, protein, ROS and enzymatic activity levels in human HepG2 hepatocytes treated with Dex for 120 h and analyze the results for various time points to produce a mathematical model.

Our study has shown that changes in mRNA, protein and enzymatic activity levels of CYP3A4/5 and CYP2C9 in HepG2 cells were induced by Dex at sub-micromolar (0.1 µM) and supra-micromolar (1.5 mM) concentrations. The induction of CYP3A4/5 and CYP2C9 enzymes during 120 h treatment with Dex may be affected by the NRs studied; GR, phosphorylated GR, PXR and CAR protein levels were also shown to be induced by Dex. The efflux transporter, P-gp's protein levels were also induced by 0.1 µM Dex, highlighting the importance of considering bioavailability of other drugs co-administered with Dex.

The results of some of these laboratory experiments have been used to produce mechanistic mathematical models by MATLAB software with reference to previous studies in rats concentrating on the effects of steroids on GR. The models developed were not effective at the lower Dex concentration of 0.1 µM but were better modelled at the higher Dex concentration of 1.5 mM. The basic mechanistic models developed using HepG2 cells in this study can be utilised to design and conduct drug-drug interaction (DDI) analyses of the induction of CYP3A4/5 and CYP2C9 in other human liver cells and starting pre-clinical studies in animals to aid in drug development.

DECLARATION:

No portion of the work referred to in the thesis has been submitted in support of an application for another degree or qualification of this or any other university or other institute of learning;

COPYRIGHT STATEMENT

The following four notes on copyright and the ownership of intellectual property rights must be included as written below:

i. The author of this thesis (including any appendices and/or schedules to this thesis) owns certain copyright or related rights in it (the "Copyright") and s/he has given The University of Manchester certain rights to use such Copyright, including for administrative purposes.

ii. Copies of this thesis, either in full or in extracts and whether in hard or electronic copy, may be made **only** in accordance with the Copyright, Designs and Patents Act 1988 (as amended) and regulations issued under it or, where appropriate, in accordance with licensing agreements which the University has from time to time. This page must form part of any such copies made.

iii. The ownership of certain Copyright, patents, designs, trade marks and other intellectual property (the "Intellectual Property") and any reproductions of copyright works in the thesis, for example graphs and tables ("Reproductions"), which may be described in this thesis, may not be owned by the author and may be owned by third parties. Such Intellectual Property and Reproductions cannot and must not be made available for use without the prior written permission of the owner(s) of the relevant Intellectual Property and/or Reproductions.

iv. Further information on the conditions under which disclosure, publication and commercialisation of this thesis, the Copyright and any Intellectual Property University IP Policy (see http://documents.manchester.ac.uk/display.aspx?DocID=24420), in any relevant Thesis restriction declarations deposited in the University Library, The University Library's regulations (see http://www.library.manchester.ac.uk/about/regulations/) and in The University's policy on Presentation of Theses.

This thesis is dedicated to my husband Amir Karimi
for his immense support through this journey
and our beautiful daughter Leila
for providing the best therapy with her laughter.

Acknowledgements

I would especially like to thank my main supervisor, Dr Costas Demonacos for his continuous support and valuable guidance throughout my PhD. I am also thankful to my co-supervisors Dr James Yates and Dr Kayode Ogungbenro for their help using MATLAB with data modelling. Emyr Bakker has given valuable assistance in using COPASI as alternative modelling software. The funding for this research study was provided by BBSRC and AstraZeneca.

Prof. Marija Krstic-Demonacos must also be thanked for her valuable suggestions and permitting some use of her lab. I would also like to thank Dr Carina Cantrill, Sue Murby and Dr Dave Hallifax for allowing use of their equipment and expertise. Dr Aris Dokoumetzidis and his students were very helpful in familiarising use of modelling for the experimental data obtained.

The previous and the current students must be mentioned for their friendships and help in the lab: Dr Travis Leung, Dr Ramkumar Rajendran, Dr Ilhem Berrou, Dr Richa Garva, Dr Daphne Chen, Subir Singh, Farra Jumuddin, Bukunola Adegbesan and many others who cannot be named on this endless list.

I am forever indebted to my parents who set me on the right track and always supported and encouraged me to persevere in my academic and professional development. My wonderful brother has been another constant source of encouragement. My extended family provided great moral support during my studies.

Chapter 1: Introduction

1.1 Introduction

This study looks at generating mechanistic mathematical models to understand the rate and extent of changes in gene expression of drug-metabolising enzymes during therapy with steroid hormones (glucocorticoids) used extensively for their anti-inflammatory properties in the treatment of chronic autoimmune diseases including arthritis and asthma, as well as various types of leukaemia and solid tumours such as prostate and breast cancer (Vermeulen, 1996; Barnes, 1998; Pui and Evans, 2006; Inaba and Pui, 2010). Understanding the molecular mechanisms implicated in drug transport and metabolism, and shedding light on the changes of gene expression of the metabolising enzymes and nuclear receptors occurring under particular environmental conditions in different individuals, is beneficial for the pharmaceutical industry especially in the early stages of the drug development process to predict the lead compound with the highest potential to reach the market and also in the clinic to avoid drug-drug interactions (DDIs) (Rogers et al., 2002) and thus individualise therapy. DDIs can unexpectedly influence the functions of other cytochrome P450 (CYP) enzymes affecting pharmacology and toxicology of the administered dose. Describing the molecular links between nuclear receptors and drug metabolising enzymes will contribute towards improving the safety and individualisation of pharmacotherapy.

The simultaneous administration of different medications and genetic differences can lead to variations in the function of transport proteins, drug targets and the enzymatic activity of CYPs among individuals, leading to differences in drug effects and may produce toxicity. Currently, it is not routine to determine CYP activity before prescribing drugs, but in the future genotyping for some CYP enzymes might become standard for drugs with a narrow therapeutic range or those with life-threatening adverse effects (Rogers et al., 2002). Drug development involves determining standard drug doses in healthy volunteers who are statistically more likely to be extensive metabolisers (Eichelbaum and Gross, 1990). The incorporation of pharmacogenomics into drug development will allow

clinicians in the future to individualise drug treatment by tailoring dosage regimens to a patient's genotype (Lesko, 2007; Huang et al., 2008).

1.2 Drug Metabolism

The effects of the body on a drug are evaluated in pharmacokinetic studies as opposed to pharmacodynamics where the effects of a drug on the body are studied. Absorption, distribution, metabolism and excretion are the pharmacokinetic processes determining the relationship between an administered dose and the concentration of the drug in the body (Cashman et al., 1996; Ansede and Thakker, 2004; Ghanbari et al., 2006). A drug is chemically altered in the body by undergoing biotransformation or metabolism. This is needed to transform non-polar, lipid soluble compounds into polar, lipid insoluble compounds that can be excreted through urine or bile. Biotransformation reactions can be divided into either Phase 1 or Phase 2 reactions. Phase 1 reactions are functionalization reactions that introduce or expose a functional group on the parent compound. The metabolites formed can be inactive or active. Phase 1 reactions usually cause the loss of pharmacological activity in drugs or lead to activation of a prodrug (Shen et al., 1997; Doherty and Charman, 2002). Phase 2 reactions are conjugation reactions that cause the formation of a covalent bond linking a functional group on the parent compound or a Phase 1 metabolite with endogenously derived glucuronic acid, sulphate, glutathione, amino acids or acetate. The conjugates formed are highly polar and can be excreted rapidly in the urine and faeces (Krishna and Klotz, 1994; Yan and Caldwell, 2001; Rushmore and Kong, 2002).

1.3 Cytochrome P450 (CYP) enzymes

The CYP enzymes are members of a super-family that are essential in the body's anabolic and catabolic metabolism of xenobiotics. The importance of this super-family has been recognised in studies showing that they are vital for survival in organisms ranging from archaebacteria to humans (Nelson et al., 1996). Figure 1.1 shows the wide-ranging fields of P450 research from toxicology to microbiology in a schematic with many of the topics being inter-related (Ioannides, 2008).

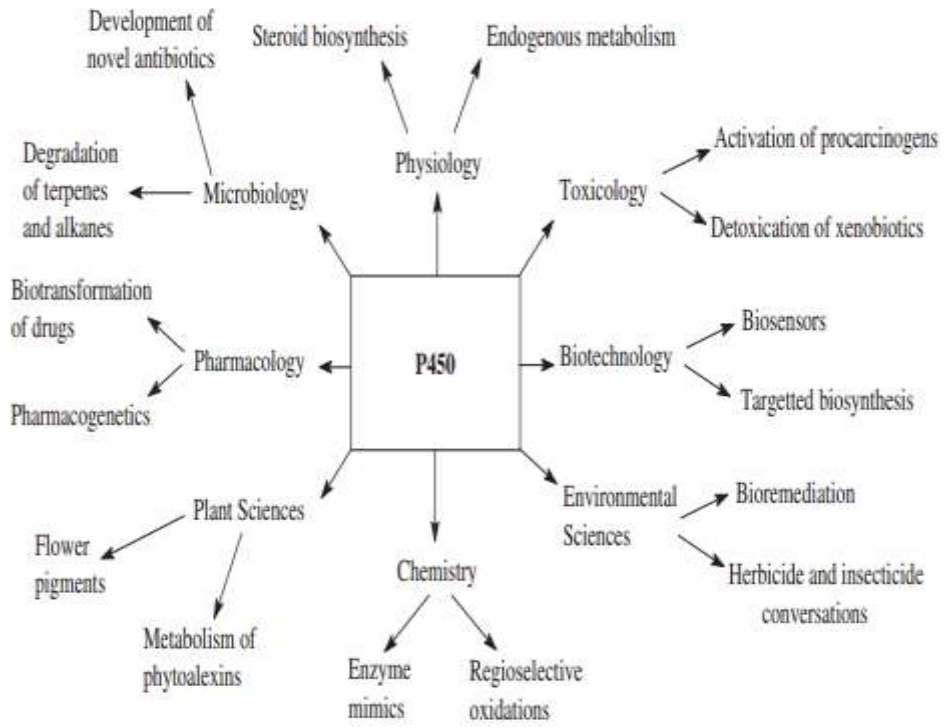

Figure 1.1: The broad fields of P450 research
Taken from Ioannides, 2008.

P450 activities of human liver samples have shown that they are affected by the recognized regulators and the other genes involved in the pathways responsible for the metabolism of drugs, fatty acids, amino acids and steroids (Musante et al., 2002).

The CYP isoforms can be sub-divided into those that metabolise endogenous chemicals and the ones responsible for Phase 1 metabolism of foreign substances (Lewis, 2004). There are 57 CYP known genes present in humans, but only members of the families CYP1, CYP2 and CYP3 have been found to have a major role in the metabolism of foreign substances (Al Omari and Murry, 2007). The other CYP enzymes in humans make up approximately half of this family and are responsible for the metabolism of endogenous compounds such as steroids, eicosanoid and fatty acids (Lewis, 2004). The clinically important aspects of CYP drug metabolism are genetic polymorphism and DDIs (Nelson et al., 1996; Wienkers and Heath, 2005; Chen and Raymond, 2006; Foti and Wahlstrom, 2008).

The CYP1 gene family is made up of 3 genes: CYP1A1, CYP1A2 and CYP1B1 (Danielson, 2002; Zanger and Schwab, 2013). Only CYP 1A2 appears to have a role in the metabolism of drugs (Zanger and Schwab, 2013) and CYP1B1 has been shown to have an enhanced appearance in a range of cancer cells whilst not being detected in normal tissues (Murray et al., 1997). The CYP2 family has the largest number of enzymes involved in drug metabolism in mammals and a total number of 13 subfamilies are included in this family (Nebert and Russell, 2002). The CYP3 gene family is comprised of two subfamilies: CYP3A in several vertebrae species including humans and CYP3B in fish (McArthur et al., 2003). The pie chart in Figure 1.2 shows the proportion of CYP metabolised drugs used clinically (Zanger and Schwab, 2013).

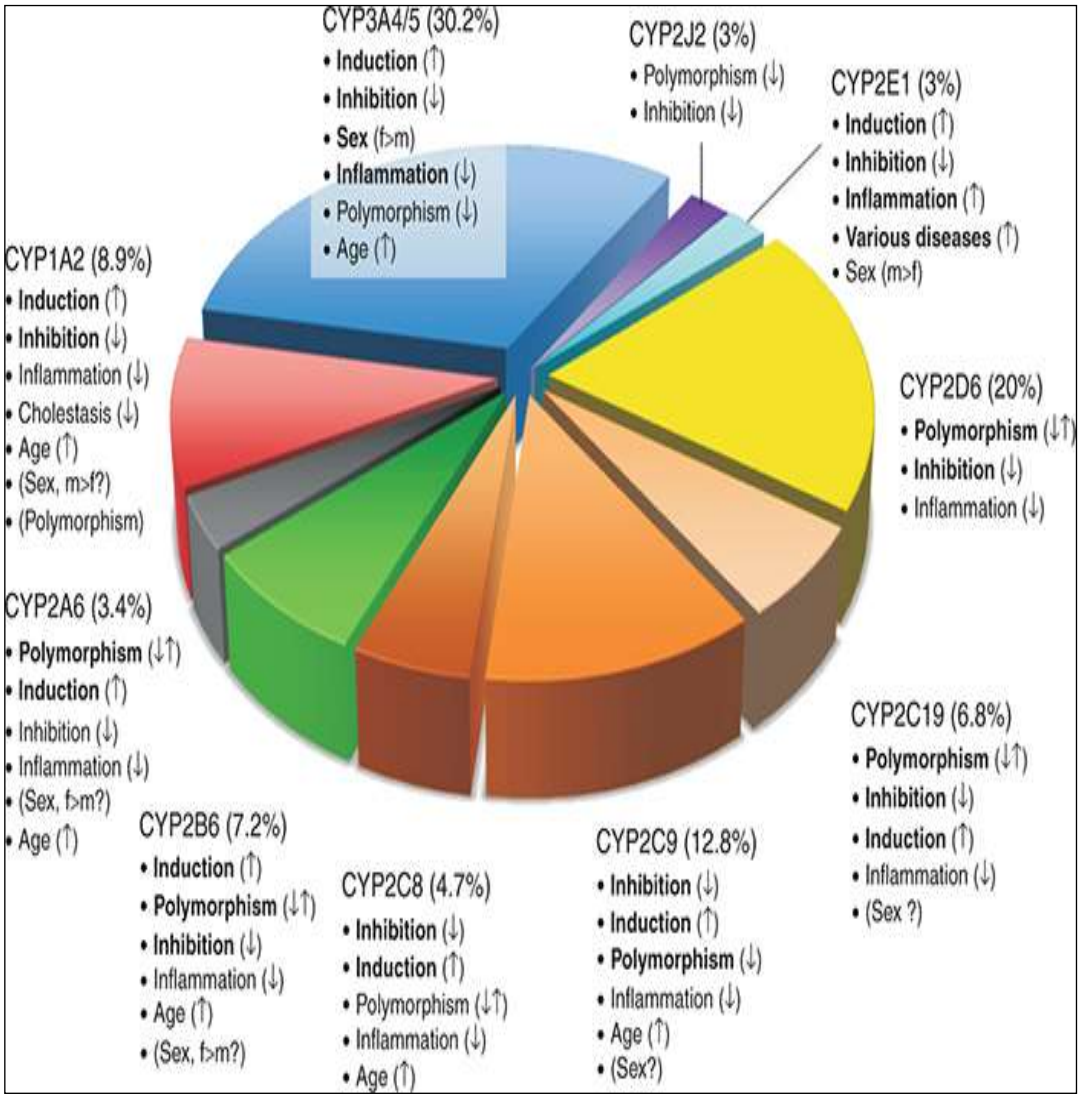

Figure 1.2: Proportions of cytochrome P450 metabolised drugs used clinically
The pie chart shows the proportion of a total of 248 drug metabolism pathways with known CYP involvement and the factors affecting their variability such as sex, polymorphism and age which can cause increased activity (↑), decreased activity (↓), increased and decreased activity (↑↓).

Figure taken from Zanger and Schwab, 2013.

CYP3A enzymes are of great importance for drugs' and xenobiotics' metabolism because of their abundant expression in the human liver and the small intestine. CYP3A enzymes show the ability to metabolise a broad range of structurally diverse compounds (Thummel and Wilkinson, 1998; Nebert and Russell, 2002). The clinically significant CYP drug-metabolising enzymes are CYP3A4/5,

CYP2C9, CYP2C19 and CYP2D6 (Huang et al., 2007; Urquhart et al., 2007; Huang et al., 2008). In combination, CYP3A4/5 and CYP2C9 are responsible for the bulk of drug metabolism in the human body, which is believed to be over 60% of drugs (Wienkers and Heath, 2005). CYP3A4 enzyme is believed to have a degradation half-life of 1-6 days (Brown et al., 2005; Galetin et al., 2006).

Table 1.1 shows the CYP involvement in the activation of metabolic pathways of chemicals such as electrophilic compounds, free radicals, carbenes and nitrenes and activated oxygen species to give reactive toxic intermediates (Vermeulen, 1996).

Initiators	*Examples*	*Reaction type*	*Targets*
Electrophiles	Michael acceptors Acyl halides Quinones	Covalent binding	Thiols
Radicals	CCl_4	Covalent binding	Thiols, nucleic acids, (phospho)lipids
	Halothane	H abstraction	Thiols, nucleic acids, (phospho)lipids
	Adriamycin	Reduction	Molecular oxygen
Reactive oxygen species	Superoxide	Reduction	Metal ions
	Peroxide	Oxidation	Thiols
	OH Radical	H abstraction	Thiols, nucleic acids, (phospho)lipids
Heavy metals	Cd, Hg, Pb, Pt, Au, Ag	Complexation	Thiols, nucleic acids
Polycations	Gentamycin Kanamycin	Charge-charge interaction	Phospholipids

Table 1.1: Chemically reactive toxic initiators, types of interactions and biological targets.

Table taken from Vermeulen, 1996.

The sequence of CYP proteins shows a motif of 10 amino acid residues making the haem-binding region:

FxxGxxxCxG

F is phenylalanine, G is glycine, C is cysteine and x is any amino acid, but the sixth position is usually a basic amino acid (Lewis et al., 1998; Kumar, 2011). This motif appears to be unique to proteins of the P450 superfamily and vital for haem-binding proteins with similar catalytic activity to P450 enzymes. Also, there are other regions of conservation in addition to the motif at the start of this L helix

which provide structural or mechanistic functions (Lewis et al., 1998; Sezutsu et al., 2013). The levels of messenger ribonucleic acids (mRNA) do not fully correlate with protein levels. The protein levels are determined by the balance of RNA and protein production and turnover. The main mechanisms controlling translation are transcript stability and protein degradation (Vogel and Marcotte, 2012). Table 1.2 shows the substrate specificity of different CYP isoforms (Nebert et al., 2013) .

gene	function(s)	disease(s)
CYP1A1	metabolism of eicosanoids; foreign chemicals	
CYP1A2	metabolism of eicosanoids; drugs and foreign chemicals	
CYP1B1	metabolism of eicosanoids; foreign chemicals	primary congenital glaucoma (buphthalmos)
CYP2A6, 2A13	metabolism of eicosanoids; drugs and foreign chemicals	
CYP2A7	nitrosamine metabolism	
CYP2B6	metabolism of eicosanoids; drugs and foreign chemicals	
CYP2C8, 2C9, 2C18, 2C19	metabolism of eicosanoids; drugs and foreign chemicals; *2C9* contributes to warfarin metabolism	
CYP2D6	metabolism of eicosanoids; drugs and foreign chemicals	
CYP2E1	metabolism of eicosanoids; drugs and foreign chemicals	
CYP2F1	metabolism of eicosanoids; drugs and foreign chemicals	
CYP2J2	metabolism of eicosanoids; drugs and foreign chemicals	
CYP2R1	vitamin D 25-hydroxylase	vitamin D 25-hydroxylase deficiency
CYP2S1	metabolism of eicosanoids; drugs and foreign chemicals; retinoids	
CYP2U1	metabolism of eicosanoids, long-chain fatty acids; drugs and foreign chemicals	
CYP2W1	metabolism of eicosanoids; drugs and foreign chemicals	
CYP3A4	metabolism of eicosanoids, sex steroids; greater than or equal to 60% of all clinically used drugs; foreign chemicals	
CYP3A5, 3A7, 3A43	metabolism of eicosanoids, sex steroids; drugs and foreign chemicals	

Table 1.2: Functions and/or diseases associated with mutations in CYP genes Adapted from Nebert et al., 2013.

The CYP enzymes found in bacteria and eukaryotic mitochondria are termed type I, whilst type II are those located in the eukaryotic endoplasmic reticulum (ER). Nicotinamide adenine dinucleotide (NADH) or nicotinamide adenine dinucleotide phosphate (NADPH) can donate electrons to the membrane-bound flavoprotein

ferredoxin reductase (FDXR) in the mitochondria, which then pass them to a soluble iron–sulphur protein ferredoxin (FDX) donating the electrons to the type I enzymes (Figure 1.3 (a)). Type II CYPs in the ER function by donation of electrons from NADPH to the protein P450 oxidoreductase (POR) (Figure 1.3 (b)) (Nebert et al., 2013).

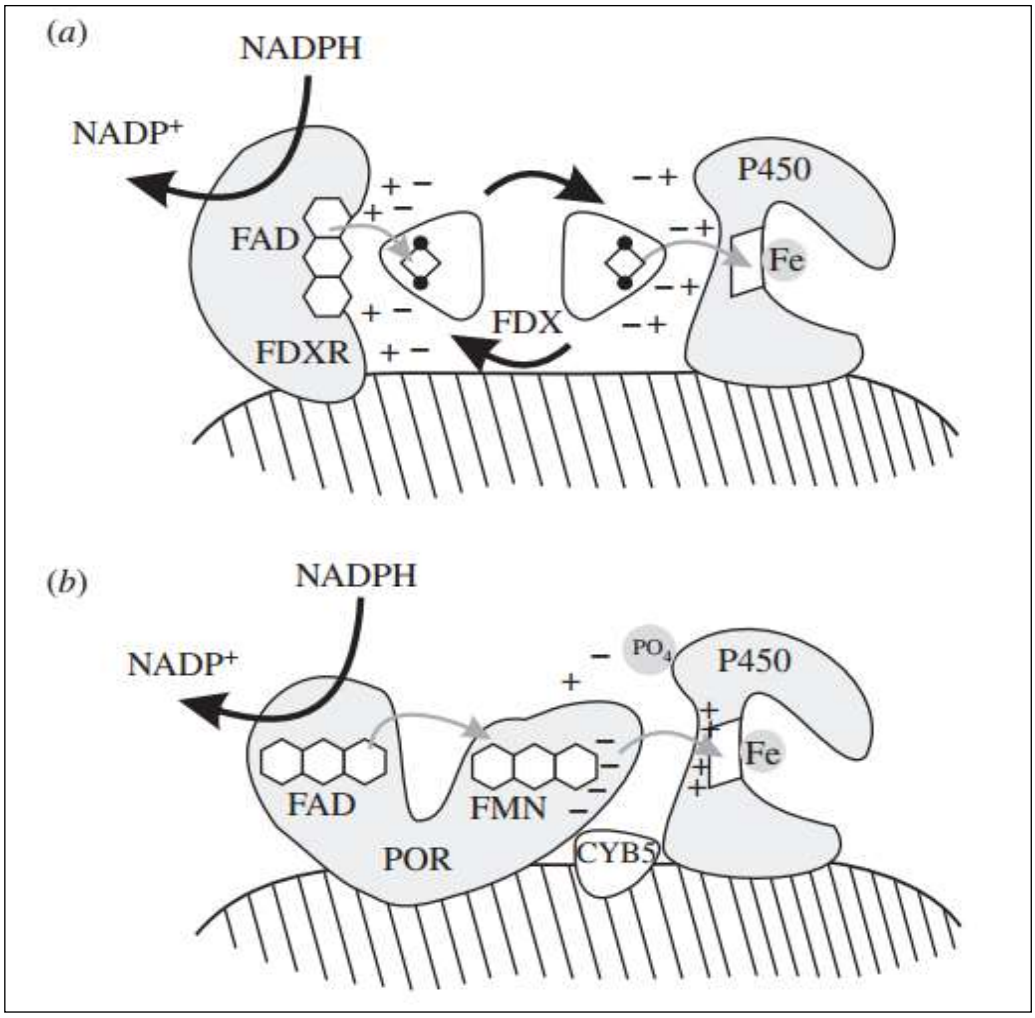

Figure 1.3: Diagram of type I P450 (a) and type II P450 (b)

FAD, flavin adenine dinucleotide; FDX, ferrodoxin; FDXR, ferrodoxin reductase; FMN, flavin mononucleotide; POR, P450 oxidoreductase; CYB5, cytochrome b5. Scheme reproduced with permission from copyright owner, WL Miller in Nebert et al., 2013.

The CYP450 enzymes which metabolise drugs such as CYP2C9 and CYP3A4/5 are mainly located in the ER in humans, but can also be present in other cellular organelles such as the mitochondria at lower levels (Neve and Ingelman-Sundberg, 2008).

1.3.1 CYP3A Subfamily

The CYP3A sub-family is considered to be most significant among the members of these families due to its high abundance in the human liver (between 30-50% of total CYP content) meaning that most chemicals will be exposed to this enzyme (Paine et al., 2006; Plant, 2007; Rostami-Hodjegan and Tucker, 2007). This sub-family has a large active site which results in substrate promiscuity and the metabolism of up to 60% of drugs currently in clinical use (Cholerton et al., 1992; Williams et al., 2004). Therefore, CYP3A appears to play an important role in the metabolism of many xenobiotics.

There is a large compendium of CYP alleles listing 40 variants for CYP3A4, 24 for CYP3A5 and 7 for CYP3A7. However, the majority of these variants have little biological significance or occur in low frequency, meaning that inter-individual variability in CYP3A activity is of little importance in response to drugs (Mizutani, 2003; Solus et al., 2004; Roy et al., 2005). CYP3A4/5 is mainly believed to contribute to CYP3A-mediated drug metabolism (Guengerich, 1999; Schuetz, 2004).

1.3.1.1 CYP3A4/5

CYP3A4/5 transcripts rise rapidly following birth after being undetectable in the foetal liver (Schuetz et al., 1994). The CYP3A4/5 family makes up 30% of the total hepatic content and 70% of the gut wall content (Chang and Kam, 1999; Paine et al., 2006). This isoform is the most abundant CYP in the adult human liver (Cholerton et al., 1992; Lacroix et al., 1997; Zanger and Schwab, 2013) and is therefore the most studied CYP3A sub-family member in humans. It is involved in the metabolism of many endogenous and exogenous compounds. The endogenous hormones metabolised by CYP3A4/5 include progesterone, estradiol, testosterone and cortisol.

It has been found that in patients with rheumatoid arthritis, low levels of endogenously produced cortisol has been measured despite the high degree of inflammation associated with this condition. GR gene polymorphism is thought to influence the immunosuppressive effects of cortisol and GC resistance (Harbuz and Jessop, 1999; Quax et al., 2015). Sensitivity to GC has also be found to differ in patients suffering with other autoimmune conditions such as MS (van Winsen et al., 2005).

CYP3A4/5 catalyses the metabolism of more than half of all drugs and is the main mode of elimination for many drugs (Schuetz, 2004). There is a wide substrate binding profile and catalytic activity for CYP3A4/5 which may include biotransformation reactions such as C- and N- oxidation, N- and O-dealkylation, nitro reduction and dehydration reactions (Gibson et al., 2002). CYP3A5 is closely related to CYP3A4 and has an equal or less metabolic capability than the latter isoform (Williams et al., 2002). The term, CYP3A is commonly used in the literature to refer to these isoforms which cannot be distinguished by either antibodies or inhibitors (Khojasteh et al., 2011). Figure 1.4 shows the metabolism of drugs by CYP3A before reaching the systemic circulation. CYP3A4 and CYP3A5 may metabolise the drug during its passage across the enteric mucosa of the proximal small bowel and through the liver before reaching the systemic circulation (Ioannides, 2008).

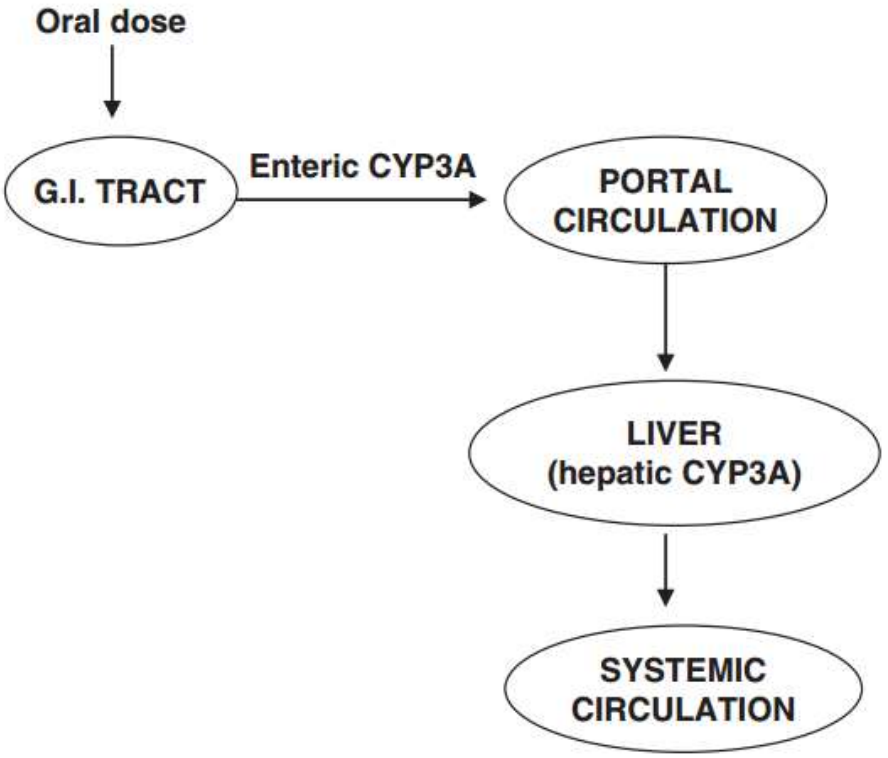

Figure 1.4: Route taken of orally administered CYP3A substrates

Possible metabolism by CYP3A4 and CYP3A5 during passage across the enteric mucosa of the proximal small bowel and through the liver before reaching the systemic circulation is shown in this schematic diagram.

Figure taken from Ioannides, 2008.

The nucleotide sequence comparison and distribution of regulatory elements in the human CYP3A4 and CYP3A5 proximal promoters is shown in Figure 1.5. The asterisks represent where the nucleotides in the two isomers are identical and the hyphens indicate the location of the absent 57 base pairs region from the CYP3A5 promoter. The arrows indicate the transcription start sites at +1 and the sequences shown are relative to this site (Nem et al., 2012).

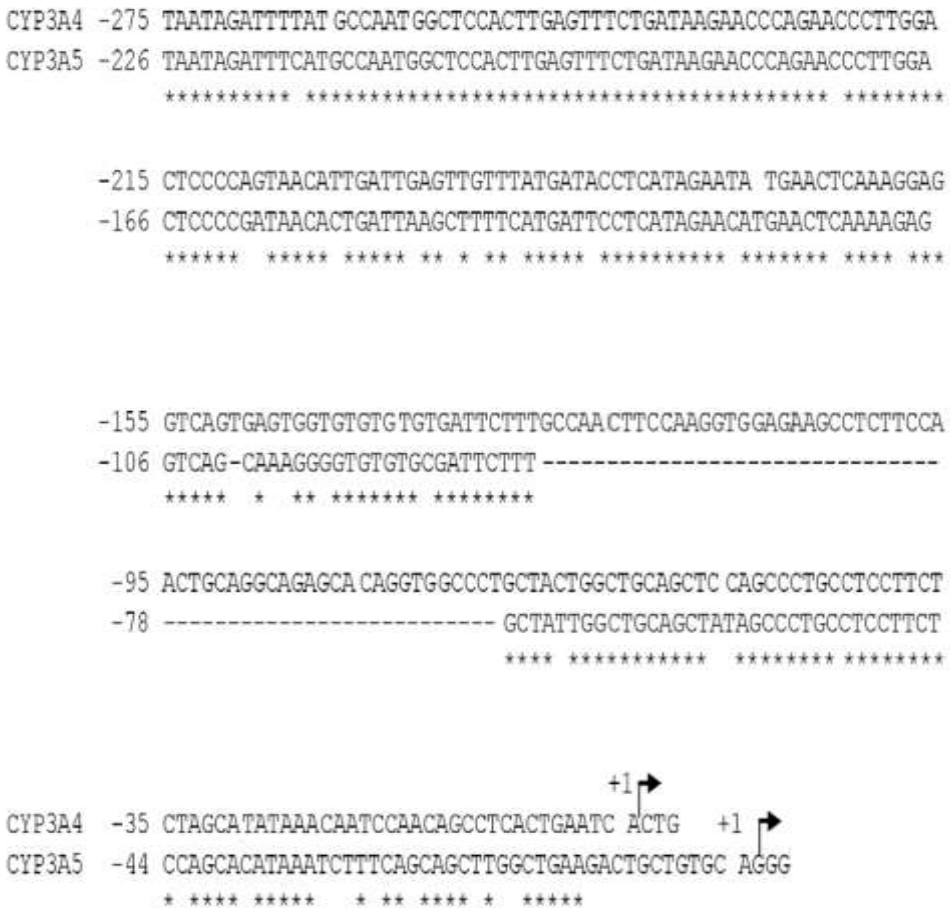

Figure 1.5: Sequence comparison in the human CYP3A4 and CYP3A5 proximal promoters

Asterisks denote identical nucleotides and hyphens represent the 57 bp region absent from the CYP3A5 promoter.

Adapted from Nem et al., 2012.

The protein sequences of the CYP3A4 and CYP3A5 enzymes in humans are shown in Figure 1.6.

CYP3A4 protein sequence (503 amino acids) in humans:

MALIPDLAME TWLLLAVSLV LLYLYGTHSH GLFKKLGIPG
PTPLPFLGNI LSYHKGFCMF DMECHKKYGK VWGFYDGQQP
VLAITDPDMI KTVLVKECYS VFTNRRPFGP VGFMKSAISI
AEDEEWKRLR SLLSPTFTSG KLKEMVPIIA QYGDVLVRNL
RREAETGKPV TLKDVFGAYS MDVITSTSFG VNIDSLNNPQ
DPFVENTKKL LRFDFLDPFF LSITVFPFLI PILEVLNICV
FPREVTNFLR KSVKRMKESR LEDTQKHRVD FLQLMIDSQN
SKETESHKAL SDLELVAQSI IFIFAGYETT SSVLSFIMYE
LATHPDVQQK LQEEIDAVLP NKAPPTYDTV LQMEYLDMVV
NETLRLFPIA MRLERVCKKD VEINGMFIPK GVVVMIPSYA
LHRDPKYWTE PEKFLPERFS KKNKDNIDPY IYTPFGSGPR
NCIGMRFALM NMKLALIRVL QNFSFKPCKE TQIPLKLSLG
GLLQPEKPVV LKVESRDGTV SGA

CYP3A5 protein sequence (502 amino acids) in humans:

MDLIPNLAVE TWLLLAVSLV LLYLYGTRTH GLFKRLGIPG
PTPLPLLGNV LSYRQGLWKF DTECYKKYGK MWGTYEGQLP
VLAITDPDVI RTVLVKECYS VFTNRRSLGP VGFMKSAISL
AEDEEWKRIR SLLSPTFTSG KLKEMFPIIA QYGDVLVRNL
RREAEKGKPV TLKDIFGAYS MDVITGTSFG VNIDSLNNPQ
DPFVESTKKF LKFGFLDPLF LSIILFPFLT PVFEALNVSL
FPKDTINFLS KSVNRMKKSR LNDKQKHRLD FLQLMIDSQN
SKETESHKAL SDLELAAQSI IFIFAGYETT SSVLSFTLYE
LATHPDVQQK LQKEIDAVLP NKAPPTYDAV VQMEYLDMVV
NETLRLFPVA IRLERTCKKD VEINGVFIPK GSMVVIPTYA
LHHDPKYWTE PEEFRPERFS KKKDSIDPYI YTPFGTGPRN
CIGMRFALMN MKLALIRVLQ NFSFKPCKET QIPLKLDTQG
LLQPEKPIVL KVDSRDGTLS GE

Figure 1.6: Translations of CYP3A4 and CYP3A5 in humans

CYP3A4 Accession NP_059488 and CYP3A5 Accession NP_000768, obtained from the National Centre for Biotechnology Information (NCBI) website, USA, http://www.ncbi.nlm.nih.gov/, accessed August 2015.

The simulation of the docking of the drug, thalidomide, into a reported structure of CYP3A4 (A) and a homology model of CYP3A5 (B) are shown in Figure 1.7. In silico analysis has shown that thalidomide closely docks to the CYP3A5 haem (displayed as 'heme' in the diagram), whilst this drug does not dock closely to the haem region of CYP3A4.

The activation phenomenon known as heterotropic cooperativity, which involves two different ligands in the active site of CYP450 enzymes are presented in Figure 1.7(C) for CYP3A4 and CYP3A5.

Comparison of the key amino acids reported in the F-helix of the two isomers is presented in Figure 1.7(D).

The different amino acids in the specified positions reveal a more flexible site and higher lipophilicity in the CYP3A5 active site which shows different characteristics in comparison to CYP3A4 for thalidomide (Okada et al., 2009).

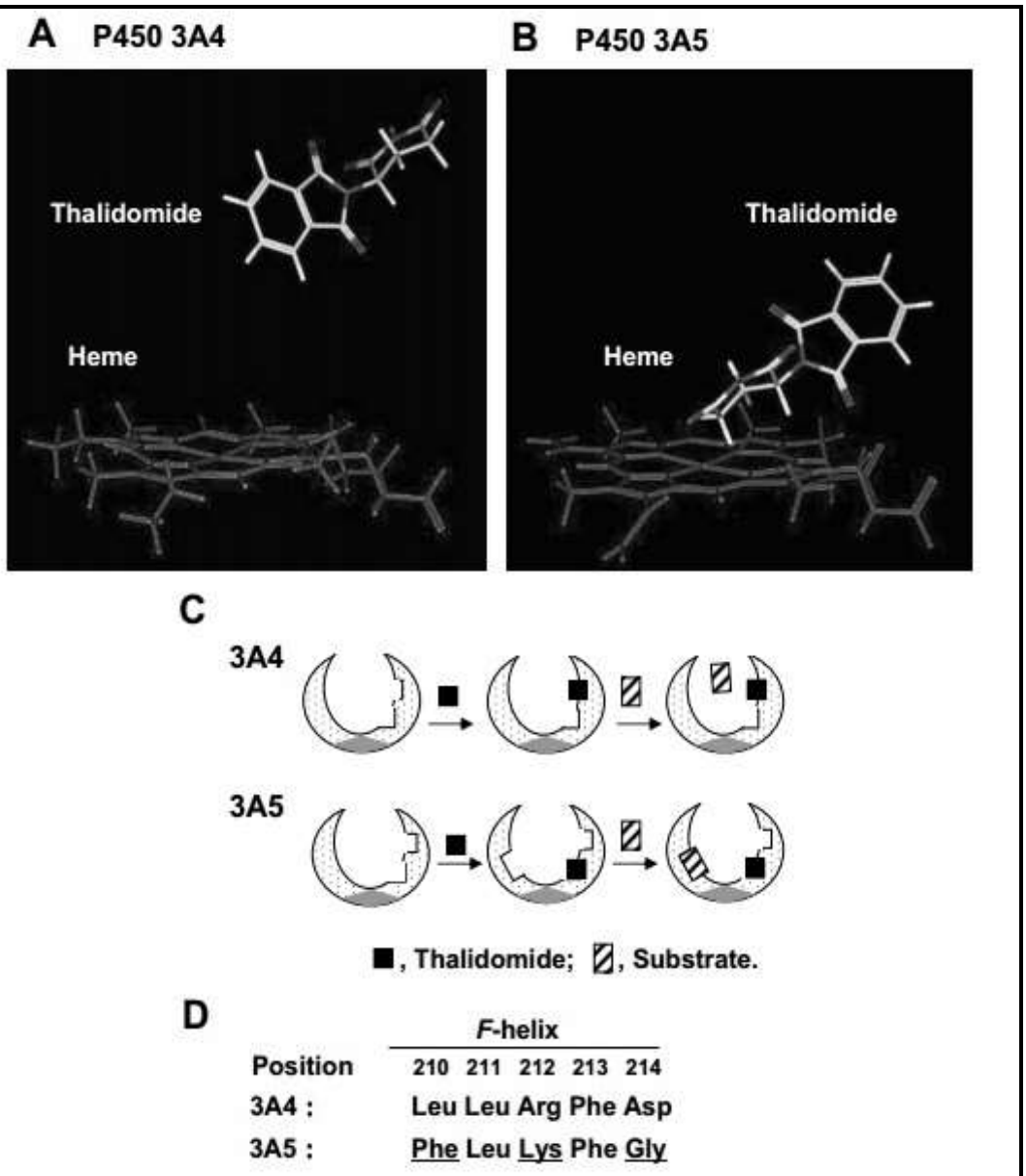

Figure 1.7 (A): Simulation of thalidomide docking in CYP3A4

(B): Simulation of thalidomide docking in CYP3A5

(C): The suggested heterotropic binding of CYP3A4 and CYP 3A5

(D): Comparison of key amino acids reported in the F-helix of the two isomers

Adapted from Okada et al., 2009.

1.3.2 CYP2C subfamily

The CYP2C subfamily of enzymes is mainly located in the liver and accounts for about 20% of the total cytochrome P450 (Shimada et al., 1994; Paine et al., 2006; Zanger and Schwab, 2013). CYP2C enzymes also play an important role in the metabolism of many currently marketed drugs.

1.3.2.1 CYP2C9

The second most abundantly expressed CYP in the human liver is the CYP2C9 which is responsible for the metabolism of commonly prescribed drugs such as phenytoin, warfarin, losartan and several non-steroidal anti-inflammatory drugs (NSAIDs) such as ibuprofen. It has been estimated that CYP2C9 metabolises around 16% of prescribed drugs and is induced by exposure to Dex, rifampicin and phenobarbital as also seen with CYP3A4/5. The protein sequence of human CYP2C9 is shown in Figure 1.8.

MDSLVVLVLCLSCLLLLSLWRQSSGRGKLPPGPTPLPVIGNILQIGIKDISKS
LTNLSKVYGPVFTLYFGLKPIVVLHGYEAVKEALIDLGEEFSGRGIFPLAE
RANRGFGIVFSNGKKWKEIRRFSLMTLRNFGMGKRSIEDRVQEEARCLVE
ELRKTKASPCDPTFILGCAPCNVICSIIFHKRFDYKDQQFLNLMEKLNENIK
ILSSPWIQICNNFSPIIDYFPGTHNKLLKNVAFMKSYILEKVKEHQESMDM
NNPQDFIDCFLMKMEKEKHNQPSEFTIESLENTAVDLFGAGTETTSTTLRY
ALLLLLKHPEVTAKVQEEIERVIGRNRSPCMQDRSHMPYTDAVVHEVQR
YIDLLPTSLPHAVTCDIKFRNYLIPKGTTILISLTSVLHDNKEFPNPEMFDPH
HFLDEGGNFKKSKYFMPFSAGKRICVGEALAGMELFLFLTSILQNFNLKSL
VDPKNLDTTPVVNGFASVPPFYQLCFIPV

Figure 1.8: Translation of CYP2C9 in humans (490 amino acids)
CYP2C9 Accession NP_000762. Obtained from NCBI website, accessed August 2015.

1.3.3 Genetic polymorphism

The activity of CYPs differs in different populations and individuals. Genetic variations within a population are known as ‘polymorphisms’ when either gene or allelic variants occur with a frequency of more than 1% (Meyer, 2000). The body's response to drugs is affected by an individual’s genetics. Testing for important DNA sequence variations or polymorphisms in key drug-metabolizing enzymes, receptors, etc. can be used to predict therapeutic failures or severe adverse drug reactions in patients. This can also reduce medical costs over the long-term.

It has been estimated that 86% of the polymorphic Phase 1 enzymes are CYPs and 56% of drugs reported in adverse drug reactions (ADR) studies are metabolised by the CYP enzymes (Phillips et al., 2001). CYP2A6, CYP2B6, CYP2C9, CYP2C19 and CYP2D6 (Martiny and Miteva, 2013) and CYP3A5 (Xie et al., 2004) are polymorphic CYP enzymes that can significantly affect the metabolism and the therapeutic efficiency of drugs.

CYP2C9 is an isoform which shows a high frequency of genetic polymorphism, being absent in about 1% of Caucasians (Hamman et al., 1997). In contrast, CYP3A4 is highly conserved in different individuals and populations with no functionally variant forms have been identified in Asians and Caucasians. This isoform does not exhibit genetic polymorphism and profiling the molecular basis for individual variation in this isoform has remained elusive (Schuetz, 2004; Xie et al., 2006). CYP3A5 is the most polymorphic isoform in the CYP3A sub-family (Burk et al., 2004; Lakhman et al., 2009) and it has been suggested that CYP3A5 may contribute up to 50% of this sub-family in individuals with increased expression of this enzyme. This isoform is expressed in only 25% of white persons and approximately 50% of African Americans (Kuehl et al., 2001). An investigation on the frequency of polymorphism in different ethnic groups found that CYP2C9 is one of the most polymorphic CYP enzymes influencing drug metabolism (Preissner et al., 2013).

Many factors other than DDIs can cause a change in the expression of CYP proteins in humans and these are summarised in Table 1.3.

Factor affecting CYP protein levels	Difference/change expected
Age	Ageing comes with changes in the physiology of many organs such as decrease in efficiency of the heart and reduction in the capacity of the kidneys. Changes in the metabolism of some drugs may remain unchanged, but the elimination of most drugs with blood-flow limited clearance is decreased in the elderly (Wauthier et al., 2007). The quantity of some isoforms may remain constant with age, but total CYP content (e.g. CYP2E1, CYP3A) and NADH reductase activity is less with age (George et al., 1995). Increase in age coincides with reduction in CYP enzyme activity in both sexes (Gurley et al., 2005).
Gender	Gender differences in the metabolic activity of CYP enzymes have been identified in humans. Women show a higher CYP3A activity on average. This variation in drug metabolising enzymes is the reason that the US FDA encourages including women as patients in clinical trials (Schwartz, 2003).
Hormones	Testosterone deficiency has been shown to decrease CYP activity. Oestrogen has also been found to decrease the oxidation of some drugs and the menstrual cycle phases can change CYP enzyme activity (Pinsonneault and Sadée, 2003).
Genetic polymorphism	Significant clinical implications in different populations have been noted for the CYP isoenzymes 2C9, 2C19, 2D6, 1A2 and 3A5 (Zhou, 2009).

Hepatic disease	Decreased gene expression of the CYP isoenzymes 1A2, 2E1 and 3A have been observed in liver cirrhosis, whereas upregulation of the 2C subfamily cellular levels have been reported in the levels of the 2C subfamily in patients suffering from hepatic carcinoma (Villeneuve and Pichette, 2004). Knowledge of how these isoenzymes are affected in these diseases, can aid in rationalising drug therapy.
Inflammation	CYP activity in humans has been reported to be suppressed by acute phase response inflammatory mediators. This can lead to high plasma levels and the toxicity of drugs metabolised by CYP-dependent enzymes (Rivory et al., 2002).
Environmental factors	Cigarette smoking and alcohol consumption induce CYP2E1 and CYP1A2 enzymatic activity (Rizzo et al., 1997).
Pregnancy	The renal excretion of unchanged drugs is increased during pregnancy whilst the metabolism of drugs catalysed by some CYPs i.e. CYP2D6 (Wadelius et al., 1997; Lind et al., 2003) and CYP2C9 are increased during pregnancy, whist the activity of other isoenzymes such as CYP1A2 and CYP3C19 is decreased (Anderson, 2005).

Table 1.3: Factors other than DDIs that affect CYP expression

1.4 Nuclear Receptors

The nuclear receptors (NRs) are a super-family of 49 members (Figure 1.9 (Ng et al., 2014)) that are the largest family of ligand-activated transcription factors implicated in regulating drug metabolism (Zhang et al., 2004).

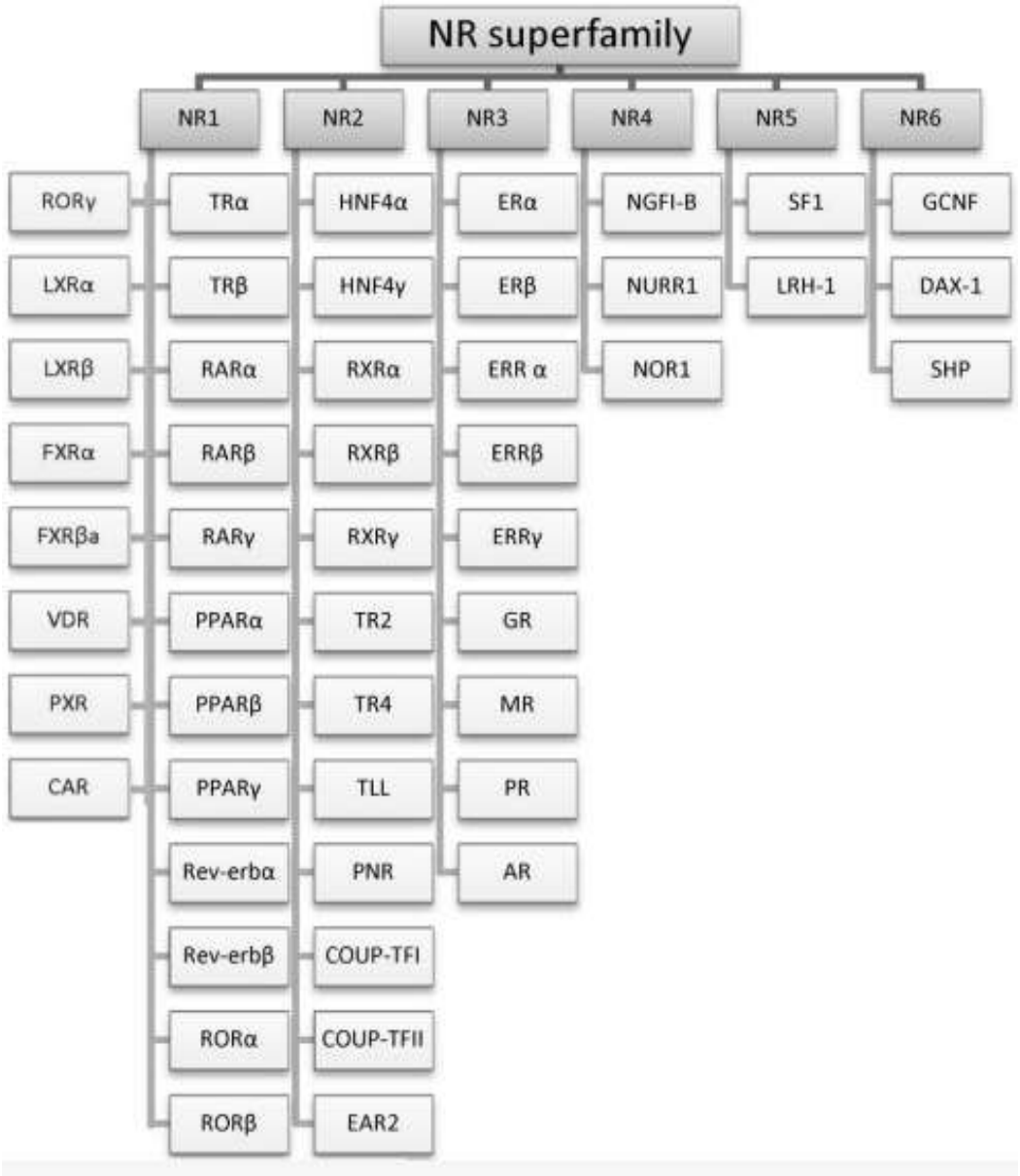

Figure 1.9: The NR superfamily

The classification of the NR superfamily and members of families 1-6 are shown. Abbreviations have been listed in the earlier section.

Figure taken from Ng et al., 2014.

NRs are transcription factors that play important parts in controlling the biological development, distinction, metabolic homeostasis and protecting the organism against the stresses induced by foreign substances (Li and Wang, 2010). 49 members of the NR superfamily have been recognised so far (Pavek and Dvorak, 2008), 48 of them in humans (Germain et al., 2006; Li and Wang, 2010). The ligands for some are unknown (orphan receptors) or have later been identified (adopted orphan receptors) (Germain et al., 2006; Li and Wang, 2010).

The interaction between NRs and CYP enzymes are shown in Figure 1.10. Where xenobiotics (X) or endobiotics (E) are ligands that can up-regulate or down-regulate the activity of CYP genes or other genes to control and generate certain cellular reactions. The ligands are degraded by specific CYP enzymes in to their oxidation products, XO and EO which may also act as ligands for NRs (Honkakoski and Negishi, 2000).

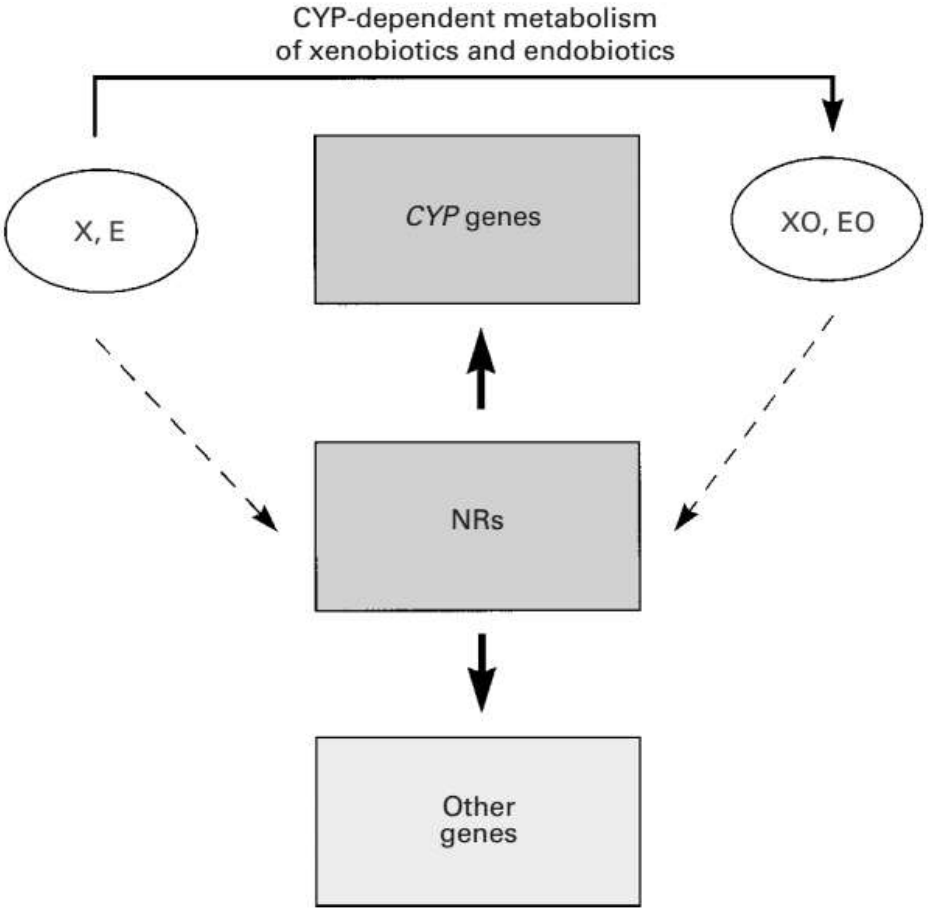

Figure 1.10: Links between the ligands of NRs, CYP genes and other genes

Figure taken from Honkakoski and Negishi, 2000.

The functional domains and the binding sites of NRs are illustrated in Figure 1.11 (A). The structure consists of DNA binding domain (DBD), ligand binding domain (LBD), C-terminal extension (CTE) required for DNA binding and activation function 2 (AF-2). Some NRs carry an independent activation function 1 (AF-1).

Figure 1.11 (B) demonstrates the binding of NR dimers to their associated DNA element DR*n*, IR*n* and ER*n*, are respectively direct, inverted and everted repeat

with *n* bp spacing. The arrows show the orientations of the half-sites currently recognised (Honkakoski and Negishi, 2000).

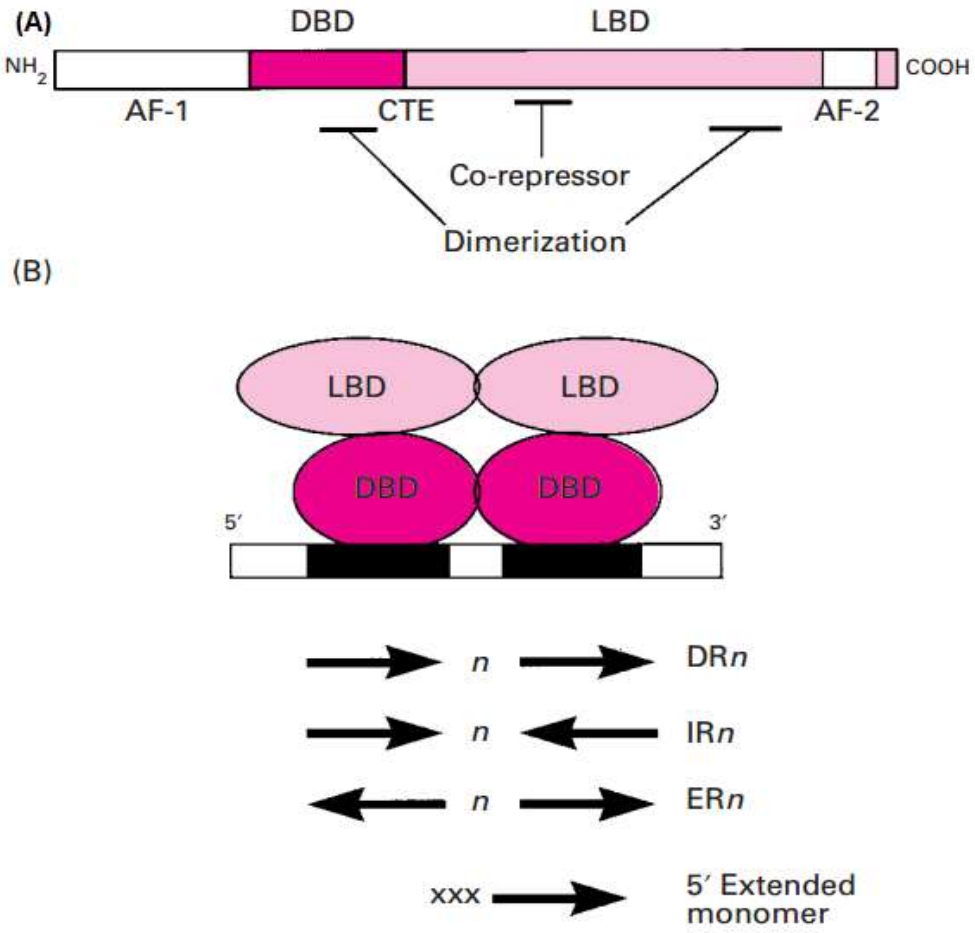

Figure 1.11: (A) Functional domains and the binding sites of NRs

Figure 1.11: (B) Binding of NR dimers to their associated DNA element DR*n*, IR*n* and ER*n*,

Various orientations of half-sites lead to different types of response elements. DR*n*, IR*n* and ER*n*, are respectively direct, inverted and everted repeat with *n* bp spacing. The arrows show the orientations of the half-sites.

Figure taken from Honkakoski and Negishi, 2000.

The gene activation and gene repression by NRs is shown in Figure 1.12 where ligand-binding or other processes that activate the NR induce its binding to the DNA element. The complexes of NR-specific and/or common co-activators or co-integrators can switch on the process to acetylate histones for activation of transcription. Some NRs bind co-repressors when there is no ligand binding or on the binding of NR antagonists, leading to deacetylation of histones (Honkakoski and Negishi, 2000).

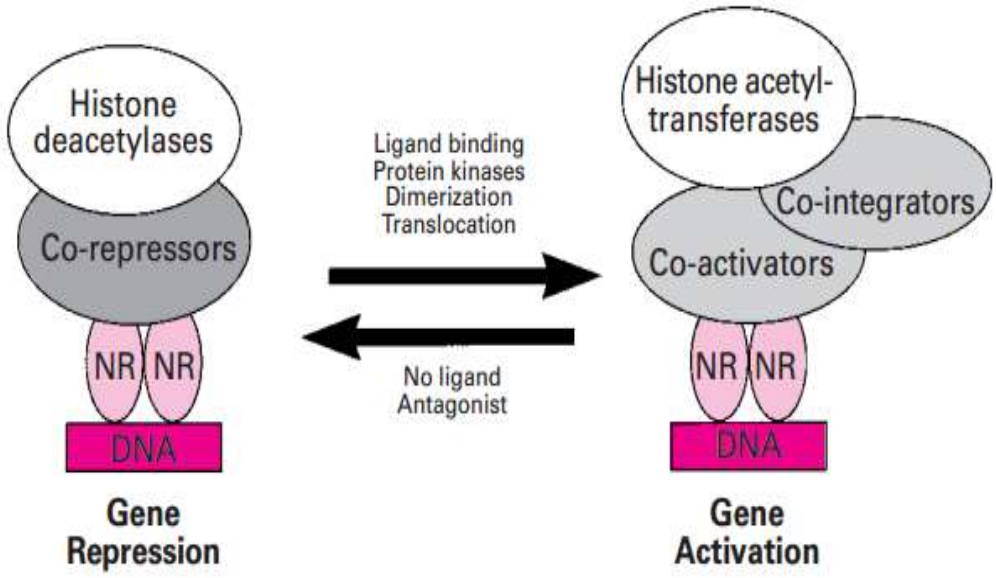

Figure 1.12: Model showing binding or absence of ligands or antagonist to NRs leading to gene activation or repression

The DNA element is shown in dark pink. NR (light pink eclipses), the co-activators and co-integrators are shown (pale grey eclipses). Histone acetyl-transferases (white eclipse).

The absence of ligand or binding of antagonists is shown in NR binding co-repressors (in grey), deacetylation of histones (white eclipse).

Figure taken from Honkakoski and Negishi.

Histones are essential in eukaryotic cells to package DNA and are important in controlling gene expression. The nucleosome is formed by the wrapping of around 150 base pairs of DNA around an octamer of core histones and this is the basic unit of chromatin which can be compacted further by linker histones. Linker histones may undergo acetylation and deacetylation by histone acetyltransferase and histone deacetylase enzymes (Honkakoski and Negishi, 2000; Over and Michaels, 2014).

1.4.1 Glucocorticoid Receptor (GR)

GR is a member of the nuclear receptor superfamily of ligand-dependent transcription factors composed of 777 amino acids. In the absence of natural or synthetic GCs which can act as ligands, GR is mainly localised in the cytosol with heat shock proteins (HSPs) acting as its chaperones (Longui, 2007; Oakley and Cidlowski, 2011). After binding GCs, GR dissociates from the HSPs and translocates to the nucleus where GR/GR homodimers form that bind to glucocorticoid response element (GRE) sequences in DNA (Figure 1.13 (Longui, 2007)). This binding to GRE can transactivate or repress the transcription of target genes. So GR can transcriptionally control a wide variety of genes such as cytokines, enzymes and receptors (Gross and Cidlowski, 2008), therefore directly and indirectly affecting gene expression (Nicolaides et al., 2010). The transcriptional regulation of the drug metabolising CYP enzymes can be via the ligand-activation of GR. This can be achieved by the direct binding of GR to the recognised gene-promoter sequence, GRE. GR can also bind indirectly to gene promoters via the formation of a multiprotein complex. GR can also up- or down regulate different CYP transcriptional regulators or NRs through the transcriptional regulatory cross-talk (Dvorak and Pavek, 2010). Synthetic glucocorticoids are extensively used in the clinic to treat many diseases, therefore better understanding of GR mediated regulation of drug-metabolising CYPs in relation to GC therapy or hormonal status will facilitate efficient patient-specific pharmacotherapy and fewer drug-drug interactions (Dvorak and Pavek, 2010).

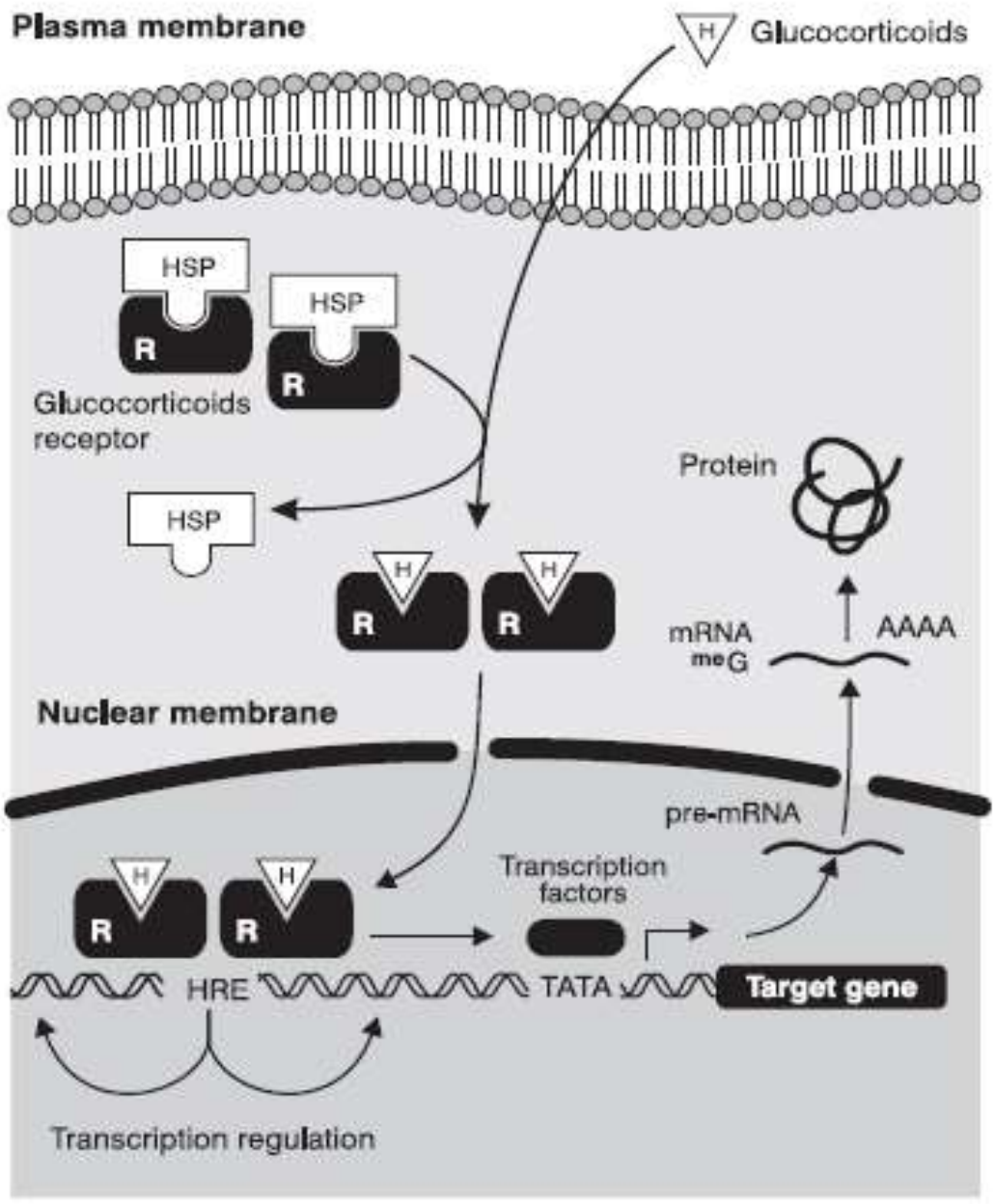

Figure 1.13: Binding of GCs to GRs

Figure taken from Longui, 2007.

Transcriptionally active GR can bind directly to the promoter of some target CYP genes, shown in Figure 1.14 (Dvorak and Pavek, 2010). The direct binding of GR to the gene promoter regions of CYP3A5 and CYP2C9 shows the direct effect of GR on these drug-metabolising enzymes. Transcriptionally active GR binds to the DNA sequence in a gene promoter in a homodimer (GR/GR). GRE

has a sequence of palindrome hexamer separated by three nucleotides (5'-AGAACAnnnTGTTCT-3') (Nordeen et al., 1990).

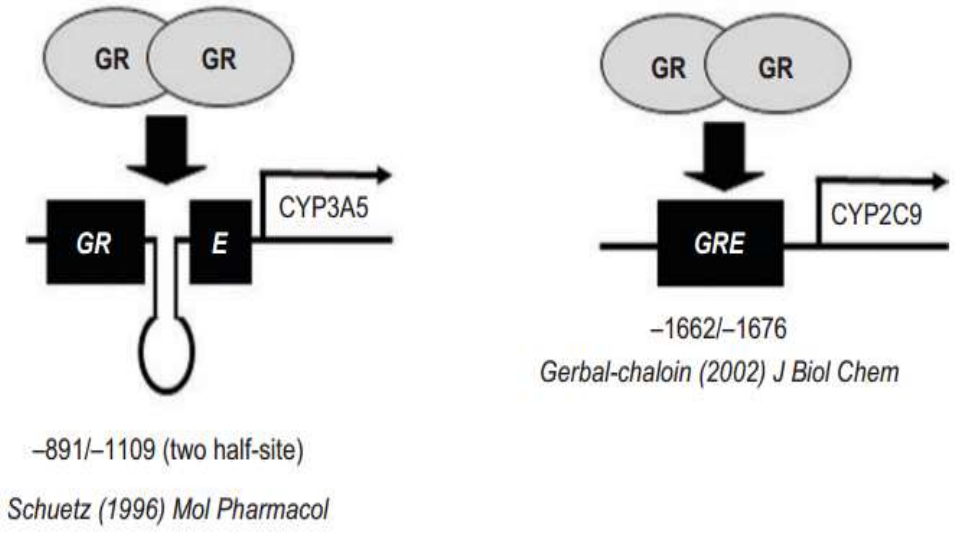

Figure 1.14: Direct binding of GR to gene promoter of CYP3A5 and CYP2C9 Figure taken from Dvorak and Pavek, 2010.

The indirect binding of GR to the gene promoter region of CYP3A4 as an example of CYP drug-metabolising enzymes is shown in Figure 1.15. GR can induce the expression of a gene that does not hold a functional GRE in the promoter region (Dvorak and Pavek, 2010).

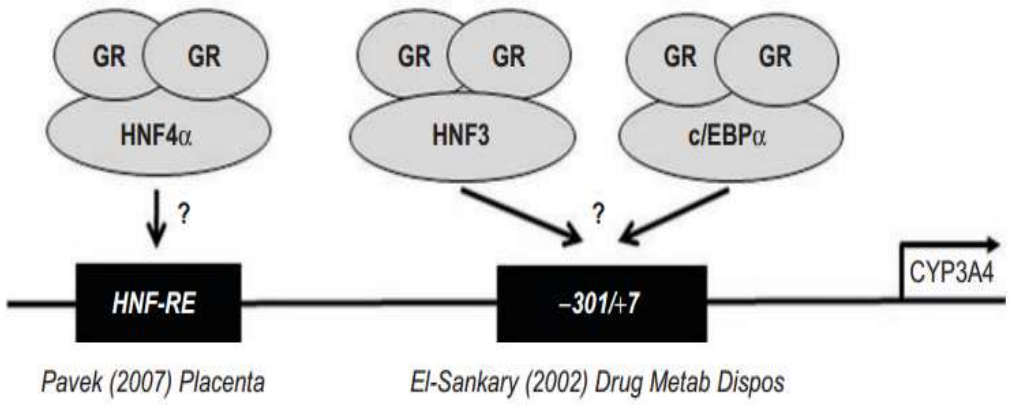

Figure 1.15: Indirect binding of GR to gene promoter of CYP3A4

Different indirect transcriptional mechanisms involved in glucocorticoid receptor-mediated regulation of human drug-metabolizing cytochrome P450 genes

Figure taken from Dvorak and Pavek, 2010.

Multiple GR isoforms can be the result of a single gene and lead to differences in GC signalling. GR subtypes can be affected by various post-translational modifications generating different GC responses and the concentration of the GC used can affect their cellular response (Oakley and Cidlowski, 2011; Oakley and Cidlowski, 2013). GRs can directly or indirectly regulate certain changes in DNA transcription leading to protein production and can act as transcription factors leading to repression or induction of target genes by interaction with GREs. The ability of the ligand-receptor complex to bind to GREs is affected by dissociation of the chaperone proteins and the consecutive phosphorylation, dimerization and nuclear translocation of GR (Buckingham, 2006).

In a study by Kirschke and colleagues, the binding of ligands to GR ligand binding domain (LBD) was monitored by measuring the increase of flurorescence polarization of fluorescin-labelled Dex (F-dex). The binding kinetics of F-dex showed standard single-phase association and dissociation. At equilibrium, the dissociation constant (K_D) was found to be 150 ± 20 nM (Kirschke et al., 2014). The anchorage of GR to the microtubule network and the interaction with heat shock protein 90 (HSP90) facilitates its nuclear translocation. It has been shown

that antagonism of HSP90 reduces the rate of GR nuclear translocation and can be overcome by disrupting the microtubule network (Galigniana et al., 1998; Nishi et al., 1999).

Trebble and colleagues have shown that the absence of the intact microtubule network does not increase the rate of GR translocation in response to Dex, whereas this does occur with non-steroidal glucocorticoid receptor ligands (Trebble et al., 2013).

1.4.1.1 Phosphorylation of GR

GC signalling is a complex process involving a crosstalk between many other regulatory pathways and regulatory processes (Beck et al., 2009). The phosphorylation is a reversible covalent association of a protein with a phosphor group and is regulated by phosphorylating kinases and dephosphorylating phosphatases(Ismaili and Garabedian, 2004). The functions of GR can be regulated by post-translational modifications such as phosphorylation which leads to modifications in the transcriptional activity of GR (Galliher-Beckley and Cidlowski, 2009; Lynch et al., 2010). Although GR can be phosphorylated in the absence of hormone, it is further phosphorylated in conjunction with agonist binding. Hormone-dependent phosphorylation of GR has been suggested to determine target promoter selectivity, cofactor interaction, strength and duration of receptor signalling, and receptor stability, sub-cellular localization and protein-protein interaction (Nicolaides et al., 2010). GR phosphorylation could affect GR-mediated transcription in a promoter-specific manner, so GR phosphorylation may have an important role in hormone signalling (Galliher-Beckley and Cidlowski, 2009). The phosphorylation of GR can be mediated by mitogen protein kinase (MAPK), cyclin-dependent kinase (CDK), glycogen synthase kinase-3 (GSK-3), extracellular-regulated kinase (ERK) and c-Jun N-terminal kinase (JNK). So GC signalling is a complex process involving a crosstalk between many other regulatory pathways and regulatory processes (Beck et al., 2009).

Six serine residues in the human GR have been characterised as phosphorylation targets: serine 113 (S113), S141, S203, S211, and S226, and more recently S404 (Beck et al., 2009) (see Figure 1.16). The kinases implicated in the phosphorylation of GR at S203 are ERK and CDK. Phosphorylated S203 fails to bind GRE-containing promoters because it is in the cytoplasmic fraction of the cell. This suggests that S203 is a transcriptionally inactive form of GR (Wang et al., 2002). On the other hand, the GR is transcriptionally more active when phosphorylated at S211 due to a conformational change and the increased recruitment to GRE-containing promoters which can lead to increased apoptosis in several cell types (Galliher-Beckley and Cidlowski, 2009). Phosphorylation of human GR at S203 and S211 are both mediated by CDK2/cyclin A kinase complexes. The interaction of CDK5 and its activator protein p35 and p25 with the GR LBD can also lead to phosphorylation of human S203 and S211 but this time result in decrease in the transcriptional activation by attenuating GR-cofactor interactions (Beck et al., 2009). S203 and S211 of human GR are phosphorylated to a greater extent in the presence of hormone. The phosphorylation of human GR at S211 has been suggested as a biomarker for activated GR *in vivo* because the transcriptional activity of GR has been found to correlate with this phosphorylation (Wang et al., 2002). Human GR is phosphorylated at S226 by the JNK pathway (Lynch et al., 2010) which can then associate with GRE-containing promoters, but its phosphorylation leads to blunted hormone signalling due to the increased nuclear export of the GR (Galliher-Beckley and Cidlowski, 2009). A conformational change within the human GR is caused by the phosphorylation at S404, which results in altered co-factor recruitment and change in the transcriptional response of GR (Galliher-Beckley and Cidlowski, 2009).

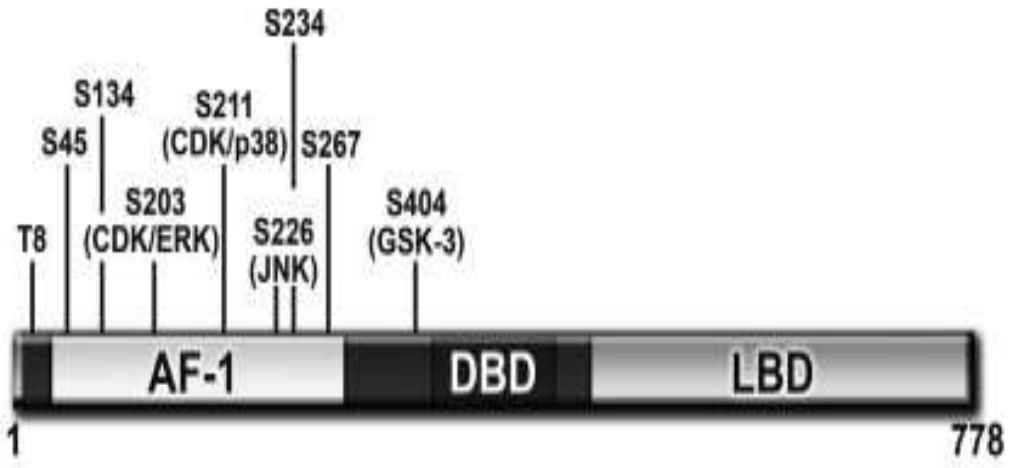

Figure 1.16: Structure of the human GR

Functional domains and phosphorylated residues of human GR are shown. The phosphorylation sites and the kinases implicated in the phosphorylation of different residues are specified.

Figure taken from Galliher-Beckley and Cidlowski, 2009.

Hormone signalling is modulated by the phosphorylation status of GR. Binding of the GC hormone to the GR, causes the translocation of this receptor to the nucleus and DNA binding.

The transcriptional response of the GR can be altered by cell and tissue-specific kinases which can phosphorylate the GR, altering its conformation, DNA binding and co-factor recruitment. This GR phosphorylation can also affect stability and half-life of the protein (Galliher-Beckley and Cidlowski, 2009). So the phosphorylation status of the GR must be taken into account to evaluate the cellular response to GCs. Chen et al. have shown that GR phosphorylation at S211 and S226 can affect receptor transcriptional activation in a gene-specific manner (Chen et al., 2008). It was shown in their study that the regulation can be both positive and negative. The receptor activity is determined by the relative phosphorylation at S211 versus S226, where higher phosphorylation at S211 relative to S226 is correlated to GR nuclear localisation and higher transcriptional activation. The opposite was true when higher phosphorylation at S226 relative to

S211 occurs (Chen et al., 2008). It has been shown that JNK mediated phosphorylation of GR at S226 affects its subcellular localisation when there is withdrawal of the hormone; a condition which favours higher GR phosphorylation at S226 and lower at S211 (Rogatsky et al., 1998; Itoh et al., 2002). Inflammatory conditions and reactive oxygen species have been shown to decrease the total amount of CYPs and inhibit their enzymatic activity, simultaneously producing oxidative stress (Proulx and du Souich, 1995; El-Kadi et al., 2000). A molecular visualisation system has been used to depict the CYP3A4 Thr264, Ser420, and Ser478 residues which can be phosphorylated in rats shown in Figure 1.17 (Wang et al., 2009).

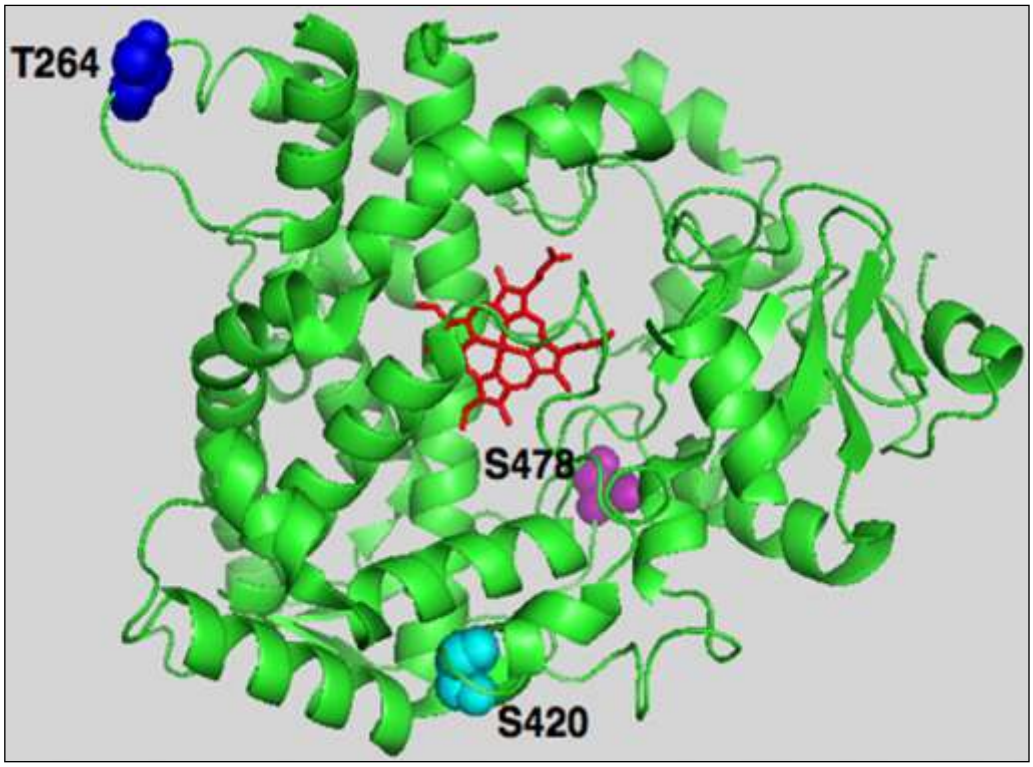

Figure 1.17: Depiction of CYP3A4 residues for phosphorylation in rats

CYP3A4 Thr264 (blue), Ser420 (cyan), and Ser478 (magenta) residues and the prosthetic heme is shown in red.

Figure taken from Wang et al., 2009.

1.4.2 Pregnane-X receptor (PXR) and constitutive androstane receptor (CAR)

Major ligand-activated, NRs such as the pregnane-X receptor (PXR, NR1I2) and the constitutive androstane receptor (CAR, NR1I3) are downstream from the GR making GR the main drug-metabolising enzyme regulator (Pascussi et al., 2003; Plant, 2004; Lim and Huang, 2008). PXR is named so because of its strong interaction with pregnane compounds (Kliewer et al., 1998) and is the most important factor in controlling and co-ordinating the response to xenobiotics with respect to CYP3A genes (Xie et al., 2000; Luo et al., 2002; Song et al., 2004). PXR was first identified in 1998 (Kliewer et al., 1998), by scanning a mouse liver cDNA library for sequences similar to the ligand-binding domain of known NRs. It should be mentioned that as well as PXR binding to the promoter/enhancer of the human CYP2C and CYP3A genes, there are several other NRs such as CAR that can bind to the response elements indicating that there is promiscuity in the specificity of response elements. The regulation of CYP2C9 and CYP3A gene expression is coordinated by an interplay between PXR and CAR (Xie et al., 2000).

The enzymes linked to drug metabolism such as CYP3A, CYP2Cs and MDR1 (P-gp) are targeted by PXR and CAR (Li and Wang, 2010). The distinct and common target genes of CAR, PXR and AhR are shown in Figure 1.18.

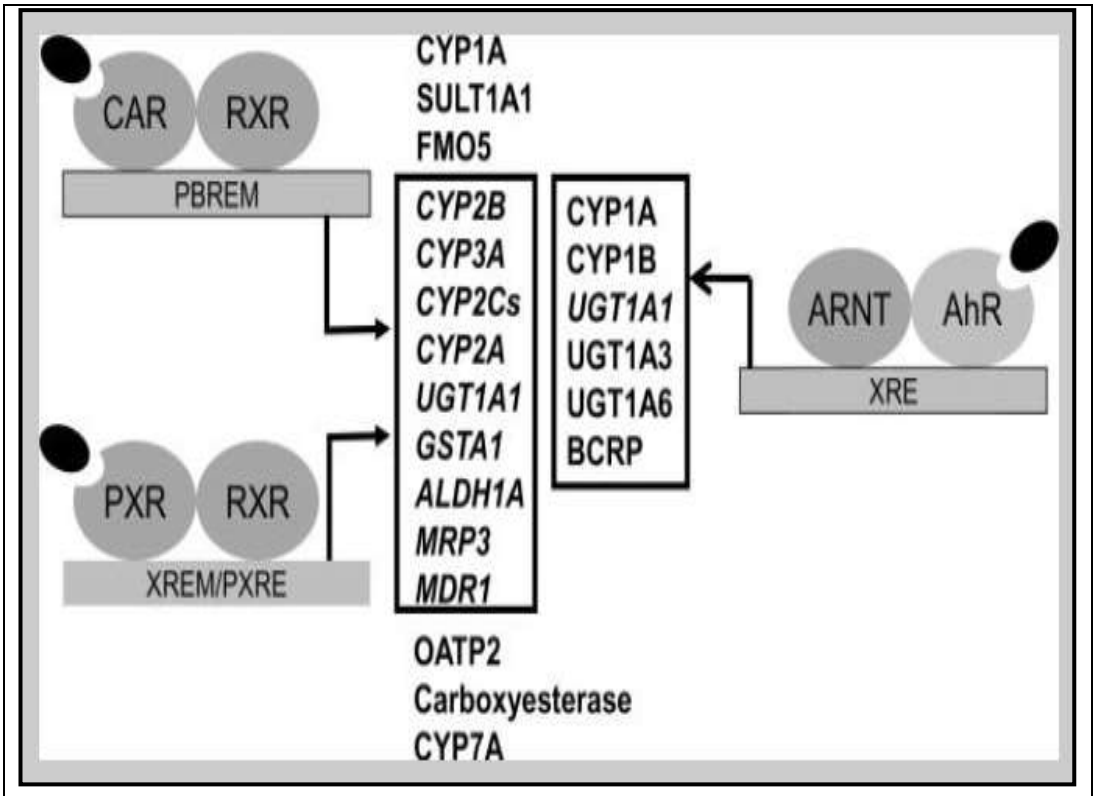

Figure 1.18: Distinct and common target genes of CAR, PXR and AhR

Figure taken from Li and Wang, 2010.

The human PXR gene, mRNA and protein organisation are shown in Figure 1.19. It is located on chromosome 3 with 4446 base pairs and 434 amino acids in isoform-1 which is considered to be the wild-type of three human PXR isoforms (Hustert et al., 2001; Kliewer et al., 2002).

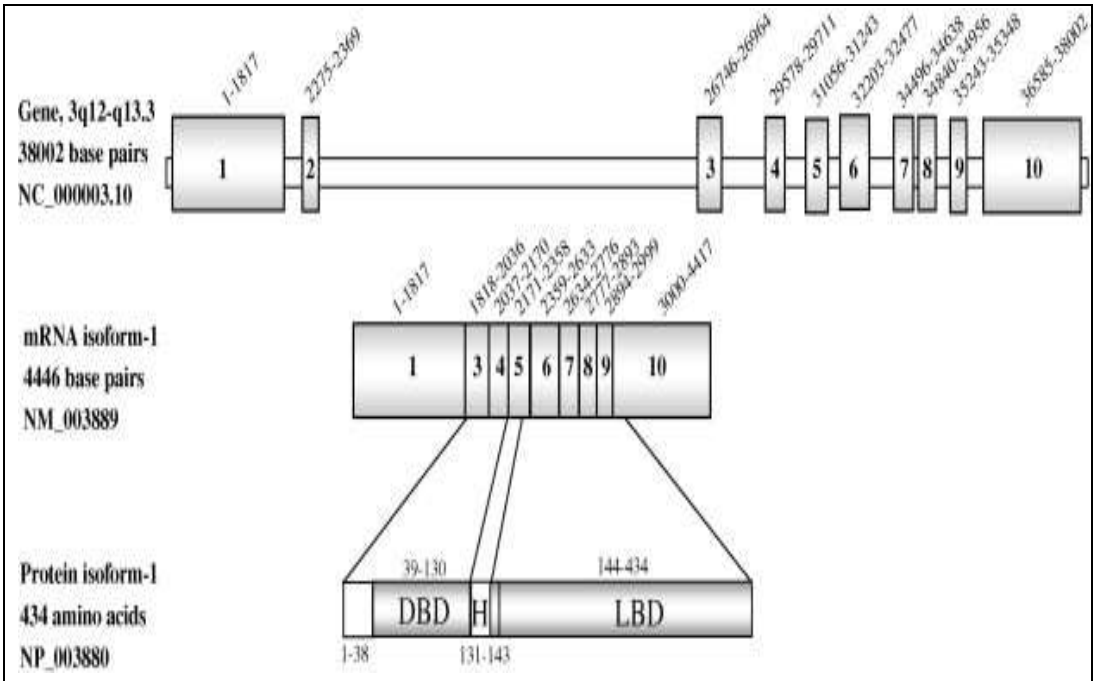

Figure 1.19: Human PXR gene, mRNA and protein organisation

Figure taken from Hustert et al.,2001 and Kliewer et al.,2002.

The human CAR gene, mRNA and protein organisation are shown in Figure 1.20. It is located on chromosome 1 with 1381 base pairs and 348 amino acids in isoform-3 which is considered to be the wild-type of twenty two human PXR isoforms (Auerbach et al., 2003; Savkur et al., 2003).

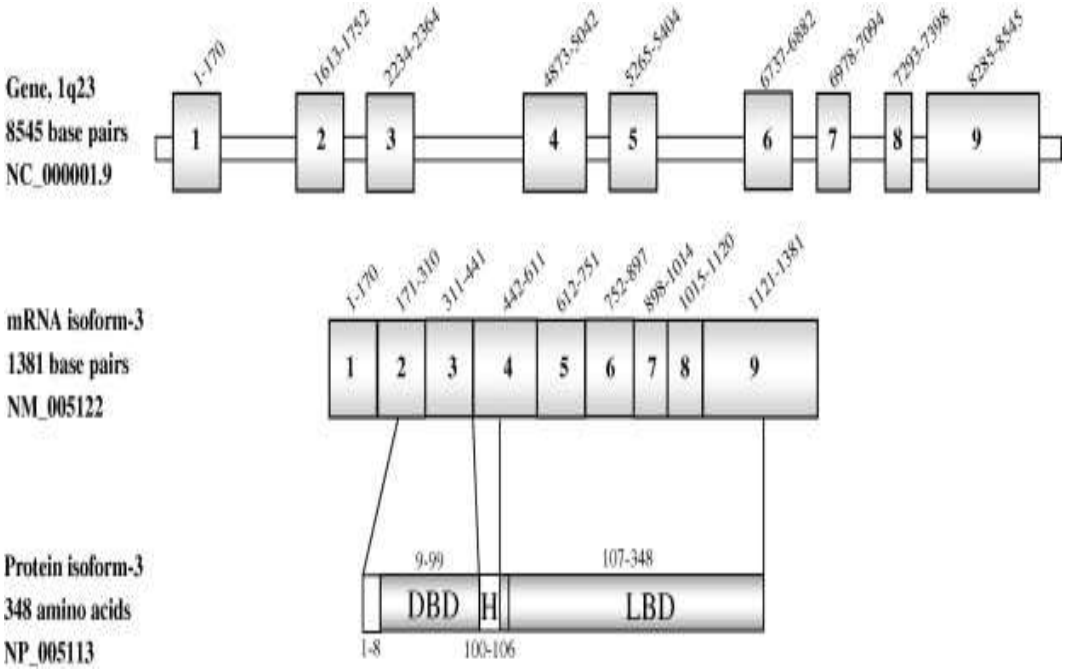

Figure 1.20: Human CAR gene, mRNA and protein organisation

Figure taken from Auerbach et al., 2003 and Savkur et al.,2003.

Recent studies have suggested that the nuclear receptors regulate the expression of each other, adding complexity to these interaction networks (Aouabdi et al., 2006; Gerbal-Chaloin et al., 2006). Delineation of the function of individual components as well as the effects of the whole interaction network will assist in explaining the observed inter-individual variation in CYP3A activity. The minor environmental and genetic changes to different factors in the network may combine to produce the variable expression seen in CYP3A genes (Plant, 2007).

1.4.3 Effect of NRs on CYP3A4/5

The activity of PXR determines the intestinal and hepatic expression of CYP3A4/5. The broad substrate specificity of PXR means that it may be activated by a range of chemical compounds found in the diet as well as many drugs. Some drug interactions are now known to be mediated through the actions of PXR (Lehmann et al., 1998). Several splice variants of PXR have been identified in the human liver and some have been shown to be defective *in vitro*, so PXR splice

variants may play a role in the differential CYP3A4/5 gene expression that has been reported to occur between individuals (Fukuen et al., 2002). However, studies have shown that genetic variants have exceedingly low allelic frequencies and only account for a small proportion of the CYP3A4/5 activity observed *in vivo* (Urquhart et al., 2007). CAR can also activate CYP3A4/5 *in vitro* and *in vivo* (Cai et al., 2002). An increase in the expression of CYP3A4/5 mRNA was seen when human hepatocarcinoma cells, HepG2 were transiently transfected with human CAR. It is likely that a cross-talk between PXR and CAR determines the expression of CYP3A4/5. The removal of PXR expression in transgenic mice has been shown to result in reduced basal expression of CYP3A11, which is the murine orthologue of CYP3A4/5. PXR binds to DNA as a heterodimer with retinoid X receptor alpha (RXRα) and may utilise response elements to form xeno-sensor-mediated pathways (Cai et al., 2002). The exact choice and/or binding efficiency the response elements depend on both the species and the genomic context of the element (Sparfel et al., 2003; Song et al., 2004). Studies on the proximal regulatory PXR response element (PXRE) show that ablation of this site reduces xenobiotic-mediated activation of CYP3A4/5 gene expression (Bombail et al., 2001). Studies have also identified two distal PXREs within the xenobiotic responsive enhancer module *(*XREM). XREM is a 230-bp distal element at -7836 to -7607 of the CYP3A4/5 gene (Goodwin et al., 1999) that appears more important in determining CYP3A4/5 gene expression and activation of its transcription by xenobiotics (Robertson et al., 2003).

The transcriptional regulation of CYP3A4 is shown in Figure 1.21. The two distal enhancer modules constitutive liver enhancer module (CLEM4) and xenobiotic response enhancer module (XREM) are closely located and contain the binding sites for the hepatocyte nuclear factor 4α (HNF4α) and PXR/CAR. The diverse transcriptional networks and interactions between HNF4α and PXR/CAR allow these nuclear receptors to control the CYP3A4 induction by xenobiotics. Enhancement of CYP3A4 gene transcription can be by interaction of the steroid receptor coactivator 1 (SRC-1) and peroxisome proliferators-activated receptor γ co-activator 1α (PGC-1α). In contrast, other nuclear receptors: the small heterodimer partner (SHP) and the chicken ovalbumin upstream promoter

transcription factor (COUP-TF) have a negative effect on the cross-talks (Jover et al., 2009).

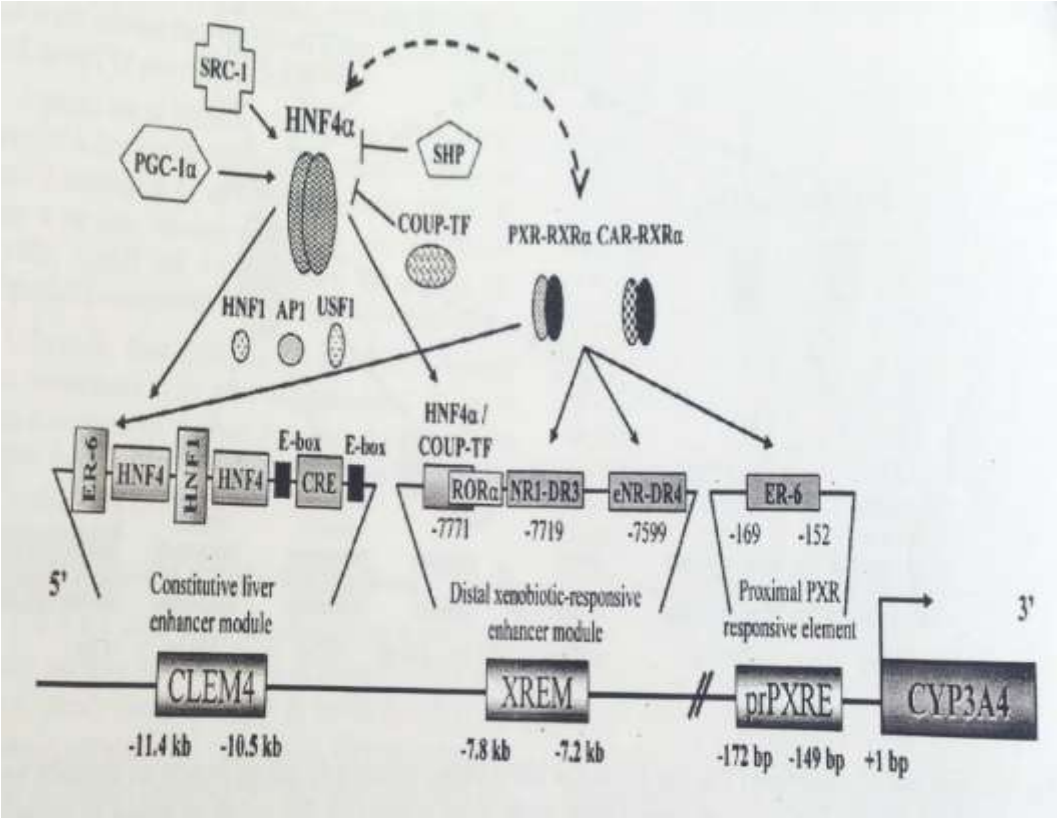

Figure 1.21: Transcriptional regulation of CYP3A4 by the NRs

Figure taken from Jover et al, 2009.

GR may also affect CYP3A4/5 expression. Studies on cultured human hepatocytes have shown that the GR agonist, Dex, induces PXR expression and causes CYP3A4/5 induction. The analysis of PXR-mediated CYP3A4/5 induction showed that the effects of Dex are biphasic. This means that at sub-micromolar concentrations (100nM), Dex triggers the signalling of GR which induces the expression of PXR and CAR, whilst at higher supra-micromolar (10μM) concentrations Dex can activate PXR directly, independently of GR (Pascussi et

al., 2001). The induction of the CAR gene and protein caused at sub-micromolar concentrations of Dex also results in increased CYP3A4/5 expression.

1.4.3.1 Effect of Dex on P-glycoprotein (P-gp)

The biotransformation by intestinal CYP3A4/5 and active efflux of absorbed drug by the a transport protein, P-gp determine the bioavailability of orally administered drugs (Kivisto et al., 2004). They are part of the intestinal defence system protecting the body against xenobiotics, and drugs which are substrates for both of these proteins have low bioavailability following oral administration (Kivisto et al., 2004; Tandon et al., 2006). Dex has been shown to induce the increase in protein levels of P-gp and CYP3A (Jin et al., 2006). The P-gp is encoded by the multidrug-resistance (MDR) gene, with MDR1 and MDR2 being present in the human genome. A study looking at MDR1 and MDR3 present in mice showed that these proteins were increased with Dex treatment of mouse hepatoma cell lines and the induction was found to be dependent on the duration of treatment as well as Dex concentration (Zhao et al., 1993). When HepG2 cells were treated with Dex, MDR1 messenger RNA levels were found to be elevated (Zhao et al., 1993). The immunosuppressive drug cyclosporine is a substrate of both P-gp and CYP3A which influence its oral bioavailability (Jin et al., 2006). The effects of P-gp compared to CYP3A4/5 have been studied *in vitro* and animals (Lin and Yamazaki, 2003; Endres et al., 2006). P-gp and CYP3A have been shown to have extensive overlap of substrates and the simultaneous activity of them means efficient intestinal first-pass metabolism of orally administered drugs (van Waterschoot and Schinkel, 2011).

1.4.4 Effect of NRs on CYP2C9

The nuclear receptors, PXR, CAR and GR, have been implicated in regulating CYP2C9 as well as CYP3A4/5 expression (Duma et al., 2006; Galliher-Beckley and Cidlowski, 2009). GRE and CAR responsive element (RE) have been identified in the regulatory region of the promoter of the CYP2C9 gene suggesting that the induction of CYP2C9 by Dex is GR and CAR mediated (Urquhart et al., 2007). The GRE is at -1697 and the two CAR/PXR-REs identified are at -2898 and -1839 base pairs upstream from the translation start site (Chen et al., 2004).

GR, CAR and PXR, can bind to these sites to mediate the induction of CYP2C9 gene expression by drugs such as rifampicin, phenobarbital, hyperforin, and Dex (Chen et al., 2005). Transcriptional regulation of CYP2C9 by NRs (A) (Jover et al., 2009) and the human CYP2C gene cluster on chromosome 10 (B) (Ioannides, 2008) are shown in Figure 1.22.

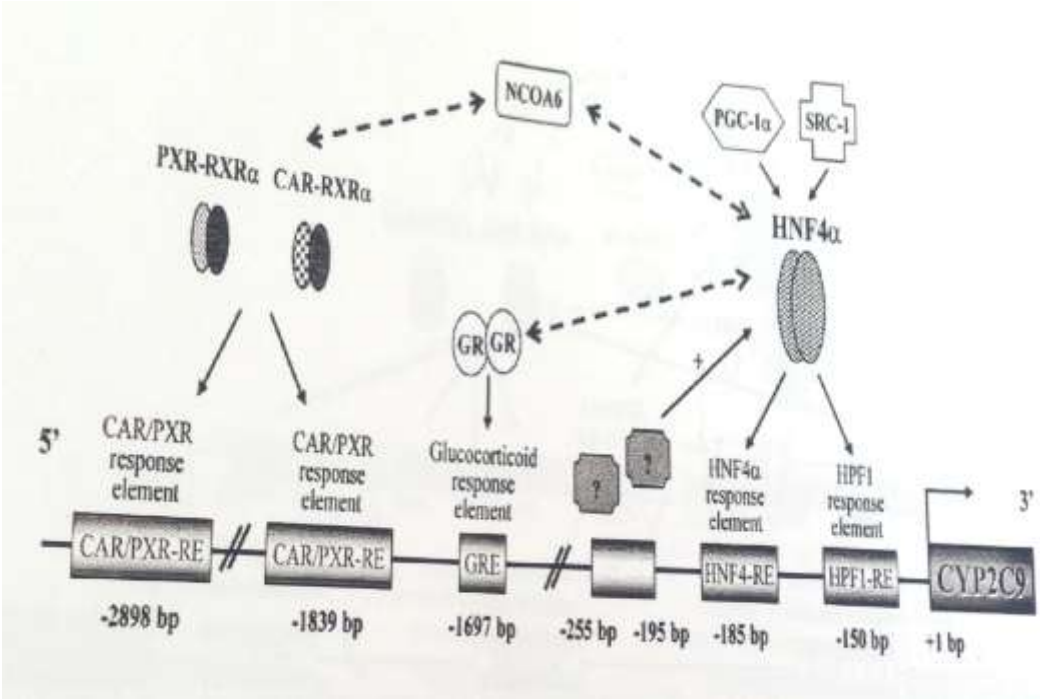

Figure 1.22 (A): Transcriptional regulation of CYP2C9 gene expression by NRs

Figure taken from Jover et al., 2009.

Figure 1.22 (B): Human CYP2C gene cluster on chromosomes 10

Figure taken from Ioannides, 2008.

CAR is responsible for the transcriptional activation of CYP2C9 seen in human primary hepatocytes and HepG2 cells. Drugs such as phenobarbital and artemisinin can act as CAR agonists (Burk et al., 2005; Li and Wang, 2010). Only modest increases are seen in the typical cell-based reporter assays which may be due to CAR accumulating in the nucleus in immortalised cells whereas it is mainly in the cytoplasm in primary hepatocytes and the liver (Maglich et al., 2003). CAR can be active without ligand binding and the drugs already mentioned can cause the nuclear translocation of CAR rather than act as its ligands (Zelko et al., 2001; Jackson et al., 2006). The PXR can also mediate the functions of CYP2C genes by the ligand-binding of drugs such as rifampicin, artemisinin and hyperforin (Burk et al., 2004; Burk et al., 2005). CYP2C9 is transcriptionally controlled by the direct binding of GR to the promoter sequence (see summary Table 1.4(a). CAR and PXR form heterodimers with RXR, while GR forms homodimers which are recognized by specific response elements within the CYP2C promoters (Chen and Goldstein, 2009). It has been found that the induction of CYP2C9 mRNA is obtained in response to sub-micromolar Dex concentration whereas significant activation of PXR by Dex requires supra-micromolar concentrations of greater or more than 10μM. It has been suggested that the CYP2C9 induction observed at 0.1 and 1μM Dex is due to GR activation (Gerbal-Chaloin et al., 2001). As already discussed in the section on the effect of nuclear receptors on CYP3A4/5, this highlights the importance of measuring the Dex concentration and its effects on the nuclear receptors under investigation.

The effects of NR activation by particular drugs metabolised by CYP3A4/5 and CYP2C9 on target gene expression are shown in Table 1.4(a) (Urquhart et al., 2007).

Target Gene	Nuclear Receptor	Nuclear Receptor Ligands	Effect on Target Gene	References
CYP3A4/5	PXR	Rifampicin, clotrimazole, phenytoin, phenobarbital, carbamazepine, dexamethasone, flucloxacillin, artemisinin, nicotine, nifedipine, nicardipine, omeprazole, paclitaxel, topotecan, etoposide	⇧	(Luo et al., 2002) (Pascussi et al., 2005) (Pascussi et al., 2001) (Huwyler et al., 2006) (Burk et al., 2005) (Lamba et al., 2004) (Drocourt et al., 2001) (Raucy et al., 2002a) (Mani et al., 2005) (Schuetz et al., 2002)
		Ritonavir, ketoconazole	⇩	(Pascussi et al., 2005) (Huang et al., 2007a)
	CAR	Artemisinin, Phenobarbital,	⇧	(Burk et al., 2005) (Sueyoshi and Negishi, 2001)
		CITCO		(Ikeda et al., 2005)
	GR	Dexamethasone	⇧	(Pascussi et al., 2000)
CYP2C9	PXR	Hyperforin, rifampicin, nifedipine, nicardipine, dexamethasone	⇧	(Chen et al., 2004) (Drocourt et al., 2001) (Gerbal-Chaloin et al., 2001)
	CAR	Phenobarbital	⇧	(Gerbal-Chaloin et al., 2001)
	GR	Dexamethasone	⇧	(Pascussi et al., 2003)

Table 1.4(a): Effects of NR activation by particular drugs metabolised by CYP3A4/5 and CYP2C9 on target gene expression

Adapted from Urquhart et al., 2007.

The effects of Dex on CYP3A4/5, CYP2C9, PXR, CAR and GR genes are summarised in Table 1.4 (b).

CYP enzyme	PXR/CAR	GR	Dex concentration
Induce CYP3A4/5	Induce both PXR and CAR	Dependent	10^{-7} M
	Induce PXR	Independent	10^{-6} M
Induce CYP2C9	Induce PXR	Dependent	0.1 and 1^{-6} M
	Induce PXR	Independent	10^{-6} M

Table 1.4(b): Effects of Dex concentration on GR dependence and independence as well as CYP3A4/5, CYP2C and PXR/CAR induction.

Table 1.5 displays the nuclear receptors and the expression of the CYP genes (Ioannides, 2008).

Nuclear receptors	*Ligands*	*CYP genes*[a]
CAR	xenobiotics	*CYP2As* ↑, *CYP2Bs* ↑, *CYP2Cs* ↑, *CYP3As* ↑, (*CYP4As* ↑)
PXR	xenobiotics	*CYP2As* ↑, *CYP2Bs* ↑, *CYP2Cs* ↑, *CYP3As* ↑,
	bile acids	*CYP24* ↑, (*CYP4As* ↑)
GR	glucocorticoids	*CYP2Bs* ↑, *CYP2Cs* ↑, *CYP3As* ↑

Table 1.5: NRs and expression of CYP genes

Direct binding of nuclear receptors to the promoter sequences has not been reported for the genes in parentheses.

Table adapted from Ioannides, 2008.

1.5 Glucocorticoids

Glucocorticoids (GCs) promote the conversion of proteins and lipids into glucose during stress-induced activation of the hypothalamic-pituitary-adrenal (HPA) axis thus they have been given this name (Gross and Cidlowski, 2008). GCs induce GR by binding to this ligand-activated receptor. 16mg of the endogenous GC,

cortisol is estimated to be secreted by normal human subjects in 24 hours (Weitzman et al., 1971). Endogenous GCs are steroid hormones produced by the adrenal cortex in human and synthetic GCs can be used as drugs for inhalation, topical application or systemic administration. The latter can be used in the diagnosis and therapy in a number of inflammatory and autoimmune disorders in the clinic (Donato et al., 1995; Pui and Evans, 2006). Various biological processes in the body are regulated by GCs via GR, including immune functions, inflammatory responses, cell proliferation and survival and embryogenesis and behaviour. It has been shown that continued GC action requires cycles of dissociation and association of the ligand to GR which depends on interaction with HSP90 (Stavreva et al., 2004; Conway-Campbell et al., 2011).

The therapeutic efficacies of GCs in treating several chronic inflammatory and autoimmune conditions appear to be caused by the interference of GR with pro-inflammatory pathways by means of various mechanisms. However, they can cause side-effects during high-dose administration and long-term use. GCs can activate both positively or negatively regulate the expression of certain genes. New findings of the molecular mechanisms of GR have initiated a number of drug discovery settings, particularly using dissociated GR-ligands, such as selective GR agonists (SEGRA). SEGRAs are being assessed for use in the clinic soon (Schäcke et al., 2007). These compounds maintain the anti-inflammatory properties of GCs whilst reducing the side effects of long-term usage of the drugs. Compound A is one such SEGRA with a unique dissociation profile of GR ligand which prevents GR dimerization both *in vitro* and *in vivo* (Lesovaya et al., 2015).

1.5.1 Dexamethasone (Dex)

Dex is widely prescribed as a synthetic GC, used as a drug in the treatment of many autoimmune diseases, inflammatory disorders and several cancers (Buckingham, 2006; Inaba and Pui, 2010). It has a long half-life of 36-54h (Singh et al., 1994) and both induces and acts as the substrate for the main drug-metabolising enzymes, CYP3A4/5 and CYP2C9 (Dvorak and Pavek, 2010). Therefore, it is important to consider the effect of this GC on the activity of these drug-metabolising enzymes when co-administering other drugs (Dvorak and

Pavek, 2010). The chemical structures of the endogenous GC, cortisol, and the synthetic GCs, prednisolone and Dex, are presented in Figure 1.23 (Inaba and Pui, 2010).

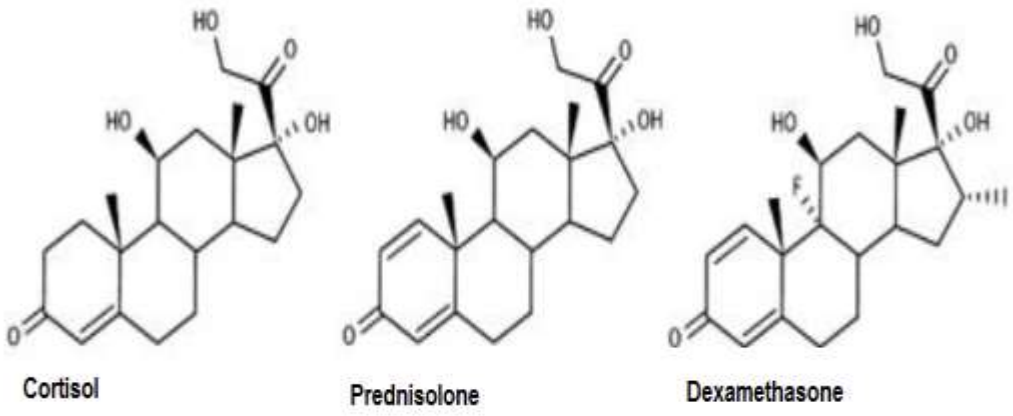

Figure 1.23: Chemical structures of GCs
Adapted from Inaba and Pui, 2010.

The regulation of CYP enzymes by GCs was first discovered in the 1980s in mice and in humans *in vivo* (Watkins et al., 1985) and in cultured rat hepatocytes (Schuetz et al., 1984).

The crystal structure of the LBD of GR complexed with Dex has been solved, making it possible to characterize the anchoring mode of the ligand within the ligand-binding cavity (Bledsoe et al., 2002). In vitro studies have also identified the contacts within the Dex-GR complex that are critical for stabilizing the complex in its active conformation (Lind et al., 2000; Bledsoe et al., 2002).

1.6 Drug-Drug Interactions (DDIs)

Toxicity issues due to chemicals being co-administered in polypharmacy are particularly dangerous and they are common in healthcare today. This can be due to multiple medications taken for complex, life-threatening diseases like cancer (Terstriep and Grothey, 2006), HIV (Sax, 2006), the treatment of multiple, long-term conditions in the elderly (Brager and Sloand, 2005; Chutka et al., 2005) or in

psychiatric patients (Tanaka, 1999; Goodwin and Vieta, 2005). The co-administration of several drugs that are metabolised by the same enzyme in a patient may lead to altered pharmacokinetics in all, some or none of the co-administered drugs. The pharmacokinetic outcome can cause the loss of clinical efficacy or the production of toxicity, which if suspected, are reported in the literature. It is estimated that adverse drug reactions is the fourth largest killer in the Western world. DDI can occur through the activation of gene transcription leading to the activation or inhibition of enzyme action (Fontana et al., 2005; Bachmann, 2006; Ghanbari et al., 2006). A narrow therapeutic index for some drugs can mean drug toxicity due to raised serum levels. DDI are the main cause of ADRs worldwide. ADRs are estimated to cause more than 100,000 deaths in the US and up to 7% of all hospital admissions in the UK and Sweden annually (Ingelman-Sundberg, 2001). Unwanted activation of PXR has been estimated to account for about 60% of the total DDIs (Evans, 2005).

Drugs inducing or inhibiting gene expression and enzymatic activity of different CYP isoforms interfere with their own or co-administered drugs' pharmacological activity and/or toxicity. As CYP enzymes are responsible for most DDIs, it is important to identify the CYPs that metabolise particular drugs and avoid co-administration of drugs metabolised by the same isoenzyme (Ingelman-Sundberg, 2001). Co-administration of two drugs that are metabolised by the same CYP enzyme means they compete for binding to the enzyme's active site, resulting in inhibition of metabolism and elevated plasma levels for one or both of the drugs. Where there is an overlap of substrate specificity by the CYP enzymes, there is high risk of DDIs (Ingelman-Sundberg, 2001; Houston and Galetin, 2008).

1.6.1 Enzyme Induction

Repeated administration of some drugs may induce CYP enzymes by increasing its rate of synthesis or reducing its rate of degradation, but the former scenario is mainly seen (Kalra, 2007). Induction then leads to an increase in the rate of metabolite production and hepatic biotransformation, decreasing drug serum half-life and the time for drug response resulting in pharmacokinetic tolerance to the drug (Xie et al., 2000; Ioannides, 2008). The extent of drug metabolism can be

affected by xenobiotics that activate the transcription and induce the expression of genes that encode drug-metabolising enzymes (Wei et al., 2000; Xie et al., 2000). The drug binds to the ligand-binding domain of the aromatic hydrocarbon (Ah) receptor which is a soluble cytosolic protein. There is conformational change in the receptor as a result of this binding and this facilitates the transportation of this complex to the nucleus by an Ah-receptor nuclear translocator and binds Ah-receptor response elements in the DNA which then induces transcription of the gene (Xie et al., 2000).

CAR regulates the inducible expression of CYP3A and is activated by a range of drugs including antibiotics, barbiturates, etc. PXR is also involved in the induction of CYP3A through a similar mechanism (Yan and Caldwell, 2001; Hasegawa et al., 2011). The CYP1A isoform is induced through the binding of a ligand to the Ah-receptor. CYP is usually induced as a result of increase in gene transcription, however, some non-transcriptional mechanisms have also been reported such as the induction of human CYP2E1 by ethanol and isoniazide which is not transcriptional and CYP2E1 protein accumulation and induction of enzymatic activity arise from protein stabilization or enhanced protein translation (Yan and Caldwell, 2001). HepG2 cells are immortalised hepatocarcinoma cells that have been used in induction studies and are an easier to handle tool compared to primary human hepatocytes in the study of upregulation of CYP enzymes (Yan and Caldwell, 2001; Westerink and Schoonen, 2007). These cells are widely used in drug metabolism and toxicology studies and have low basal expression of CYP enzymes (Vermeir et al., 2005; Chu et al., 2009) which means possible inductions in these enzymes is easier to detect.

1.6.2 Enzyme Inhibition

It is important to identify the isoenzyme that metabolises a particular drug to be able to predict potential DDIs. Inhibition is often specific, e.g. fluoxetine inhibits the metabolism of tricyclic antidepressants like desipramine. The interaction can vary in duration depending on the half-life of the drug. There is a decrease in the rate of hepatic biotransformation of drugs leading to an increase in serum

concentration and toxicity due to enzyme inhibition (McGinnity and Riley, 2001; Fowler and Zhang, 2008). The inhibition of CYP enzymes can be classified into reversible and irreversible inhibition based on enzymatic mechanism.

1.6.2.1 Reversible inhibition

Reversible inhibition is the most common cause of DDIs occurring as a result of direct competition between the substrate and inhibitor for the binding site on CYP enzymes (McGinnity and Riley, 2001; Fowler and Zhang, 2008). This competition can be for the haem prosthetic group or for other regions in the active site. For instance, cimetidine, which is an H2-receptor antagonist used to treat gastric ulcers, contains an imidazole ring which binds in a competitive manner to the H_2 receptor. However, the imidazole ring of cimetidine can also inhibit biotransformation reactions catalysed by CYP3A4/5 by binding to the haem prosthetic group (McGinnity and Riley, 2001). Ketoconazole is another drug containing the imidazole ring and is thought to be a more potent CYP inhibitor than cimetidine because it has stronger hydrophobic interactions (McGinnity and Riley, 2001; Khojasteh et al., 2011).

1.6.2.2 Irreversible inhibition

Irreversible inhibition is caused by reactive metabolites produced from CYP-catalysed reactions. The inhibition of CYP3A by erythromycin is an example of irreversible inhibition resulting from a metabolic intermediate (MI) complex (McGinnity and Riley, 2001; Galetin et al., 2006; Zhou, 2008; VandenBrink and Isoherranen, 2010). N-hydroxylation, N-demethylation and N-oxidation are transformation reactions catalysed by CYP3A which generate a nitroso metabolite that binds tightly to the haem portion of the CYP enzyme forming a stable MI complex. Erythromycin inhibits a number of drug oxidation reactions catalysed by CYP3A4/5 which are important considering that it is a potent antibiotic (Kanamitsu et al., 2000). Erythromycin inhibits the oxidation of terfenadine, cyclosporine and various other drugs *in vitro* (Kenworthy et al., 1999). A study carried out in Dex-treated female rats showed the CYP3A inhibitors, ketoconazole and erythromycin, extensively inhibited the metabolism of midazolam (Kanazu et al., 2004). In another study, the antagonist of GR, azole anti-mycotic

ketoconazole, inhibited the expression of PXR and CAR receptors and their target genes: CYP2B6, CYP2C9, and CYP3A4/5 in primary human hepatocytes (Duret et al., 2006). Ketoconazole and erythromycin are drugs which can be used in the current study to distinguish the inhibition of CYP3A4/5 and CYP2C9 gene expression through their effect(s) on the nuclear receptors from the inhibition of enzymatic activity of these CYPs.

Accumulation of substrates metabolised by CYP3A4/5 can cause serious drug interactions. Drugs that are potent inhibitors of this isoform like erythromycin and ketoconazole can cause increased substrate levels leading to prolonged QT interval (a measurement of the heart's electrical cycle which is dependent on the heart rate) and even death. Grape fruit juice can cause decrease of CYP3A4/5 production in the small intestine (Gertz et al., 2008), possibly increasing the bioavailability of drugs such as felodipine and cyclosporine (Bailey et al., 1998).

Inhibition of CYP2C9 can lead to important DDIs, for example, fluconazole, metronidazole and amiodarone are examples of drugs that can significantly inhibit warfarin metabolism (Rettie et al., 1992; Limdi and Veenstra, 2008). Warfarin is a widely prescribed anticoagulant that is metabolised by CYP2C9, and has a narrow therapeutic index meaning that under-dosing of warfarin increases the risk of thrombosis and its overdose may lead to internal bleeding in the patient. Variations in inter-individual responses to warfarin may be explained by CYP2C9 induction. Inhibition of warfarin metabolism increases prothrombin time (PT), increasing the anticoagulant effect of warfarin. The interaction of amiodarone with warfarin is more serious because amiodarone has a long half-life and the clinical onset of interaction may be delayed by 1 week to 2 months. PT can remain elevated for 1-3 weeks after amiodarone treatment is stopped. Reducing the dose of warfarin by 25% when amiodarone treatment is started can account for this interaction (Rettie et al., 1992; Limdi and Veenstra, 2008).

The up-regulation of CYP gene expression by GR means that anti-GC factors or stimuli would also have negative effects on CYP gene expression. In some studies it has been shown that the pro-inflammatory cytokines interleukin-6 (IL-6) and IL-1β downregulated CAR and PXR, which led to a loss of CYP2 and CYP3 gene

expression in primary human hepatocytes (Assenat et al., 2004). Another study in human hepatocytes showed that CYP2C9 and CYP3A4 responses to inflammation are independently regulated and indicated that this may have an important influence on human drug responses during the various stats of disease (Aitken and Morgan, 2007).

1.6.3 CYP enzymes and reactive oxygen species (ROS)

The microsomal monooxygenase (MMO) system in many cells generate physiologically significant amount of ROS (Zangar et al., 2004). The uncoupling of the P450 catalytic cycle produces ROS which can make changes to cellular macromolecules and lead to several toxic reactions such as lipid peroxidation, protein dysfunction and nucleic acid oxidation (Bondy and Naderi, 1994; Rashba-Step and Cederbaum, 1994; Zhukov and Ingelman-Sundberg, 1999). The auto-regulatory loops have evolved to decrease CYP levels following increase in oxidative stress. There might be faster effects via changes in CYP stability, particularly in CYP3A and CYP2E1 which generate high levels of ROS (Marí and Cederbaum, 2001; Kim et al., 2009). Protein phosphorylation and cell signalling pathways appear to regulate the CYP protein-protein interactions and CYP oxidase activity are shown in Figure 1.24 as a schematic diagram (Zangar et al., 2004).

Xenobiotic inducers such as drugs and phenylalanine hydroxylase can be toxic to the cell by causing P450 uncoupling leading to ROS generation. The inactivation and degradation of P450 is an antioxidant process achieved through conversion of fatty acid hydro peroxide (FAOOH) to a fatty acid radical (FAO) and vice versa. ROS can cause decrease in nuclear factor 1 (NF1) activity and the interaction of aryl hydrocarbon receptor (AhR) through nuclear factor kappa B (NFκB) which lead to a decrease in P450 transcription. Caspase 3 and Cyt. C release can cause cell death. Protection from toxicity is provided by catalase and glutathione S-transferase (GST) activity.

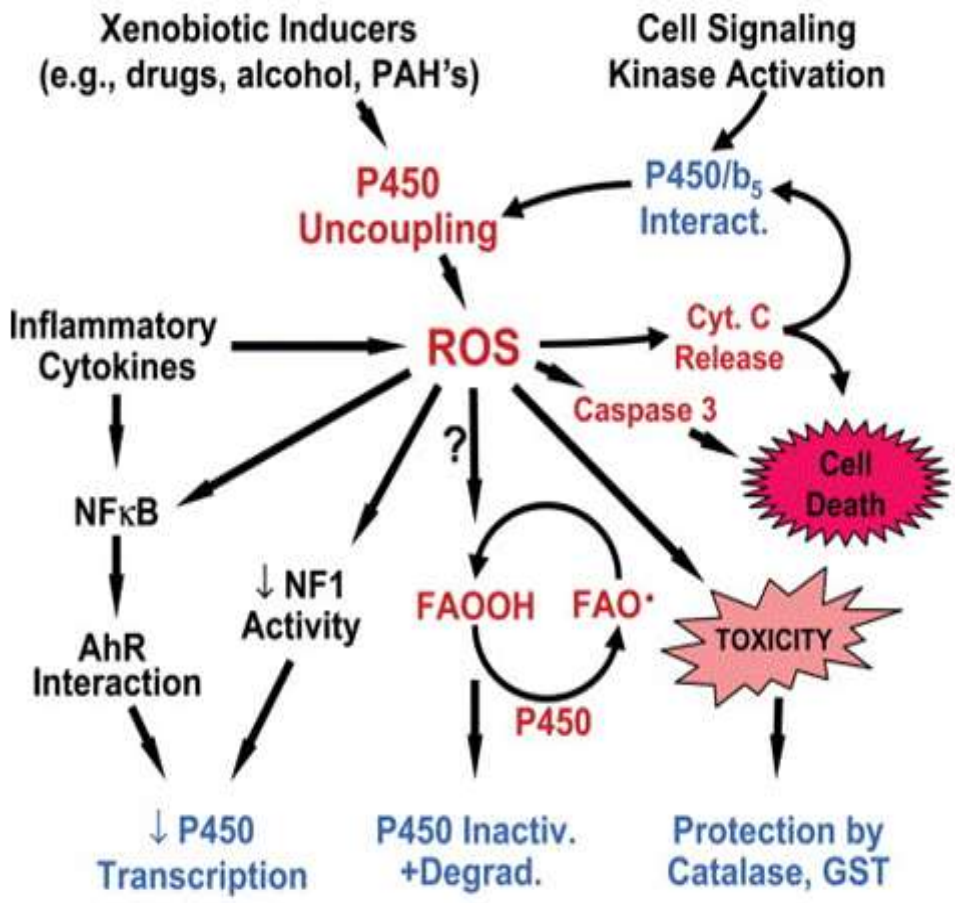

Figure 1.24: The feedback loops that regulate ROS generation by CYP microsomes

The abbreviations have been listed earlier. The steps associated with toxicity are shown in red and antioxidant processes are blue.

Figure taken from Zangar, 2004.

1.7 Mathematical modelling

The DDIs expected after Dex treatment are due to enzyme induction. Empirical models have been used in the past by looking at the external behaviour of the whole system rather than the precise structural connectivity and the functional mechanism. Mechanistic models, on the other hand, can include more specifically the expression characteristics that occur between the administration of the drug and its effect. These specific expressions include target binding and activation, pharmacodynamic interaction, transduction and so on (Danhof et al., 2005). The development of this mechanistic mathematical model would allow the prediction of the influence of synthetic GCs on other drugs metabolised by the CYP3A4/5 and CYP2C9 enzymes and allow extrapolation to *in-vivo* data in humans. Mechanism-based pharmacokinetic-pharmacodynamic (PK-PD) modelling would allow the prediction of drug effects in humans based on information collected in pre-clinical *in-vitro* and *in-vivo* studies. The use of this mechanistic mathematical model in drug development can lead to better predictions of drug efficacy and safety, therefore, reducing the time spent and financial costs in drug discovery (van de Waterbeemd and Gifford, 2003).

The time course of drug response following its administration may be affected by interaction with receptors, enzymes, transporters and possibly other biological molecules. The recent development of many mechanism-based pharmacodynamic models, essentially recognise the non-linear drug-target interaction (Mager et al., 2003). The prediction of drug response has been targeted by generating cellular assays to evaluate the *in vitro* response of cultured cell lines to chemotherapeutic agents. A number of genes and proteins have been recognised as possible predictive markers of drug activity. This may lead for better drug selection and individualised therapy (Robert et al., 2004) . A recent review on idiosyncratic liver injury looked at how this rare and unpredictable injury may occur as a result of drug administration. It may lead to acute liver failure, refusal of marketing authorisation, safety alerts or even withdrawal from the market (Muller, 2007). Studies have shown that the time course of drug effect are often delayed compared to the time course of the system's exposure to it. The delay is often difficult to be accounted for mathematically by using standard pharmacodynamic models. The use of the transit compartment model has been shown to simulate the data more

accurately than the standard pharmacodynamic models (Mager and Jusko, 2001; Lobo and Balthasar, 2002). The period of time between the cause and its effects is the time lag. A series of transit compartments can represent the delayed response profile reflecting the time taken for the drug's initial effect to be translated to the final response. When compared to the lag-time models used in previous studies, the use of the transit compartment model provided better goodness of fit shown by the lower objective function value (OFV) and better fitting graphs to the data (Savic et al., 2007).

A population pharmacokinetic/pharmacodynamic (PK/PD) model developed by Hong and colleagues looks at the effects of four major systemic corticosteroids on lymphocyte trafficking and responsiveness. The immunosuppressive dynamics of these four corticosteroids was captured by the population PK/PD model with the merging of some variability for numerous model components. More variability of the system and dynamic parameters compared to pharmacokinetic parameters allowed improvements in modelling systemic corticosteroid effects (Hong et al., 2007). Newer PK-PD models often account for the basic theories of capacity limitation and the operation of turnover processes to mechanistically model pharmacological effects over a time course. *In silico, in vitro* and preclinical data need to be effectively linked with available models to aid in the discovery and development of new drugs (Mager and Jusko, 2008; Mager et al., 2009).

Since the 1990s, there has been an increase in the development and application of mechanistic PK/PD models to predict the time course of drug response. The major processes determining drug effect are shown in Figure 1.25. Determining factors include the concentration in the central compartment (C_P), biophase distribution (K_{eo}), biophase concentration (C_e), inhibition or stimulation (H) of production (K_{in}) or removal (K_{out}) of the biosignal which results in the response (R).

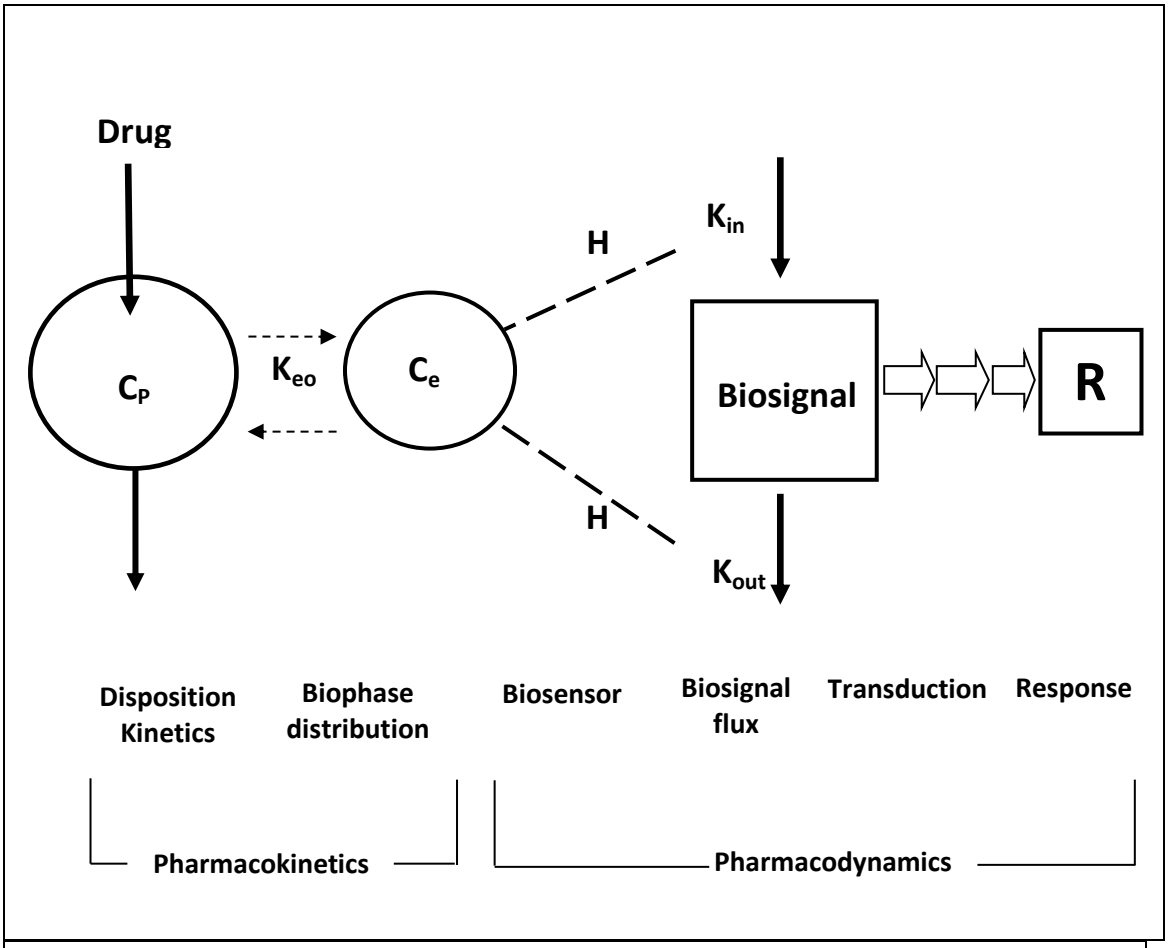

Figure 1.25: Factors influencing drug action

Adapted from Mager and Jusko, 2001.

The model shown in Figure 1.25 is complete from the administration of the drug, its absorption through to the drug response (Mager and Jusko, 2001). However, the model currently looked at in this project is using *in-vitro* data where absorption and distribution of the drug is limited to transport of the drug from the medium to inside the HepG2 cells. At this stage, it is difficult to incorporate the complexities involved in drug absorption which can often affect metabolism.

Time-dependent transduction of the response by the drug is shown in Figure 1.26 (Mager and Jusko, 2001). This model shows the interaction of the free drug (D) with the available receptor (R) which may reversibly or irreversibly form a drug-receptor complex (DR). The intrinsic efficacy of the drug (ε) causes the biologic effector signal (E*) leading to the effect (E) after the transit time (τ).

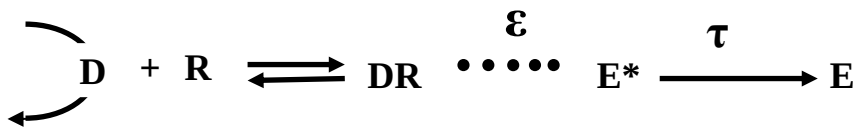

Figure 1.26: Model showing time-dependent transduction of the drug signal Adapted from Mager and Jusko, 2001.

The recently obtained 3D crystal structures of human CYPs have been derived and these allow more accurate prediction of these enzymes' metabolism of certain compounds and direct the process of drug-design (de Groot, 2006). The study of gene network is used in systems biology which essentially integrates experimental data with modelling. A set of computable assumptions represent the model which must be tested against the recognised experimental facts (Kitano, 2002).

Successful implementation of translational PK-PD approach is able to integrate various test platforms during the discovery and development in a mechanistic structure and have an important role in the efficiency and success of pharmaceutical research (Musante et al., 2002; Agoram et al., 2007). The main cause of slow speed in the drug development process is toxicity, which is mainly found pre-clinically in new molecular technologies and the established use of rodent toxicology studies (Balant and Gex-Fabry, 2000; Kramer et al., 2007).

A similar study to the present one was conducted by Chen and colleagues where quantitative models to study c-Jun, Bim and Erg signalling and their interactions with GR were used to form Ordinary Differential Equation (ODE) models (Chen et al., 2012).

Hazra and colleagues evaluated the effect of methylprednisolone on receptor/gene mediated events in rats. Significant down regulation in GR mRNA, followed by a delayed rebound phase was described in a mechanistic pharmacokinetic/pharmacodynamic model showing the interplay of exogenous and endogenous corticosteroid effects on hepatic GR mRNA and cytosolic free

GR in normal rats (Hazra et al., 2007a; Hazra et al., 2007b). Sukumaran and co-workers later developed a mechanism–based model to describe the effect of methylprednisolone on the pharmacodynamics of GR in rats. This study obtained parameter values for GR mRNA expression and the receptor dynamics shown in Table 1.6 (Sukumaran et al., 2011). CV% is the percentage coefficient of variation.

Parameter values for GR mRNA expression and receptor dynamics

Parameter	Definition	Estimate	CV%
$a_{0,GRm}$	Fourier coefficient for GR mRNA	2215.9	Fixed
$a_{1,GRm}$	Fourier coefficient for GR mRNA	−273.2	Fixed
$a_{2,GRm}$	Fourier coefficient for GR mRNA	65.91	Fixed
$b_{1,GRm}$	Fourier coefficient for GR mRNA	−10.86	Fixed
$b_{2,GRm}$	Fourier coefficient for GR mRNA	10.08	Fixed
$k_{d,GRm}$ (h^{-1})	Loss rate for GR mRNA	0.3117	26.12
$IC_{50,GRm}$ (nM)	Inhibition of GR mRNA production	15.6	Fixed
$k_{d,GR}$ (h^{-1})	Loss rate for GR	0.05	Fixed
$k_{s,GR}$ $(nM/h)(mol/ng)^{-1}$	Production rate for GR	0.00196	30.78
k_{on} ($nM^{-1} \cdot h^{-1}$)	Association constant	0.016	Fixed
f_{mpl}	Fraction unbound of MPL	0.23	Fixed
k_{re} (h^{-1})	Loss rate constant for DR_n	1.31	Fixed
R_f	Recycling factor for DR_n	0.93	Fixed
k_t (h^{-1})	Translocation rate for DR	58.2	Fixed
$GR_m(0)$ (mol/ng)	GR mRNA initial concentration (control)	2050	Fixed
$GR_{m,mpl}(0)$ (mol/ng)	GR mRNA initial concentration (drug treatment)	2200	Fixed
$R(0)$ (nM)	Free GR initial concentration	86.15	30.78
$DR(0)$ (nM)	DR initial concentration	0	Fixed
$DR_n(0)$ (nM)	DR_n initial concentration	0	Fixed

Table 1.6: GR and receptor dynamic parameters

Table taken from Sukumaran et al., 2011.

The researchers considered the influence of circadian rhythms and the glucose/free fatty acid/insulin system in white adipose tissue in the rat. In their study, GR mRNA was measured alongside other data to form a 2-comparment pharmacokinetic model and biphasic pharmacodynamic profiles for this GC (Sukumaran et al., 2011).

A dynamic model of the induction of the genes and proteins in the GR signalling pathway has been developed by Chen and colleagues (Chen et al., 2010). The simulations obtained by this model are in agreement with the experimental data and help in understanding GR function. Some of the data measured in these studies were used in modelling the experimental data obtained in the current study.

Chapter 2: Aims and hypothesis

2.1 Aims

The overall aim of this project was to develop a mechanistic mathematical model based on laboratory data (mRNA, protein, ROS and enzymatic activity levels of CYP3A4/5 and CYP2C9) obtained from Dex treated human hepatocytes, HepG2 cells.

The mathematical model can find application in the prediction of drug response, metabolic rate and drug-drug interactions caused by differences in gene expression and enzymatic activity of these phase I drug metabolising enzymes. This study will take into account several factors affected by Dex such as GR, PXR and CAR, and posttranslational modifications such as GR phosphorylation, as well as monitoring the influence of Dex on the efflux transporter, P-gp.

The model can allow the prediction of changes in the metabolic rate of other drugs metabolized by the CYP3A4/5 and CYP2C9 enzymes and permit adjustment of the drug-dose during short-term or chronic use of Dex in combination with other drug therapies. This adjustment can reduce the toxicity of drugs interacting with GCs, thus optimizing and personalizing therapy. As such, this model will be useful for both the clinic and the pharmaceutical industry to select the lead GC with the higher potential to reach the market.

2.2 Hypothesis

The hypothesis of this project was that in Dex-treated hepatocytes GR, PXR and CAR mediated changes in CYP2C9 and CYP3A4/5 gene expression coinciding with changes in CYP2C9 and CYP3A4/5 enzymes' mRNA, protein, ROS and enzymatic activity levels thereby affecting the pharmacological window and thus the therapeutic activity of drugs metabolized by these two enzymes during chronic use of Dex.

2.3 Mathematical models

The parameters used to make this mathematical model were mRNA levels measured by qRT-PCR, protein levels determined by western blots, ROS assays estimated by flow cytometry and enzymatic activity assessed using the P450-Glo luminogenic assays for CYP3A4/5 and CYP2C9 after treatment with Dex; these are displayed in Figure 2.1. The rate of change of these four parameters in HepG2 cells were used to form mechanistic mathematical models using the MATLAB software.

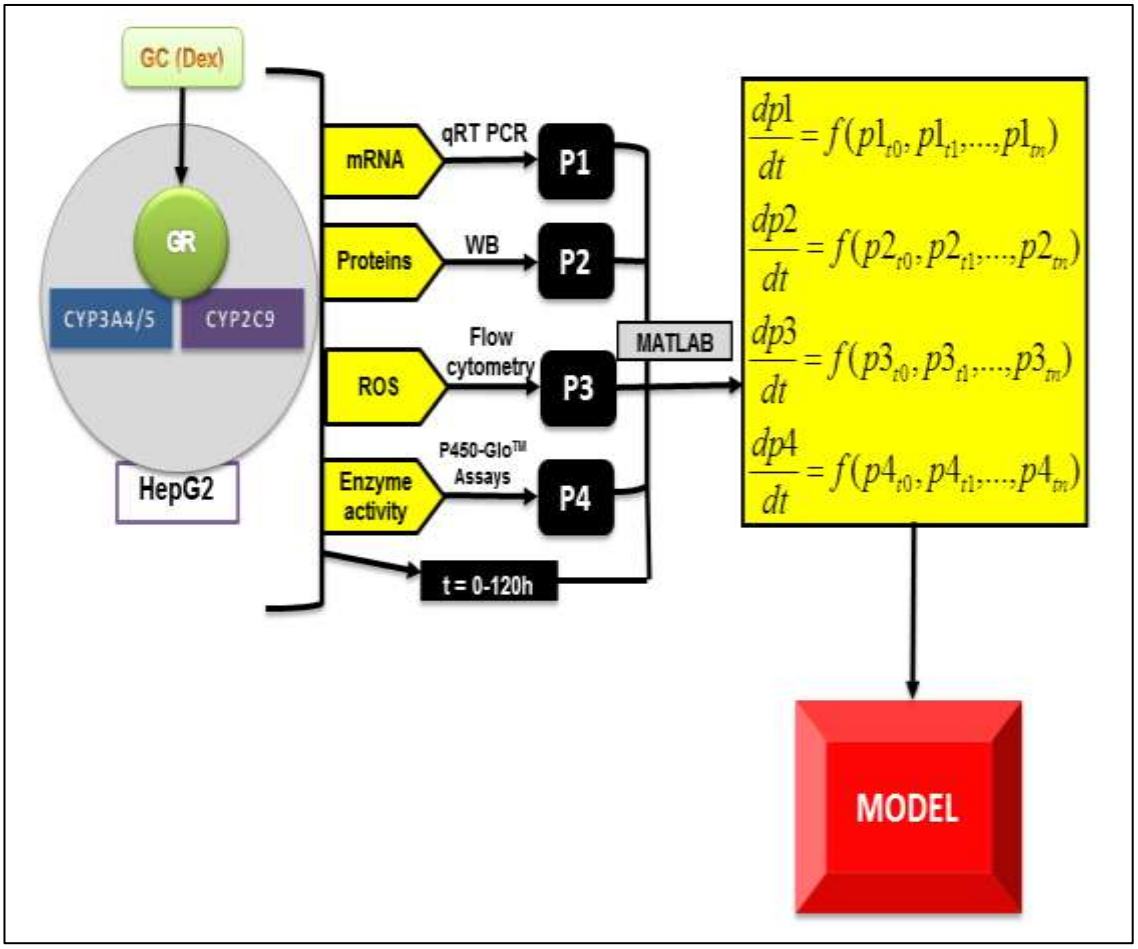

Figure 2.1: Parameters used to form the mathematical model

Chapter 3: Materials and Methods

3.1 Materials

3.1.1 Chemicals

The chemicals and reagents used in this study and their suppliers are listed in Table 3.1.

Materials used	Supplier	Product code
2-Mercaptoethanol	Sigma, UK	M3148
Acrylamide	Sigma, UK	A6050
Ammonium per sulphate (APS)	Flowgen, UK	H17423
Chemiluminescent substrate (ECL reagent)	Chembio Ltd, Hertforshire, UK	16031
ColorPlus Prestained Protein Ladder	New England Biolabs, UK	P7711
Cryovials	Scientific laboratory supplies, UK	G122263
Dichlorodihydrofluorescein diacetate (H_2DCF-DA)	Invitrogen, Paisley, UK	D-399
Diclofenac	Sigma-Aldrich, Madrid, Spain	-
Dexamethasone (Dex)	Sigma-Aldrich, UK	D1756
Dexamethasone (water-soluble)	Sigma-Aldrich, UK	D2915
Dimethylsulphoxide (DMSO)	Sigma-Aldrich, UK	D8418
Dithiothreitol (DTT)	Sigma-Aldrich, UK	D0632
Ethanol absolute	Fisher, UK	E/0600/05
Ethylene diamine tetra acetatic acid (EDTA)	Sigma-Aldrich, UK	EDS
Gel loading tips	Star labs, UK.	I1010-3000
Glycerol	VWR BDH Prolabo, UK	24387.361

Materials used	Supplier	Product code
HEPES	Sigma-Aldrich, UK	H-4034
4′-Hydroxydiclofenac	Ultrafine, Manchester, UK	-
1′-Hydroxymidazolam	Ultrafine, Manchester, UK	-
4-hydroxytolbutamide	Toronto Chemical Research, Toronto, Canada	-
Immobilon-P PVDF membrane	Millipore, MA, USA	IPVH00010
Ketoconazole	Sigma-Aldrich, Dorset, UK	K1003
Isopropanol	Fisher, UK	P/7490/15
Methanol	Fisher, UK	BPE1105-1
Midazolam	Ultrafine, Manchester, UK	-
Nonidet P-40 (NP-40)	VWR BDH Prolabo, UK	A2239.0100
Phenylmethylsulphonylfluoride (PMSF)	Sigma-Aldrich, UK	P7626
Polyvinylidene Difluoride (PVDF) membrane	Millipore, UK	IPVH00010
Sodium acetate 3 hydrate	VWR BDH Prolabo, UK	27652.298
Sodium butyrate	Sigma, UK	B5887
Sodium carbonate	VWR BDH Prolabo, UK	27766.292
Sodium chloride	Fisher, UK	BPE358-1
Sodium dihydrogen phosphate	Fisher, UK	S/4480/60
Sodium dodecyl sulphate (SDS)	Fisher, UK	S/P530/48

Materials used	Supplier	Product code
Sodium hydroxide	VWR BDH Prolabo, UK	28244.262
Sodium hydrogen carbonate	VWR BDH Prolabo, UK	27778.293
Sodium orthovandate	Sigma-Aldrich, UK	S6508
Sodium pyrophosphate	Sigma-Aldrich, UK	221368
Sulfaphenazole	Santa Cruz Biotechnology, Germany	sc-215926
SYBR Green I	Sigma-Aldrich, UK	S9430
Tetra methyl ethylene diamine (TEMED)	VWR BDH Prolabo, UK	443083G
Tris base	Fisher, UK	BPE152-1
Triton X100	Sigma-Aldrich, UK	T8787
Tween 20	Sigma-Aldrich, UK	P9416
X-Ray film Rx	Fuji Films, UK	Super Rx

Table 3.1: Chemicals and reagents used in this study

3.1.2 Biological materials

The cell culture media and other biological materials used in this study are listed in Table 3.2.

Materials used	Supplier	Product code
Dextran Coated Charcoal treated FBS (DCC FBS) was purchased from Hyclone	Hyclone, USA	SH30068.03HI
Dissociation buffer	Gibco, UK	13151-014
Dulbecco's Modified Eagle's Medium (DMEM)	Sigma-Aldrich, UK	D5796
Dulbecco's Modified Eagle's Medium (DMEM) without phenol red and L-glutamine	Sigma-Aldrich, UK	D1145
Foetal calf serum (FCS)	Gibco	10500
Penicillin/Streptomycin	Sigma, UK	DE17-602E
Trypsin with EDTA	Sigma-Aldrich, UK	T3924

Table 3.2: Media and other biological materials

3.1.3 Antibodies and assays used

The antibodies and kits used in this study and their supplier details are listed in Table 3.3.

Materials used	Supplier	Product code	Dilution
β-actin antibody	Abcam, UK	ab8227	1:5000
CAR1/2 (M-127)	Santa Cruz Biotechnology, UK	sc-13065	1:500
CYP2C9	Abcam, UK	ab4236	1:1000
CYP3A4/5 (HL3)	Santa Cruz Biotechnology, UK	sc-53850	1:2000
ECL mouse IgG (Secondary antibody)	Amersham Biosciences, UK	NA931	1:5000
ECL Rabbit IgG (Secondary antibody)	Amersham Biosciences (UK)	NXA931	1:5000
Glucocorticoid receptor antibody (M-20)	Santa Cruz Biotechnology, UK	sc-1004	1:500
Mdr-1 (D-11)	Santa Cruz Biotechnology, UK	sc-55510	1:250
P450-Glo CYP2C9 Assay (Luciferin-H)	Promega, Madison, USA	V8791/2	-
P450-Glo CYP3A4/5 Assay (Luciferin-IPA)	Promega, Madison, USA	V9001/2	-
Phospho-Glucocorticoid Receptor (Ser211) Antibody	Cell Signalling, USA	4161S	1:1000
PXR (H-160)	Santa Cruz Biotechnology, UK	sc-25381	1:250

Table 3.3: Antibodies and assays used

3.1.4 Buffers and general solutions

All the buffers and general solutions used in this study and their ingredients are listed in Table 3.4.

Solution	Ingredients
10% APS	Ammonium persulphate in H20
Blocking solution (western)	5% Milk in PBS 0.1% Tween-20
10x Running buffer (western)	25mM Tris, 190mM Glycine, 35mM SDS
10% SDS	SDS powder in H2O
3X SDS sample buffer	187mM Tris base, 30% Glycerol, 6% SDS, 15% 2-mercapto ethanol, 0.01% bromophenol blue.
Stripping buffer	100mM 2-Mercaptoethanol, 2% SDS, 62.5mM Tris-HCl pH 6.7
Western transfer buffer	25mM Tris, 192mM Glycine, 15% Methanol

Table 3.4: Buffers and general solutions

3.2 Cell Culture

The cell line used was HepG2 cells that were originally derived from human hepatocarcinoma of a 15-year old Caucasian male. These cells are commonly used as a model for the human liver. The HepG2 cells were obtained from the European Cell Culture Collection (ECACC no. 85011430, Salisbury, UK). The medium used to grow the cells was Dulbecco's Modified Eagle's Medium (DMEM) supplemented with 10% foetal bovine serum and 0.5% penicillin and streptomycin (Cambrex, NJ, USA) in 75 cm^2 tissue culture flasks (Fisher, UK). The cells (passages 19-25) were grown in a humidified atmosphere of 5% CO_2 at 37°C. The medium was changed twice weekly and the cell monolayers were split with 0.05% trypsin/0.02% EDTA when they reached more than 80% confluence. The cells were treated with 0.1 µM Dex (Sigma, MO, USA) at indicated time points (0, 2, 6, 24, 48 and 120 h). The low concentration of Dex was decided based on reports which have indicated that 0.1 µM of this hormone is sufficient to induce GR transcriptional activity (Sommer et al., 2007; Lynch et al., 2010). The higher 1.5 mM Dex concentration was determined to be used by conducting

mRNA experiments of 3A4 and 2C9 enzymes between 0.00015 and 15 mM Dex concentration, noting the higher concentrations used in rat studies to develop models (Sukumaran et al., 2011; Li et al., 2012).

24 hours before treatment with Dex the media was changed to DMEM supplemented with 10% charcoal stripped foetal bovine serum so that any endogenous steroid hormones present in the untreated foetal bovine serum (FBS) would not influence the results. During treatment, the media was changed and Dex added again every 24 h to allow the assumption that the Dex concentration was constant throughout the experiments.

3.2.1 Cell counting

The cells were counted before the start of each experiment. The bright line haemocytometer used for cells counting was obtained from Hausser Scientific, USA. The haemocytometer used for cell counting is shown in Figure 3.1 with the equation for counting the cells.

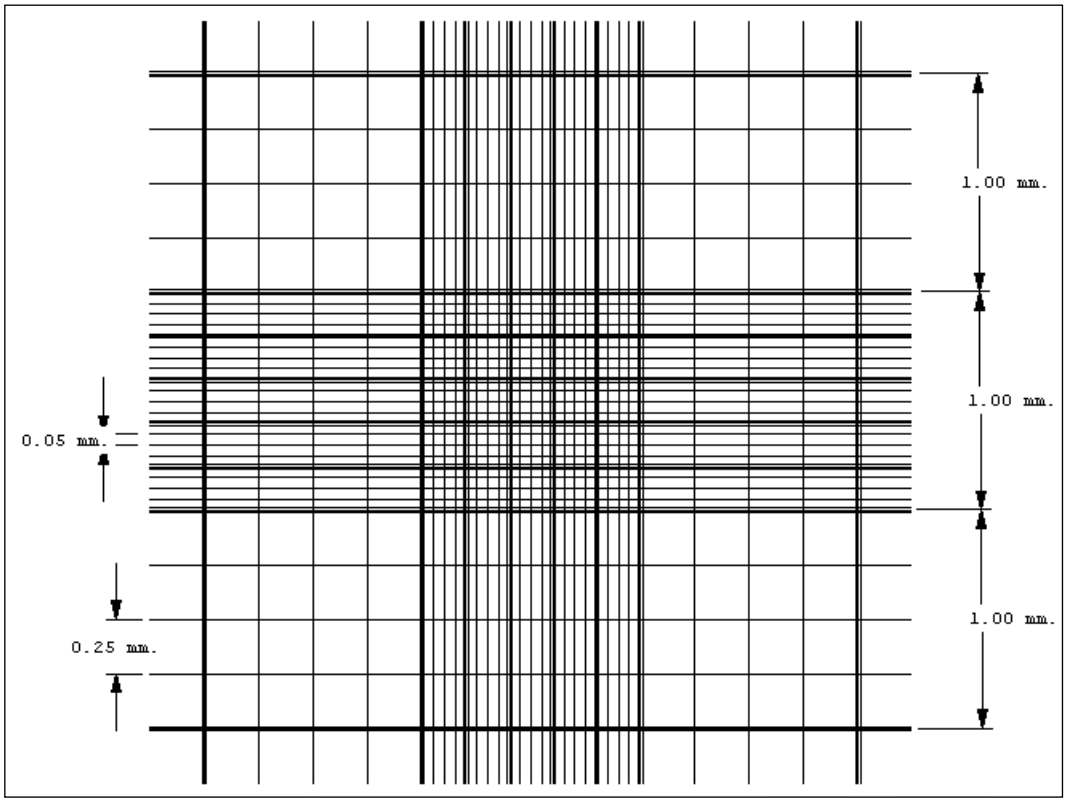

Figure 3.1: Haemocytometer for cell counting

Haemocytometer Figure taken from the Hausser Scientific website (HausserScientific, 2015).

Viable Cell Count (live cells per millilitre) =

$$\frac{\text{Number Live Cells Counted}}{\text{Number of large corner Squares counted}} \times \text{Dilution} \times 10{,}000$$

3.2.2 Protein levels

3.2.2.1 Preparation of cellular extracts

The cells were washed twice with cold PBS to remove traces of serum. 300 µl of high salt lysis buffer (400 mM NaCl, 45 mM HEPES pH7.5, 1 mM EDTA, 10% glycerol, 0.5% NP-40, 1 M DTT, 100 mM PMSF, protease inhibitor mixture including 1 µg/ml aprotinin, 1 µg/ml leupeptin, 1 µg/ml pepstatin, 20 mM b-

glycerophosphate, 5 mM sodium pyrophosphate and 2 mM sodium orthovanadate and dH2O) was then added. The cells were scraped off the petri dishes and put in 1.5 ml eppendorf tubes. The samples were rotated at 4ºC for 20 min and centrifuged at 13000 rpm for 15 min in a microcentrifuge at 4ºC. The pellet was then discarded and the supernatant containing the proteins was stored at -70°C.

3.2.2.2 Determination of protein concentration

The concentration of proteins in the samples was determined using Bio-Rad protein assay (Bio-Rad laboratories, Munich, Germany). This uses the Bradford method (Bradford, 1976) to quantify the proteins extracted. The Coomassie Brilliant Blue dye used in this assay binds to protein to give changes in colour reflecting the protein concentration. 800 µl of dH_2O and 200 µl of Bio-Rad solution had 2 µl of samples added in a cuvette and mixed thoroughly. The colour was allowed to develop for 2 mins and the absorbance was then measured at a wavelength of 595 nm using the spectrophotometer (WPA UV 1101 Biotech Photometer, Cambridge, UK). The blank used to calibrate the machine contained only dH_2O and Bio-Rad solution without any protein sample. The absorbance readings for the samples were used to calculate the relative concentrations for Dex treated and untreated cells with the lowest concentration in each group being used as a maximum of 20 µl sample with 10 µl 3x SDS.

3.2.2.3 SDS-PAGE and Western blot (Immunoblot)

The proteins under study were separated according to size using polyacrylamide gel electrophoresis (PAGE). The 7.5% gel was used for the proteins with larger molecular weight and the 10% gel was found to be more suitable to study the lower range of proteins (Table 3.5).

Western blots are usually used to determine the purity and molecular weight of a protein. It was used on the samples of various experiments to determine the presence of a specific protein in the samples. The specific antibody for the protein of interest is added in this analysis to bind to the particular protein present in small amounts.

The enzyme-linked immunosorbent assay (ELISA) is used to detect the presence of an antibody or an antigen in a sample. In ELISA an unknown amount of

antigen is affixed to a surface, and then a specific antibody is washed over the surface so that it can bind to the antigen. This antibody is linked to an enzyme, and in the final step a substance is added that the enzyme can convert to some detectable signal.

In comparison with ELISA, performing western blots have higher specificity and are more independent of the specificity of the antibodies. Western blot method is also less likely to give false positive results (Schmitt et al., 2005).

Solutions	**7.5% Resolving Gel**	**10% Resolving Gel**	**Stacking Gel**
H_2O	13.3 ml	10.94 ml	6.73 ml
30% Acrylamide	7 ml	9.33 ml	1.67 ml
1.5M Tris pH 8.95	7 ml	7 ml	-
1.0M Tris pH 6.95	-	-	1.25 ml
0.2M EDTA	0.28 ml	0.28 ml	100 µl
10% SDS	0.28 ml	0.28 ml	100 µl
10% APS	157 µl	157 µl	100 µl
TEMED	17 µl	17 µl	10 µl

Table 3.5: Ingredients used to make different percentage resolving gels and the stacker for 3 gels

3.2.2.4 Preparation of samples

Proteins in the supernatant were diluted with 3x sample buffer (1 M Tris at pH 6.95, 10% SDS, 60% sucrose, 0.001% bromophenol blue, 0.2M EDTA, water) depending on the protein concentration determined earlier. The proteins were then

denatured by boiling the samples for 3 min. A short spin in the centrifuge allowed the sample contents to remix before being loaded on to the gel.

3.2.2.5 Casting the gel

The resolving gel was poured inside the gel cassette up to the comb line and was covered with water and cling film to prevent evaporation. After 1 hour, the resolving gel was polymerised and the water was poured off. The stacking gel was then added and the comb was inserted immediately. The stacker was allowed to set and the comb was removed carefully once set.

3.2.2.6 Loading the samples

The gel was placed in tank buffer and up to 30µl samples were loaded in adjacent wells. This was run at 80V for the samples to pass the stacker, then increased to 1 hour at 110V to allow stacking and separation of the proteins. A pre-stained protein ladder was run alongside the samples to help determine the protein sizes and ensure correct transfer later.

3.2.2.7 Transfer

The proteins needed to be accessible to antibody detection, so they were electrophoretically transferred from within the gel to transferred to PVDF membrane. This involved the assembly of the transfer sandwich consisting of 2 sponges, 2 blotting papers, the PVDF membrane and the gel in the centre. The membrane was soaked in methanol and then in transfer buffer. The sponges were also soaked in transfer buffer for 10 min before use. The transfer sandwich was made in a cassette and inserted into the transfer apparatus with the membrane side facing the anode electrode as shown in Figure 3.2. An ice block was also inserted in the apparatus and it was left to run on a stir plate at 0.4 amps for 2 hours. The cooling and stirring processes allowed a homogenous low temperature to be maintained in the transfer apparatus.

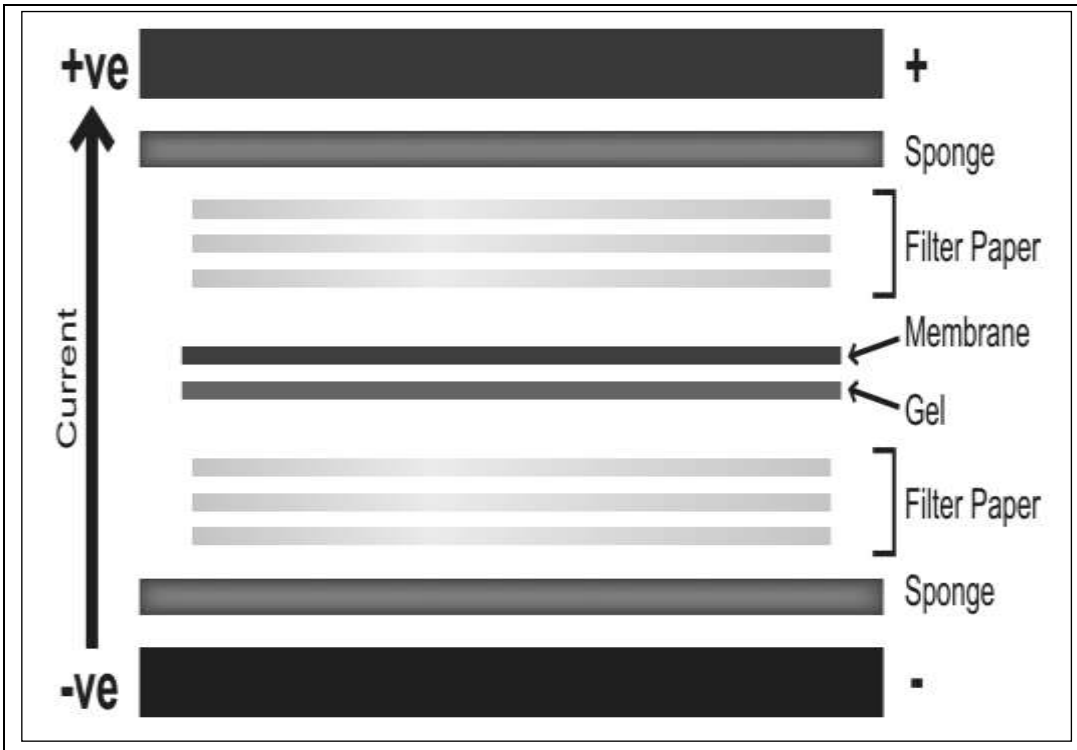

Figure 3.2: Western blot transfer sandwich

Figure taken from the Abcam website (Abcam, 2015)

3.2.2.8 Blocking

After the transfer, blocking of non-specific binding was achieved by placing the membrane in 5% (w/v) non-fat milk solution for 1 hour. This was made by dissolving non-fat dry milk powder in phosphate-buffered saline (PBS) (14.8 g sodium chloride, 7.34 g $NaH_2PO_4 \cdot 2H_2O$ and 19.87 g Anhydrous Na_2HPO_4 made to 2 L with deionised water). The membrane was washed 3 times in this solution.

3.2.2.9 Antibodies and Detection

The membrane was incubated with the appropriate antibody diluted in 2.5% (w/v) milk PBS tween solution, under gentle agitation overnight at 4°C. The antisera against the following proteins were used: actin, CYP3A4/5 and CYP2C9 (Abcam, Cambridge, UK), phosphorylated GR at s211 (Cell Signalling, MA, USA), GR M20 (Santa Cruz Biotechnology, Germany), PXR and CAR (Santa Cruz Biotechnology, Germany). The following day, the membrane was washed in PBS tween for 10 min (3 times) to remove unbound primary antibody. The membrane was incubated in 1:50,000 dilution (in 5% milk) of appropriate horseradish

peroxidase-conjugated anti-mouse or anti-rabbit secondary antibodies (GE Healthcare, UK) at room temperature for 1 hour under agitation. The membrane was subsequently washed three times in PBS tween to remove the milk. Excess liquid was removed and chemiluminescence solution (Chembio Ltd, Hertfordshire, UK) was applied to the membrane for 1 min. Excess chemiluminescence solution was drained from the membrane and light emission was detected using photographic film developed in the dark room.

3.2.2.10 Data analysis

The programme ImageJ (Schneider et al., 2012) was used to compare the western blots obtained and densitometry values were expressed as fold changes. Densitometry readings were statistically analysed using a Student T test and the standard deviation was shown as error bars on graphs depicting the results. The Summit software (Version 4.3, DAKO, Denmark) was used to analyse ROS data and produce histograms for comparison. The median was used as the average to give more accurate results.

The results in Figure 4.6 and Figure 5.8 are the products of the following formula: total GR (A)/actin (B) = X. The ratio of the intensities of total GR versus actin (X) was then used to determine the relative intensity of GR phosphorylated at S211. Phosphorylated GR (C) / (X) = relative phosphorylated GR levels (Y), which have been shown in the GR phosphorylation Figures. The western blot bands considered for the quantification are shown in panels (A) and (B).

In order for a result to be considered statistically significant, the probability of obtaining its value had to be less than 5% ($p < 0.05$). Experiments were carried out to give two or three sets of independent results to allow statistical analysis.

3.2.3 mRNA levels

3.2.3.1 RNA extraction

The cells were grown in 6-well at were harvested and the total RNA was extracted using RNeasy® plus mini kit and QIAshredder (Qiagen, Hilden, Germany).

RLT Plus buffer was freshly prepared with 10 µl BME added per 1 ml of RLT Buffer. 350 µl of BME-RLT buffer was added to the dishes and the cells were

scraped with a cell scraper and transferred to a QIAshredder spin column with 2 ml collection tube. The lysate was centrifuged for 2 min at 12000 rpm. The homogenised lysate was transferred into a gDNA eliminator spin column with 2 ml collection tube and centrifuged for 30 seconds at 8000 rpm. 700 µl of freshly prepared ethanol 70% was added to the supernatant and mixed by pipetting. 700 µl of the supernatant was transferred to RNeasy spin column with 2 ml collection tube and centrifuged for 15 seconds at 8000rpm. The flow-through was discarded. This step was repeated until all the supernatant had gone through the column. 700 µl of RW1 buffer was added to the column and centrifuged for 15 seconds at 8000 rpm. The flow through was discarded and this step repeated again. 500 µl of RPE buffer was added and centrifuged for 15 seconds at 8000rpm and the flow through was discarded. Another 500 µl of RPE buffer was added and centrifuged for 2 min at 8000 rpm to wash the column. The column was placed in a new 2 ml collection tube and centrifuged for 1 min at 12000 rpm. The spin column was placed into a 1.5 ml collection tube with 50 µl preheated 45ºC RNase free water added to the centre of the column. This was allowed to sit for 2-3 min and the column was centrifuged for 1 min at 8000 rpm for elution. The extracted RNA was stored at -70ºC**.**

3.2.3.2 Quantitative real-time polymerase chain reaction (qRT-PCR)

The extracted RNA was converted to cDNA by reverse transcription and used in real-time PCR to measure the gene expression in the same vial according to the manufacturer's directions (One-Step RT-PCR, Qiagen, UK). One-step qRT-PCR was performed using the Quantifast SYBR Green RT-PCR kit in 96-well plates. The steps of the reaction are shown in Table 3.6.

Step	Temperature	Time	Comments
Reverse Transcription	50°C	10min	
PCR Initial activation step	95°C	5min	DNA Polymerase is activated by this step (maximal/ fast mode)
Two-step cycling			
Denaturation	95°C	10sec	Maximal/ fast mode
Combined annealing/extension	60°C	30sec	Perform fluorescence data collection
Number of cycles= 40			

Table 3.6: qRT-PCR set up for amplification of genes of interest

The kit used for this measurement allowed both reverse transcription and real-time PCR to take place in the same well which reduced the risk of any contamination in conducting the RNA measurements. The kit included enzymes that exhibited a high affinity for RNA, facilitating efficient and sensitive reverse transcription. After transcription, the DNA polymerase was activated by heating to 95°C for 5 min. This enzyme remained in an inactive state during reverse transcription. The denaturation step was followed by combined annealing/extension and was repeated for 40 cycles. After the denaturation step, the primers anneal to their targets and the SYBR Green dye is released. During the annealing/extension step, the PCR product is generated.

SYBR Green I binds to all double-stranded DNA molecules, emitting a fluorescent signal which was measured. The excitation and emission maxima of SYBR Green I are at 494 nm and 521 nm, respectively. The qRT-PCR method allows continuous data logging during the plate read out at each cycle during the assay. The specificity of such assay depends on primer specificity (Bustin and

Mueller, 2005). PCR reactions work by amplifying a region of double-stranded DNA flanked by two known sequences. The two primers (forward and reverse) hybridise to their complementary sequence. The qRT-PCR amplification curves (fluorescence signal versus the cycle) are shown in Figure 3.3 (Bustin and Mueller, 2005).

The baseline area below the threshold represents the noise level in early cycles where no significant fluorescence is measured and the $C_{t,}$value measures where the threshold cycle shows a significant increase in fluorescence. The arrows in the graph point to C_t values of three samples reaching threshold and crossing baseline. The readings given in the results section are for the differences in C_t (ΔC_t) for the control untreated cells versus the Dex-treated cells.

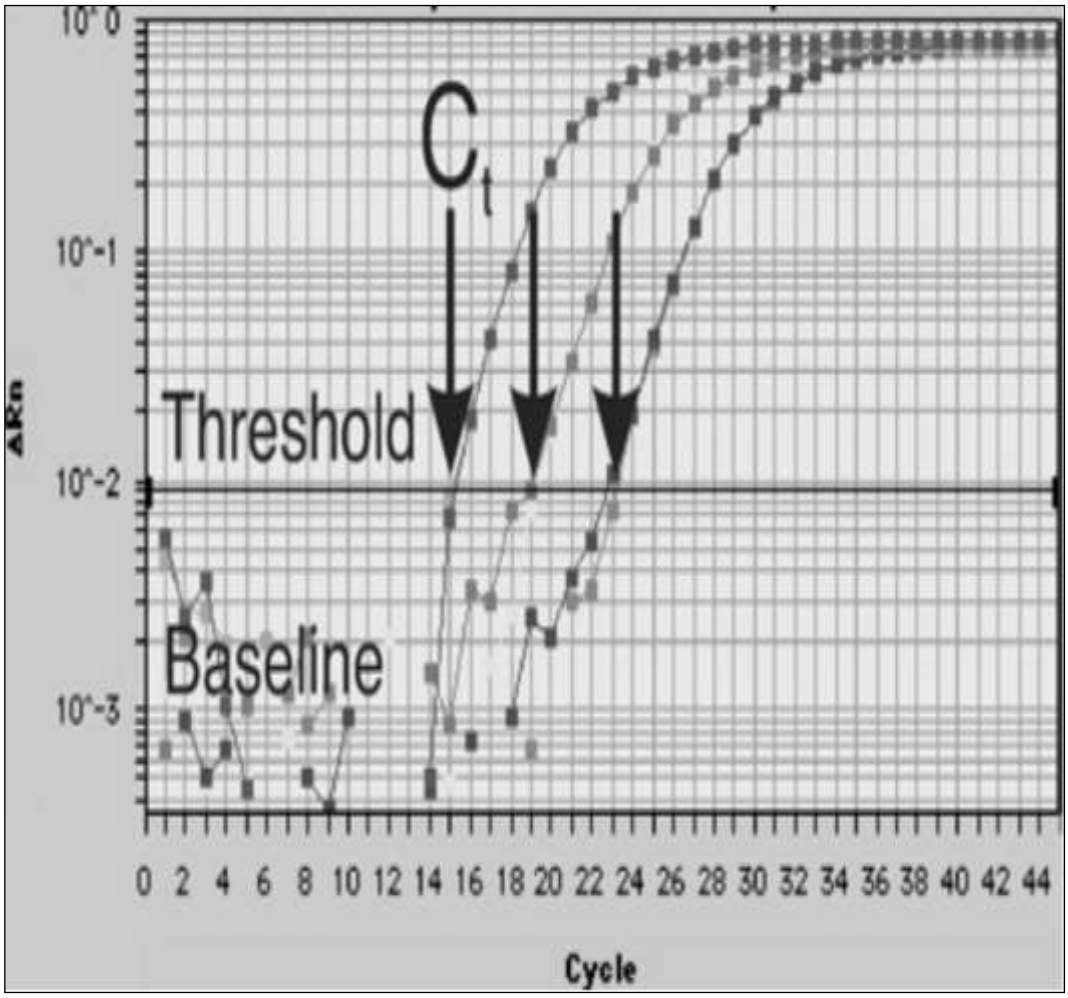

Figure 3.3: Diagram showing the qRT-PCR amplification curve (fluorescence signal versus the cycle)

Adapted from Bustin and Mueller (2005).

The qRT-PCR melting curve to verify the PCR product amplified is shown in Figure 3.4 (Bustin and Mueller, 2005).

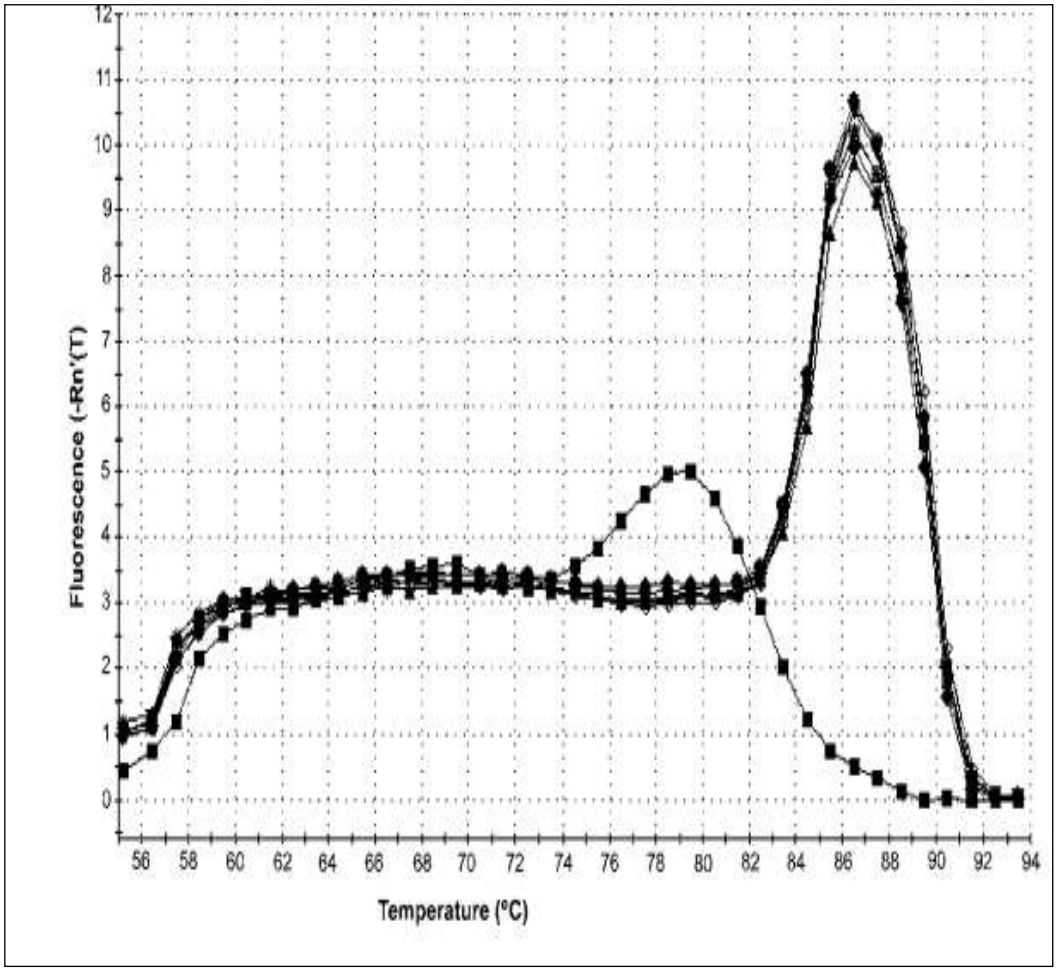

Figure 3.4: qRT-PCR melting curve

The qRT –PCR is used to verify the PCR product amplified. Figure taken from Bustin and Mueller (2005).

3.2.3.3 Primers used

The gene-specific PCR primers were designed by certain criteria such as the primer T_m being +/- 1 60°C, primer length 18-15 bases and the GC content 40-60%. This generated unique and short PCR products of between 60-150 base pairs (Udvardi et al., 2008). The qRT-PCR was performed and the standard curve analysis was carried out using the Opticon Monitor software version 3.1. The primers used are shown in Table 3.7. All values were normalized with ribosomal protein 19 (RPL19) control.

Primer	Forward	Reverse
RPL19	ATGTATCACAGCCTGTACCTG	TTCTTGGTCTCTTCCTCCTTG
CYP2C9	GCACGAGGTCCAGAGATACA	GTTGTGCCCTTGGGAATGAG
CYP3A4/5	CTCAAGGAGATGGTCCCTAT	CCTGTCACCTTGAAAGACGTC

Table 3.7: Primers used for qRT-PCR reactions

3.2.4 Measurement of Intracellular ROS generation by fluorescence-activated cell sorting (FACS)

The cells were grown in 60 mm dishes and treated with Dex at the mentioned time points. After 5 days all samples were washed with dissociation buffer (1 ml each dish) to detach the cells. The dishes were put in the incubator for 2 min and the dissociation buffer was then neutralised with DMEM media (3 ml). The cells were put in 25 ml tubes and centrifuged for 3 min at 12000 rpm. The media was carefully aspirated without disturbing the cell pellet and 1 ml media was added. The cells were transferred to 1.5 ml eppendorf tubes and allowed to sit in the tube for 30 min. The cells were centrifuged at 3000 rpm for 3 min. The cells were washed twice with PBS and 100 µl of 100 µM H_2DCF-DA (Invitrogen, Paisley, UK) in PBS was added to each sample. The samples were left in the dark for 30 min. After 30 min the samples were again washed with PBS twice and 500 µl PBS was added per sample. The samples were measured using a flow cytometer (Cyan ADP) and analysed Summit software version 4.3 (Dako, Denmark). 20,000 of the healthy cells were gated to be displayed on the histograms.

The 5- (and 6-) chloromethyl-2',7' dichlorodihydrofluorescein diacetate (H2-DCFDA) are isomers and probes for intracellular oxidants to measure ROS (Macey, 2007). The method used in ROS measurement consists of a flow cytometer containing a flow cell, sheath stream, laser beam, sensing system computer, charging collar, deflection plates and droplet collection after separation is shown in Figure 3.5.

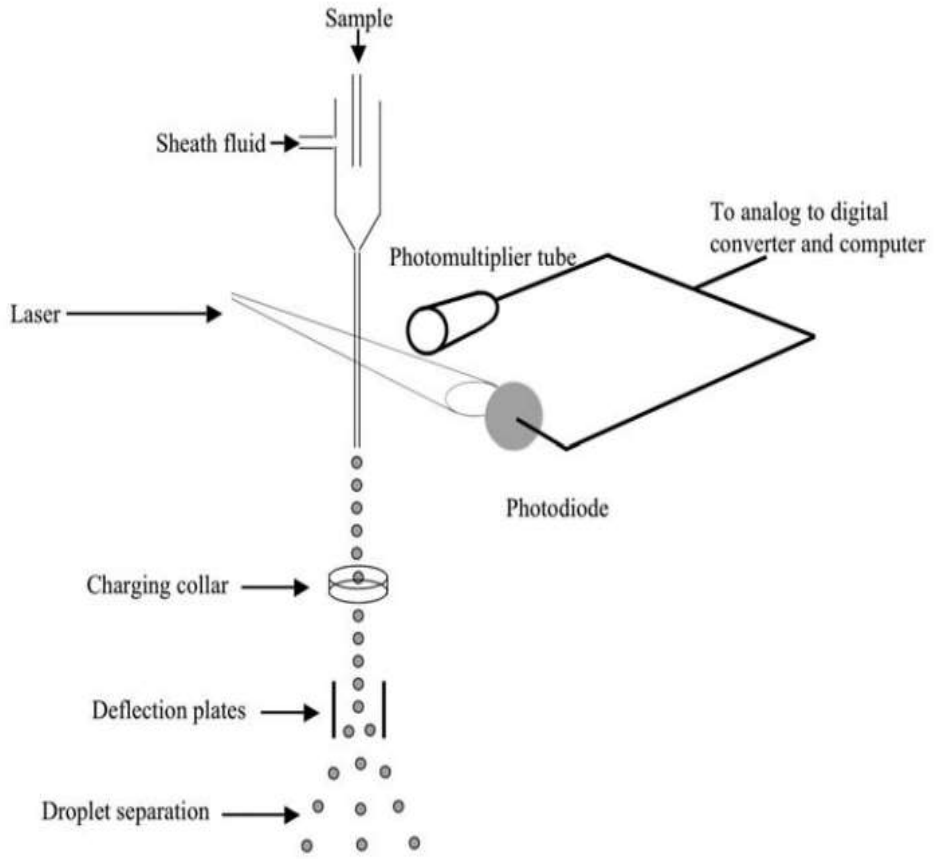

Figure 3.5: Schematic of the flow cytometry principle

Figure taken from Macey, 2007.

Fluorescence was determined by FACS analysis. The reactions within the cell to give ROS measurements are shown in Figure 3.6 (Macey, 2007). H2-DCFHDA is taken up by cells and converted to the fluorescent product dichlofluorescein (DCF) which is cell impermeable and measures ROS in the cell.

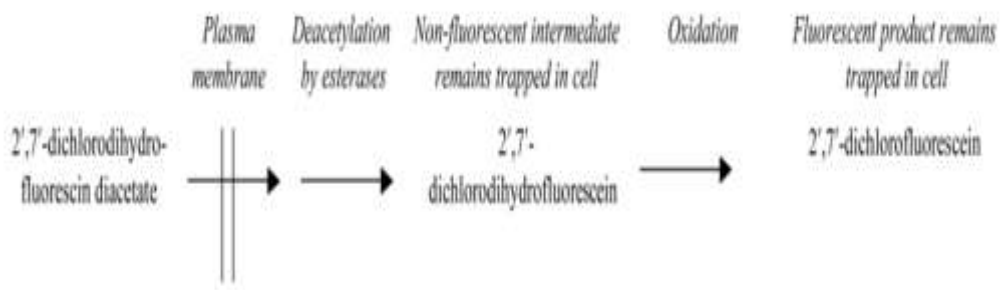

Figure 3.6: ROS reactions within the cell

Taken from Macey, 2007.

The inhibition of CYP 3A enzymatic activity is selective by the antifungal drug, ketoconazole (Keto). It selectively inhibits CYP3A at 0.3 µM not affecting other CYP enzymes at this concentration. The inhibition caused is mixed-type, meaning that it inhibits by mixed competitive and non-competitive processes (Greenblatt et al., 2011). Inhibition of CYP2C9 enzymatic activity was by sulfaphenazole (SPZ). This antibacterial drug is a potent and very selective inhibitor of CYP2C9 at 0.1 µM, not thought to affect other CYP enzymes at this concentration. It functions by competitive inhibition (Afzelius et al., 2001). Concentrations of inhibitors were taken from the FDA 2006, Guidance for Industry on the FDA website (FDA, 2006).

3.2.5 Analysis of enzymatic activity

3.2.5.1 Liquid chromatography–mass spectrometry (LC-MS)

$1x10^6$ HepG2 cells seeded in 6-well plates were treated with 0.1 µM Dex for 2, 6, 24 and 48 hours. These cells were treated with the appropriate substrate concentrations as shown in Table 3.8. Following incubation of the cells with the substrates, aliquots of the incubation medium were taken and centrifuged at 1000g. The supernatant was stored at -80°C prior to analysis.

P450 Enzyme	Reaction	Substrate Concentration µM	Incubation Times (min)	Internal Standard
CYP2C9	Tolbutamide 4-hydroxylation	100, 500	30, 60	Diclofenac (10 µM)
CYP3A4/5	Midazolam 1-hydroxylation	10, 50	15, 30	Diazepam (10 µM)

Table 3.8: Substrates used for the CYPs studied and incubation times

3.2.5.2 Metabolite Determinations for LC-MS

The metabolites for CYP2C9 and CYP3A4/5 were 4-hydroxytolbutamide and 1′-hydroxymidazolam respectively. These were formed and released into the culture medium and were quantified by high-performance liquid chromatography tandem mass spectrometry. This system is comprised of a Micromass Quattro Micro (Waters, Milford MA) triple quadrupole mass spectrometer in the electrospray ionization mode, interfaced with an Alliance 2795 HPLC (Waters). Chromatography was performed at 35°C, and an aliquot (20 µl) of incubation extract was injected into a Teknokroma C18 column (100 mm × 2.1 mm, 3 µm particle size) at a flow rate of 0.4 ml/min. The tandem mass spectrometry analysis was performed with a triple quadrupole analyser operating in the multiple reaction monitoring mode using argon as collision gas as described previously by Donato and colleagues (Donato et al., 2010).

3.2.5.3 P450-Glo assay

The P450-Glo assay method functioned by combining the CYP enzymatic activity with the firefly luciferase luminescence technique. Measurement of induction or inhibition of CYP enzyme activity was possible with this luminogenic assay in cultured hepatocytes (Cali et al., 2006). HepG2 cells were cultured in 96-well

plates and treated with Dex for 5 days at various time points. After treatment the culture medium was replaced with medium containing the P450 substrate required. The cells were then incubated for 1 hour with Luciferin-IPA for CYP3A4/5 or 4 hours with Luciferin-H for CYP2C9. The incubation times varied depending on the assay being used. After the required incubation period, a volume of the medium was transferred to a white multi-well Plate and combined with an equal volume of luciferin detection reagent (LDR) given in the kit. The luminescence was read by a luminometer (Labtech BMG, Fluostar Optima Luminometer).

3.3 Mathematical modelling using computational methods

A set of ordinary differential equations can be used to mathematically describe biological processes. These mathematical equations will vary depending on the type of bimolecular interactions used in the model.

Michaelis-Menten equations may be used to describe irreversible enzyme catalysed reactions whilst mass action equations describe complex-bindings.

Mass action reactions of two substrates (S1 + S2) producing product (P), by first-order kinetics:

$$S_1 + S_2 \xrightarrow{k} P$$

Where *k* is the net rate or the kinetic constant.

The ordinary differential equations (ODE) describing the reaction rate are:

$$\frac{d[S1]}{dt} = -k \cdot [S1] \cdot [S2]$$

$$\frac{d[S2]}{dt} = -k \cdot [S1] \cdot [S2]$$

$$\frac{d[P]}{dt} = k \cdot [S1] \cdot [S2]$$

The reaction rate is proportional to the concentration of each of the reactants S1 and S2 and the reaction is known as a bimolecular reaction (Klipp et al., 2005).

Given that the reaction rate is directly proportional to the reactant concentration, mass action kinetics can be utilised to describe the dynamics of the reactants and products in a chemical reaction. This kinetic model has been used effectively in GR transduction models (Jin et al., 2003).

ODEs are used to describe the rate of change of a particular species concentration during a fixed time period. Several software have been developed to simulate and model biological systems using ODEs. This method allows using the detailed knowledge in consideration of individual interactions in gene regulation (Babu et al., 2006). None the less, finding the kinetic constants is extremely challenging.

Using Bayesian networks is an alternative method using probabilistic graphical models. These networks are made up of nodes representing variables such as genes, and the arcs representing the link of statistical dependence among the variables. Gene analysis of microarray measurements by Bayesian networks has been found promising because of its tolerance to the inherent noise in the microarray method (Friedman et al., 2000).

3.3.1 Comparison of computational modelling using MATLAB and COPASI software

Both software packages can be utilised to model systems of reaction equations.

3.3.1.1 Requirements to model reaction systems in MATLAB

MATLAB is the abbreviation for MATrix LABoratory where the software can be used for linear algebra and also to solve algebraic and differential equations.
For example, modelling protein reaction systems in this software package requires details of the protein-protein interactions, kinetic rates and concentration data and more detailed understanding of mathematical manipulation and theory including matrix algebra and differential equations.

3.3.1.2 Requirements to model reaction systems in COPASI

COPASI stands for COmplex PAthway Simulator and can be used for the simulation and analysis of biochemical networks and their dynamics.

Modelling protein reaction systems in this software package also requires details of the protein-protein interactions, kinetic rates and concentration data and simple understanding of how simulations tools work (Tindall, 2012).

COPASI does not require that the user understands how the underlying mathematical model is derived which makes modelling with this software less complex.

Source codes of MATLAB scripts used in this study are in Appendices 1 and 2. The data for treatment with 0.1 µM Dex, test concentrations of Dex and 1.5 mM treatment with Dex are in Appendices 3, 4 and 5 respectively.

Chapter 4: Results of low Dex concentration

The amounts of Dex which were used in this study correspond to dosages administered to patients for the treatment of several autoimmune diseases, inflammation, allergies, leukaemia and solid cancers such as prostate and breast cancer (Pui and Evans, 2006; Inaba and Pui, 2010). The dosage of Dex administered for these conditions result in final blood concentrations of 0.1 μM - 0.015 mM. The low concentration of 0.1 μM forms the basis of the following results.

4.1 Assessment of CYP3A4 and CYP2C9 mRNA levels in hepatocytes treated with 0.1 μM Dex (low dose of Dex)

Drugs and environmental chemicals modulate their own metabolism and excretion by regulating the activity of transcription factors which in turn alter the gene expression of metabolizing enzymes and drug transporter in multiple tissues including the liver (Pavek and Dvorak, 2008) thereby exerting profound effects on human health. Members of the NR superfamily such as GR, CAR and PXR are well known regulators of gene expression of phase I metabolizing enzymes such as CYP family members (Handschin and Meyer, 2003) and drug transporters including P-gp. The synthetically produced GC Dex is one of the most extensively prescribed drugs in clinical practice (Buckingham, 2006) because of the wide spectrum of its pharmacological effects which are mainly due to anti-inflammatory functions (Barnes, 1998). The pharmacological effects of Dex are mediated by binding of this hormone to its specific cellular receptor namely GR at the receptor's LBD (Galliher-Beckley and Cidlowski, 2009). Apart from GR, Dex has been shown to stimulate the transcriptional activity of other members of the nuclear receptor superfamily, the so called "orphan" receptors CAR and PXR (Germain et al., 2006; Li and Wang, 2010). Taken together all the above mentioned observations allow the hypothesis that Dex treatment would alter the mRNA levels of the CYP metabolizing enzymes through induction of the transcriptional activity of the nuclear receptors GR, CAR or PXR in a Dex concentration and duration of the treatment manner.

The main function of the haem-containing cytochrome P450 (CYP) superfamily is to convert endogenous compounds and drugs to ionic water soluble derivatives so that are easier to be excreted or more susceptible to further biotransformation (Guengerich, 1991). In this context, CYP3A4/5 and CYP2C9 are the most extensively active enzymes since both are responsible for the phase I metabolism of more than 60% of drugs and xenobiotics (Williams et al., 2004; Wienkers and Heath, 2005). In order to test the hypothesis that Dex alters the gene expression of CYP family members and in particular of the most active members CYP3A4 and CYP2C9, the gene expression of these enzymes was followed in HepG2 cells treated with 0.1 μM Dex for different time points employing qRT-PCR. The oligos used for qRT-PCR of CYP3A4 were specific to this isoform and not CYP3A5 according to the RNA sequences previously mentioned. The concentration of Dex was used based on reports indicating that 0.1 μM of this hormone is sufficient to induce GR transcriptional activity on human small cell lung cancer cells and human lymphoblastic leukemia cells (Sommer et al., 2007; Lynch et al., 2010). The data were obtained by treating HepG2 cells with 0.001 mM for 120 h, and samples were collected at 0, 0.5, 1, 2, 6, 24, 48 and 120 h. The media was changed and Dex added again every 24 h to allow the assumption that the Dex concentration was constant throughout the experiments.

4.1.1 CYP3A4 mRNA levels

To investigate gene expression of CYP3A4 enzyme in HepG2 cells treated with 0.1 µM Dex, the mRNA levels of CYP3A4 were determined by qRT-PCR.

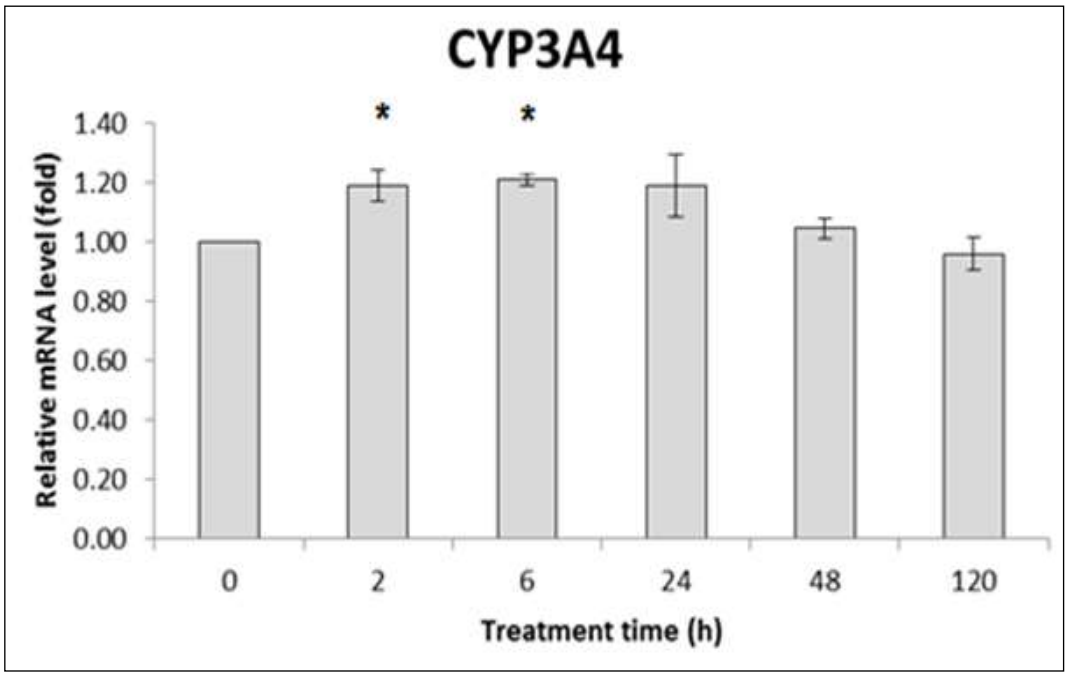

Figure 4.1: qRT-PCR analysis of CYP3A4 mRNA levels in Dex treated HepG2 cells

Total RNA from HepG2 cells treated with 0.1 µM Dex for 2, 6, 24, 48 and 120 hours or untreated (0 h) as indicated, and extracted and reverse transcribed. The cDNAs were then subjected to qRT-PCR using specific primers amplifying CYP3A4 mRNA. Rpl19 was used as an internal control. The data were analysed by the Opticon Monitor 3 software and are representative of three independent experiments each performed in duplicates. Error bars represent standard deviations of three independent experiments. An asterisk indicates a significant difference of $p < 0.05$.

A slight induction of CYP3A4 mRNA levels was observed in HepG2 cells treated with Dex at 2 h and remained at these levels in cells treated 6 and 24 h with the hormone and started declining 48 h after the addition of Dex to reach the basal level after 120 h of Dex treatment (Figure 4.1). These results indicate that Dex induced CYP3A4 gene expression in relatively early stages after the addition of

the hormone in accord with published reports (Pichard et al., 1992; Schuetz et al., 1993; Pascussi et al., 2001).

4.1.2 CYP2C9 mRNA levels

As well as CYP3A4, CYP2C9 has been shown to be induced in response to Dex treatment (Gerbal-Chaloin et al., 2001; Raucy et al., 2002).

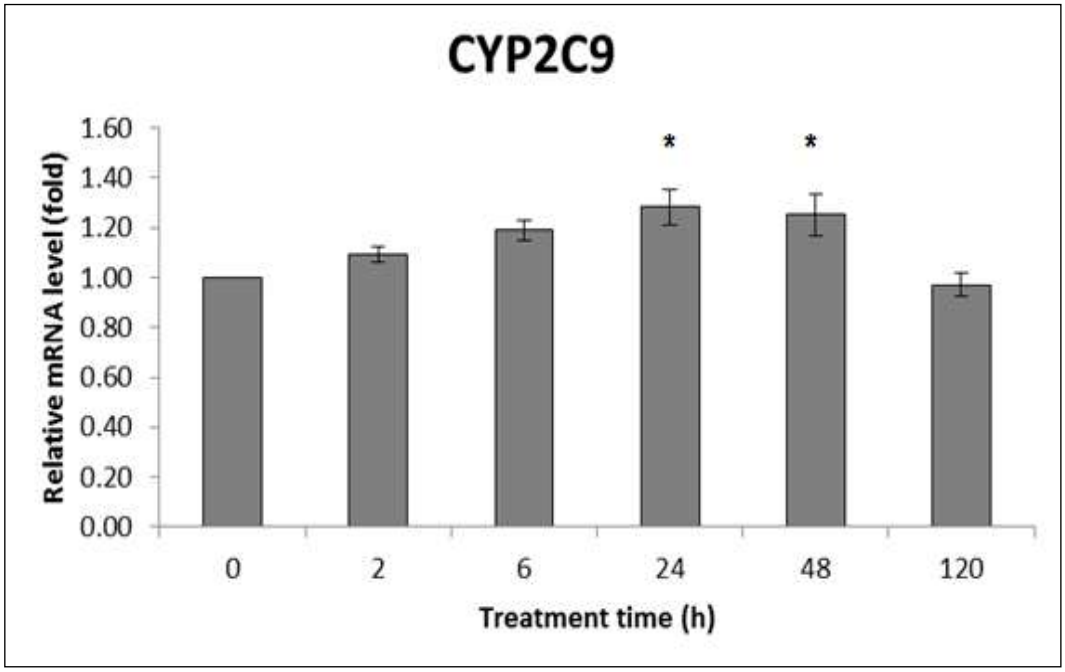

Figure 4.2: qRT-PCR analysis of CYP2C9 mRNA levels in Dex treated HepG2 cells

Total RNA from HepG2 cells treated with 0.1 µM Dex for 2, 6, 24, 48 and 120 hours or untreated (0 h) as indicated, and was extracted and reverse transcribed. The cDNAs were then subjected to qRT-PCR using specific primers amplifying CYP2C9 mRNA. Rpl19 was used as an internal control. The data were analyzed by the Opticon Monitor 3 software and are representative of three independent experiments each performed in duplicates. Error bars represent standard deviations of three independent experiments. An asterisk indicates a significant difference of $p < 0.05$.

A delayed statistically significant induction of CYP2C9 mRNA levels compared to CYP3A4 mRNA levels was observed in HepG2 cells treated with Dex at 24 and 48h, declining to return to baseline 120h after the addition of Dex (see Figure

4.2). These results indicate that Dex-mediated induction of CYP2C9 occurs at slower rates compared to CYP3A4 (compare Figure 4.1 with Figure 4.2).

4.2 Assessment of CYP3A4/5, CYP2C9, GR, phosphorylated GR at S211, PXR, CAR and P-gp protein levels in hepatocytes treated with 0.1 µM Dex

The levels of mRNA transcripts do not always correlate with the protein level (Maier et al., 2009). The protein levels are determined by the balance of RNA and protein production and turnover (Vogel and Marcotte, 2012). The main mechanisms controlling translation are transcript stability and protein degradation (Schwanhäusser et al., 2011; Chalancon et al., 2012). The control of gene expression mainly occurs by regulation of transcription initiation (Fickett and Hatzigeorgiou, 1997) whilst this does not regulate mRNA stability (Wilusz et al., 2001). The model can be more accurate with the inclusion of delays that are evident between the emergence of gene mRNA and the functional protein, which account for a number of intermediate biological steps such as translation (Zak et al., 2005).

Western blot analysis of CYP3A4, CYP2C9, GR, phosphorylated GR at S211, PXR, CAR and P-gp protein levels (normalised to actin) in 0.1 µM Dex treated HepG2 cells relative to untreated cells was conducted to show the protein expression of these CYP enzymes and NRs.

4.2.1 CYP3A4/5 protein levels

Hepatic CYP3A4/5 is regulated by GR, CAR and PXR agonists (Xie et al., 2000; Sahi et al., 2009). GR binds indirectly to the promoter region of CYP3A4 and can induce the expression of a gene that does not hold a functional GRE in its promoter region and directly binds to the promoter region of CYP3A5 (Dvorak and Pavek, 2010). The antibody used for this protein level cannot distinguish between the 3A4 and the 3A5 isoforms therefore the two proteins are measured together and are indicated as CYP3A4/5. The CYP3A4/5 protein levels were determined by western immunoblotting in HepG2 cells and quantification of the intensity of the CYP3A4/5 bands compared to that of Actin for each time point using Image J densitometric analysis (Schneider et al., 2012) as described in

details in the Materials and Methods section. Western blot analysis indicated of CYP3A4/5 protein levels in Dex treated cells relative to untreated cells and one representative blot is shown at the indicated time points (Figure 4.3).

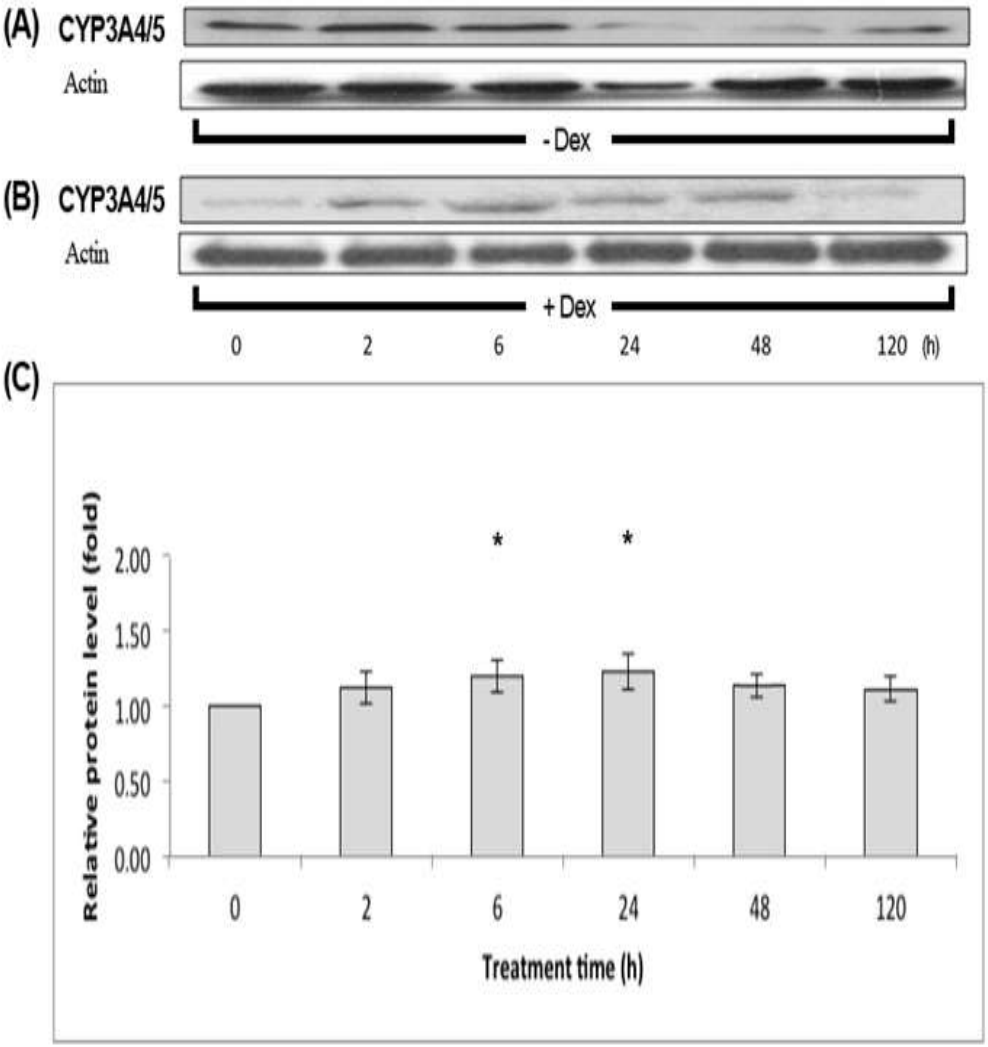

Figure 4.3: CYP3A4/5 protein levels in HepG2 cells

(A) HepG2 cells were treated only with vehicle for the indicated time points. Subsequent to the treatment, cells were harvested with high salt lysis buffer and equal amount of protein lysate was loaded and resolved on 10% PAGE. Antibodies targeting CYP3A4/5 and actin were used to detect the respective proteins. Actin was used as loading control. (B) HepG2 cells were treated with 0.1 µM Dex for the indicated time points and processed the same way as that described in (A). Data shown in (A) and (B) panels are representative of 3

independent experiments. (C) Densitometric analysis carried out using Image J to measure the intensity of each CYP3A4/5 and actin bands in panels (A) and (B).
The intensity of the CYP3A4/5 bands shown at the top in panel (B) was divided by the respective band of actin at the bottom of the same panel. The value obtained from this calculation was normalised to the value obtained from the estimation of the intensity of CYP3A4/5 bands divided by the intensity of the respective actin in panel (A).
For example, the calculation for the intensity of the CYP3A4/5 bands at 2 hours treatment was performed as follows:

$$\frac{\text{(B) 2h CYP3A4/5 / 2h Actin}}{\text{(A) 2h CYP3A4/5 / 2h Actin}} = \text{bar shown in panel (C)}$$

The intensity of the CYP3A4/5 band was normalized to the intensity of the corresponding actin band for each time point and the average of three independent experiments was plotted. Error bars represent standard deviations of three independent experiments. The asterisks indicate a significant difference of $p < 0.05$.
Statistically significant induction of relative CYP3A4/5 protein levels was apparent at 6 and 24h after treatment with this Dex concentration and was not seen at the later time points (Figure 4.3).

4.2.2 CYP2C9 protein levels

Similar to CYP3A4/5, CYP2C9 is regulated by agonists of GR, CAR and PXR in human hepatocytes (Sahi et al., 2009; Dvorak and Pavek, 2010). Dex can activate the CYP2C promoters via GR and CYP2C9 is transcriptionally controlled by the direct binding of GR to the promoter sequence (Pascussi et al., 2003; Dvorak and Pavek, 2010). Western blot analysis of CYP2C9 protein levels in Dex treated cells relative to untreated cells and one representative blot is displayed at the indicated time points (Figure 4.4).

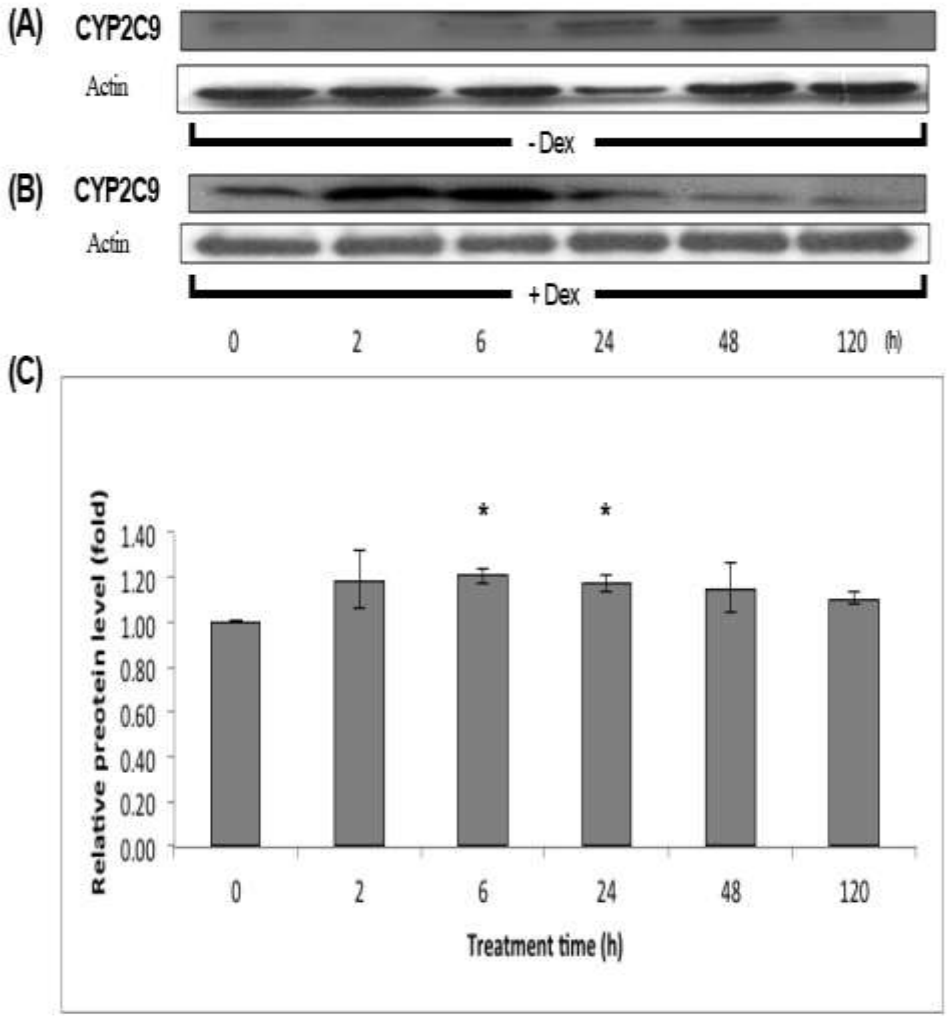

Figure 4.4: CYP2C9 protein levels in HepG2 cells

(A) HepG2 cells were treated only with vehicle for the indicated time points. Subsequent to the treatment, cells were harvested with high salt lysis buffer and equal amount of protein lysate was loaded and resolved on 10% PAGE. Antibodies targeting CYP2C9 and actin were used to detect the respective proteins. Actin was used as loading control. (B) HepG2 cells were treated with 0.1 µM Dex for the indicated time points and processed the same way as that described in (A). Data shown in (A) and (B) panels are representative of 3 independent experiments. (C) Densitometric analysis carried out using Image J to measure the intensity of each CYP2C9 and actin bands in panels (A) and (B). The

intensity of the CYP2C9 band was normalized to the intensity of the corresponding actin band for each time point and the average of three independent experiments was plotted.

The values and the results plotted have been analysed as described in Figure 4.3. Error bars represent standard deviations of three independent experiments. The asterisks indicate a statistically significant difference of $p < 0.05$.

Statistically significant induction of relative CYP2C9 protein levels was again apparent at 6 and 24 h after treatment with this Dex concentration and was not seen at the later time points (compare Figure 4.3 and Figure 4.4).

4.2.3 GR protein levels

Multiple GR isoforms can be the result of a single gene and lead to differences in GC signalling. GR subtypes can be affected by various post-translational modifications generating different GC responses and the concentration of the GC used can affect their cellular response (Oakley and Cidlowski, 2013). GRs can directly or indirectly regulate certain changes in DNA transcription leading to protein production and can act as transcription factors leading to repression or induction of target genes by interaction with GREs. The ability of the ligand-receptor complex to bind to GREs is affected by dissociation of the chaperone proteins and the consecutive phosphorylation, dimerization and nuclear translocation of GR (Buckingham, 2006).

Western blot analysis of GR protein levels in Dex treated cells relative to untreated cells. One representative blot is shown at the indicated time points (Figure 4.5).

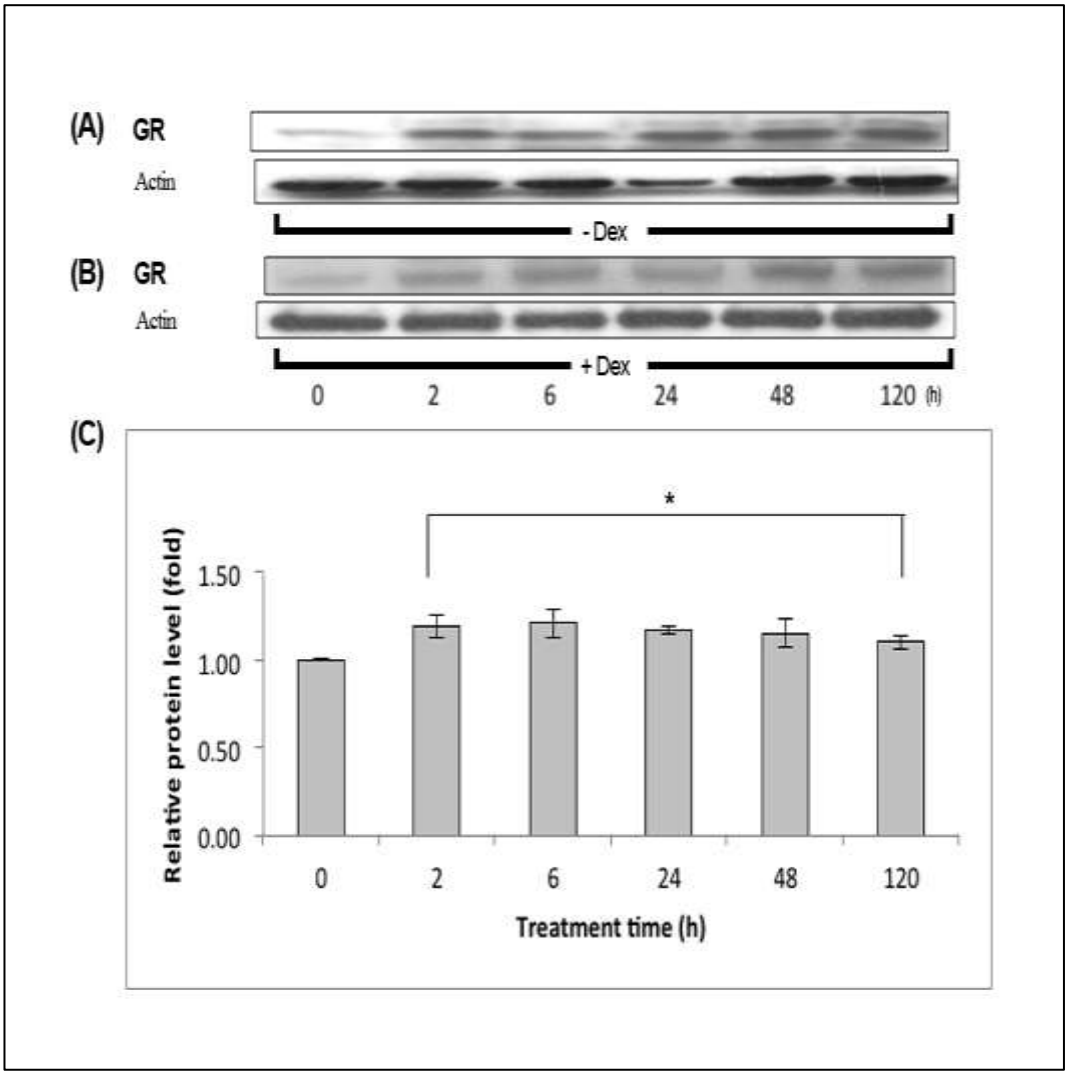

Figure 4.5: GR protein levels in HepG2 cells

(A) HepG2 cells were treated only with vehicle for the indicated time points. Subsequent to the treatment, cells were harvested with high salt lysis buffer and equal amount of protein lysate was loaded and resolved on 10% PAGE. Antibodies targeting GR and actin were used to detect the respective proteins. Actin was used as loading control. (B) HepG2 cells were treated with 0.1 µM Dex for the indicated time points and processed the same way as that described in (A). Data shown in (A) and (B) panels are representative of 3 independent experiments. (C) Densitometric analysis carried out using Image J to measure the intensity of each GR and actin bands in panels (A) and (B).

The intensity of the GR band was normalized to the intensity of the corresponding actin band for each time point and the average of three independent experiments was plotted.

The values and the results plotted have been analysed as described in Figure 4.3. Error bars represent standard deviations of three independent experiments. The asterisks indicate a statistically significant difference of $p < 0.05$.

Statistically significant induction of relative GR protein levels was obtained throughout the Dex treatment from 2 - 120h (Figure 4.5).

4.2.4 Phosphorylated GR at S211 protein levels

The phospho-GR is a phosphoprotein and its phosphorylation can be both ligand-independent and ligand-dependent (Bodwell et al., 1991; Ismaili and Garabedian, 2004). Cyclin E/ cdk2 and cyclin A/ cdk2 phosphorylate GR at S203, whilst GR phosphorylation at S211 is mediated by cyclin A/ cdk2 (Krstic et al., 1997) and p38 MAPK (Miller et al., 2005). Phosphorylation of GR at S203 and S211 enhances GR transcriptional activity (Wang et al., 2003). The MAPK family member, JNK, phosphorylates GR at S226, reducing its transcriptional activity (Krstic et al., 1997; Rogatsky et al., 1998; Davies et al., 2008). Phosphorylation at this site by JNK has also been shown to enhance nuclear export of GR upon glucocorticoids withdrawal (Itoh et al., 2002). GR phosphorylation is important for the regulation of its transcriptional activity since this post translational modification affects its biding specificity with transcriptional cofactors, thereby modulating its transcriptional target selectivity (Davies et al., 2008; Davies et al., 2011; Chen et al., 2008). The functions of GR can also be regulated by post-translational modifications such as phosphorylation which leads to modifications in the transcriptional activity of GR (Galliher-Beckley and Cidlowski, 2009; Lynch et al., 2010).

Although GR can be phosphorylated in the absence of hormone, it is further phosphorylated in conjunction with agonist binding. Hormone-dependent phosphorylation of GR has been suggested to determine target promoter selectivity, cofactor interaction, strength and duration of receptor signalling, and receptor stability, sub-cellular localization and protein-protein interaction

(Nicolaides et al., 2010). GR phosphorylation could affect GR-mediated transcription in a promoter-specific manner, so GR phosphorylation may have an important role in hormone signalling (Galliher-Beckley and Cidlowski, 2009). The phosphorylation of GR can be mediated by MAPK, CDK, GSK-3, ERK and JNK. GC signalling is a complex process involving a crosstalk between many other regulatory pathways and regulatory processes (Beck et al., 2009).

Western blot analysis of S211 phosphorylated GR protein levels in Dex treated cells relative to untreated cells. One representative blot is shown at the indicated time points (Figure 4.6).

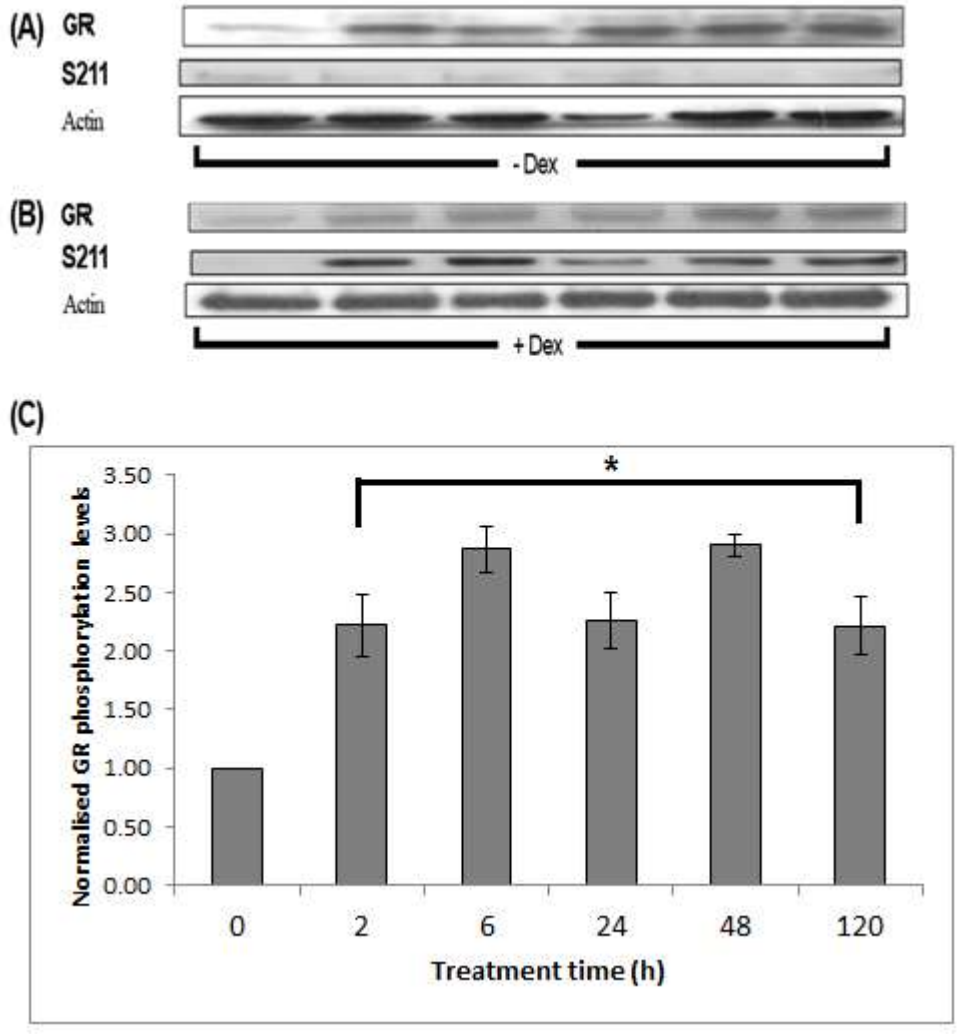

Figure 4.6: S211 Phospho-GR protein levels in HepG2 cells

(A) HepG2 cells were treated only with vehicle for the indicated time points. Subsequent to the treatment, cells were harvested with high salt lysis buffer and equal amount of protein lysate was loaded and resolved on 10% PAGE. Antibodies targeting GR, S211 phospho-GR and actin were used to detect the respective proteins. Actin was used as loading control. (B) HepG2 cells were treated with 0.1 μM Dex for the indicated time points and processed the same way as that described in (A). Data shown in (A) and (B) panels are representative of 3 independent experiments. (C) Densitometric analysis was carried out using Image J to measure the intensity of each GR, S211 phospho-GR and actin bands in panels (A) and (B).

The values and the results plotted have been analysed as described in the Methods section (3.2.2.10 Data analysis). The intensity of the S211 phospho-GR band was normalized to the intensity of the corresponding total GR and actin band for each time point and the average of three independent experiments was plotted.

Error bars represent standard deviations of three independent experiments. The asterisks indicate a statistically significant difference of $p < 0.05$.

As with total GR protein levels, induction of relative phosphorylated GR at serine 211 protein levels was detected and calculated to be statistically significant throughout the Dex treatment from 2 - 120h. The values of phosphorylated GR at S211 compared to total GR were approximately 1.5 - 2 folds (Compare Figure 4.5 and Figure 4.6).

4.2.5 PXR protein levels

PXR can regulate the expression of CYP3A4/5 and CYP2C9 gene activity and protein levels (Pascussi et al., 2003; Sahi et al., 2009).

Western blot analysis of PXR protein levels in Dex treated cells relative to untreated cells. One representative blot is shown at the indicated time points (Figure 4.7).

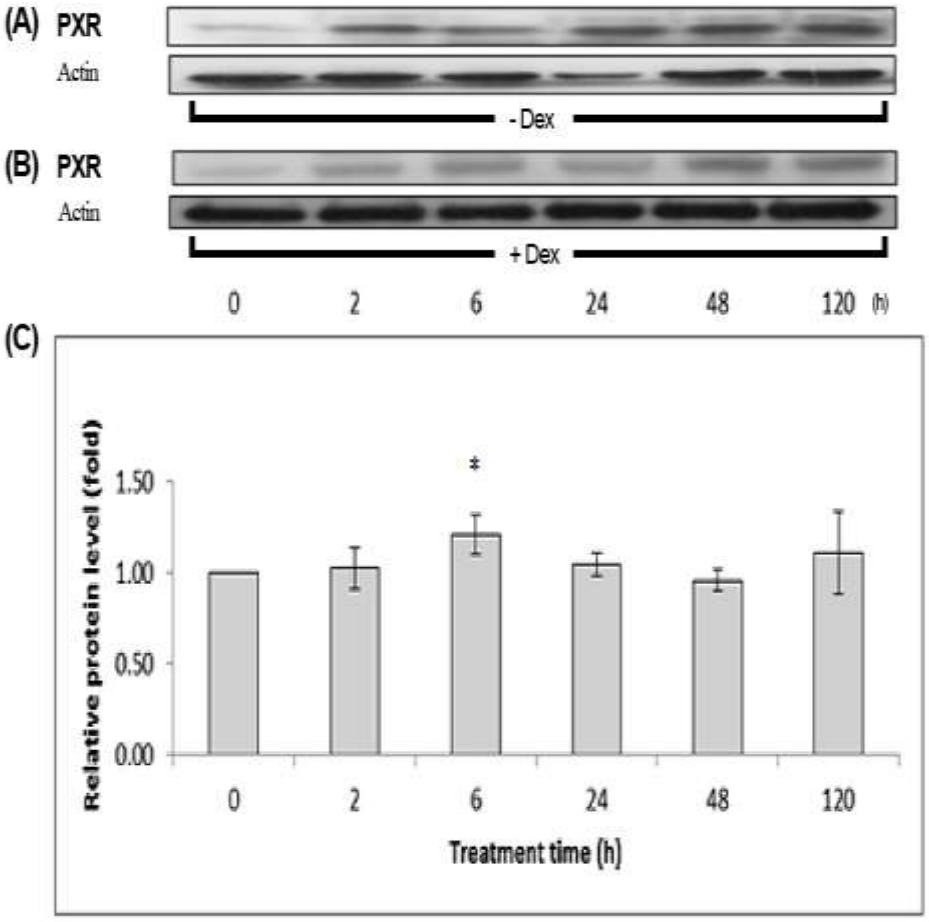

Figure 4.7: PXR protein levels in HepG2 cells

(A) HepG2 cells were treated only with vehicle for the indicated time points. Subsequent to the treatment, cells were harvested with high salt lysis buffer and equal amount of protein lysate was loaded and resolved on 10% PAGE. Antibodies targeting PXR and actin were used to detect the respective proteins. Actin was used as loading control. (B) HepG2 cells were treated with 0.1µM Dex for the indicated time points and processed the same way as that described in (A). Data shown in (A) and (B) panels are representative of 3 independent experiments. (C) Densitometric analysis carried out using Image J to measure the intensity of each PXR and actin bands in panels (A) and (B).

The intensity of the PXR band was normalized to the intensity of the corresponding actin band for each time point and the average of three independent experiments was plotted.
The values and the results plotted have been analysed as described in Figure 4.3.
Error bars represent standard deviations of three independent experiments. The asterisks indicate a statistically significant difference of $p < 0.05$.

The relative protein levels of PXR were only statistically significant at 6 h and did not show induction of this NR at any other time point compared with untreated cells (see Figure 4.7).

4.2.6 CAR protein levels

CAR can also regulate the expression of CYP3A4/5 and CYP2C9 gene activity and protein levels (Dickins, 2004; Sahi et al., 2009).
Western blot analysis of CAR protein levels in Dex treated cells relative to untreated cells and actin as the internal control. One representative blot is shown at the indicated time points (Figure 4.8).

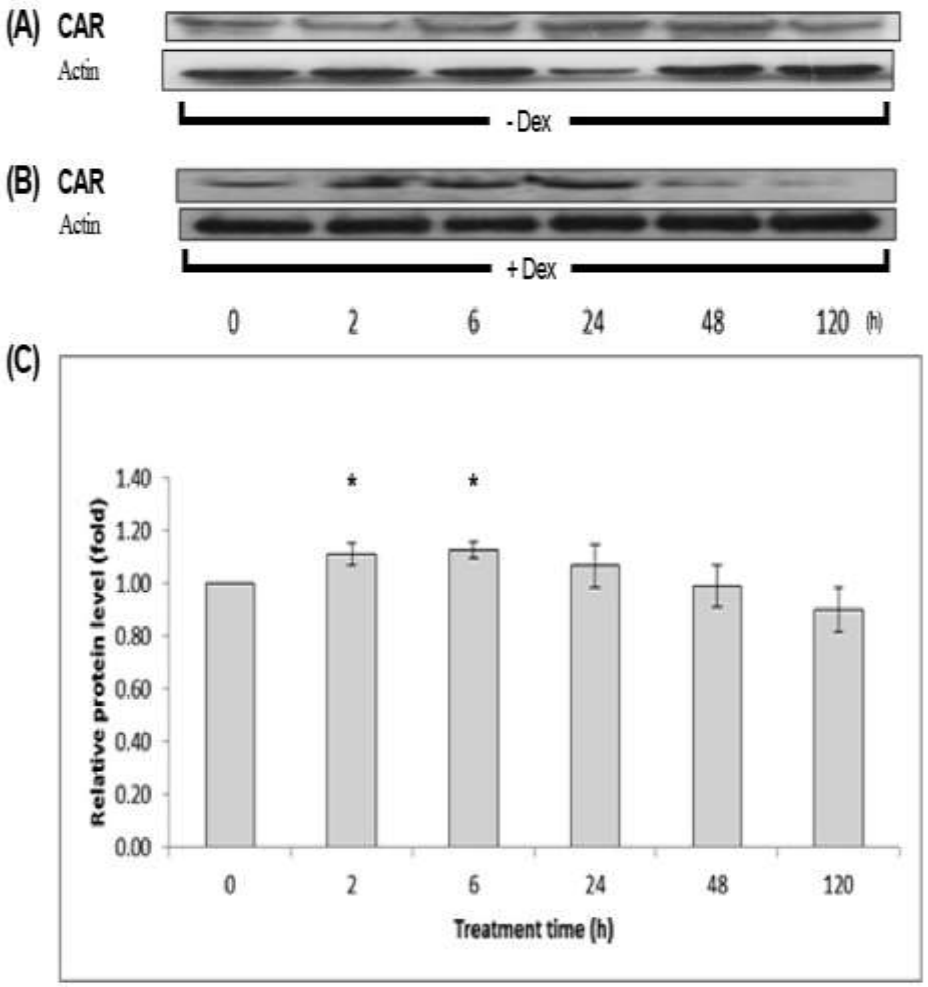

Figure 4.8: CAR protein levels in HepG2 cells

(A) HepG2 cells were treated only with vehicle for the indicated time points. Subsequent to the treatment, cells were harvested with high salt lysis buffer and equal amount of protein lysate was loaded and resolved on 10% PAGE. Antibodies targeting CAR and actin were used to detect the respective proteins. Actin was used as loading control. (B) HepG2 cells were treated with 0.1 µM Dex for the indicated time points and processed the same way as that described in (A). Data shown in (A) and (B) panels are representative of 3 independent experiments. (C) Densitometric analysis carried out using Image J to measure the intensity of each CAR and actin bands in panels (A) and (B).

The intensity of the CAR band was normalized to the intensity of the corresponding actin band for each time point and the average of three independent experiments was plotted.

The values and the results plotted have been analysed as described in Figure 4.3. Error bars represent standard deviations of three independent experiments. The asterisks indicate a statistically significant difference of $p < 0.05$.

CAR relative protein levels showed statistically significant induction at 2 and 6 h after treatment with Dex and then the protein levels decreased at the following time points (Figure 4.8).

4.2.7 P-gp protein levels

Responses to GC hormones may be affected by several mechanisms such as the control of GC bioavailability by the efflux transporter, P-gp (Meijer et al., 2003).

Western blot analysis of P-gp protein levels in Dex treated cells relative to untreated cells and actin as the internal control. One representative blot is shown at the indicated time points (Figure 4.9).

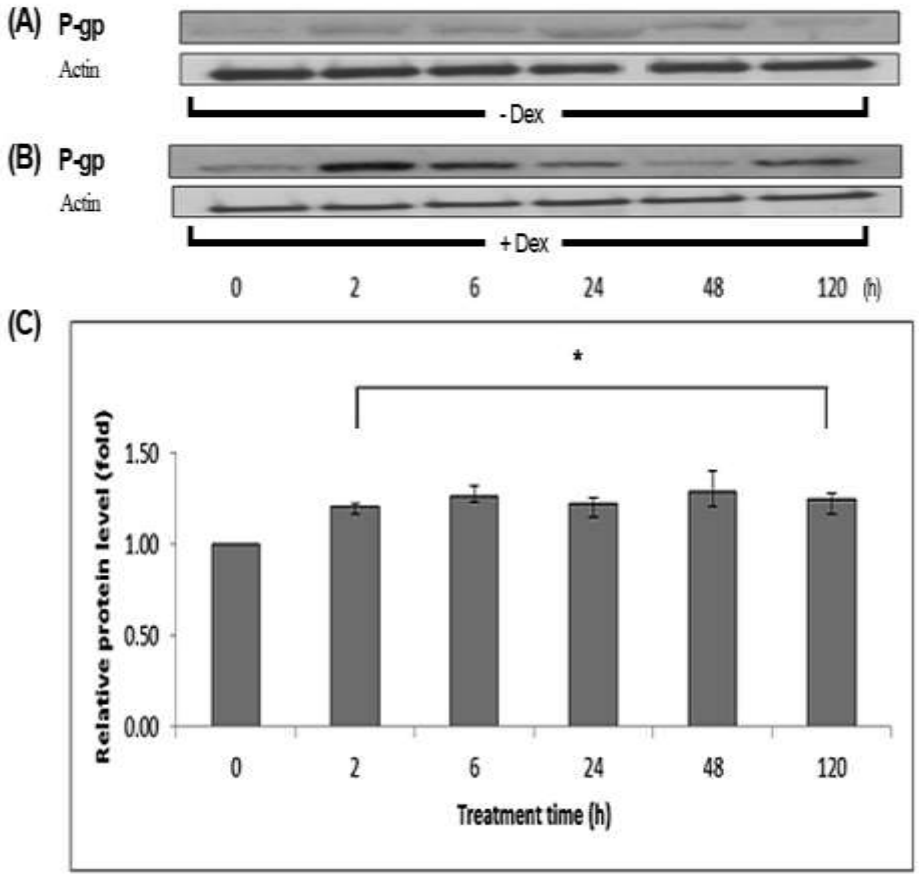

Figure 4.9: P-gp protein levels in HepG2 cells

(A) HepG2 cells were treated only with vehicle for the indicated time points. Subsequent to the treatment, cells were harvested with high salt lysis buffer and equal amount of protein lysate was loaded and resolved on 7.5% PAGE. Antibodies targeting P-gp and actin were used to detect the respective proteins. Actin was used as loading control. (B) HepG2 cells were treated with 0.1 µM Dex for the indicated time points and processed the same way as that described in (A). Data shown in (A) and (B) panels are representative of 3 independent experiments. (C) Densitometric analysis carried out using Image J to measure the intensity of each P-gp and actin bands in panels (A) and (B).

The intensity of the P-gp band was normalized to the intensity of the corresponding actin band for each time point and the average of three independent experiments was plotted. The values and the results plotted have been analysed as

described in Figure 4.3. Error bars represent standard deviations of three independent experiments. The asterisks indicate a statistically significant difference of $p < 0.05$.

P-gp relative protein levels were significantly induced at all measured time points following treatment with 0.1 µM Dex (See Figure 4.9).

4.3 ROS levels

4.3.1 ROS levels with/without CYP3A4 or CYP2C9 inhibitors and/or Dex

Inflammatory conditions and reactive oxygen species have been shown to decrease the total amount of CYPs and inhibit their enzymatic activity, simultaneously producing oxidative stress (Proulx and du Souich, 1995; El-Kadi et al., 2000).

The abundance of CYP3A4 in human liver microsomes has shown that it plays an important role in producing ROS (Puntarulo and Cederbaum, 1998). It has been shown that low ROS levels produced by CYP3A4 influence the secretion of paracrine and autocrine factors in HepG2 cells (Zangar et al., 2011). A variety of human liver diseases is caused by the change in the production and secretion of amphiregulin (AmR), intracellular adhesion molecule 1 (ICAM1), matrix metalloprotease 2 (MMP2), platelet derived growth factor (PDGF) and vascular endothelial growth factor (VEGF) (Qin and Tang, 2004). The secretion of these proteins were found to be increased in connection with the amount of ROS produced (Zangar et al., 2011). CYP2C9 is an important source of ROS in coronary arteries (Givens et al., 2003). A study looking at the CYP2C9 inhibitor sulfaphenazole has shown that it reduced ischemia-reperfusion injury by reducing the superoxide level and also scavenging oxygen free radicals generated in the reperfused heart (Khan et al., 2007).

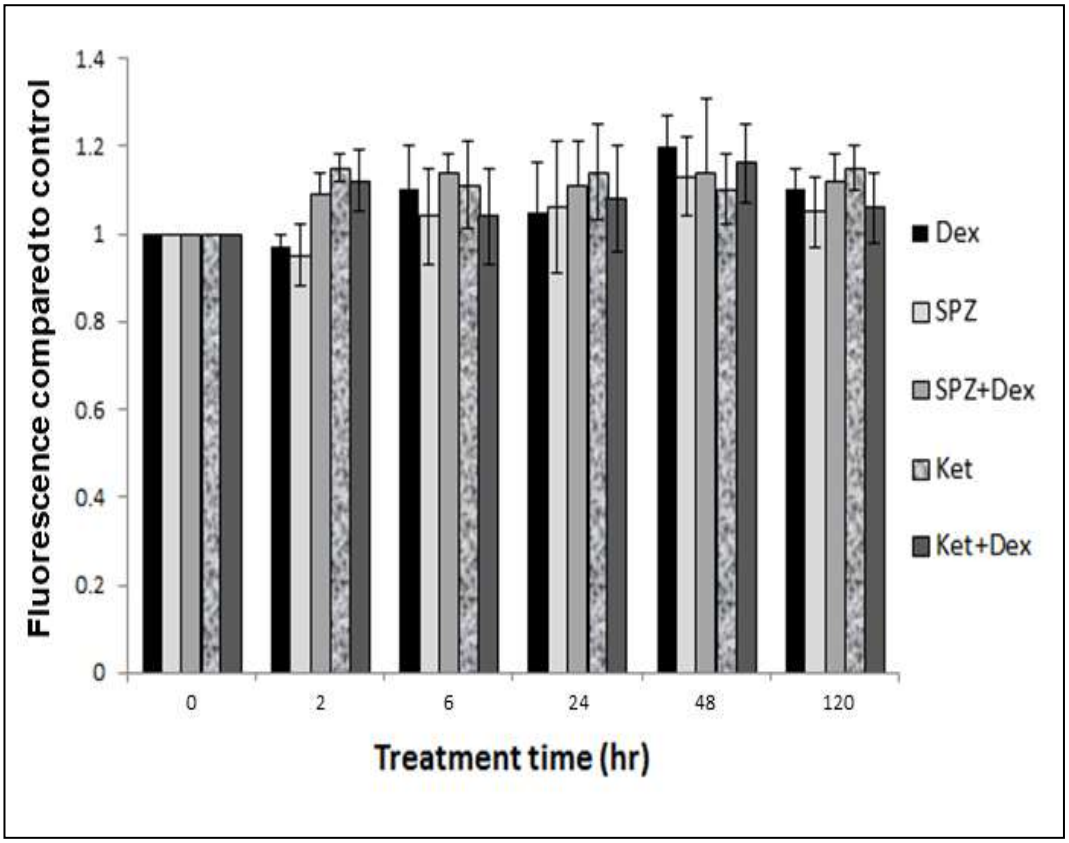

Figure 4.10: ROS levels measured in HepG2 cells treated with different compounds

The measurements were taken using flow cytometry to analyse the level of fluorescence indicative of ROS in the cells in three independent experiments. The absence of asterisk indicates no statistically significant difference of $p < 0.05$.

The levels of ROS were measured by flow cytometry in cells treated with 0.1 µM Dex, 0.3 µM SPZ, SPZ + Dex, 0.1 µM Ket and Ket + Dex. The results were calculated relative to untreated cells (Figure 4.10) and did not show any statistically significant change compared to control.

4.4 Enzymatic activity levels of CYP3A4 and CYP2C9 during treatment with 0.1 µM Dex

CYP3A4 and CYP2C9 enzymatic activity was initially measured by LC-MS and following the lack of success in sighting induction in HepG2 cells (data not shown), luminogenic cytochrome P450 assays were used by utilizing specific substrates for this method (P450-Glo™, Promega, USA). The assays couple CYP

enzyme activity to firefly luciferase luminescence and the luminometric substrates are derivatives of d-luciferin which are converted to d-luciferin by CYP enzymes (Cali et al., 2006).

4.4.1 CYP3A4 enzymatic activity levels

The substrate used for measuring enzymatic activity in HepG2 cells treated with Dex was Luciferin-IPA. This is the most sensitive and selective substrate for CYP3A4 and shows minimal cross-reactivity with CYP3A5 and 3A7 according to the manufacturer. CYP3A4 enzymatic activity and was selectively measured by this method (Figure 4.11).

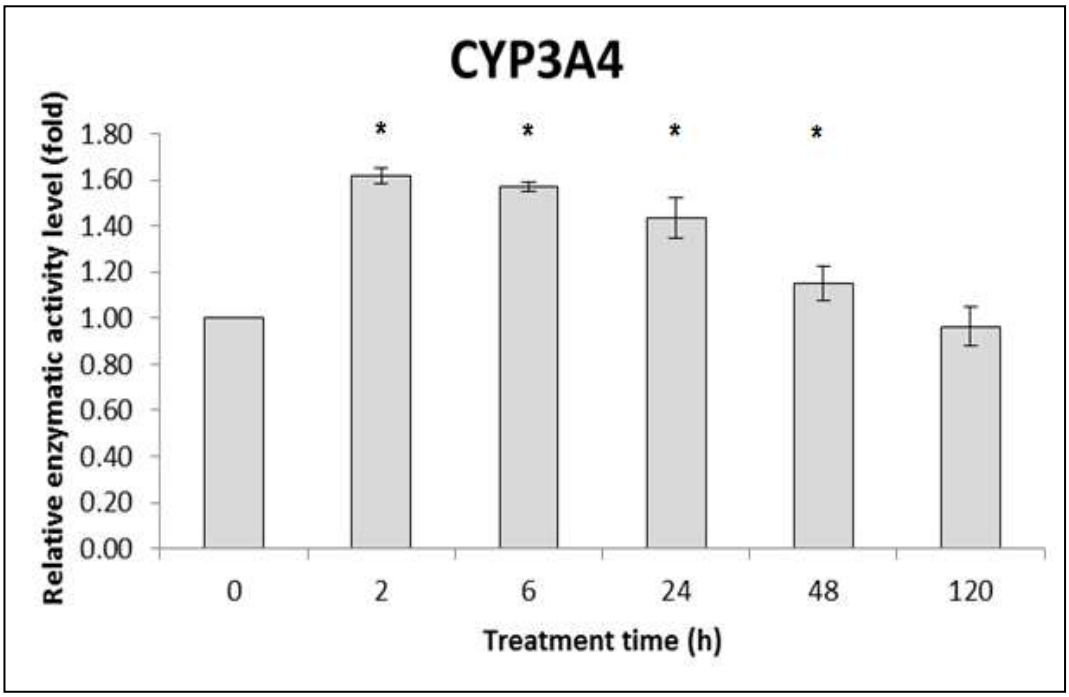

Figure 4.11: CYP3A4 enzymatic activity levels in HepG2 cells

Error bars represent standard deviations of three independent experiments. An asterisk indicates a statistically significant difference of $p < 0.05$.

The enzymatic activity measured of CYP3A4 after Dex treatment showed statistical significance at 2, 6, 24 and 48 h (Figure 4.11).

4.4.2 CYP2C9 enzymatic activity levels

The substrate used for measuring enzymatic activity in cells treated with Dex was by using the substrate Luciferin-H which is the most sensitive and selective substrate for CYP2C9 and shows minimal cross-reactivity with other CYP enzymes according to the manufacturer. CYP2C9 enzymatic activity was measured by this method (Figure 4.12).

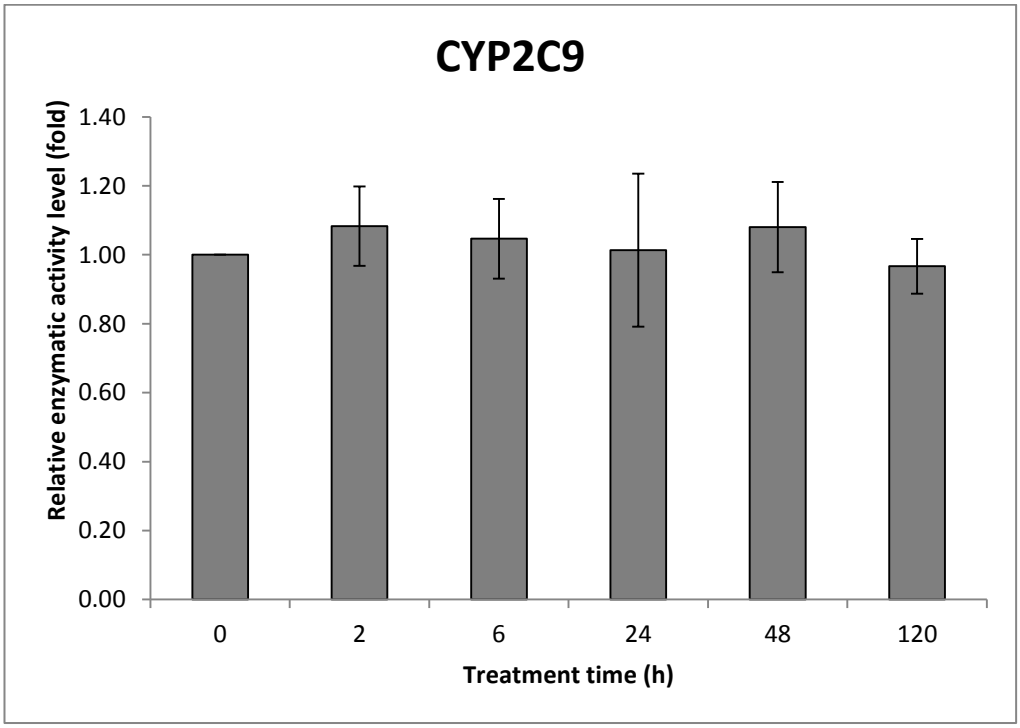

Figure 4.12: CYP2C9 enzymatic activity levels

Error bars represent standard deviations of three independent experiments. The absence of asterisk indicates no statistically significant difference of $p < 0.05$.

The enzymatic activity measured of CYP2C9 after Dex treatment showed no statistical significance at any time points measured (Figure 4.12).

Chapter 5: Results of high Dex concentration

The GC methylprednisolone can be used at a high dose short-term by oral or intravenous administration for 3 - 5 days (500 – 1000 mg daily) to speed up recovery from multiple sclerosis (MS) relapses (Myhr and Mellgren, 2009). These high concentrations can lead to mM concentrations of methylprednisolone in the blood (0.4 - 0.5 mM). The following data were obtained by treating HepG2 cells with 1.5 mM Dex for 120 h, and samples were collected at 0, 0.5, 1, 2, 6, 24, 48 and 120 h. The media was changed and Dex added again every 24 h to allow the assumption that the Dex concentration was constant throughout the experiments.

5.1 Effect of different Dex concentrations on mRNA levels of CYP3A4 and CYP2C9

Some studies have been conducted in GC responsive and GC resistant leukaemia cells looking at GC-induced apoptosis in acute lymphoblastic leukaemia by a systems biology approach (Chen et al., 2010; Chen et al., 2012). Other modelling techniques have used *in vivo* studies in rats to monitor the effects of Dex or other GCs on mRNA, protein and enzymatic activity (Hazra et al., 2007a; Sukumaran et al., 2011; Li et al., 2012). The *in vivo* research looked at higher GC concentrations and we investigated the effect of 0.15 – 15 mM concentrations of Dex on CYP3A4 and CYP2C9 mRNA levels in human HepG2 cells at 30 min and 2 h.

5.1.1 CYP3A4 and CYP2C9 mRNA levels after 30 min treatment with Dex

To investigate gene expression of CYP3A4 and CYP2C9 enzymes in HepG2 cells treated with 0.00015 – 15 mM Dex, the mRNA levels of CYP3A4 and CYP2C9 were determined by qRT-PCR.

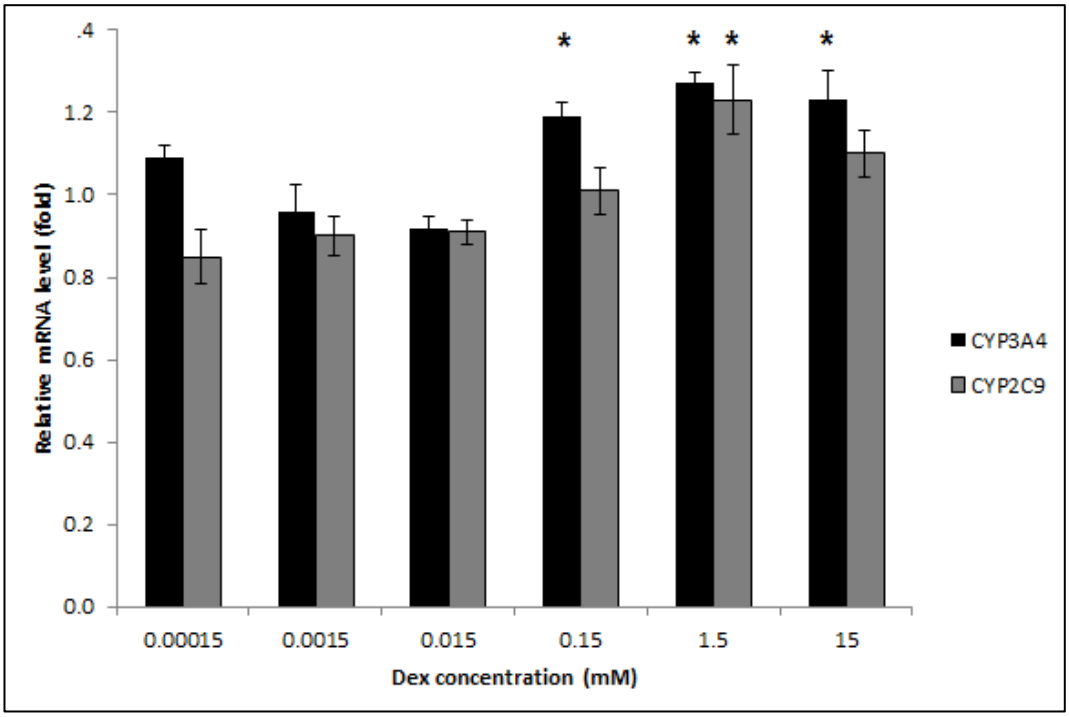

Figure 5.1: CYP3A4 and CYP2C9 mRNA levels after 30 min treatment with Dex

qRT-PCR analysis of CYP3A4 and CYP2C9 mRNA levels in Dex treated HepG2 cells. Total RNA from HepG2 cells treated with 0.00015, 0.0015, 0.015, 0.15, 1.5 and 15 mM Dex for 30 min or untreated was extracted and reverse transcribed. The cDNAs were then subjected to qRT-PCR using specific primers amplifying CYP3A4 mRNA. Rpl19 was used as an internal control. The data were analysed by the Opticon Monitor 3 and are representative of two independent experiments each performed in duplicates. CYP3A4 and CYP2C9 mRNA levels in Dex treated cells relative to untreated cells were normalised to RPL19 at different Dex concentrations after 30 min treatment. Error bars represent standard deviations of two independent experiments. An asterisk indicates a statistically significant difference of $p < 0.05$.

Statistically significant induction of CYP3A4 mRNA levels was observed in HepG2 cells treated with 0.15, 1.5 and 15 mM Dex for 30 min (Figure 5.1) whilst induction of CYP2C9 mRNA levels was only statistically significant in HepG2 cells treated with 1.5 mM Dex for 30 min (Figure 5.1). The results indicated that Dex induced CYP3A4 and CYP2C9 gene expression in higher concentrations of

the hormone in accord with an *in vivo* published report in rats analysing CYP3A1/2 (Li et al., 2012).

5.1.2 CYP3A4 and CYP2C9 mRNA levels after 2 h treatment with Dex

To investigate gene expression of CYP3A4 and CYP2C9 enzymes in HepG2 cells treated with 0.00015 – 15 mM Dex, the mRNA levels of CYP3A4 and CYP2C9 were determined by qRT-PCR.

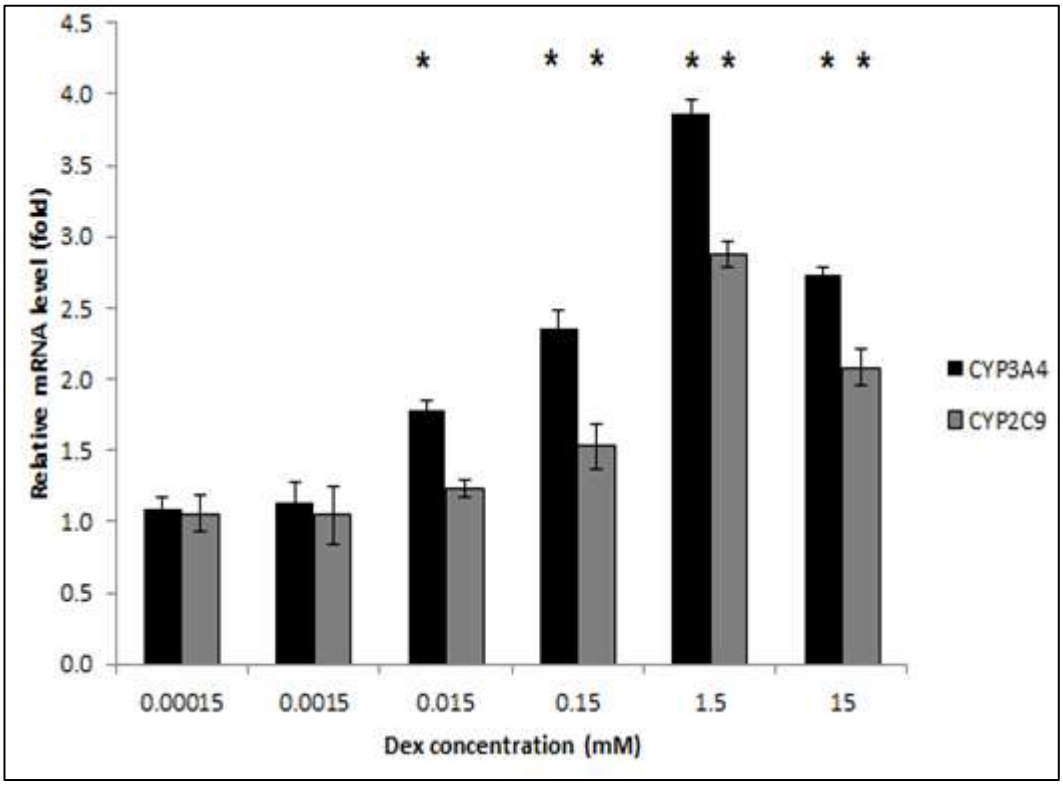

Figure 5.2: CYP3A4 and CYP2C9 mRNA levels after 2 h treatment with Dex

Total RNA from HepG2 cells treated with 0.00015, 0.0015, 0.015, 0.15, 1.5 and 15 mM Dex for 2 h or untreated, was extracted and reverse transcribed. The cDNAs were then subjected to qRT-PCR using specific primers amplifying CYP3A4 mRNA. Rpl19 was used as an internal control. The data were analysed by the Opticon Monitor 3 software and are representative of two independent experiments each performed in duplicates. CYP3A4 and CYP2C9 mRNA levels in Dex treated cells relative to untreated cells were normalised to RPL19 at different Dex concentrations after 2 h treatment. Error bars represent standard deviations of two independent experiments. An asterisk indicates a statistically significant difference of $p < 0.05$.

Induction of CYP3A4 mRNA levels was observed in HepG2 cells treated with 0.015, 0.15, 1.5 and 15 mM Dex for 2 h (Figure 5.2). Induction of CYP2C9 mRNA levels was observed in HepG2 cells treated with 0.15, 1.5 and 15 mM Dex for 2 h (Figure 5.2).

The results indicated that Dex induced CYP3A4 and CYP2C9 gene expression in higher concentrations of the hormone in accord with *in vivo* published reports in rats analysing CYP3A1/2 (Li et al., 2012). CYP3A4 and CYP2C9 mRNA levels in Dex treated cells relative to untreated cells normalised to RPL19 at different Dex concentrations after 2 h treatment. The concentration of 1.5 mM Dex was found to have the most increase in both CYP3A4 and CYP2C9 mRNA levels whilst at 0.015 mM an increase was only observed in CYP3A4. The higher concentration of 15 mM still presented with statistically significant increases in both CYP3A4 and CYP2C9 mRNAs but less than the 10-fold lower concentration of 1.5 mM (Figure 5.2).

This experiment has shown that 1.5 mM Dex concentration is the most suitable to use in the following experiments for monitoring induction of CYP3A4 and 2C9 enzymes.

5.2 Assessment of CYP3A4 and CYP2C9 mRNA levels in hepatocytes treated with 1.5 mM Dex

5.2.1 qRT-PCR analysis of CYP3A4 mRNA levels

To investigate gene expression of CYP3A4 enzyme in HepG2 cells treated with 1.5 mM Dex the mRNA levels of CYP3A4 were determined by qRT-PCR.

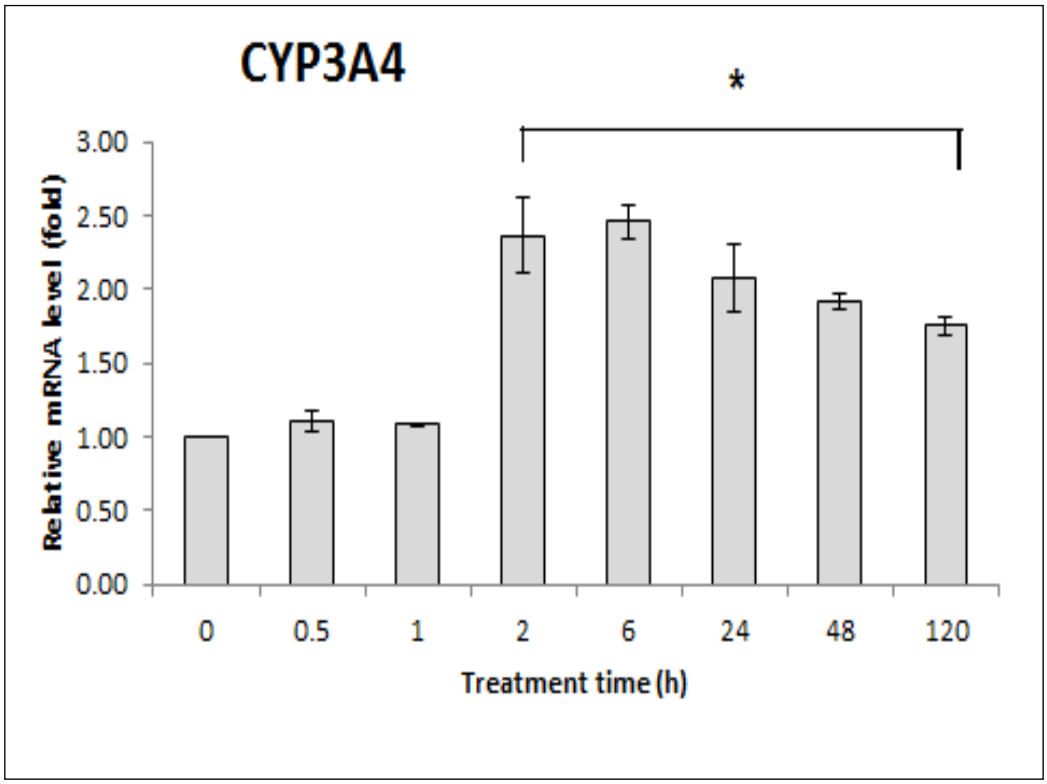

Figure 5.3: qRT-PCR analysis of CYP3A4 mRNA levels in 1.5 mM Dex treated HepG2 cells

Total RNA from HepG2 cells treated with 1.5 mM Dex for 0.5, 1, 2, 6, 24, 48 and 120 hours or untreated (0 h) as indicated was extracted and reverse transcribed. The cDNAs were then subjected to qRT-PCR using specific primers amplifying CYP3A4 mRNA. Rpl19 was used as an internal control. The data were analysed by the Opticon Monitor 3 software and are representative of two independent experiments each performed in duplicates. Error bars represent standard deviations of two independent experiments. An asterisk indicates a statistically significant difference of $p < 0.05$.

Induction of CYP3A4 mRNA levels was observed in HepG2 cells treated with Dex for 2 - 120 h but showed less induction at 24, 48 and 120 h Dex treatment (Figure 5.3). These results indicate that Dex induced CYP3A4 gene expression 2 h after the addition of the hormone in accord with published reports of *in vivo* studies in rats (Hazra et al., 2007a; Sukumaran et al., 2011; Li et al., 2012).

5.2.2 qRT-PCR analysis of CYP2C9 mRNA levels

To investigate gene expression of CYP2C9 enzyme in HepG2 cells treated with 1.5 mM Dex the mRNA levels of CYP2C9 were determined by qRT-PCR.

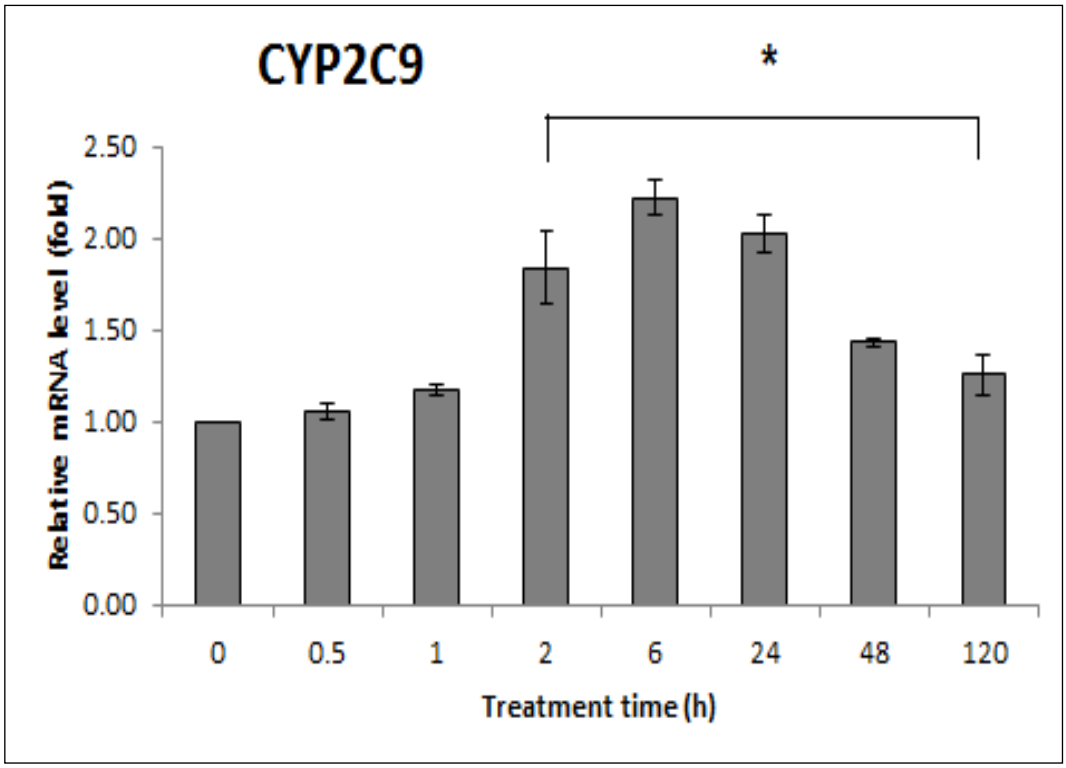

Figure 5.4: qRT-PCR analysis of CYP2C9 mRNA levels in Dex treated HepG2 cells

Total RNA from HepG2 cells treated with 1.5 mM Dex for 0.5, 1, 2, 6, 24, 48 and 120 hours or untreated (0 h) as indicated was extracted and reverse transcribed. The cDNAs were then subjected to qRT-PCR using specific primers amplifying CYP2C9 mRNA. Rpl19 was used as an internal control. The data were analysed by the Opticon Monitor 3 software and are representative of two independent experiments each performed in duplicates. Error bars represent standard deviations of two independent experiments. An asterisk indicates a statistically significant difference of $p < 0.05$.

As well as inducing CYP3A4, induction of CYP2C9 mRNA levels was observed in HepG2 cells treated with Dex for 2 - 120 h but showed less induction at 24, 48 and 120 h (compare Figure 5.3 and Figure 5.4). These results indicate that Dex

induced CYP2C9 and CYP3A4 gene expression 2 h after the addition of the hormone in accord with published reports of *in vivo* studies in rats (Hazra et al., 2007a; Sukumaran et al., 2011; Li et al., 2012).

5.3 Assessment of CYP3A4/5, CYP2C9, GR, phosphorylated GR at S211 and PXR protein levels in hepatocytes treated with 1.5 mM Dex

The levels of mRNA transcripts do not always correlate with the protein level (Maier et al., 2009). The protein levels are determined by the balance of RNA and protein production and turnover (Vogel and Marcotte, 2012). The main mechanisms controlling translation are transcript stability and protein degradation (Schwanhäusser et al., 2011; Chalancon et al., 2012). The control of gene expression mainly occurs by regulation of transcription initiation (Fickett and Hatzigeorgiou, 1997) whilst this does not regulate mRNA stability (Wilusz et al., 2001). The model can be more accurate with the inclusion of delays that are evident between the emergence of gene mRNA and the functional protein, which account for a number of intermediate biological steps such as translation. The levels of mRNA transcripts do not fully correlate with the protein level (Maier et al., 2009). The protein levels are determined by the balance of RNA and protein production and turnover.

Western blot analysis of CYP3A4, CYP2C9, GR, phosphorylated GR at S211, PXR protein levels (normalised to actin) in 1.5 mM Dex treated HepG2 cells relative to untreated cells was conducted to show the protein expression of these CYP enzymes and NRs.

5.3.1 CYP3A4/5 protein levels

Hepatic CYP3A4/5 is regulated by GR, CAR and PXR agonists (Xie et al., 2000; Sahi et al., 2009). GR binds indirectly to the promoter region of CYP3A4 and can induce the expression of a gene that does not hold a functional GRE in its promoter region and directly binds to the promoter region of CYP3A5 (Dvorak and Pavek, 2010). The antibody used for this protein level cannot distinguish between CYP3A4 and CYP3A5 isoforms, therefore the two proteins are measured together and are indicated as CYP3A4/5. The CYP3A4/5 protein levels were determined by western immunoblotting in HepG2 cells and quantification of the

intensity of the CYP3A4/5 bands compared to that of Actin for each time point using Image J densitometric analysis (Schneider et al., 2012) as described in details in the Materials and Methods section. Western blot analysis indicated of CYP3A4/5 protein levels in Dex treated cells relative to untreated cells and one representative blot is shown at the indicated time points (Figure 5.5).

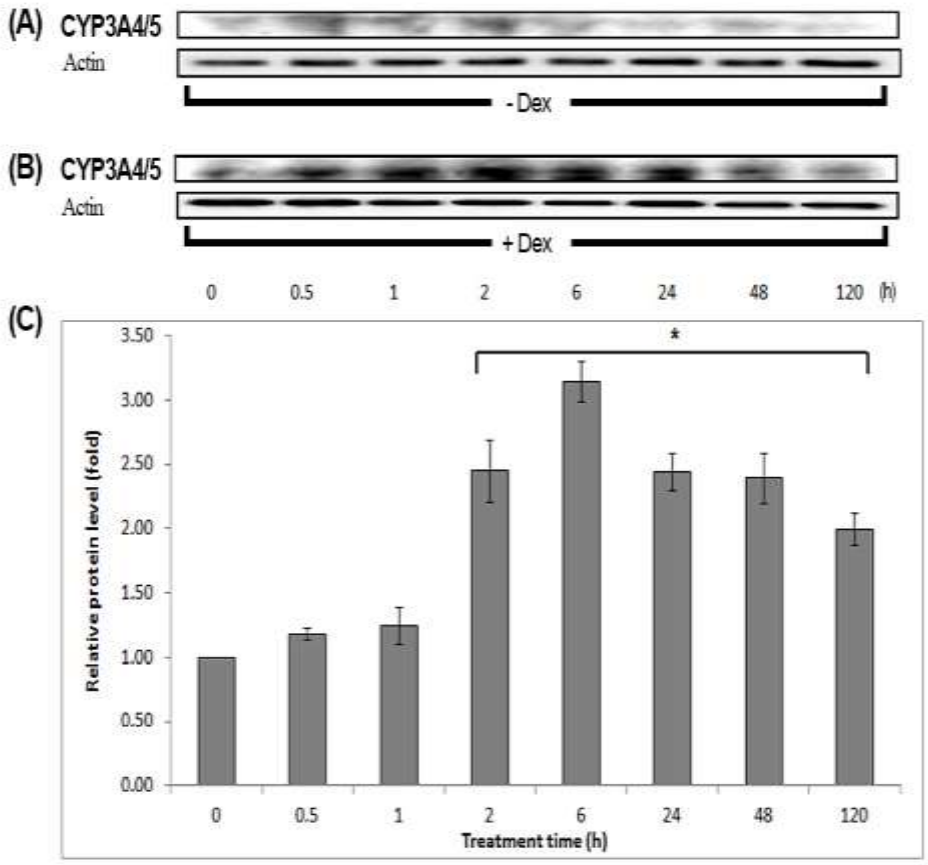

Figure 5.5: CYP3A4/5 protein levels in HepG2 cells treated with 1.5 mM Dex

(A) HepG2 cells were treated only with vehicle for the indicated time points. Subsequent to the treatment, cells were harvested with high salt lysis buffer and equal amount of protein lysate was loaded and resolved on 10% PAGE. Antibodies targeting CYP3A4/5 and actin were used to detect the respective proteins. Actin was used as loading control. (B) HepG2 cells were treated with 1.5 mM Dex for the indicated time points and processed the same way as that described in (A). Data shown in (A) and (B) panels are representative of two

independent experiments. (C) Densitometric analysis carried out using Image J to measure the intensity of each CYP3A4/5 and actin bands in panels (A) and (B).
The intensity of the CYP3A4/5 band was normalized to the intensity of the corresponding actin band for each time point and the average of two independent experiments was plotted.
The values and the results plotted have been analysed as described in Figure 4.3.
Error bars represent standard deviations of two independent experiments. The asterisks indicate a statistically significant difference of $p < 0.05$.

Statistically significant induction of relative CYP3A4/5 protein levels was observed at 2 - 120 h after treatment with 1.5 mM Dex and peaked at 6 h decreasing at the following time points (see Figure 5.5).

5.3.2 CYP2C9 protein levels

CYP2C9 is also regulated by agonists of GR, CAR and PXR in human hepatocytes (Sahi et al., 2009; Dvorak and Pavek, 2010) Dex can activate the CYP2C promoters in via GR and CYP2C9 is transcriptionally controlled by the direct binding of GR to the promoter sequence (Pascussi et al., 2003; Dvorak and Pavek, 2010)

Western blot analysis of CYP2C9 protein levels in Dex treated cells relative to untreated cells and one representative blot is shown at the indicated time points (Figure 5.6).

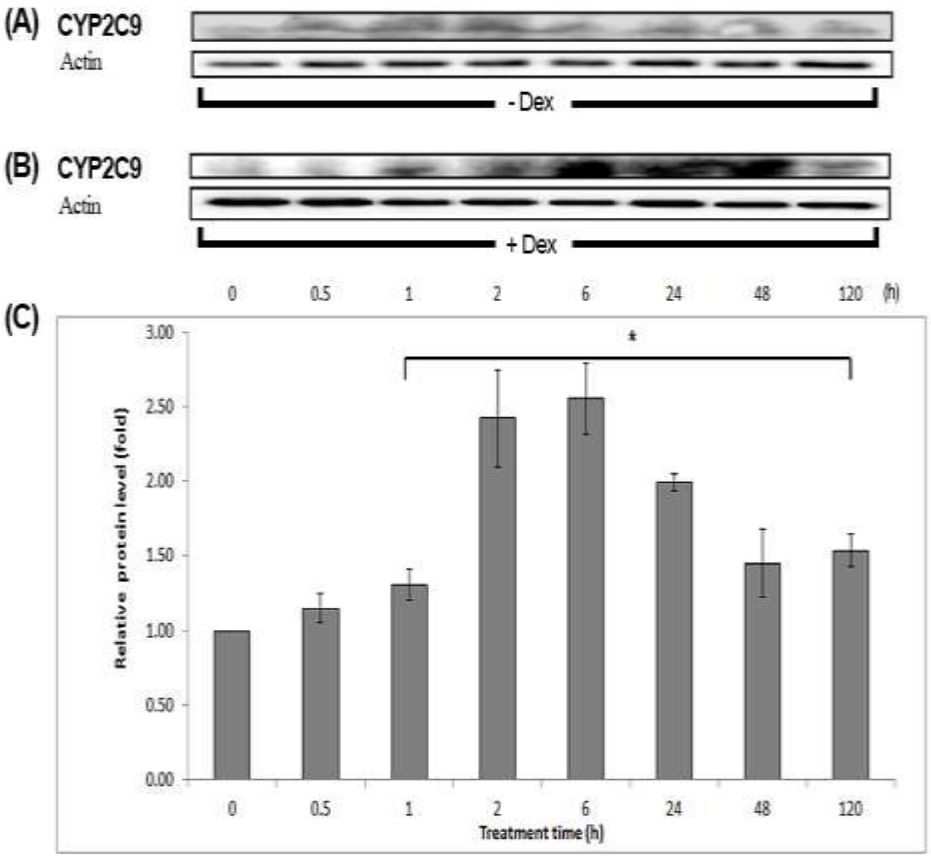

Figure 5.6: CYP2C9 protein levels in HepG2 cells treated with 1.5 mM Dex

(A) HepG2 cells were treated only with vehicle for the indicated time points. Subsequent to the treatment, cells were harvested with high salt lysis buffer and equal amount of protein lysate was loaded and resolved on 10% PAGE. Antibodies targeting CYP2C9 and actin were used to detect the respective proteins. Actin was used as loading control. (B) HepG2 cells were treated with 1.5 mM Dex for the indicated time points and processed the same way as that described in (A). Data shown in (A) and (B) panels are representative of two independent experiments. (C) Densitometric analysis carried out using Image J to measure the intensity of each CYP2C9 and actin bands in panels (A) and (B). The intensity of the CYP2C9 band was normalized to the intensity of the corresponding actin band for each time point and the average of two independent experiments was plotted.

The values and the results plotted have been analysed as described in Figure 4.3. Error bars represent standard deviations of two independent experiments. The asterisks indicate a statistically significant difference of $p < 0.05$.

Statistically significant induction of relative CYP2C9 protein levels was measured at 1 – 120 h after treatment with this 1.5 mM Dex and similar to CYP3A4 protein levels, the measurements peaked at 6 h and decreased at the following time points (compare Figure 5.5 and Figure 5.6).

5.3.3 GR protein levels

Western blot analysis of GR protein levels in Dex treated cells relative to untreated cells and a representative blot is shown at the indicated time points (Figure 5.7).

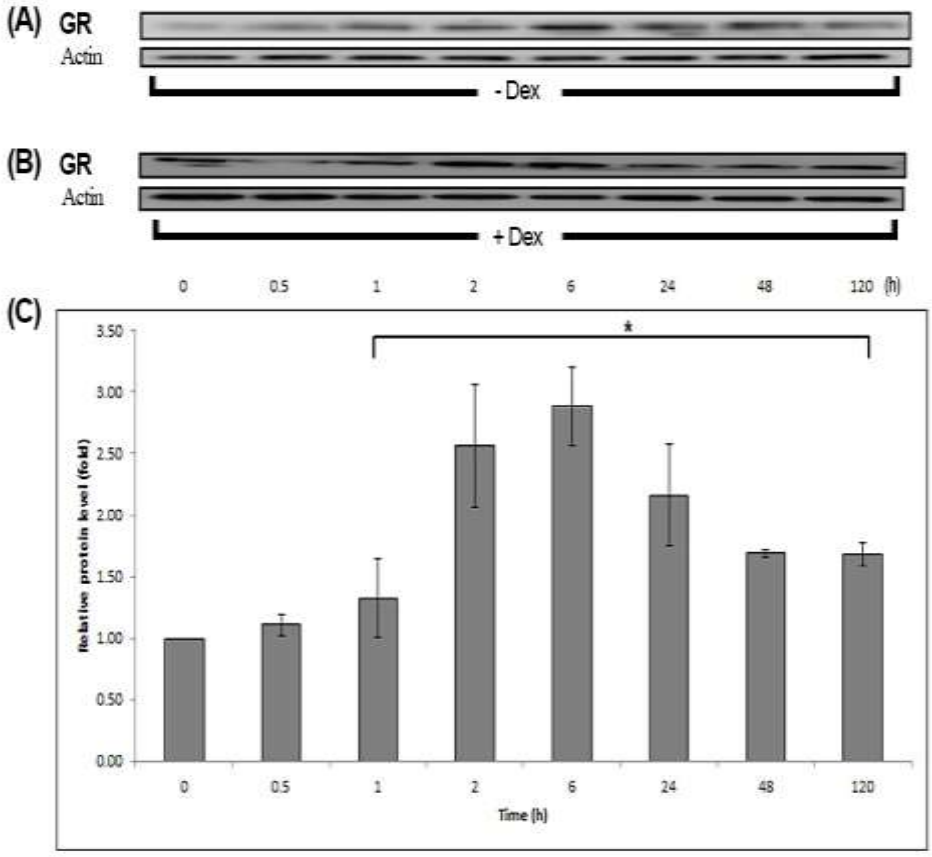

Figure 5.7: GR protein levels in HepG2 cells treated with 1.5 mM Dex

(A) HepG2 cells were treated only with vehicle for the indicated time points. Subsequent to the treatment, cells were harvested with high salt lysis buffer and equal amount of protein lysate was loaded and resolved on 10% PAGE. Antibodies targeting GR and actin were used to detect the respective proteins. Actin was used as loading control. (B) HepG2 cells were treated with 1.5 mM Dex for the indicated time points and processed the same way as that described in (A). Data shown in (A) and (B) panels are representative of two independent experiments. (C) Densitometric analysis carried out using Image J to measure the intensity of each GR and actin bands in panels (A) and (B). The intensity of the GR band was normalized to the intensity of the corresponding actin band for each time point and the average of two independent experiments was plotted.

The values and the results plotted have been analysed as described in Figure 4.3. Error bars represent standard deviations of two independent experiments. The asterisks indicate a statistically significant difference of $p < 0.05$.

Statistically significant inductions of relative GR protein levels were obtained after Dex treatment from 1 - 120 h (Figure 5.7).

5.3.4 Phosphorylated GR at S211 protein levels

Western blot analysis of S211 phosphorylated GR protein levels in Dex treated cells relative to untreated cells and one representative blot is shown at the indicated time points (Figure 5.8).

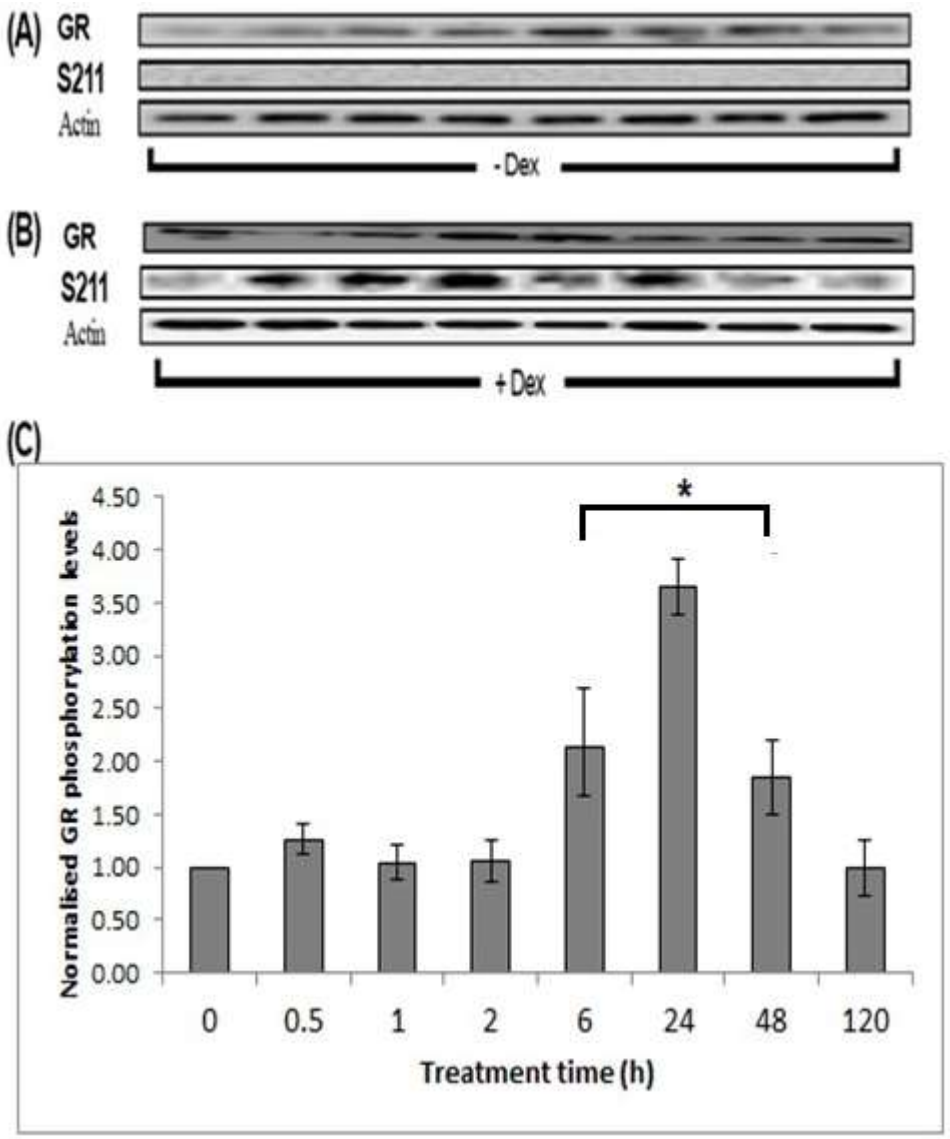

Figure 5.8: S211 phospho-GR protein levels in HepG2 cells treated with 1.5 mM Dex

(A) HepG2 cells were treated only with vehicle for the indicated time points. Subsequent to the treatment, cells were harvested with high salt lysis buffer and equal amount of protein lysate was loaded and resolved on 10% PAGE. Antibodies targeting GR, S211 phospho-GR and actin were used to detect the respective proteins. Actin was used as loading control. (B) HepG2 cells were treated with 1.5 mM Dex for the indicated time points and processed the same way as that described in (A). Data shown in (A) and (B) panels are representative of two independent experiments. (C) Densitometric analysis carried out using

Image J to measure the intensity of each GR, S211 phospho-GR and actin bands in panels (A) and (B).

The values and the results plotted have been analysed as described Figure 4.6. Error bars represent standard deviations of two independent experiments. The asterisks indicate a statistically significant difference of $p < 0.05$. The intensity of the S211 band was normalized to the intensity of the corresponding total GR and actin band for each time point and the average of two independent experiments was plotted.

Only the measurements at 6 – 48 h were found to be statistically significant. The values of phosphorylated GR at S211 compared to total GR were approximately 1.5 fold higher (compare Figure 5.7 and Figure 5.8).

5.3.5 PXR protein levels

PXR can regulate the expression of CYP3A4/5 and CYP2C9 gene activity and protein levels (Sahi et al., 2009).

Western blot analysis of PXR protein levels in Dex treated cells relative to untreated cells and one representative blot is shown at the indicated time points (Figure 5.9).

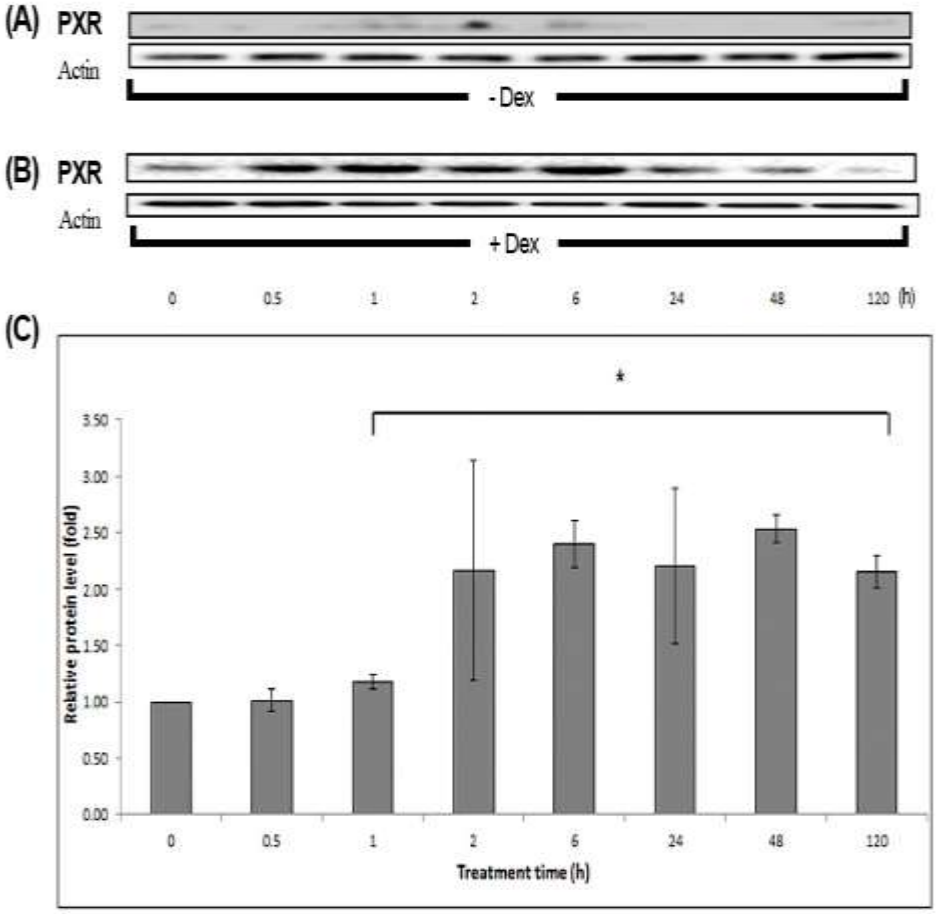

Figure 5.9: PXR protein levels in HepG2 cells treated with 1.5 mM Dex

(A) HepG2 cells were treated only with vehicle for the indicated time points. Subsequent to the treatment, cells were harvested with high salt lysis buffer and equal amount of protein lysate was loaded and resolved on 10% PAGE. Antibodies targeting PXR and actin were used to detect the respective proteins. Actin was used as loading control. (B) HepG2 cells were treated with 1.5 mM Dex for the indicated time points and processed the same way as that described in (A). Data shown in (A) and (B) panels are representative of two independent experiments. (C) Densitometric analysis carried out using Image J to measure the intensity of each PXR and actin bands in panels (A) and (B). The intensity of the PXR band was normalized to the intensity of the corresponding actin band for each time point and the average of two independent experiments was plotted.

The values and the results plotted have been analysed as described in Figure 4.3. Error bars represent standard deviations of two independent experiments. The asterisks indicate a statistically significant difference of $p < 0.05$.

Statistically significant inductions of relative PXR protein levels were obtained during the Dex treatment from 1 – 120 h (Figure 5.9).

5.4 Enzymatic activity levels of CYP3A4 and CYP2C9 during treatment with 1.5 mM Dex

5.4.1 CYP3A4 enzymatic activity levels

CYP3A4 enzymatic activity was measured by luciferase luminescence analysis. The substrate used for measuring enzymatic activity in HepG2 cells treated with Dex was Luciferin-IPA which is the most sensitive and selective substrate of CYP3A4 and shows minimal cross-reactivity with CYP3A5 and CYP3A7 according to the manufacturer. CYP3A4 enzymatic activity was selectively measured by this method (Figure 5.10).

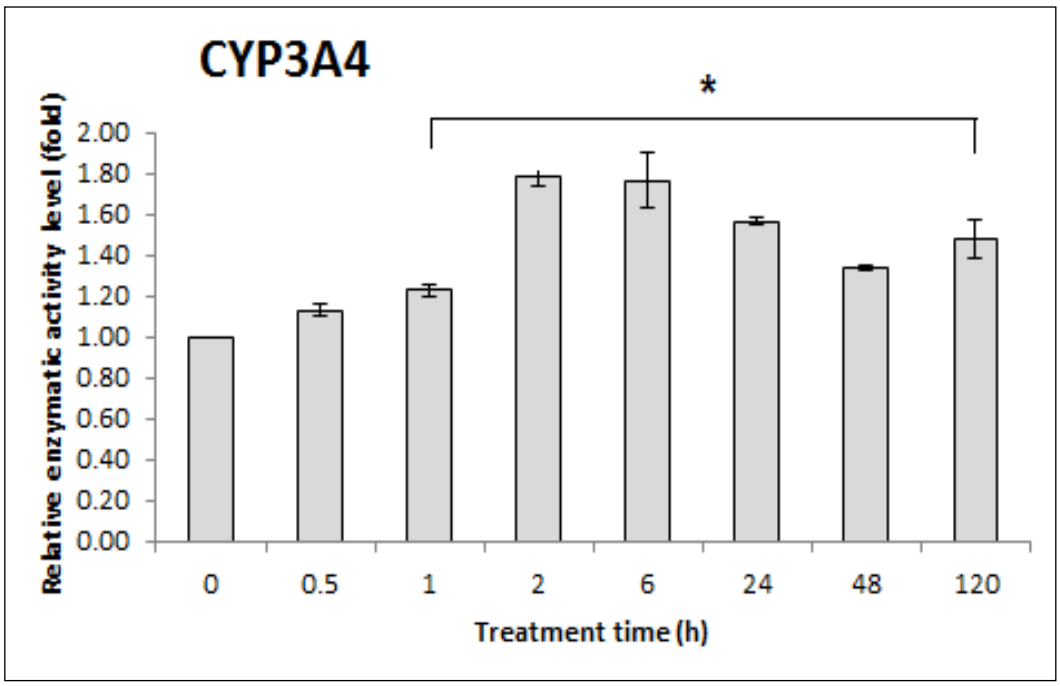

Figure 5.10: CYP3A4 enzymatic activity levels

Error bars represent standard deviations of two independent experiments. An asterisk indicates a statistically significant difference of $p < 0.05$.

The enzymatic activity of CYP3A4 is significantly increased following treatment of HepG2 cells with 1.5 mM Dex from 1 – 120 h (Figure 5.10).

5.4.2 CYP2C9 enzymatic activity level

CYP2C9 enzymatic activity was measured by luciferase luminescence analysis. The substrate used for measuring enzymatic activity in cells treated with Dex was by using the substrate Luciferin-H which is the most sensitive and selective substrate for CYP2C9 and shows minimal cross-reactivity with other CYP enzymes according to the manufacturer. CYP2C9 enzymatic activity was measured by this method (Figure 5.11).

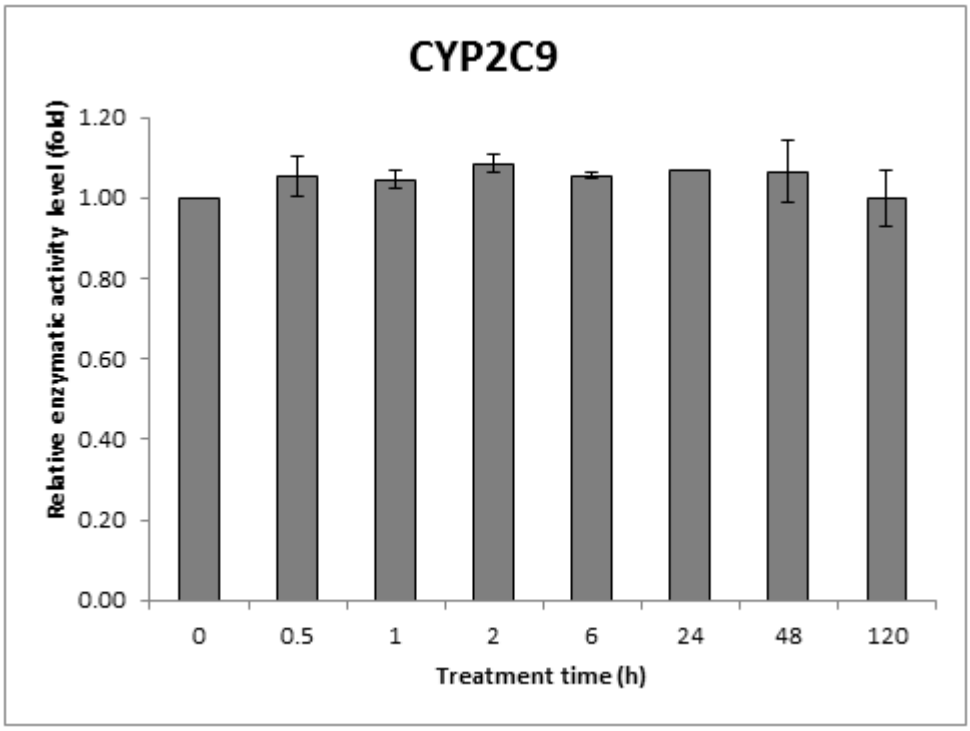

Figure 5.11: CYP2C9 enzymatic activity levels

Error bars represent standard deviations of two independent experiments. The absence of asterisk indicates no statistically significant difference of $p < 0.05$.

This analysis lacked the sensitivity to monitor the induction in CYP2C9 enzymatic activity of HepG2 cells, unlike that seen with the CYP3A4 enzyme in these cells treated with Dex at the same concentration and evaluated at the same time points (compare Figure 5.10 and Figure 5.11).

Chapter 6: Modelling of relative CYP3A4/5 and CYP2C9 mRNA, protein and enzymatic activity in Dex treated hepatocytes

The process of elevation of the cellular concentration and/or the consequent increase of the activity of an enzyme is called induction of this enzyme and usually occurs through mRNA or protein stabilization of this enzyme or increased gene transcription (Zanger and Schwab, 2013). Enzyme induction of CYP enzymes is usually a consequence of transcriptional activation of their gene expression, a process mediated by nuclear hormone receptors (Honkakoski and Negishi, 2000; Wang and LeCluyse, 2003; Qatanani and Moore, 2005; Tirona and Kim, 2005). Increased protein levels and enzymatic activities of CYP enzymes affect various pharmacokinetic parameters altering the hepatic clearance of drugs (reduced AUC, Cmax, and half-life) metabolized by these enzymes (Park et al., 2004; Mueller et al., 2006). Changes in AUC, Cmax and half-life caused by one drug might significantly alter the pharmacological effects of another which is co-administered or in some instances, such as in the case of Dex, the administered drug induces pharmacokinetic changes that affect its own pharmacological effects, a phenomenon known as auto-induction (Bertilsson et al., 1980; Simonsson et al., 2003). Taken into account the constantly increasing number of older adults using multiple prescription together with over the counter medications (Brown and Bussell, 2011) it is concluded that the drug-drug interactions occur more frequently as well as there is a need to design novel drugs with reduced risk of inducing the activity of metabolizing enzymes. Thus the development of a mathematical model enabling the prediction of the enzymatic activity of metabolizing enzymes and potential drug-drug interactions is useful in both clinical practice and pharmaceutical industry.

Transcriptional activation mediated by nuclear hormone receptors takes place in the presence of a ligand which activates the transcriptional activity of the receptor triggering its dissociation from transcriptional repressors in the cytoplasm and subsequent nuclear translocation and homo- or hetero- dimerization, and binding

to DNA in the DNA responsive element present on the regulatory region of the promoter of the target gene (Harmsen et al., 2007).

One of the technical concerns when developing mathematical models that would be able to predict induction and auto-induction of metabolizing enzymes is the selection of the appropriate biological system to study these phenomena taking into account the fact that results obtained in animal models are not entirely reproducible in humans and cells grown in cell culture are not accurate representations of physiological conditions. For the purpose of the present study the simple model of the human hepatocytes, HepG2 cells were used to assess the induction effects of Dex on CYP3A4/5 and CYP2C9.

6.1 The model using MATLAB software

The schematic model presented in Figure 6.1 indicates the ligand binding to GR and the transcriptional effects of the activated GR on CYP gene expression (mRNA), translation (protein) and enzymatic activity. The model has been adapted with modifications from two studies on the effects of the steroid methylprednisolone on GR in rats in (A) (Hazra et al., 2007a; Sukumaran et al., 2011) and a study on the effect of Dex on CYP3A1 and CYP3A2 in rats (B) (Li et al., 2012). (B) includes the use of laboratory results obtained experimentally in our study.

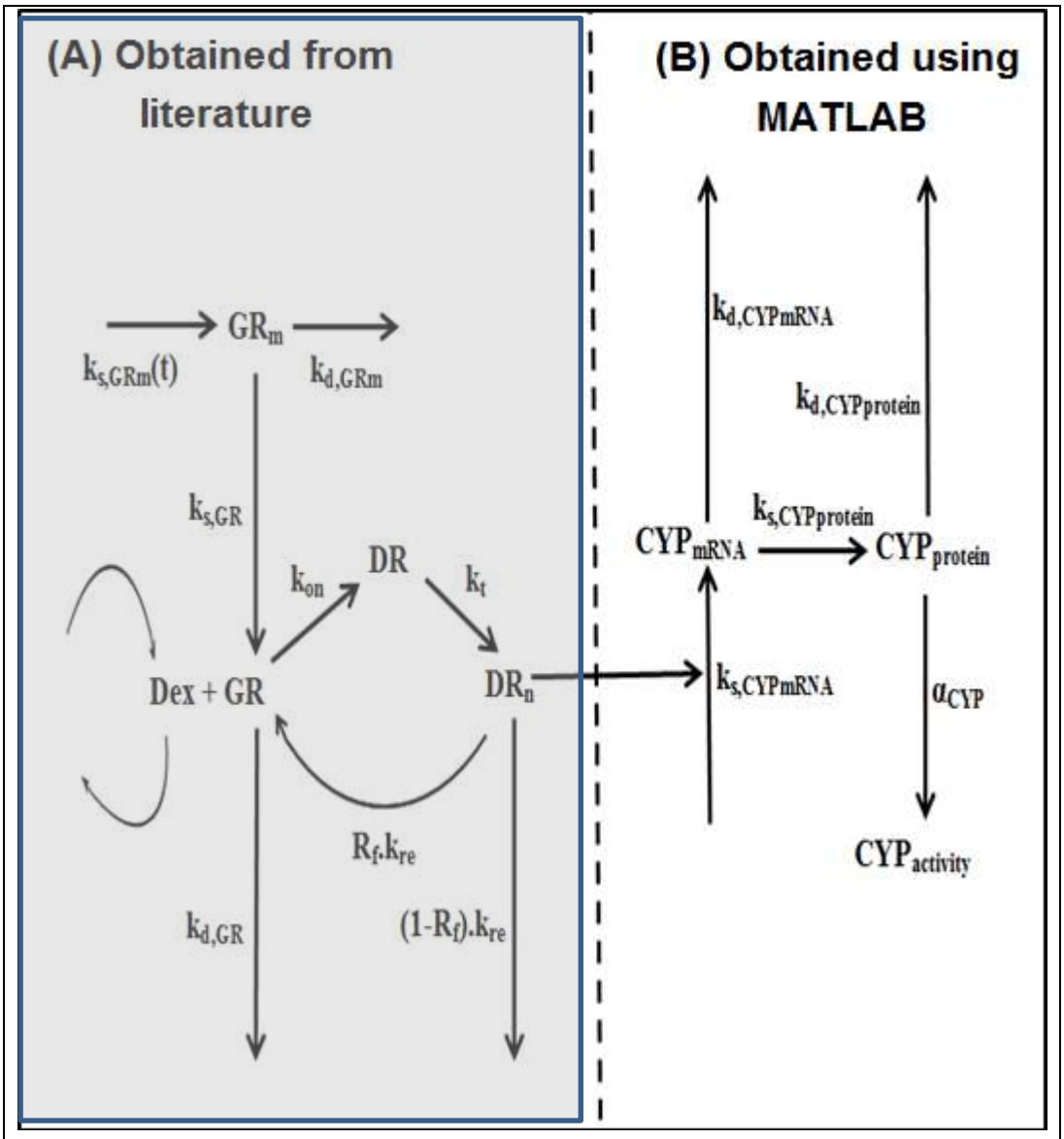

Figure 6.1: Schematic model of parameters from the literature and experimental values from laboratory data obtained in this study

Schematic model adapted from Hazra et al, 2007(b), Sukumaran et al., 2011 and Li et al., 2012 with modifications. Section (A) has been obtained from the literature and section (B) includes laboratory data measured to represent CYP induction.

The parameters used in this schematic are listed in Table 6.1.

GR is produced from its mRNA by a first-order rate constant of free receptor from the translation of GR mRNA which is time-dependent ($k_{s,GRm}(t)$). The time-dependent production rate constant was described by a two harmonics function. It was then degraded by a first-order rate constant (k_d,*GR*). R represents the free cytosolic receptor which can interact with the free ligand to form the drug-receptor complex in the cytosol (DR) and this complex translocates to the nucleus with a first order rate constant k_t, forming DR_n. This drug-receptor complex may recycle back to the cytosol ($R_f.k_{re}$) or may degrade with rate constant of $(1-R_f).k_{re}$.

DR_n in turn induces CYP3A4/5 and CYP2C9 gene expression by first-order rate constant (k_s,CYPm) which is degraded by a first-order rate constant (k_d,CYPm). CYP_{mRNA} gives rise to CYP protein synthesis ($CYP_{protein}$) by a first-order rate constant (kd,$CYP_{protein}$). The synthesized stable CYP protein is active and is related to activity by a proportionality constant α_{CYP}.

$k_{s,GRm}(t)$	GR mRNA synthesised by a time-dependent synthesis rate
$k_{d,GRm}$	degradation rate of GR mRNA
$k_{s,GR}$	Synthesis rate constant of free receptor from the translation of GR mRNA
k_{on}	Rate constant for formation of the drug-receptor complex
$k_{d,GR}$	Rate constant for degradation of the free receptor
k_t	First order rate constant of translocation of the drug-receptor complex from the cytosol (DR) into the nucleus (DR_n)
$R_f.k_{re}$	Rate constant of some DR recycled back into the cytosol
$(1-R_f).k_{re}$	Rate constant of degradation
$k_{d,GR}$	Rate constant of GR protein degradation
$k_{in,CYPm}$	Transcription rate of CYP mRNA
$k_{out,CYPm}$	Degradation rate constant for CYP mRNA
$k_{s,CYPprotein}$	Rate constant of CYP protein synthesis
$k_{d,CYPprotein}$	Degradation rate constant for CYP protein
$\alpha_{,CYP}$	Enzymatic activity of CYP

Table 6.1: Parameters used in the schematic (Figure 6.1)

The differential equations and initial conditions (IC) that describe the schematic in Figure 6.1 were implemented in equations (1-11)

6.2 The data

The data were obtained by treating HepG2 cells with 0.001 mM or 1.5 mM Dex for 120 h, and samples were collected at 0, 0.5, 1, 2, 6, 24, 48 and 120 h (0.5 and 1h measurement were not taken for 0.0001 mM treatment). The media was changed and Dex added again every 24 h to allow the assumption that the Dex concentration was constant throughout the experiments. Data was also obtained for 0.5 and 2 h Dex treatment at a range of 10-fold change of concentrations between 0.00015 and 15 mM. The relative mRNA levels of these cells were analysed by qRT-PCR of CYP3A4 and CYP2C9 in untreated cells providing the

fold change in Dex treated cells. The relative protein levels of CYP3A4/5 and CYP2C9 in HepG2 cellular extracts were obtained by densitometric analysis of the intensity of the respective bands on western blots normalised to actin for each time point. The fold change in Dex-treated cells was calculated by dividing the value obtained from the normalised densitometric value of the CYP/actin bands in the control (untreated) cells at the same time point. The enzymatic activity of CYP3A4 and CYP2C9 was assessed by luminogenic cytochrome P450 assays using specific substrates for each CYP enzyme specified and calculated as fold change between Dex-treated versus untreated cells. All the experimental data obtained were used for parameter estimation. The units used for all of the values obtained from these experiments were arbitrary and this is how they were used in modelling. The data collected for the different Dex concentrations are included in appendices 3 - 5.

6.3 Parameter estimation using MATLAB software

The differential equations and initial conditions (IC) that describe the model above (Figure 6.1) were implemented as follows:

$$\frac{dGRm}{dt} = k_{s,GRm}(t) - k_{d,GRm}.GR_m \qquad IC=GR_m(0) \tag{1}$$

The production rate constant was time-dependent and described by a two-harmonics function:

$$k_{s,GRm}(t) = a_{0,GRm} \cdot k_{d,GRm} + \left(a_{1,GRm} \cdot k_{d,GRm} + \frac{2\pi b_{1,GRm}}{24}\right) \cdot \cos\left(\frac{2\pi T}{24}\right)$$

$$+ \left(b_{1,GRm} \cdot k_{d,GRm} + \frac{2\pi a_{1,GRm}}{24}\right) \cdot \sin\left(\frac{2\pi T}{24}\right) + \left(a_{2,GRm} \cdot k_{d,GRm}\right.$$

$$+ \frac{2\pi b_{2,GRm}}{12} \cdot \cos\left(\frac{2\pi T}{12}\right) + \left(b_{2,GRm} \cdot k_{d,GRm} + \frac{2\pi a_{2,GRm}}{12}\right) \cdot \sin\left(\frac{2\pi T}{12}\right) \tag{2}$$

a_1, a_2, b_1 *and* b_2 are Fourier coefficients associated with harmonic oscillations.

The harmonics function was taken from a previously published paper on GR using GC methylprednisolone in rats and utilising circadian rhythms to model the effects on the glucose / fatty acid / insulin system (Sukumaran et al., 2011).

$$\frac{dR}{dt} = k_{s,GR}..GR_m - k_{d,GR}..R\text{-}k_{on.}..Conc.R + k_{re}.R_{f.DR}\,DR_n \quad IC=R(0) \qquad (3)$$

Where Conc is the concentration of Dex.

$$\frac{dDR}{dt} = k_{\text{on}}.Conc.R - k_{\text{t.DR}}.\text{DR} - k_{\text{on}}.DR \quad IC=DR(0) \qquad (4)$$

$$\frac{dDRn}{dt} = k_t.DR - k_{re}.DR_n \quad IC=DR_n(0) \qquad (5)$$

$$\frac{dCYP3A4m}{dt} = k_{\text{in}}.(1 + \text{slo\_mRNA}.\text{DR}_n) - k_{\text{out}}.CYP3A4_{\text{m}} \quad \text{slo\_mRNA=1} \qquad (6)$$

slo_mRNA describes the delay in transcription.

IC for CYP mRNA compartment = $\frac{kin}{kout}$

IC for CYP proteins= $\frac{ksyn}{kdeg}.\frac{kin}{kout}^{m}$

M is the amplification factor

$$\frac{dCYP3A4protein}{dt} = k_{\text{syn}}.CYP3A4mRNA^m - k_{\text{deg}}.CYP3A4_{\text{protein}} \qquad (7)$$

$$\text{CYP3A4\_act} = \alpha.\text{CYP3A4}_{\text{protein}} \qquad (8)$$

Where CYP3A4/2C9_act was enzymatic activity and described to be proportional to protein concentrations.

$$\frac{dCYP2C9m}{dt} = k_{\text{in}}.(1 + \text{slo\_mRNA}.\text{DR}_n) - k_{\text{out}}.CYP2C9_{\text{m}} \quad \text{slo\_mRNA=1} \qquad (9)$$

$$\frac{dCYP2C9protein}{dt} = k_{\text{syn}} . CYP2C9mRNA^{m} - k_{\text{deg}}.CYP2C9_{\text{protein}} \quad (10)$$

$$\text{CYP2C9\_act} = \alpha .CYP2C9_{\text{protein}} \quad (11)$$

Equation (1) describes the production of GR protein from its mRNA and its degradation. Equation (2) describes time-dependent two-harmonics function of the GR production rate constant. The production of the receptor is described in equation (3) and the formation and the separation of the DR complex is shown in equation (4). The translocation of DR to the nucleus is described by equation (5). Equations (6) - (11) relate to the mRNA, protein and enzymatic activity levels of CYP3A4/5 and CYP2C9. The equations were solved using the ODE45 solver.

The differential equations were implemented in MATLAB (R2013a 8.1.0.604. The MathWorks Inc., USA) and parameter estimation was performed using the lsqnonlin nonlinear least squares optimisation function. The difference between the observed data and model prediction was weighted by the prediction at each time point and used to calculate a final objective function of the sum of the squared weighted differences which was subsequently minimised. The objective function was derived for simultaneous fitting of all the data; mRNA, protein and activity separately for CYP3A4 and CYP2C9. The relative standard errors (SE) were calculated as described by Landaw and DiStefano (Landaw and DiStefano, 1984). The standard error (SE) is the standard deviation of the sampling statistical measure, which is usually the sample mean. The standard error measures how accurately the sample represents the actual population from which the sample was drawn.

6.4 Results of parameter estimation

6.4.1 Final parameter estimates

The estimated parameters (obtained from (Sukumaran et al., 2011) and the measured experimental parameters acquired by fittings of the models to the data are listed in Table 6.2.

Parameter	Definition	Estimate	SE
$a_{0,GRm}$	Fourier coefficient for GR mRNA	2215.9	Fixed
$a_{1,GRm}$	Fourier coefficient for GR mRNA	-273.2	Fixed
$a_{2,GRm}$	Fourier coefficient for GR mRNA	65.91	Fixed
$b_{1,GRm}$	Fourier coefficient for GR mRNA	-10.86	Fixed
$b_{2,GRm}$	Fourier coefficient for GR mRNA	10.08	Fixed
kd,GRm	Loss rate for GR mRNA	0.3117	Fixed
$k$on	Association constant	0.016	Fixed
$k$re	Loss rate constant for DRn	1.31	Fixed
Rf	Recycling factor for DRn	0.93	Fixed
kt	Translocation rate for DR	58.2	Fixed
GRm(0)	GR mRNA initial concentration (control)	2050	Fixed
GR	GR mRNA initial concentration (drug treatment)	2200	Fixed
$k_{s,R}$	Rate constant of receptor protein synthesis	0.00057	0.00025
$k_{d,GR}$	Rate constant of GR protein degradation	0.0708	0.65105
$k_{in,CYPm}$	Transcription rate of CYP mRNA	1.1098	0.27505
$k_{out,CYPm}$	Degradation rate constant for CYP mRNA	0.89595	0.23634
$k_{s,CYPprotein}$	Rate constant of CYP protein synthesis	1.6275	1.4499
$k_{d,CYPprotein}$	Degradation rate constant for CYP protein	1.6114	1.4328
m	Amplification factor	0.96013	0.14383
$\alpha_{,CYP}$	CYP enzymatic activity	0.97153	0.06118

$k_{s,R}$	Rate constant of receptor protein synthesis	0.00018	0.00038
$k_{d,GR}$	Rate constant of GR protein degradation	0.73901	305.39
$k_{in,CYPm}$	Transcription rate of CYP mRNA	0.56827	0.0988
$k_{out,CYPm}$	Degradation rate constant for CYP mRNA	0.50751	0.0945
$k_{s,CYPprotein}$	Rate constant of CYP protein synthesis	14.927	67.329
$k_{d,CYPprotein}$	Degradation rate constant for CYP protein	13.298	60.058
m	Amplification factor	0.77036	0.1258
$\alpha_{,CYP}$	CYP enzymatic activity	0.78575	0.0376

Table 6.2: Parameters that describe the model

The parameters with dark grey background have been taken from published data (Sukumaran et al., 2011), the parameters with light grey and white backgrounds have been estimated by fitting the data obtain in this study for CYP3A4/5 and CYP2C9, respectively.

6.4.1.a Modelling of CYP3A4 mRNA levels in hepatocytes treated with different Dex concentrations

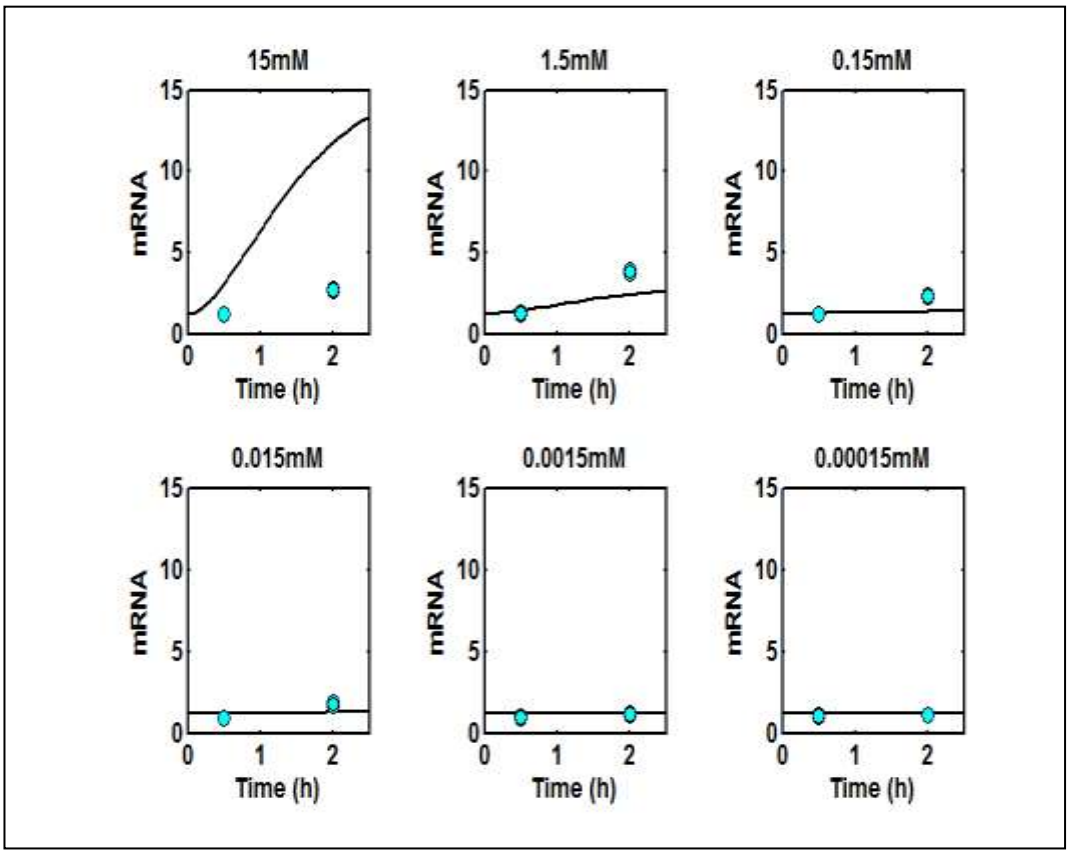

Figure 6.2: Experimental data and predictions of CYP3A4 mRNA levels

The relative mRNA level of CYP3A4 measured by qRT-PCR showed no increase in Dex-treated cells compared to control at 0.00015 - 0.015 mM Dex concentration. There was a slight increase in the experimental data and the prediction at 0.15 and 1.5 mM. The prediction at 15 mM was significantly over-predicted compared to the experimental data obtained.

6.4.1.b Modelling of relative CYP3A4/5 mRNA, protein and enzymatic activity levels in hepatocytes treated with 0.0001 mM Dex

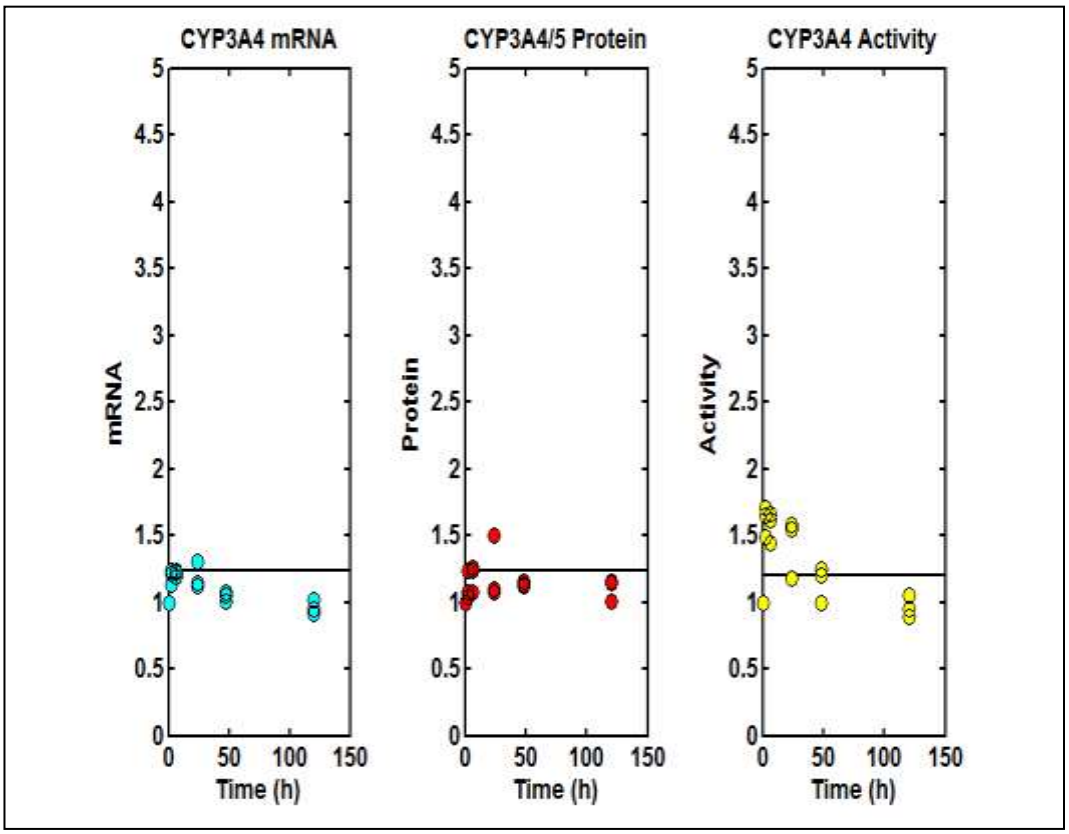

Figure 6.3: Experimental data for CY3A4/5 mRNA, protein and enzymatic activity levels in HepG2 cells treated with 0.0001 mM Dex

Figure 6.3 showed experimental data for relative CYP3A4 mRNA (blue circles), protein (red circles) and enzymatic activity (yellow circles) levels and the fittings obtained for the HepG2 cells treated with 0.0001 mM Dex.

The relative mRNA, protein and enzymatic activity levels for treatment at the low concentration of Dex showed a small degree of induction for all three classes of measurements. The mRNA levels peaked at approximately 2 – 6 h after Dex treatment and gradually decreased to baseline at the following time-points.

Protein levels were also induced at 6 and 24 h in Dex treated cells relative to untreated cells. This measurement returned to baseline at 120 h.

The enzymatic activity level experimentally showed the highest level of induction at approximately 2 – 6 h and slowly subsided at other treatment time points, returning to baseline at 120 h.

The predicting models for the three sets of data showed a constant induction of approximately 1.25 relative fold increases throughout the treatment period of 120 h for mRNA, protein and enzymatic activity levels.

6.4.1.c Modelling of relative CYP3A4/5 mRNA, protein and enzymatic activity levels in hepatocytes treated with 1.5 mM Dex

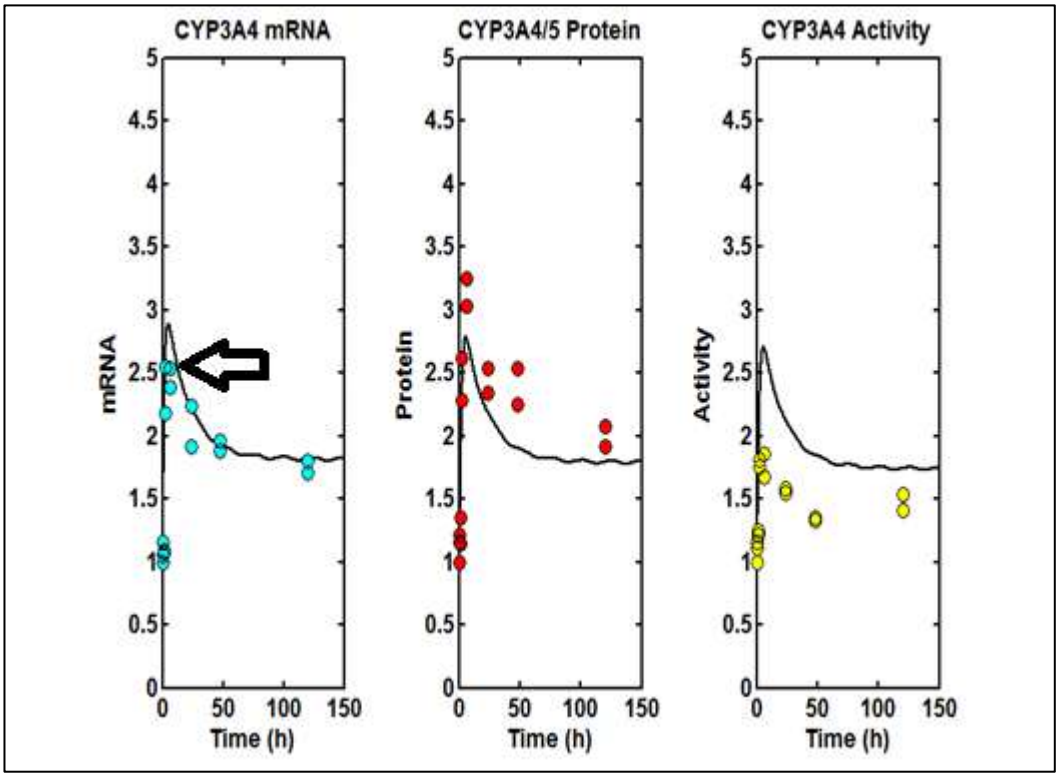

Figure 6.4: Experimental data for CY3A4/5 mRNA, protein and enzymatic activity levels in HepG2 cells treated with 1.5 mM Dex

Figure 6.4 showed experimental data for relative CYP3A4 mRNA (blue circles), protein (red circles) and enzymatic activity (yellow circles) levels and the fittings obtained for the HepG2 cells treated with 1.5 mM Dex.

The models for 1.5 mM Dex treatment were able to better capture the changes of mRNA, protein and enzymatic activity levels of the CYP3A4/5 data obtained. The

model for mRNA levels were reflective of the experimental data obtained and accurately followed the peak and decrease in mRNA at each time point. The maximum CYP3A4 mRNA measurements at 6 hours which are followed by decline at later time points are shown by the black arrow in the Figure. The model for protein levels was lower than the experimental data obtained from the laboratory.

The model for the enzymatic activity level was an over-prediction compared to experimental data due to the proportionality of the models between protein and enzymatic activity described previously. The models obtained were a compromise of under-predictions and over-predictions of the experimental protein and enzymatic activity levels respectively.

6.4.1.d Simulated profiles of GR, R, DR and DR_n dynamics controlling CYP3A4/5 regulation following treatment with 1.5 mM Dex

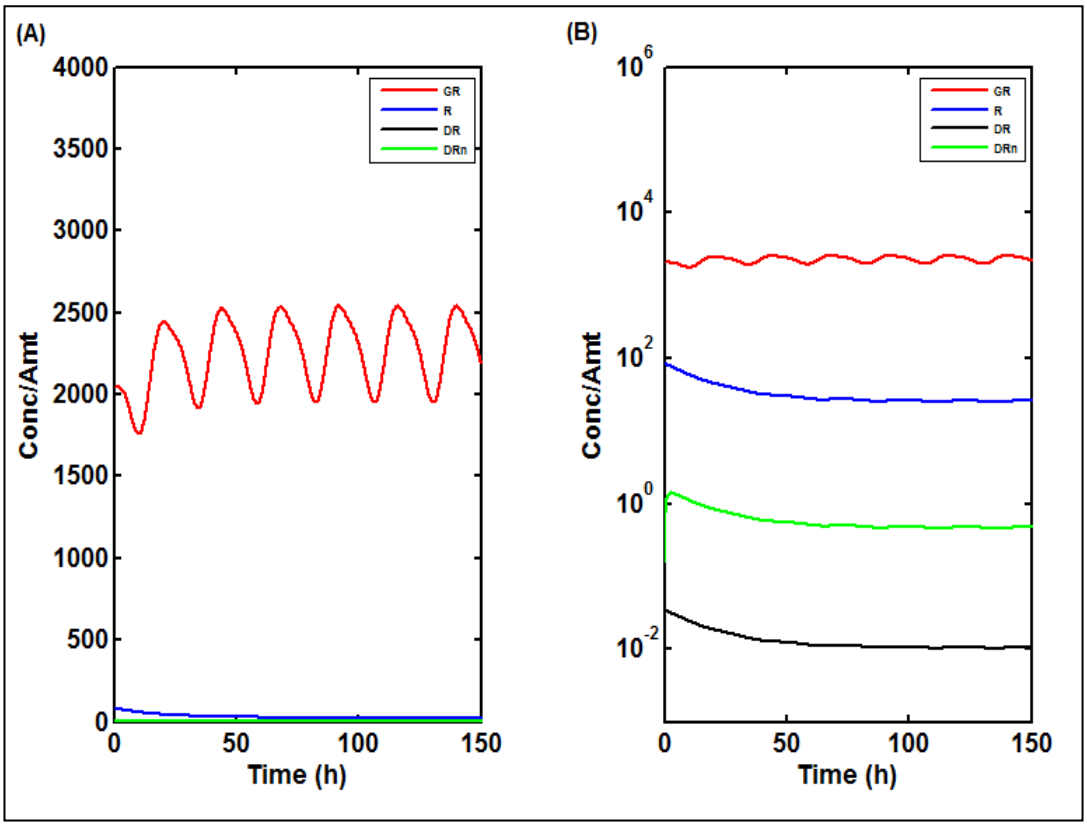

Figure 6.5: GR, R, DR and DR_n dynamics controlling CYP3A4/5 regulation

Figure 6.5 (A) is the normal simulated profile whilst Figure 6.5(B) is the semilog(y) profile displaying the changes of dynamics more clearly. The dynamics of GR in relation to CYP2C9 GR appear to oscillate with respect to Dex treatment over time and increase at each peak to reach a constant oscillation at 48h. R, DR and DRn begin at lower levels respectively and reach plateaus at approximately 50 h.

6.4.1.e Modelling of CYP2C9 mRNA levels in hepatocytes treated with different Dex concentrations

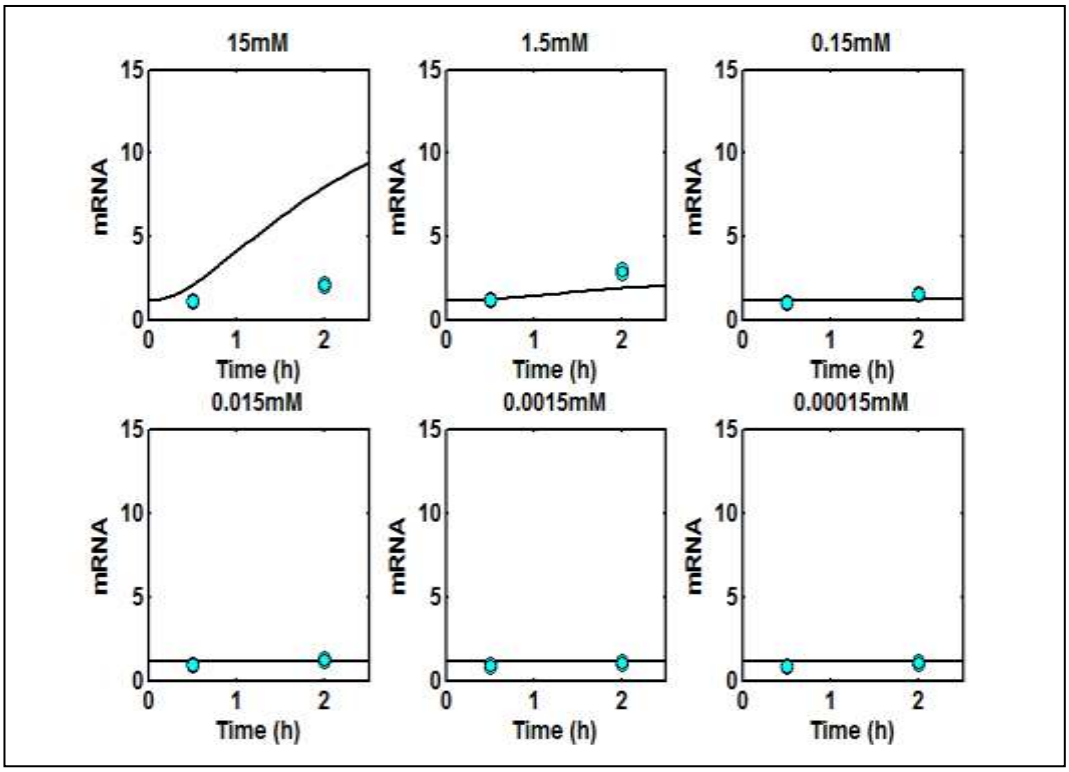

Figure 6.6: Experimental data and predictions of CYP2C9 mRNA levels

The relative mRNA level of CYP2C9 measured by qRT-PCR showed little increase in Dex-treated cells compared to control at 0.00015 - 0.015 mM Dex concentration, however there was a slight increase in the experimental data and the prediction at 0.15 and 1.5 mM, but the prediction at 15 mM was a significant over-prediction compared to the experimental data obtained.

6.4.1.f Modelling of relative CYP2C9 mRNA, protein and enzymatic activity levels in hepatocytes treated with 0.0001 mM Dex

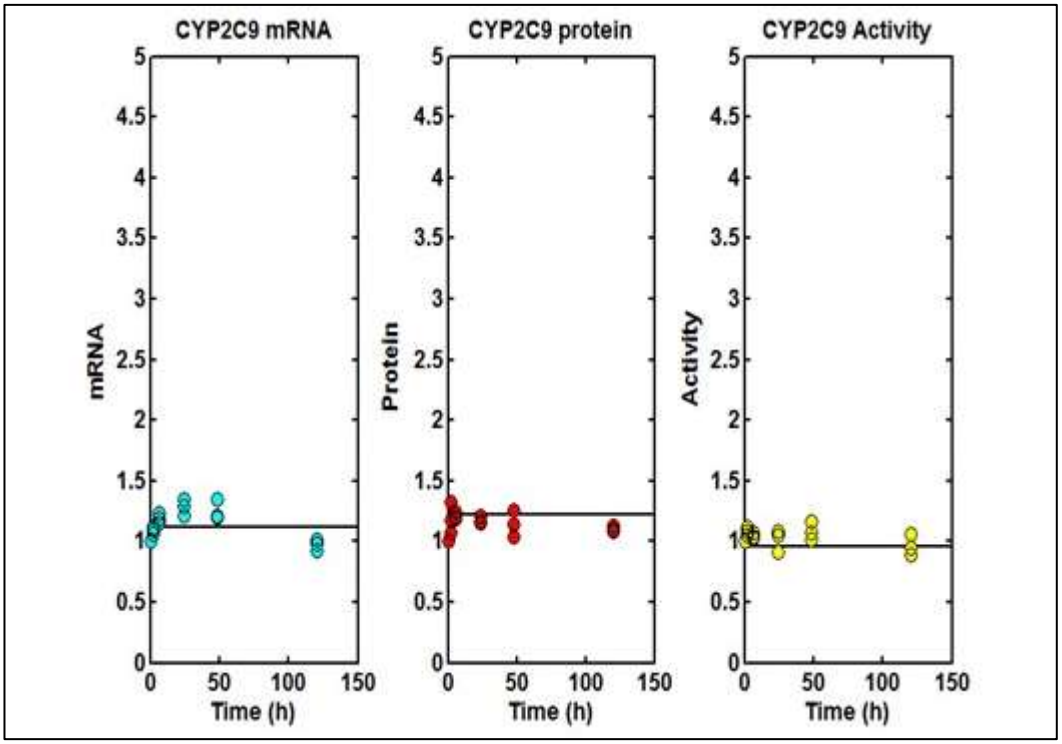

Figure 6.7: Experimental data and predictions for CYP2C9 mRNA, protein and enzymatic activity at 0.0001 mM Dex

The relative CYP2C9 mRNA and protein showed slight induction early in Dex treatment and returned to baseline at 120 h. The two models for mRNA and protein levels present as constant predictions of induction at about 1.1 and 1.2 respectively. The enzymatic activity levels for the low concentration of Dex (0.0001 mM) did not show significant induction in the experimental results or the model.

6.4.1.g Modelling of relative CYP2C9 mRNA, protein and enzymatic activity levels in hepatocytes treated with 1.5 mM Dex

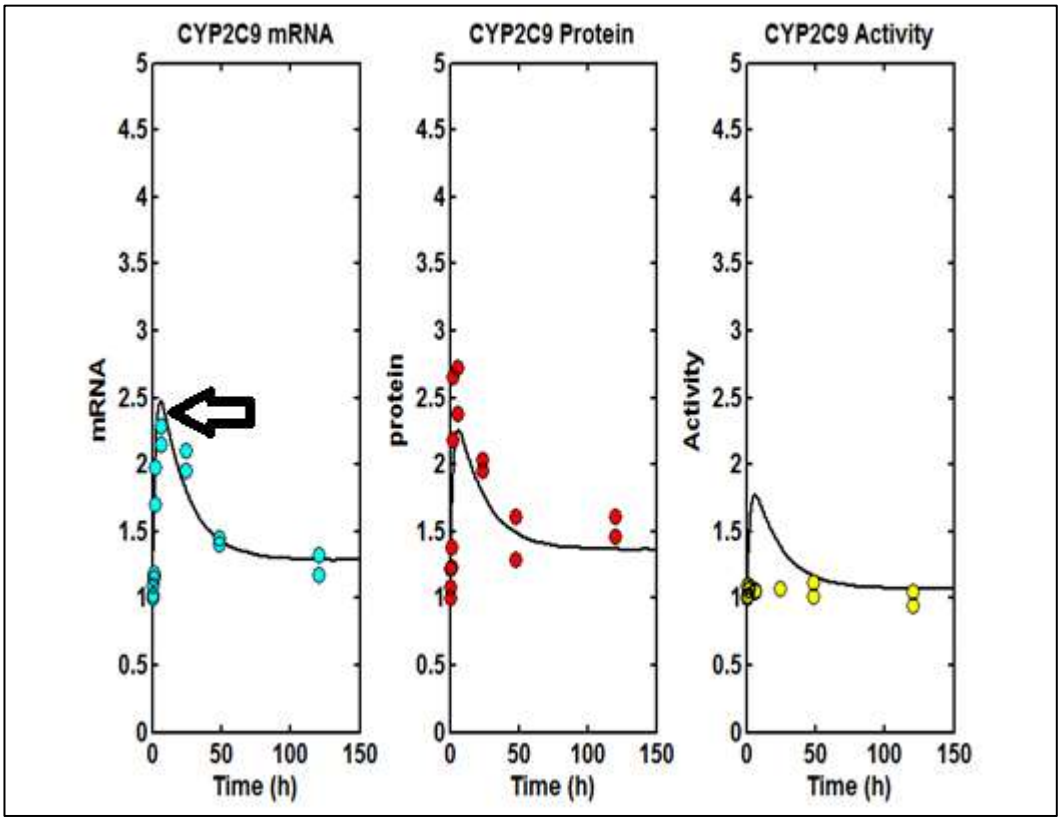

Figure 6.8: Experimental data for CYP2C9 mRNA, protein and enzymatic activity levels in HepG2 cells treated with 1.5 mM Dex

Figure 6.8 showed experimental data for CYP2C9 mRNA (blue circles), protein (red circles) and enzymatic activity (yellow circles) levels and the fittings obtained for HepG2 cells treated with 1.5 mM Dex.

The models obtained for the mRNA and protein levels of the experimental data were closely linked to the data obtained in the laboratory, but the enzymatic activity model presented an over-prediction compared to the experimental data obtained. The maximum CYP2C9 mRNA measurements at 6 hours which are followed by decline at later time points are shown by the black arrow in the Figure.

6.4.1.h Simulated profiles of GR, R, DR and DR_n dynamics controlling CYP2C9 regulation following treatment with 1.5 mM Dex

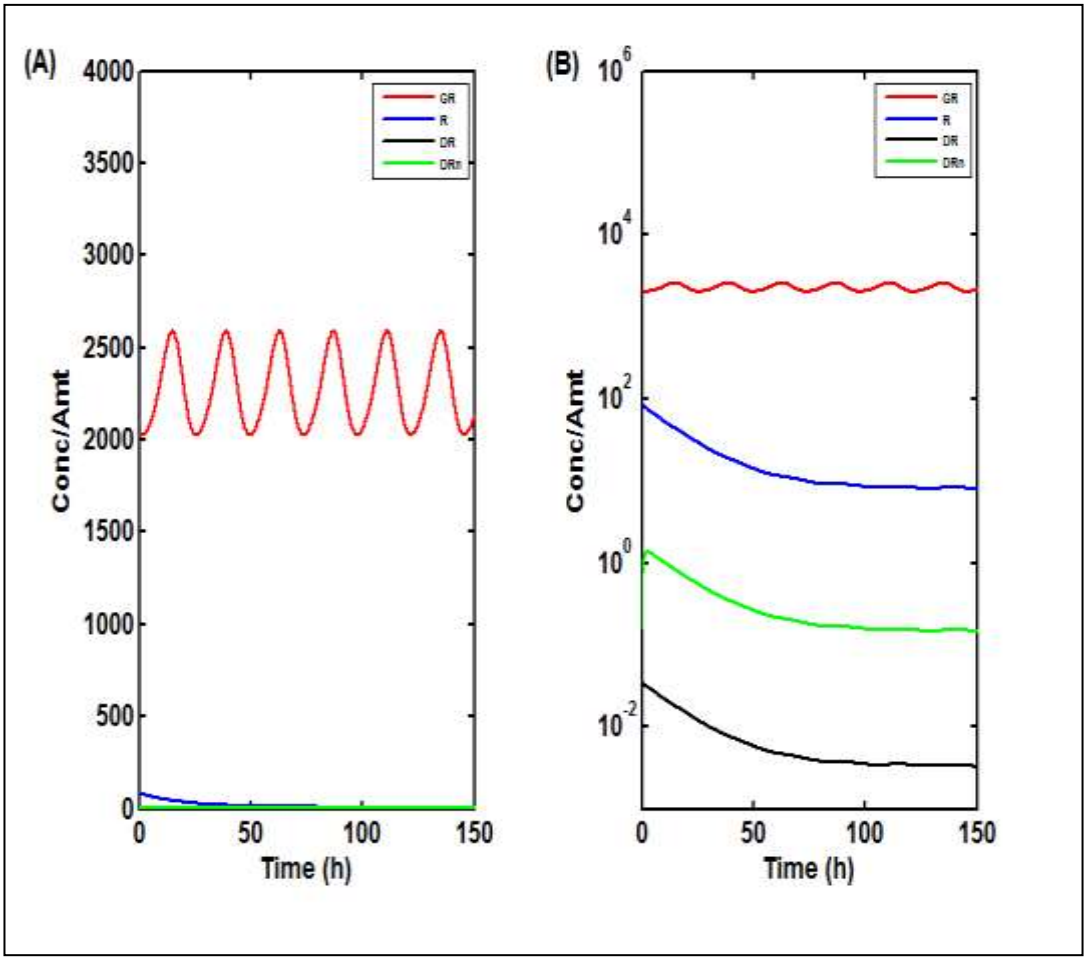

Figure 6.9: GR, R, DR and DR_n dynamics controlling CYP2C9 regulation

Figure 6.9(A) is the normal simulated profile whilst Figure 6.9(B) is the semilog(y) profile displaying the changes of dynamics more clearly. The dynamics of GR in relation to CYP2C9 appear to oscillate with respect to Dex treatment over time and oscillate at a constant rate throughout the 150 h shown. R, DR and DR_n begin at lower levels respectively and reach plateaus at approximately 75 h (see Figure 6.9 (B)).

Utilising MATLAB software to develop the model using the combination of different Dex concentrations and estimation of parameters was not successful as apparent in Figure 6.3, Figure 6.4, Figure 6.7 and Figure 6.8. There is no fit between the protein levels and enzymatic activity despite the link by a simple relation of proportionality. Also, the parameters estimated in Table 6.2 show large standard error values which define the uncertainty of parameter estimation.

6.5 Discussion

The interaction of Dex with the cytosolic GR, leads to GR conformational changes and subsequent translocation of the receptor in the nucleus. GR nuclear translocation might be affected by phosphorylation of the receptor upon Dex treatment and activation of the receptor (Schaaf and Cidlowski, 2002).

Figure 6.2 shows that the relative mRNA level of CYP3A4 showed no increase in Dex-treated cells compared to control at 0.00015 - 0.015 mM Dex concentration, however there was a slight increase in the experimental data and the prediction at 0.15 and 1.5 mM. Nonetheless, the prediction at 15 mM was an over-prediction compared to the experimental data obtained. Similarly, the relative mRNA, protein and enzymatic activity levels for the low concentration of Dex (0.0001 mM) did not show much induction in the experimental results or the model (Figure 6.3). However, the models for the higher concentration of 1.5 mM Dex used (Figure 6.4) were able to better capture the levels of the experimental data. Figure 6.5 shows the simulated profiles of GR, R, DR and DR_n dynamics controlling CYP3A4/5 regulation following treatment with 1.5 mM Dex. The Figure 6.5(A) is the normal simulated profile whilst Figure 6.5(B) is the semilog(y) profile displaying the changes of dynamics more clearly. The dynamics of CYP3A4 GR appear to oscillate with respect to Dex treatment over time and increase to reach a plateau at 48 h.

Figure 6.6 shows that the relative mRNA level of CYP2C9 displays little increase in Dex-treated cells compared to control at 0.00015 - 0.015 mM Dex concentration, however there was a slight increase in the experimental data and the prediction at 0.15 and 1.5 mM, but the prediction at 15 mM was an over-prediction compared to the experimental data obtained. The relative CYP2C9

mRNA, protein and enzymatic activity levels for the low concentration of Dex (0.0001 mM) also did not show significant induction in the experimental results or the model (Figure 6.7). However, the models for the higher concentration of 1.5 mM Dex used (Figure 6.8) were able to better capture the levels of the experimental data. Figure 6.9 shows the simulated profiles of GR, R, DR and DR_n dynamics controlling CYP2C9 regulation following treatment with 1.5 mM Dex. Figure 6.9(A) is the normal simulated profile whilst Figure 6.9(B) is the semilog(y) profile displaying the changes of dynamics more clearly. The dynamics of CYP2C9 GR appear to oscillate with respect to Dex treatment over time and reach plateau at approximately 75 h.

The mRNA regulation of CYPs is the major player in the signalling pathway downstream of the induction of these important enzymes, and must be taken account of during drug development (Dickins, 2004). The delayed onset of maximum induction of mRNA observed in CYP3A4/5 (approximately 6 h) and CYP2C9 (approximately 6 h) was reflected in the fittings of the model. The induction of CYP3A4/5 and CYP2C9 protein levels followed this increase in mRNA. However, unlike that of CYP3A4/5, the enzymatic activity level of CYP2C9 did not follow that of the mRNA and protein levels. An analysis using specific inhibitors of CYPs may be more suitable to follow changes in CYP2C9 enzymatic activity similar to the study by Westerink et al. (Westerink and Schoonen, 2007). Other than much lower enzymatic activity of CYP2C9 compared to CYP3A4, the CYP enzymes exhibited mRNA and protein levels that are similar and aligned with the fittings of the mathematical model obtained.

Several recent studies have looked at the effects of the nuclear receptors on CYP450 expression in animal *in vivo* and liver microsomal experiments. Hasegawa and colleagues examined the enzymatic activities and mRNA expression of CYP3A4 and CYP2C9 in chimeric mice with a humanized liver. This study found that the nuclear receptor PXR can mediate the induction of CYP3A4 and the CYP2C subfamily (Hasegawa et al., 2011). The study of Lee et al. also demonstrated that rifampicin treatment caused an increase in microsomal protein levels, total CYP content and CYP reductase activity of CAR/PXR double

humanized mice as opposed to normal mice (Lee et al., 2015). Another study on double transgenic mice which expressed human PXR and CYP3A4 (TgCYP3A4/hPXR), demonstrated that following treatment with rifampicin hepatic human CYP3A4 and mouse CYP3A genes and proteins were both induced. Also, following this CYP3A expression, the CYP3A activity in liver microsomes of TgCYP3A4/hPXR mice increased by approximately 5 fold (Ma et al., 2008). A study by Kim and colleagues on cynomolgus monkey and human hepatocytes demonstrated that the two known human inducers, rifampicin and hyperforin, resulted in increased RNA expression and enzymatic activity of CYP3A8 and CYP3A4, respectively (Kim et al., 2010). The study used in modelling for CYP3A4/5 and CYP2C9 was from Li and colleagues who used an indirect response model with a series of transit compartments to describe the induction of mRNA, protein and enzyme activity levels in CYP3A1/2 of rats via the DEX-PXR complex formed following Dex treatment (Li et al., 2012). The two-harmonics function of the GR production rate constant with respect to time, was used in modelling of the experimental data in MATLAB with reference to previous studies (Sukumaran et al., 2011). This function was used for CYP3A4/5 and CYP2C9 mRNA, protein and enzymatic activity levels, and correlated more with the data obtained for CYP3A4/5 (see Figure 6.4).

Chapter 7: Discussion

The system used in this study is human hepatocytes, HepG2 cells which are an immortalised cell line. The results in this study show that at 0.1 µM Dex, CYP3A4/5 and CYP2C9 enzyme mRNA, protein and enzymatic activity levels are not significantly induced whereas in other reports using 10 – 100 nM Dex in primary hepatocytes, the enzymes mentioned are significantly induced (4 fold) (Gerbal-Chaloin et al., 2001; Pascussi et al., 2001; Raucy et al., 2002). A study in cell culture on human osteosarcoma cell line U2OS with the addition of a mouse mammary tumour virus (MMTV), has found that long-term exposure to low concentration GCs causes a persistent repression by GCs. This continued repression uses a chromatin-dependant mechanism in disrupting binding of GR-dependant and also GR- independent transcription complexes (Burkhart et al., 2009). This can been seen in the current results in this study, where following an increase after 24 hours, there appears to be a decrease in the induction response of HepG2 cells to Dex at 48 and 120 h constant treatment.

The level of cytokines in hepatoma cell lines is high compared to other cell lines (Hammerich and Tacke, 2014). This is whilst cytokines can reduce CYP3A4 and CYP2C9 enzymes, and the overexpression of IL-6 and the activation of nuclear factor kappa B (NFkB) inhibits CAR and GR activation (Assenat et al., 2004; Aitken and Morgan, 2007). Also, the cross talk of GR with the transcription factors activator protein 1 (AP1) and NFkB can lead to GC insensitivity (Van Bogaert et al., 2010). It has been found that in patients with rheumatoid arthritis, low levels of endogenously produced cortisol are measured despite the high degree of inflammation associated with this condition. GR gene polymorphism is thought to influence the immunosuppressive effects of cortisol and GC resistance (Harbuz and Jessop, 1999; Jessop and Harbuz, 2005; Quax et al., 2015). Sensitivity to GC has also be found to differ in patients suffering with other autoimmune conditions such as MS (van Winsen et al., 2005). The current study

has been conducted using diseased liver cancer cells (HepG2 cell line) in humans, therefore the results cannot be extrapolated for use in healthy individuals.

7.1 mRNA and protein correlation

The mRNA and protein stability have important roles in the complicated processes of transcription to protein production. The rate of mRNA degradation and synthesis, as well as protein stability can affect protein levels (Hargrove and Schmidt, 1989). The rate of degradation of different mRNAs and proteins can vary with the cell cycle, the process of differentiation or nutritional needs. The average mRNA half-life in mammalian cells is typically 24 h whilst the average half-life of proteins is 48 - 72 h (Hargrove and Schmidt, 1989; Ing, 2005). Steroid hormones control mRNA stability by post transcriptional regulation and GCs predominantly influence gene expression via transcriptional initiation (Hargrove and Schmidt, 1989; Ing, 2005). The dynamics of these processes were described by the time-dependent two-harmonics function of the GR production rate constant used in modelling of the experimental data measured for CYP3A4/5 and CYP2C9 mRNA, protein and enzymatic activity levels.

The increases in the typical cell-based reporter assays are low, which may be due to CAR accumulating in the nucleus in immortalised cells whereas it is mainly in the cytoplasm in primary hepatocytes and the liver (Maglich et al., 2003). CAR can be active without ligand binding and the drugs already mentioned can cause the nuclear translocation of CAR rather than act as its ligands (Zelko et al., 2001; Jackson et al., 2006). It has been suggested that the CYP2C9 induction observed at 0.1 and 1 μM Dex is due to GR activation (Gerbal-Chaloin et al., 2001). HepG2 cells are immortalised hepatocarcinoma cells that have been used in induction studies and are an easier to handle tool compared to primary human hepatocytes in the study of upregulation of CYP enzymes (Yan and Caldwell, 2001; Westerink and Schoonen, 2007).

7.2 CYP3A4 mRNA levels at different concentrations of Dex

This study has shown that the mRNA levels of CYP3A4 increased at 2 an 6 h before starting to decline from 24 h with 0.1 µM Dex treatment (Figure 4.1), but 1.5 mM Dex treatment showed at least 2 fold induction between 2 – 120 h (Figure 5.3).

It can be concluded from these results that higher Dex concentration leads to more constant induction of CYP3A4 mRNA. In a study using HepG2 cell lines constitutively and stably expressing human CYP3A4 showed that acetaminophen did not increase CYP-mRNA whilst an increase in CYP3A4 content and activity was determined with this drug (Feierman et al., 2002). The activity of NFkB has been found to regulate CYP3A4 protein levels (Zangar et al., 2008). The rate of mRNA degradation and its translational efficiency determine gene expression in eukaryotes (Roy and Jacobson, 2013).

7.3 CYP2C9 mRNA levels at different concentrations of Dex

Treatment with 0.1 µM Dex produced statistically significant increases in CYP2C9 mRNA at later time points compared to CYP3A4 at 24 and 48 h (Figure 4.2), whilst treatment with 1.5 mM Dex presented with a similar increase to CYP3A4 mRNA levels (compare Figure 5.3 and Figure 5.4).

7.4 CYP3A4/5 protein levels at different concentrations of Dex

Protein levels of CYP3A4/5 in HepG2 ells treated with 0.1 µM Dex showed statistically significant increases at 6 and 24 h (Figure 4.3) whilst treatment with 1.5 mM showed a longer induction period from 2 – 120 h (Figure 5.5). However, the level of induction of the protein started to decline at 6 h and continued to decrease until the end of 120 h. At both of these concentrations, the induction of the CYP3A4/5 protein may be due to the induction of NRs: GR, phosphorylated GR at S211and PXR which were induced at both 0.1 µM and 1.5 mM. CAR was also found to be induced at 0.1 µM Dex concentration.

7.5 CYP2C9 protein levels at different concentrations of Dex

CYP2C9 protein levels treated with 0.1 µM Dex showed statistically significant increase at 6 and 24 h (see Figure 4.4). The induction of CYP2C9 protein levels treated with 1.5 µM Dex was from 1-120 h (see Figure 5.6). Induction of the NRs monitored was also seen at this Dex concentration and they may be responsible for CYP2C9 protein induction as suggested by other studies in human hepatocytes (Sahi et al., 2009).

7.6 GR protein levels at different concentrations of Dex

GR protein levels treated with 0.1 µM Dex showed statistically significant increase at 2 – 120 h (Figure 4.5). After treatment with 1.5 µM Dex the induction was apparent from 1 – 120 h (see Figure 5.7).

It has been shown by Pavek and co-workers that human placental cells do not mediate the transcriptional regulation of CYP2C9 and CYP3A4 via GR, whilst hepatic HepG2 cells demonstrated GR-mediated transcriptional regulation of these genes (Pavek et al., 2007).

7.7 S211-GR protein levels at different concentrations of Dex

The protein levels of phosphorylated GR at S211 treated with 0.1 µM Dex showed statistically significant increase at 2 – 120 h (see Figure 4.6). The induction of S211-GR protein levels treated with 1.5 µM Dex was seen earlier from 0.5 – 120 h (see Figure 5.8).

A study on GC signalling in human U2-OS osteosarcoma cells, has shown that transcriptional activity of GR correlated with the amount of S211 phosphorylation and the phosphorylated GR at S211 was localised in both the nuclear and cytoplasmic parts of the cell (Wang et al., 2002). The human GR phosphorylated at S211 has also been shown to be more transcriptionally active due to binding to a number of GRE-containing promoters (Blind and Garabedian, 2008).

The interaction of GCs (Dex in our study) with the cytosolic GR, results in GR conformational changes and subsequent translocation of the receptor to the nucleus (Longui, 2007; Galliher-Beckley and Cidlowski, 2009). The findings of our study show GR phosphorylation with respect to Dex treatment, so it may be

assumed that this GC-treatment led to GR nuclear translocation, the phosphorylation of the receptor and its activation, which confirm earlier studies (Schaaf and Cidlowski, 2002).

The increase in protein levels of phosphorylated GR at S211 was in correlation with the increase in CYP3A4/5 protein levels. This supports the finding by Wang and co-workers who studied the relationship between the transcriptional activity of GR and the amount of S211 phospho-GR *in vivo*, and suggested that this phosphorylation is a biomarker for activated GR (Wang et al., 2002). The increase in protein levels of phosphorylated GR at S211 was also in correlation with the increase in CYP3A4/5 and CYP2C9 protein levels. This also supports the finding by Wang and co-workers (Wang et al., 2002).

7.8 PXR protein levels at different concentrations of Dex

PXR was induced most significantly at 6 h with 0.1 µM Dex (see Figure 4.7) and at all time points measured from 1 - 120 h with 1.5 mM Dex treatment (Figure 5.9). This is in agreement with findings that sub-micromolar concentrations of Dex induces indirect expression of PXR through signalling of GR whilst at supra-micromolar concentrations PXR is directly activated (Pascussi et al., 2001). PXR is also thought to induce CYP3A4 and CYP2C9 which is in support of the findings in our study which shows induction of both these enzymes at the Dex concentrations used (Gerbal-Chaloin et al., 2001; Pascussi et al., 2003).

7.9 CAR protein levels at 0.1 µM Dex concentration

CAR was induced most significantly at 2 and 6 h with 0.1 µM Dex (see Figure 4.8). This is in agreement with findings that sub-micromolar concentrations of Dex induces indirect expression of CAR through signalling of GR whilst at supra-micromolar concentrations, PXR is directly activated (Pascussi et al., 2001). CAR is also thought to induce CYP3A4 and CYP2C9 which is in support of the findings in our study which shows induction of both these enzymes at the Dex concentrations used (Gerbal-Chaloin et al., 2002; Pascussi et al., 2003).

The expression of CAR is induced by sub-micromolar concentrations of Dex indirectly through GR signalling, in the same way as PXR. However at supra-

micromolar concentrations, it is regulated by activation of PXR (Gerbal-Chaloin et al., 2002; Pascussi et al., 2003).

CAR, PXR and GR agonists have been found to act as transcriptional regulators to control CYP gene induction (Qatanani and Moore, 2005; Tirona and Kim, 2005; Westerink and Schoonen, 2007; Korhonova et al., 2015). A study by Westerink and Schoonen, investigated the expression levels of CYP enzymes in HepG2 cells after 24 h exposure to several PXR/CAR agonists. The transcription of CYP2C8, 2D6, and 2E1 were not enhanced by the CAR/PXR agonists but the mRNA levels of CYP1A1, 1A2, 2B6 and 3A4 were induced by the tested activators (Westerink and Schoonen, 2007). Regulation of CYP3A4 by CAR and PXR have shown in several studies (Waxman, 1999; Moore et al., 2003; Faucette et al., 2006), but PXR has been recognised as the main mediator of CYP3A gene induction (Hewitt et al., 2007). GR binds to the GREs and regulates selective gene transcription in different ways in various cells. A study by So et al. using A549 human lung cells found that gene-specific regulatory effects are influenced by GR binding sites and various GREs (So et al., 2007). Our study has shown that these NRs and CYP3A4/5 and CYP2C9 are induced by varying concentrations of Dex in human liver cells (HepG2).

7.10 P-gp protein levels at 0.1 µM Dex concentration

P-gp protein levels were induced most significantly at 2 and 6 h with 0.1 µM Dex (see Figure 4.9). The herbal antidepressant St. John's wart has been shown to produce simultaneous induction of both CYP3A4 and p-gp. The intestinal carcinoma cells used in this study showed induction of P-gp expression which can be responsible for the decrease in bioavailability of co-administered drugs (Obach, 2000; Perloff et al., 2001). The findings of our study also present the importance of the induction of CYP3A4/5 and P-gp by Dex which will affect the bioavailability of other drugs simultaneously administered.

7.11 ROS levels of HepG2 cells treated with 0.1 µM Dex

Inflammation and infection can suppress the CYP enzymes in the liver during disease. The human hepatoma cell line, HepaRG and primary human hepatocytes were used in a recent study by Rubin and co-workers to show that CYP3A4 mRNA levels and catalytic activity were affected by pro-inflammatory mediators IL-6 and IL-8 (Rubin et al., 2015). However, we did not measure statistically significant ROS effects on CYP3A4 or CYP2C9 in HepG2 cells with and without the specific inhibitors for these enzymes treated with 0.1 µM Dex (Figure 4.10).

7.12 CYP3A4 enzymatic activity at different concentrations of Dex

The enzymatic activity of CYP3A4 was statistically significant at 2 – 48 h after treatment with 0.1 µM Dex (see Figure 4.11) and showed statistically significant enzymatic activity at the time points between 1 – 120 h treatments with 1.5 mM Dex (see Figure 5.10). A study looking at assessing the drug-drug interactions of CYP3A4 enzyme using its irreversible inhibitors has determined the degradation half-life of CYP3A4 to be 1 - 6 days in the collated data used (Galetin et al., 2006). Our findings of the enzymatic activity of CYP3A4 confirm that treatment with 1.5 mM Dex causes continued induction of its enzymatic activity until day 5 when the experiment was stopped.

7.13 CYP2C9 enzymatic activity at different concentrations of Dex

Whilst the enzymatic activity of CYP3A4 enzymes increased with Dex treatment at both 0.1 µM and 1.5 mM, no statistically significant enzymatic activity was seen at either Dex concentration for CYP2C9 (see Figure 4.12 and Figure 5.11). The lack of enzymatic activity of CYP2C9 was evident in measuring by the CYP2C9-specific luminogenic assay. Enzymatic activity of CYP2C9 was not measurably increased with Dex-treatment by using LC-MS to measure its effects on tolbutamide which is another CYP2C9 substrate (data not shown). This may be due to analysis of enzymatic activity not being sensitive enough to monitor induction and may need to be compared to inhibitors.

7.14 Mathematical model

The mathematical model developed in this study followed the experimental data at the lower Dex concentration (0.1 μM) and the higher Dex concentration of 1.5 mM for CYP3A4/5 and CYP2C9. The mRNA, protein and enzymatic activity levels of these enzymes were normalised to untreated cells at each corresponding time point. CYP2C9 tracked the mRNA and protein levels of CYP3A4 in experimental data and modelling, but enzymatic activity of this enzyme did not reflect the transcription of mRNA or protein levels (compare Figure 6.4 and Figure 6.8).

The mRNA regulation of CYPs is the major player in the signalling pathway downstream of the induction of these important enzymes, and must be taken account of during drug development (Dickins, 2004). The delayed onset of maximum induction of mRNA observed in CYP3A4/5 and CYP2C9 was reflected in the fittings of the model designed. Analysis using specific inhibitors of CYPs may be more appropriate to follow changes in CYP2C9 enzymatic activity as studied by Westerink et al. (Westerink and Schoonen, 2007). Other than the lack of upregulation of enzymatic activity of CYP2C9 compared with the significant upregulation of CYP3A4 enzymatic activity, the two CYP enzymes exhibited mRNA and protein levels that were similar and aligned with the fittings of the mathematical model designed.

The basic pharmacodynamic mechanism-based model in HepG2 cells were developed in this study by designing the model using MATLAB. These attempts at estimating parameters could help design and carryout DDI analysis of the induction of CYP3A4 and CYP2C9 in other human cells and possibly starting pre-clinical studies in other organisms to aid in drug development.

A homology model which is the comparative modelling of proteins has been used by Lewis and co-workers to determine that the fold induction of CYP3A4 is under the control of the human GR (Lewis et al., 2002). A study in human hepatocytes and liver donors has also shown that CYP2C9 is differentially regulated by agonists of CAR and PXR, and although the regulatory mechanisms are similar with CYP2B6 and CYP3A4, CYP2C9 displays an induction profile more in line

with that of CYP3A4 (Sahi et al., 2009). The findings of the present study which show that Dex induced mRNA, protein and enzymatic activity levels of CYP3A4/5 and CYP2C9 whilst also demonstrating induction of the NRs: GR, S211-GR, PXR and CAR protein levels at high (1.5 mM) and low (0.1 µM) Dex concentrations, are in confirmation with the earlier studies by the groups mentioned.

The human hepatocarcinoma cell line used in this *in vitro* study is easy to handle and delivers a human system which is reproducible, but it will not exactly reflect the CYP3A4 and CYP2C9 profile present in the human liver because its expression of drug-metabolising enzymes is different to the *in vivo* condition (Wilkening et al., 2003). Therefore, this study requires further evaluation in other human cells and *in vivo* studies using animals.

Chapter 8: Conclusion and Future work

8.1 Conclusion

Our study has shown that the changes in mRNA, protein and enzymatic activity levels of CYP3A4/5 and CYP2C9 in human HepG2 cells was induced by Dex at sub-micromolar (0.1 µM) and supra-micromolar (1.5 mM) concentrations.

The induction of CYP3A4/5 and CYP2C9 enzymes during 120 h treatment with Dex may be affected by NRs: GR, phosphorylated GR, PXR and CAR, as shown by the induction of proteins of these NRs. The efflux transporter, P-gp's protin levels, were also induced by Dex at the lower concentration of Dex used (0.1 µM), highlighting the importance of considering bioavailability of other drugs co-administered with Dex. The results of these laboratory experiments have been used to produce a mechanistic mathematical model in MATLAB with reference to previous studies on rats concentrating on the effects of steroids on GR (Sukumaran et al., 2011; Li et al., 2012). The model was not effective at the lower Dex concentration of 0.1 µM but was better modelled at the higher Dex concentration of 1.5 mM. The MATLAB model combined the data for the different Dex concentrations.

This was an initial effort for the development of the mathematical model of the data experimentally obtained for CYP3A4/5 and CYP2C9 enzymes in HepG2 cells. Changes in mRNA and protein levels were not reflected in enzymatic activity by the methods used in our study. The basic mechanistic model in HepG2 cells developed in this study could help design and carryout DDI analysis of the induction of CYP3A4/5 and CYP2C9 in other human cells and starting pre-clinical studies in other organisms to aid in drug-development.

8.2 Future work

The mathematical model developed in this study may be extended to evaluating the effects of phosphorylated GR on CYP3A4/5 and CYP2C9 or other CYP enzymes significantly affected by ROS such as CYP2E1. Other inducers such as rifampicin may be compared to the results obtained with this model. Also, CYP induction by Dex can be followed in a range of human cells such as breast cancer

cells and compared to the liver HepG2 cells used here. Further study of P-gp effects on the induction of drugs in HepG2 cells can be conducted by shorter treatment time points to gain an accurate evaluations of this efflux transporter.

Variability in compound sensitivity has been recognised in natural as well as synthetic corticosteroids. The roles of CYP3A4 and GR polymorphism in corticosteroid metabolism has been analysed in children with acute lymphoblastic leukaemia (Fleury et al., 2004). This difference in GC action, leading to GC insensitivity needs to be taken account of in future experiments.

The long-standing view that the side effects of chronic GC use is due to GR transactivation and the anti-inflammatory effects are caused by transrepression of GR, has been questioned in recent studies that the dimerization-deficient GR mutant can not only activate gene transcription but also form dimers (Nixon et al., 2013). The formation of dimers can directly influence the role of CYP450 enzymes in drug metabolism (Dvorak and Pavek, 2010). Hence, it is difficult to predict how the use of SEGRAs instead of Dex may affect GR and other NRs which regulate CYP450 enzymes. The recent findings that GR can potentially express various functions, depending on the tissue, ligand and receptor types as well as cofactor surroundings and target gene promoters, has highlighted that the development of ligands to cause only the wanted outcomes of therapy has not yet been achieved (De Bosscher, 2010).

SEGRAs have to be carefully assessed for use as therapeutic compounds in inflammatory diseases because they may cause immunostimulation in some of these diseases. Compound A is a SEGRA that blocks NFkB, whilst not blocking AP1. Further understanding of the GR ligand mechanisms will help to realize well-rounded and more cost-effective therapy (Vandevyver et al., 2013).

Appendix 1

Source code of individual fitting of data obtained in the laboratory to the model for CYP3A4/5 in MATLAB (Ind_fit1):

```
clear
format short g

%% load data
%% conc=1.5mM
data_1=load('data_1b_2b.txt');

time_1=data_1(:,1);
mRNA_1=data_1(:,2);
CYP3A4_1=data_1(:,3);
Conc_1=1.5;
exid_1=data_1(:,5);
CYP3A4_act_1=data_1(:,6);

%% conc=0.0001mM
data_2=load('data_low_conc.txt');

time_2=data_2(:,1);
mRNA_2=data_2(:,2);
CYP3A4_2=data_2(:,3);
Conc_2=0.0001;
CYP3A4_act_2=data_2(:,6);

%% conc=15mM
data_3=load('data_text_1.txt');
% data=load('data.txt');

time_3=data_3(:,1);
mRNA_3=data_3(:,2);
Conc_3=15;
exid_3=data_3(:,4);

%% conc=1.5mM
data_4=load('data_text_2.txt');
% data=load('data.txt');

time_4=data_4(:,1);
mRNA_4=data_4(:,2);
Conc_4=1.5;
exid_4=data_4(:,4);

%% conc=0.15mM
data_5=load('data_text_3.txt');
% data=load('data.txt');

time_5=data_5(:,1);
```

```
mRNA_5=data_5(:,2);
Conc_5=0.15;
exid_5=data_5(:,4);

%% conc=0.015mM
data_6=load('data_text_4.txt');
% data=load('data.txt');

time_6=data_6(:,1);
mRNA_6=data_6(:,2);
Conc_6=0.015;
exid_6=data_6(:,4);

%% conc=0.0015mM
data_7=load('data_text_5.txt');
% data=load('data.txt');

time_7=data_7(:,1);
mRNA_7=data_7(:,2);
Conc_7=0.0015;
exid_7=data_7(:,4);

%% conc=0.00015mM
data_8=load('data_text_6.txt');
% data=load('data.txt');

time_8=data_8(:,1);
mRNA_8=data_8(:,2);
Conc_8=0.00015;
exid_8=data_8(:,4);

%% Parameter estimates
ks_R=0.0009321;
kd_GR=1065.5;       %0.3117;    % (/hr)     - FIXED

% mRNA
kin=2.017;
kout=1.0047;

% protein
ksyn=3.0087;
kdeg=3.0128;
m=1.3147;

% Activity
alpha=0.1;

%% Vector of parameters
theta0=[ks_R kd_GR kin kout ksyn kdeg m alpha];

ncomp=6;                        % Number of compartments (states in
the differential equations)
Conc=1.5;                       % Initial incubation experiment mM

%% Optimisation (Estimation/Optimisation)
options=optimset('Diagnostics','on','Display','iter','MaxFunEvals'
,10000,'Maxiter',40,'TolX',1e-8,'PrecondBandWidth',inf);
```

```
[theta,resnorm] =
lsqnonlin(@obj_fun,theta0,zeros(size(theta0)),[],options,ncomp,tim
e_1,mRNA_1,CYP3A4_1,CYP3A4_act_1,Conc_1,...
    time_2,mRNA_2,CYP3A4_2,CYP3A4_act_2,Conc_2,...
    time_3,mRNA_3,Conc_3,...
    time_4,mRNA_4,Conc_4,...
    time_5,mRNA_5,Conc_5,...
    time_6,mRNA_6,Conc_6,...
    time_7,mRNA_7,Conc_7,...
    time_8,mRNA_8,Conc_8)

THETA=theta;

% pred
pred=all_pred(THETA,ncomp,time_1,Conc_1,time_2,Conc_2,time_3,Conc_
3,...
    time_4,Conc_4,...
    time_5,Conc_5,...
    time_6,Conc_6,...
    time_7,Conc_7,...
    time_8,Conc_8);

pred=pred';

% data
mRNA_data=[mRNA_1; mRNA_2; mRNA_3; mRNA_4; mRNA_5; mRNA_6; mRNA_7;
mRNA_8];
CYP3A4_data=[CYP3A4_1; CYP3A4_2];
CYP3A4_act=[CYP3A4_act_1; CYP3A4_act_2];

data=[mRNA_data;CYP3A4_data;CYP3A4_act];

res=data-pred;              % residual (data-prediction)

wt_pred=pred;
for k=1:length(wt_pred);
    if pred(k)==0
        wt_pred(k)=1;
    end
end
OF=sum((res.^2)./(wt_pred.^2)); % objective function this must be
equal to "resnom" or f(x) at the last iteration of the LSQnonlin
%OF=sum(res.^2); % objective function this must be equal to
"resnom" or f(x) at the last iteration of the LSQnonlin

J =
Jac(THETA,ncomp,time_1,Conc_1,time_2,Conc_2,time_3,Conc_3,time_4,C
onc_4,time_5,Conc_5,time_6,Conc_6,time_7,Conc_7,time_8,Conc_8);
nparam=length(THETA);

FIM=zeros(nparam);
for i=1:length(J)
    v=wt_pred(i)^2;
    FIM=((J(:,i)*J(:,i)')/v) + FIM;
end
FIM=FIM/(sum((res.^2)./wt_pred.^2)/(length(J)-nparam));
```

```
dt=det(FIM)           % determinant
Cov=inv(FIM)          % Var-Cov

se=sqrt(diag(Cov));
se=se'                % se
cv=se./THETA*100      % cv se(%)

%% Prediction
TT=0:0.1:150;

[mRNA_pred1,CYP3A4_pred1,GR_pred1,R_pred1,DR_pred1,DRn_pred1,CYP3A
4_actpred_1]=ext_model(THETA,Conc_1,TT,ncomp);
[mRNA_pred2,CYP3A4_pred2,GR_pred2,R_pred2,DR_pred2,DRn_pred2,CYP3A
4_actpred_2]=ext_model(THETA,Conc_2,TT,ncomp);
[mRNA_pred3,CYP3A4_pred3,GR_pred3,R_pred3,DR_pred3,DRn_pred3,CYP3A
4_actpred_3]=ext_model(THETA,Conc_3,TT,ncomp);
[mRNA_pred4,CYP3A4_pred4,GR_pred4,R_pred4,DR_pred4,DRn_pred4,CYP3A
4_actpred_4]=ext_model(THETA,Conc_4,TT,ncomp);
[mRNA_pred5,CYP3A4_pred5,GR_pred5,R_pred5,DR_pred5,DRn_pred5,CYP3A
4_actpred_5]=ext_model(THETA,Conc_5,TT,ncomp);
[mRNA_pred6,CYP3A4_pred6,GR_pred6,R_pred6,DR_pred6,DRn_pred6,CYP3A
4_actpred_6]=ext_model(THETA,Conc_6,TT,ncomp);
[mRNA_pred7,CYP3A4_pred7,GR_pred7,R_pred7,DR_pred7,DRn_pred7,CYP3A
4_actpred_7]=ext_model(THETA,Conc_7,TT,ncomp);
[mRNA_pred8,CYP3A4_pred8,GR_pred8,R_pred8,DR_pred8,DRn_pred8,CYP3A
4_actpred_8]=ext_model(THETA,Conc_8,TT,ncomp);

%% Plotting
set(0,'DefaultFigureWindowStyle','docked')

%% (1)
figure()

subplot(1,3,1), h1=plot(TT,mRNA_pred1,time_1,mRNA_1,'o');

set(h1(1),'LineWidth',1.5,'Color','k','LineStyle','--')
set(h1(2),'MarkerSize',7.5,'LineWidth',1,'MarkerEdgeColor','k','Ma
rkerFaceColor','c')

xlabel('Time (h)','FontSize', 14, 'fontweight','b')
ylabel('mRNA','FontSize', 14, 'fontweight','b')
title('CYP3A4 mRNA','FontSize', 14, 'fontweight','b')
xlim([0 150])
ylim([0 5])

h=gca;
set(h,'FontSize',14,'fontweight','b','LineWidth',1.5)

subplot(1,3,2),
h1=plot(TT,CYP3A4_pred1,time_1,CYP3A4_1,'o','LineWidth',1.5);

set(h1(1),'LineWidth',1.5,'Color','k','LineStyle','--')
set(h1(2),'MarkerSize',7.5,'LineWidth',1,'MarkerEdgeColor','k','Ma
rkerFaceColor','r')

xlabel('Time (h)','FontSize', 14, 'fontweight','b')
ylabel('Protein','FontSize', 14, 'fontweight','b')
```

```
title('CYP3A4/5 Protein','FontSize', 14, 'fontweight','b')
xlim([0 150])
ylim([0 5])

h=gca;
set(h,'FontSize',14,'fontweight','b','LineWidth',1.5)

subplot(1,3,3),
h1=plot(TT,CYP3A4_actpred_1,time_1,CYP3A4_act_1,'o','LineWidth',1.
5);

set(h1(1),'LineWidth',1.5,'Color','k','LineStyle','--')
set(h1(2),'MarkerSize',7.5,'LineWidth',1,'MarkerEdgeColor','k','Ma
rkerFaceColor','y')

xlabel('Time (h)','FontSize', 14, 'fontweight','b')
ylabel('Activity','FontSize', 14, 'fontweight','b')
title('CYP3A4 Activity','FontSize', 14, 'fontweight','b')
xlim([0 150])
ylim([0 5])

h=gca;
set(h,'FontSize',14,'fontweight','b','LineWidth',1.5)

%% (2)
figure()

subplot(1,3,1), h1=plot(TT,mRNA_pred2,time_2,mRNA_2,'o');

set(h1(1),'LineWidth',1.5,'Color','k','LineStyle','--')
set(h1(2),'MarkerSize',7.5,'LineWidth',1,'MarkerEdgeColor','k','Ma
rkerFaceColor','c')

xlabel('Time (h)','FontSize', 14, 'fontweight','b')
ylabel('mRNA','FontSize', 14, 'fontweight','b')
title('CYP3A4 mRNA','FontSize', 14, 'fontweight','b')
xlim([0 150])
ylim([0 5])

h=gca;
set(h,'FontSize',14,'fontweight','b','LineWidth',1.5)

subplot(1,3,2),
h1=plot(TT,CYP3A4_pred2,time_2,CYP3A4_2,'o','LineWidth',1.5);

set(h1(1),'LineWidth',1.5,'Color','k','LineStyle','--')
set(h1(2),'MarkerSize',7.5,'LineWidth',1,'MarkerEdgeColor','k','Ma
rkerFaceColor','r')

xlabel('Time (h)','FontSize', 14, 'fontweight','b')
ylabel('Protein','FontSize', 14, 'fontweight','b')
title('CYP3A4/5 Protein','FontSize', 14, 'fontweight','b')
xlim([0 150])
ylim([0 5])

h=gca;
set(h,'FontSize',14,'fontweight','b','LineWidth',1.5)
```

```
subplot(1,3,3),
h1=plot(TT,CYP3A4_actpred_2,time_2,CYP3A4_act_2,'o','LineWidth',1.
5);

set(h1(1),'LineWidth',1.5,'Color','k','LineStyle','--')
set(h1(2),'MarkerSize',7.5,'LineWidth',1,'MarkerEdgeColor','k','Ma
rkerFaceColor','y')

xlabel('Time (h)','FontSize', 14, 'fontweight','b')
ylabel('Activity','FontSize', 14, 'fontweight','b')
title('CYP3A4 Activity','FontSize', 14, 'fontweight','b')
xlim([0 150])
ylim([0 5])

h=gca;
set(h,'FontSize',14,'fontweight','b','LineWidth',1.5)

%% (3)
figure()

subplot(2,3,1), h1=plot(TT,mRNA_pred3,time_3,mRNA_3,'o');

set(h1(1),'LineWidth',1.5,'Color','k','LineStyle','--')
set(h1(2),'MarkerSize',7.5,'LineWidth',1,'MarkerEdgeColor','k','Ma
rkerFaceColor','c')

xlabel('Time (h)','FontSize', 14, 'fontweight','b')
ylabel('mRNA','FontSize', 14, 'fontweight','b')
title('15mM','FontSize', 14, 'fontweight','b')
xlim([0 2.5])
ylim([0 15])

h=gca;
set(h,'FontSize',14,'fontweight','b','LineWidth',1.5)

% (4)
subplot(2,3,2), h1=plot(TT,mRNA_pred4,time_4,mRNA_4,'o');

set(h1(1),'LineWidth',1.5,'Color','k','LineStyle','--')
set(h1(2),'MarkerSize',7.5,'LineWidth',1,'MarkerEdgeColor','k','Ma
rkerFaceColor','c')

xlabel('Time (h)','FontSize', 14, 'fontweight','b')
ylabel('mRNA','FontSize', 14, 'fontweight','b')
title('1.5mM','FontSize', 14, 'fontweight','b')
xlim([0 2.5])
ylim([0 15])

h=gca;
set(h,'FontSize',14,'fontweight','b','LineWidth',1.5)

%(5)
subplot(2,3,3), h1=plot(TT,mRNA_pred5,time_5,mRNA_5,'o');

set(h1(1),'LineWidth',1.5,'Color','k','LineStyle','--')
```

```
set(h1(2),'MarkerSize',7.5,'LineWidth',1,'MarkerEdgeColor','k','Ma
rkerFaceColor','c')

xlabel('Time (h)','FontSize', 14, 'fontweight','b')
ylabel('mRNA','FontSize', 14, 'fontweight','b')
title('0.15mM','FontSize', 14, 'fontweight','b')
xlim([0 2.5])
ylim([0 15])

h=gca;
set(h,'FontSize',14,'fontweight','b','LineWidth',1.5)

% (6)
subplot(2,3,4), h1=plot(TT,mRNA_pred6,time_6,mRNA_6,'o');

set(h1(1),'LineWidth',1.5,'Color','k','LineStyle','--')
set(h1(2),'MarkerSize',7.5,'LineWidth',1,'MarkerEdgeColor','k','Ma
rkerFaceColor','c')

xlabel('Time (h)','FontSize', 14, 'fontweight','b')
ylabel('mRNA','FontSize', 14, 'fontweight','b')
title('0.015mM','FontSize', 14, 'fontweight','b')
xlim([0 2.5])
ylim([0 15])

h=gca;
set(h,'FontSize',14,'fontweight','b','LineWidth',1.5)

% (7)
subplot(2,3,5), h1=plot(TT,mRNA_pred7,time_7,mRNA_7,'o');

set(h1(1),'LineWidth',1.5,'Color','k','LineStyle','--')
set(h1(2),'MarkerSize',7.5,'LineWidth',1,'MarkerEdgeColor','k','Ma
rkerFaceColor','c')

xlabel('Time (h)','FontSize', 14, 'fontweight','b')
ylabel('mRNA','FontSize', 14, 'fontweight','b')
title('0.0015mM','FontSize', 14, 'fontweight','b')
xlim([0 2.5])
ylim([0 15])

h=gca;
set(h,'FontSize',14,'fontweight','b','LineWidth',1.5)

% (8)
subplot(2,3,6), h1=plot(TT,mRNA_pred8,time_8,mRNA_8,'o');

set(h1(1),'LineWidth',1.5,'Color','k','LineStyle','--')
set(h1(2),'MarkerSize',7.5,'LineWidth',1,'MarkerEdgeColor','k','Ma
rkerFaceColor','c')

xlabel('Time (h)','FontSize', 14, 'fontweight','b')
ylabel('mRNA','FontSize', 14, 'fontweight','b')
title('0.00015mM','FontSize', 14, 'fontweight','b')
xlim([0 2.5])
ylim([0 15])
```

```
h=gca;
set(h,'FontSize',14,'fontweight','b','LineWidth',1.5)
%%
figure()
subplot(1,2,1), h1=plot(TT,GR_pred1,'-r',TT,R_pred1,'-
b',TT,DR_pred1,'-k',TT,DRn_pred1,'-g','LineWidth',1.5);

xlabel('Time (h)','FontSize', 14, 'fontweight','b')
ylabel('Conc/Amt','FontSize', 14, 'fontweight','b')
title('','FontSize', 14, 'fontweight','b')

xlim([0 150])
ylim([0 4000])

h=gca;
set(h,'FontSize',14,'fontweight','b','LineWidth',1.5)

hleg = legend('GR','R','DR','DRn','Location','northeast');
set(hleg,'FontSize',6)

subplot(1,2,2), h1=semilogy(TT,GR_pred1,'-r',TT,R_pred1,'-
b',TT,DR_pred1,'-k',TT,DRn_pred1,'-g','LineWidth',1.5);

xlabel('Time (h)','FontSize', 14, 'fontweight','b')
ylabel('Conc/Amt','FontSize', 14, 'fontweight','b')
title('','FontSize', 14, 'fontweight','b')

xlim([0 150])
ylim([0.001 1000000])

h=gca;
set(h,'FontSize',14,'fontweight','b','LineWidth',1.5)

hleg = legend('GR','R','DR','DRn','Location','northeast');
set(hleg,'FontSize',6)
```

Appendix 2

Source code of individual fitting of data obtained in the laboratory to the model for CYP2C9 in MATLAB (Ind_fit2):

```
clear
format short g

%% load data
%% conc=1.5mM
data_1=load('data_1b_2c.txt');

time_1=data_1(:,1);
mRNA_1=data_1(:,2);
CYP2C9_1=data_1(:,3);
Conc_1=1.5;
exid_1=data_1(:,5);
CYP2C9_act_1=data_1(:,6);

%% conc=0.0001mM
data_2=load('data_low_conc_2c.txt');

time_2=data_2(:,1);
mRNA_2=data_2(:,2);
CYP2C9_2=data_2(:,3);
Conc_2=0.0001;
CYP2C9_act_2=data_2(:,6);

%% conc=15mM
data_3=load('data_text_1_2c.txt');
% data=load('data.txt');

time_3=data_3(:,1);
mRNA_3=data_3(:,2);
Conc_3=15;
exid_3=data_3(:,4);

%% conc=1.5mM
data_4=load('data_text_2_2c.txt');
% data=load('data.txt');

time_4=data_4(:,1);
mRNA_4=data_4(:,2);
Conc_4=1.5;
exid_4=data_4(:,4);

%% conc=0.15mM
data_5=load('data_text_3_2c.txt');
% data=load('data.txt');

time_5=data_5(:,1);
mRNA_5=data_5(:,2);
Conc_5=0.15;
exid_5=data_5(:,4);
```

```
%% conc=0.015mM
data_6=load('data_text_4_2c.txt');
% data=load('data.txt');

time_6=data_6(:,1);
mRNA_6=data_6(:,2);
Conc_6=0.015;
exid_6=data_6(:,4);

%% conc=0.0015mM
data_7=load('data_text_5_2c.txt');
% data=load('data.txt');

time_7=data_7(:,1);
mRNA_7=data_7(:,2);
Conc_7=0.0015;
exid_7=data_7(:,4);

%% conc=0.00015mM
data_8=load('data_text_6_2c.txt');
% data=load('data.txt');

time_8=data_8(:,1);
mRNA_8=data_8(:,2);
Conc_8=0.00015;
exid_8=data_8(:,4);

%% Parameter estimates

ks_R=0.0009321;
kd_GR=1065.5;       %0.3117;    % (/hr)     - FIXED

% mRNA
kin=1.017;
kout=1.0047;

% protein
ksyn=2.0087;
kdeg=3.0128;
m=1.3147;

% Activity
alpha=0.01;

%% Vector of parameters
theta0=[ks_R kd_GR kin kout ksyn kdeg m alpha];

ncomp=6;                        % Number of compartments (states in
the differential equations)
Conc=1.5;                       % Initial incubation experiment mM

%% Optimisation (Estimation/Optimisation)
options=optimset('Diagnostics','on','Display','iter','MaxFunEvals'
,10000,'Maxiter',40,'TolX',1e-8,'PrecondBandWidth',inf);
[theta,resnorm] =
lsqnonlin(@obj_fun,theta0,zeros(size(theta0)),[],options,ncomp,tim
e_1,mRNA_1,CYP2C9_1,CYP2C9_act_1,Conc_1,...
```

```
    time_2,mRNA_2,CYP2C9_2,CYP2C9_act_2,Conc_2,...
    time_3,mRNA_3,Conc_3,...
    time_4,mRNA_4,Conc_4,...
    time_5,mRNA_5,Conc_5,...
    time_6,mRNA_6,Conc_6,...
    time_7,mRNA_7,Conc_7,...
    time_8,mRNA_8,Conc_8)

THETA=theta;

% pred
pred=all_pred(THETA,ncomp,time_1,Conc_1,time_2,Conc_2,time_3,Conc_
3,...
    time_4,Conc_4,...
    time_5,Conc_5,...
    time_6,Conc_6,...
    time_7,Conc_7,...
    time_8,Conc_8);

pred=pred';

% data
mRNA_data=[mRNA_1; mRNA_2; mRNA_3; mRNA_4; mRNA_5; mRNA_6; mRNA_7;
mRNA_8];
CYP2C9_data=[CYP2C9_1; CYP2C9_2];
CYP2C9_act=[CYP2C9_act_1; CYP2C9_act_2];

data=[mRNA_data;CYP2C9_data;CYP2C9_act];

res=data-pred;              % residual (data-prediction)

wt_pred=pred;
for k=1:length(wt_pred);
    if pred(k)==0
        wt_pred(k)=1;
    end
end
OF=sum((res.^2)./(wt_pred.^2)); % objective function this must be
equal to "resnom" or f(x) at the last iteration of the LSQnonlin
%OF=sum(res.^2); % objective function this must be equal to
"resnom" or f(x) at the last iteration of the LSQnonlin

J =
Jac(THETA,ncomp,time_1,Conc_1,time_2,Conc_2,time_3,Conc_3,time_4,C
onc_4,time_5,Conc_5,time_6,Conc_6,time_7,Conc_7,time_8,Conc_8);
nparam=length(THETA);

FIM=zeros(nparam);
for i=1:length(J)
    v=wt_pred(i)^2;
    FIM=((J(:,i)*J(:,i)')/v) + FIM;
end
FIM=FIM/(sum((res.^2)./wt_pred.^2)/(length(J)-nparam));


dt=det(FIM)          % determinant
Cov=inv(FIM)         % Var-Cov
```

```
se=sqrt(diag(Cov));
se=se'                  % se
cv=se./THETA*100        % cv se(%)

%% Prediction
TT=0:0.1:150;

[mRNA_pred1,CYP2C9_pred1,GR_pred1,R_pred1,DR_pred1,DRn_pred1,CYP2C
9_actpred_1]=ext_model(THETA,Conc_1,TT,ncomp);
[mRNA_pred2,CYP2C9_pred2,GR_pred2,R_pred2,DR_pred2,DRn_pred2,CYP2C
9_actpred_2]=ext_model(THETA,Conc_2,TT,ncomp);
[mRNA_pred3,CYP2C9_pred3,GR_pred3,R_pred3,DR_pred3,DRn_pred3,CYP2C
9_actpred_3]=ext_model(THETA,Conc_3,TT,ncomp);
[mRNA_pred4,CYP2C9_pred4,GR_pred4,R_pred4,DR_pred4,DRn_pred4,CYP2C
9_actpred_4]=ext_model(THETA,Conc_4,TT,ncomp);
[mRNA_pred5,CYP2C9_pred5,GR_pred5,R_pred5,DR_pred5,DRn_pred5,CYP2C
9_actpred_5]=ext_model(THETA,Conc_5,TT,ncomp);
[mRNA_pred6,CYP2C9_pred6,GR_pred6,R_pred6,DR_pred6,DRn_pred6,CYP2C
9_actpred_6]=ext_model(THETA,Conc_6,TT,ncomp);
[mRNA_pred7,CYP2C9_pred7,GR_pred7,R_pred7,DR_pred7,DRn_pred7,CYP2C
9_actpred_7]=ext_model(THETA,Conc_7,TT,ncomp);
[mRNA_pred8,CYP2C9_pred8,GR_pred8,R_pred8,DR_pred8,DRn_pred8,CYP2C
9_actpred_8]=ext_model(THETA,Conc_8,TT,ncomp);

%% Plotting
set(0,'DefaultFigureWindowStyle','docked')

%% (1)
figure()

subplot(1,3,1), h1=plot(TT,mRNA_pred1,time_1,mRNA_1,'o');

set(h1(1),'LineWidth',1.5,'Color','k','LineStyle','--')
set(h1(2),'MarkerSize',7.5,'LineWidth',1,'MarkerEdgeColor','k','Ma
rkerFaceColor','c')

xlabel('Time (h)','FontSize', 14, 'fontweight','b')
ylabel('mRNA','FontSize', 14, 'fontweight','b')
title('CYP2C9 mRNA','FontSize', 14, 'fontweight','b')
xlim([0 150])
ylim([0 5])

h=gca;
set(h,'FontSize',14,'fontweight','b','LineWidth',1.5)

subplot(1,3,2),
h1=plot(TT,CYP2C9_pred1,time_1,CYP2C9_1,'o','LineWidth',1.5);

set(h1(1),'LineWidth',1.5,'Color','k','LineStyle','--')
set(h1(2),'MarkerSize',7.5,'LineWidth',1,'MarkerEdgeColor','k','Ma
rkerFaceColor','r')

xlabel('Time (h)','FontSize', 14, 'fontweight','b')
ylabel('protein','FontSize', 14, 'fontweight','b')
title('CYP2C9 Protein','FontSize', 14, 'fontweight','b')
xlim([0 150])
```

```
ylim([0 5])

h=gca;
set(h,'FontSize',14,'fontweight','b','LineWidth',1.5)

subplot(1,3,3),
h1=plot(TT,CYP2C9_actpred_1,time_1,CYP2C9_act_1,'o','LineWidth',1.
5);

set(h1(1),'LineWidth',1.5,'Color','k','LineStyle','--')
set(h1(2),'MarkerSize',7.5,'LineWidth',1,'MarkerEdgeColor','k','Ma
rkerFaceColor','y')

xlabel('Time (h)','FontSize', 14, 'fontweight','b')
ylabel('Activity','FontSize', 14, 'fontweight','b')
title('CYP2C9 Activity','FontSize', 14, 'fontweight','b')
xlim([0 150])
ylim([0 5])

h=gca;
set(h,'FontSize',14,'fontweight','b','LineWidth',1.5)

%% (2)
figure()

subplot(1,3,1), h1=plot(TT,mRNA_pred2,time_2,mRNA_2,'o');

set(h1(1),'LineWidth',1.5,'Color','k','LineStyle','--')
set(h1(2),'MarkerSize',7.5,'LineWidth',1,'MarkerEdgeColor','k','Ma
rkerFaceColor','c')

xlabel('Time (h)','FontSize', 14, 'fontweight','b')
ylabel('mRNA','FontSize', 14, 'fontweight','b')
title('CYP2C9 mRNA','FontSize', 14, 'fontweight','b')
xlim([0 150])
ylim([0 5])

h=gca;
set(h,'FontSize',14,'fontweight','b','LineWidth',1.5)

subplot(1,3,2),
h1=plot(TT,CYP2C9_pred2,time_2,CYP2C9_2,'o','LineWidth',1.5);

set(h1(1),'LineWidth',1.5,'Color','k','LineStyle','--')
set(h1(2),'MarkerSize',7.5,'LineWidth',1,'MarkerEdgeColor','k','Ma
rkerFaceColor','r')

xlabel('Time (h)','FontSize', 14, 'fontweight','b')
ylabel('protein','FontSize', 14, 'fontweight','b')
title('CYP2C9 protein','FontSize', 14, 'fontweight','b')
xlim([0 150])
ylim([0 5])

h=gca;
set(h,'FontSize',14,'fontweight','b','LineWidth',1.5)
```

```
subplot(1,3,3),
h1=plot(TT,CYP2C9_actpred_2,time_2,CYP2C9_act_2,'o','LineWidth',1.
5);

set(h1(1),'LineWidth',1.5,'Color','k','LineStyle','--')
set(h1(2),'MarkerSize',7.5,'LineWidth',1,'MarkerEdgeColor','k','Ma
rkerFaceColor','y')

xlabel('Time (h)','FontSize', 14, 'fontweight','b')
ylabel('protein','FontSize', 14, 'fontweight','b')
title('CYP2C9 Activity','FontSize', 14, 'fontweight','b')
xlim([0 150])
ylim([0 5])

h=gca;
set(h,'FontSize',14,'fontweight','b','LineWidth',1.5)

%% (3)
figure()

subplot(2,3,1), h1=plot(TT,mRNA_pred3,time_3,mRNA_3,'o');

set(h1(1),'LineWidth',1.5,'Color','k','LineStyle','--')
set(h1(2),'MarkerSize',7.5,'LineWidth',1,'MarkerEdgeColor','k','Ma
rkerFaceColor','c')

xlabel('Time (h)','FontSize', 14, 'fontweight','b')
ylabel('mRNA','FontSize', 14, 'fontweight','b')
title('15mM','FontSize', 14, 'fontweight','b')
xlim([0 2.5])
ylim([0 15])

h=gca;
set(h,'FontSize',14,'fontweight','b','LineWidth',1.5)

% (4)
subplot(2,3,2), h1=plot(TT,mRNA_pred4,time_4,mRNA_4,'o');

set(h1(1),'LineWidth',1.5,'Color','k','LineStyle','--')
set(h1(2),'MarkerSize',7.5,'LineWidth',1,'MarkerEdgeColor','k','Ma
rkerFaceColor','c')

xlabel('Time (h)','FontSize', 14, 'fontweight','b')
ylabel('mRNA','FontSize', 14, 'fontweight','b')
title('1.5mM','FontSize', 14, 'fontweight','b')
xlim([0 2.5])
ylim([0 15])

h=gca;
set(h,'FontSize',14,'fontweight','b','LineWidth',1.5)

%(5)
subplot(2,3,3), h1=plot(TT,mRNA_pred5,time_5,mRNA_5,'o');

set(h1(1),'LineWidth',1.5,'Color','k','LineStyle','--')
set(h1(2),'MarkerSize',7.5,'LineWidth',1,'MarkerEdgeColor','k','Ma
rkerFaceColor','c')
```

```
xlabel('Time (h)','FontSize', 14, 'fontweight','b')
ylabel('mRNA','FontSize', 14, 'fontweight','b')
title('0.15mM','FontSize', 14, 'fontweight','b')
xlim([0 2.5])
ylim([0 15])

h=gca;
set(h,'FontSize',14,'fontweight','b','LineWidth',1.5)

% (6)
subplot(2,3,4), h1=plot(TT,mRNA_pred6,time_6,mRNA_6,'o');

set(h1(1),'LineWidth',1.5,'Color','k','LineStyle','--')
set(h1(2),'MarkerSize',7.5,'LineWidth',1,'MarkerEdgeColor','k','Ma
rkerFaceColor','c')

xlabel('Time (h)','FontSize', 14, 'fontweight','b')
ylabel('mRNA','FontSize', 14, 'fontweight','b')
title('0.015mM','FontSize', 14, 'fontweight','b')
xlim([0 2.5])
ylim([0 15])

h=gca;
set(h,'FontSize',14,'fontweight','b','LineWidth',1.5)

% (7)
subplot(2,3,5), h1=plot(TT,mRNA_pred7,time_7,mRNA_7,'o');

set(h1(1),'LineWidth',1.5,'Color','k','LineStyle','--')
set(h1(2),'MarkerSize',7.5,'LineWidth',1,'MarkerEdgeColor','k','Ma
rkerFaceColor','c')

xlabel('Time (h)','FontSize', 14, 'fontweight','b')
ylabel('mRNA','FontSize', 14, 'fontweight','b')
title('0.0015mM','FontSize', 14, 'fontweight','b')
xlim([0 2.5])
ylim([0 15])

h=gca;
set(h,'FontSize',14,'fontweight','b','LineWidth',1.5)

% (8)
subplot(2,3,6), h1=plot(TT,mRNA_pred8,time_8,mRNA_8,'o');

set(h1(1),'LineWidth',1.5,'Color','k','LineStyle','--')
set(h1(2),'MarkerSize',7.5,'LineWidth',1,'MarkerEdgeColor','k','Ma
rkerFaceColor','c')

xlabel('Time (h)','FontSize', 14, 'fontweight','b')
ylabel('mRNA','FontSize', 14, 'fontweight','b')
title('0.00015mM','FontSize', 14, 'fontweight','b')
xlim([0 2.5])
ylim([0 15])

h=gca;
set(h,'FontSize',14,'fontweight','b','LineWidth',1.5)
```

```
%%
figure()
subplot(1,2,1), h1=plot(TT,GR_pred1,'-r',TT,R_pred1,'-
b',TT,DR_pred1,'-k',TT,DRn_pred1,'-g','LineWidth',1.5);

xlabel('Time (h)','FontSize', 14, 'fontweight','b')
ylabel('Conc/Amt','FontSize', 14, 'fontweight','b')
title('','FontSize', 14, 'fontweight','b')

xlim([0 150])
ylim([0 4000])

h=gca;
set(h,'FontSize',14,'fontweight','b','LineWidth',1.5)

hleg = legend('GR','R','DR','DRn','Location','northeast');
set(hleg,'FontSize',6)

subplot(1,2,2), h1=semilogy(TT,GR_pred1,'-r',TT,R_pred1,'-
b',TT,DR_pred1,'-k',TT,DRn_pred1,'-g','LineWidth',1.5);

xlabel('Time (h)','FontSize', 14, 'fontweight','b')
ylabel('Conc/Amt','FontSize', 14, 'fontweight','b')
title('','FontSize', 14, 'fontweight','b')

xlim([0 150])
ylim([0.001 1000000])

h=gca;
set(h,'FontSize',14,'fontweight','b','LineWidth',1.5)

hleg = legend('GR','R','DR','DRn','Location','northeast');
set(hleg,'FontSize',6)
```

Appendix 3

Data for 0.1 µM Dex treatment

ID	Time	Dex conc. (uM)	3A4	2C9	M20	S211	PXR	CAR	p-gp	3A4 protein SPZ+Dex	2C9 protein Ket +Dex	mRNA 3A4	mRNA 2C9	ROS Dex	ROS SPZ	ROS SPZ+ Dex	ROS Ket	ROS Ket+ Dex	P-glo 3A4	P-glo 2C9
1	0	0.1	1.00	1.00	1.00	1.00	1.00	1.00	1.00	1.00	1.00	1.00	1.00	1.00	1.00	1.00	1.00	1.00	1.00	1.00
1	2	0.1	1.08	1.32	1.11	1.97	1.14	1.10	1.18	1.05	1.01	1.23	1.12	1.02	0.97	0.95	0.95	1.15	1.71	1.12
1	6	0.1	1.08	1.24	1.12	2.10	1.14	1.09	1.23	0.95	1.02	1.19	1.19	1.23	1.10	1.04	0.87	1.11	1.66	1.04
1	24	0.1	1.50	1.21	1.15	1.40	1.11	1.12	1.24	0.97	0.92	1.12	1.21	1.34	1.05	1.06	0.92	1.14	1.58	1.08
1	48	0.1	1.16	1.26	1.09	1.83	1.02	0.92	1.35	1.13	1.25	1.08	1.20	1.15	1.20	1.13	0.97	1.10	1.00	1.16
1	120	0.1	1.14	1.13	1.05	1.84	1.02	0.86	1.22	1.15	1.31	0.91	0.92	1.09	1.10	1.05	0.93	1.15	0.89	1.06
2	0	0.1	1.00	1.00	1.00	1.00	1.00	1.00	1.00	1.00	1.00	1.00	1.00	1.00	1.00	1.00	1.00	1.00	1.00	1.00
2	2	0.1	1.23	1.17	1.19	1.53	0.92	1.16	1.21	1.09	1.05	1.13	1.06	1.08	1.08	1.04	1.01	1.16	1.65	1.08
2	6	0.1	1.26	1.19	1.26	1.88	1.34	1.13	1.33	0.90	1.09	1.23	1.15	1.12	1.12	1.06	1.09	1.21	1.61	1.03
2	24	0.1	1.10	1.15	1.12	1.79	0.99	0.97	1.25	0.87	1.07	1.14	1.35	1.31	1.21	1.16	1.03	1.15	1.55	1.05
2	48	0.1	1.13	1.14	1.25	2.04	0.90	0.97	1.36	1.16	1.11	1.05	1.21	1.19	1.09	1.13	0.98	1.09	1.20	1.07
2	120	0.1	1.16	1.08	1.08	1.47	0.95	0.84	1.28	1.12	1.22	1.02	0.98	1.12	1.18	1.02	0.96	1.02	1.05	0.95
3	0	0.1	1.00	1.00	1.00	1.00	1.00	1.00	1.00	1.00	1.00	1.00	1.00	1.00	1.00	1.00	1.00	1.00	1.00	1.00
3	2	0.1	1.04	1.07	1.22	1.65	1.01	1.07	1.22	0.95	1.08	1.21	1.10	1.05	1.02	0.92	0.89	1.12	1.49	1.05
3	6	0.1	1.24	1.20	1.25	2.11	1.16	1.16	1.23	0.89	1.13	1.22	1.23	1.13	1.09	1.11	0.91	1.25	1.44	1.07
3	24	0.1	1.08	1.16	1.13	1.87	1.04	1.11	1.19	1.13	1.24	1.31	1.29	1.21	1.18	1.06	0.94	1.18	1.18	0.91
3	48	0.1	1.12	1.04	1.16	2.09	0.97	1.08	1.35	1.15	1.15	1.01	1.35	1.29	1.08	1.10	0.91	1.08	1.25	1.01
3	120	0.1	1.01	1.10	1.12	1.46	1.37	1.00	1.24	1.02	1.19	0.95	1.01	1.01	0.97	1.09	0.85	1.11	0.95	0.89

Appendix 4

Data for 0.00015 µM – 15 mM concentrations of Dex treatment for relative CYP3A4 and CYP2C9 mRNA levels

ID	Time (h)	Dex conc. (uM)	Dex conc. (mM)	mRNA 3A4	mRNA 2C9
1	0.5	15000.0	15mM	1.25	1.05
2	0.5	1500.0	1.5mM	1.22	1.19
3	0.5	150.0	0.15mM	1.17	0.99
4	0.5	15.0	15uM	0.89	0.87
5	0.5	1.5	1.5uM	0.98	0.96
6	0.5	0.15	0.15uM	1.14	0.81
1	0.5	15000.0	15mM	1.21	1.14
2	0.5	1500.0	1.5mM	1.31	1.26
3	0.5	150.0	0.15mM	1.21	1.03
4	0.5	15.0	15uM	0.94	0.95
5	0.5	1.5	1.5uM	0.94	0.84
6	0.5	0.15	0.15uM	1.04	0.89
1	2	15000.0	15mM	2.79	1.98
2	2	1500.0	1.5mM	3.76	3.02
3	2	150.0	0.15mM	2.29	1.57
4	2	15.0	15uM	1.68	1.12
5	2	1.5	1.5uM	1.07	0.98
6	2	0.15	0.15uM	1.06	0.97
1	2	15000.0	15mM	2.68	2.17

2	2	1500.0	1.5mM	3.96	2.73
3	2	150.0	0.15mM	2.4	1.49
4	2	15.0	15uM	1.88	1.34
5	2	1.5	1.5uM	1.21	1.11
6	2	0.15	0.15uM	1.12	1.15

Appendix 5

Data for 1.5 mM Dex treatment

ID	Time=IDV	Dex conc. (uM)	3A4	2C9	M20	S211	PXR	mRNA 3A4	mRNA 2C9	P-glo 3A4	P-glo 2C9
b1	0.0	1500.0	1.00	1.00	1.00	1.00	1.00	1.00	1.00	1.00	1.00
b1	0.5	1500.0	1.15	1.08	1.17	1.25	0.92	1.05	1.03	1.15	1.09
b1	1.0	1500.0	1.14	1.23	1.55	1.45	1.13	1.08	1.15	1.25	1.06
b1	2.0	1500.0	2.62	2.65	2.92	2.73	1.47	2.18	1.70	1.75	1.10
b1	6.0	1500.0	3.03	2.72	3.11	3.55	2.55	2.54	2.29	1.86	1.06
b1	24.0	1500.0	2.54	1.95	1.87	3.88	2.69	1.91	2.10	1.58	1.07
b1	48.0	1500.0	2.25	1.29	1.71	2.54	2.45	1.96	1.45	1.33	1.12
b2	120.0	1500.0	1.91	1.61	1.62	1.84	2.25	1.80	1.33	1.41	1.05
b2	0.0	1500.0	1.00	1.00	1.00	1.00	1.00	1.00	1.00	1.00	1.00
b2	0.5	1500.0	1.21	1.22	1.05	1.15	1.08	1.15	1.09	1.11	1.02
b2	1.0	1500.0	1.35	1.38	1.10	1.21	1.22	1.09	1.19	1.21	1.03
b2	2.0	1500.0	2.28	2.19	2.21	2.45	2.85	2.55	1.98	1.81	1.07
b2	6.0	1500.0	3.25	2.38	2.66	4.59	2.25	2.38	2.15	1.67	1.05
b2	24.0	1500.0	2.34	2.03	2.45	4.25	1.72	2.24	1.95	1.55	1.07
b2	48.0	1500.0	2.53	1.61	1.67	2.04	2.62	1.88	1.41	1.35	1.01
b2	120.0	1500.0	2.08	1.46	1.75	1.47	2.05	1.71	1.18	1.54	0.95

Chapter 9: References

Abcam (2015) General western blot protocol, http://www.abcam.com/protocols/general-western-blot-protocol (Accessed: August 2015).

Afzelius L, Zamora I, Ridderström M, Andersson TB, Karlén A, and Masimirembwa CM (2001) Competitive CYP2C9 inhibitors: enzyme inhibition studies, protein homology modeling, and three-dimensional quantitative structure-activity relationship analysis. *Mol Pharmacol* **59:**909-919.

Agoram BM, Martin SW, and van der Graaf PH (2007) The role of mechanism-based pharmacokinetic-pharmacodynamic (PK-PD) modelling in translational research of biologics. *Drug Discov Today* **12:**1018-1024.

Aitken AE and Morgan ET (2007) Gene-specific effects of inflammatory cytokines on cytochrome P450 2C, 2B6 and 3A4 mRNA levels in human hepatocytes. *Drug Metab Dispos* **35:**1687-1693.

Al Omari A and Murry DJ (2007) Pharmacogenetics of the Cytochrome P450 Enzyme System: Review of Current Knowledge and Clinical significance. *J Pharm Pract* **20:**206-218.

Anderson GD (2005) Pregnancy-induced changes in pharmacokinetics: a mechanistic-based approach. *Clin Pharmacokinet* **44:**989-1008.

Ansede JH and Thakker DR (2004) High-throughput screening for stability and inhibitory activity of compounds toward cytochrome P450-mediated metabolism. *J Pharm Sci* **93:**239-255.

Aouabdi S, Gibson GG, and Plant N (2006) Transcriptional regulation of PXR: Identification of a PPRE within the proximal promoter responsible for fibrate-mediated transcriptional activation of PXR. *Drug Met Disp* **34:**138–144.

Assenat E, Gerbal-Chaloin S, Larrey D, Saric J, Fabre J-M, Maurel P, Vilarem M-J, and Pascussi JM (2004) Interleukin 1β inhibits CAR-induced expression of hepatic genes involved in drug and bilirubin clearance. *Hepatology* **40:**951-960.

Auerbach SS, Ramsden R, Stoner MA, Verlinde C, Hassett C, and Omiecinski CJ (2003) Alternatively spliced isoforms of the human constitutive androstane receptor. *Nucleic Acids Res* **31:**3194-3207.

Babu SCV, Song EJ, and Yoo YS (2006) Modeling and simulation in signal transduction pathways: a systems biology approach. *Biochimie* **88:**277-283.

Bachmann KA (2006) Inhibition constants, inhibitor concentrations and the prediction of inhibitory drug drug interactions: pitfalls, progress and promise. *Curr Drug Met* **7:**1–14.

Bailey DG, Malcolm J, Arnold O, and Spence JD (1998) Grapefruit juice-drug interactions. *Br J Clin Pharmacol* **58:**S831-843.

Balant LP and Gex-Fabry M (2000) Modelling during drug development. *Eur J Pharm Biopharm* **50:**13-26.

Barnes PJ (1998) Anti-inflammatory actions of glucocorticoids: molecular mechanisms. *Clin Sci (Lond)* **94:**557-572.

Beck IM, Vanden Berghe W, Vermeulen L, Yamamoto KR, Haegeman G, and De Bosscher K (2009) Crosstalk in inflammation: the interplay of glucocorticoid receptor-based mechanisms and kinases and phosphatases. *Endocr Rev* **30:**830-882.

Bertilsson L, Höjer B, Tybring G, Osterloh J, and Rane A (1980) Autoinduction of carbamazepine metabolism in children examined by a stable isotope technique. *Clin Pharmacol Ther* **27:**83-88.

Bledsoe RK, Montana VG, Stanley TB, Delves CJ, Apolito CJ, McKee DD, Consler TG, Parks DJ, Stewart EL, Willson TM, Lambert MH, Moore JT, Pearce KH, and Xu HE (2002) Crystal structure of the glucocorticoid receptor ligand binding domain reveals a novel mode of receptor dimerization and coactivator recognition. *Cell* **110:**93-105.

Blind RD and Garabedian MJ (2008) Differential recruitment of glucocorticoid receptor phospho-isoforms to glucocorticoid-induced genes. *J Steroid Biochem Mol Biol* **109:**150-157.

Bodwell JE, Ortí E, Coull JM, Pappin DJ, Smith LI, and Swift F (1991) Identification of phosphorylated sites in the mouse glucocorticoid receptor. *J Biol Chem* **266:**7549-7555.

Bombail V, Plant N, and Gibson G (2001) Mapping of protein–DNA interactions in the CYP3A4 proximal promoter. *Toxicology* **168:**129–130.

Bondy SC and Naderi S (1994) Contribution of hepatic cytochrome P450 systems to the generation of reactive oxygen species. *Biochem Pharmacol* **48:**155-159.

Bradford MM (1976) A rapid and sensitive method for the quantitation of microgram quantities of protein utilizing the principle of protein-dye binding. *Anal Biochem* **72:**248-254.

Brager R and Sloand E (2005) The spectrum of polypharmacy. *Nurse Pract* **30:**44–50.

Brown HS, Ito K, Galetin A, and Houston JB (2005) Prediction of in vivo drug-drug interactions from in vitro data: impact of incorporating parallel pathways of drug elimination and inhibitor absorption rate constant. *Br J Clin Pharmacol* **60:**508-518.

Brown MT and Bussell JK (2011) Medication adherence: WHO cares? *Mayo Clin Proc* **86:**304-314.

Buckingham JC (2006) Glucocorticoids: exemplars of multi-tasking. *Br J Pharmacol* **147 Suppl 1:**S258-268.

Burk O, Arnold KA, Nussler AK, Schaeffeler E, Efimova E, Avery BA, Avery MA, Fromm MF, and Eichelbaum M (2005) Antimalarial artemisinin drugs induce cytochrome P450 and MDR1 expression by activation of xenosensors pregnane X receptor and constitutive androstane receptor. *Mol Pharmacol* **67:**1954-1965.

Burk O, Koch I, Raucy J, Hustert E, Eichelbaum M, Brockmöller J, Zanger UM, and Wojnowski L (2004) The induction of cytochrome P450 3A5 (CYP3A5) in the human liver and intestine is mediated by the xenobiotic sensors pregnane X receptor (PXR) and constitutively activated receptor (CAR). *J Biol Chem* **279:**38379-38385.

Burkhart BA, Ivey ML, and Archer TK (2009) Long-term low level glucocorticoid exposure induces persistent repression in chromatin. *Mol Cell Endocrinol* **298:**66-75.

Bustin SA and Mueller R (2005) Real-time reverse transcription PCR (qRT-PCR) and its potential use in clinical diagnosis. *Clin Sci (Lond)* **109:**365-379.

Cai Y, Konishi T, Han G, Campwala KH, French SW, and Wan YJ (2002) The role of hepatocyte RXR alpha in xenobiotic-sensing nuclear receptor-mediated pathways. *Eur J Pharm Sci* **15:**89-96.

Cali JJ, Ma D, Sobol M, Simpson DJ, Frackman S, Good TD, Daily WJ, and Liu D (2006) Luminogenic cytochrome P450 assays. *Expert Opin Drug Metab Toxicol* **2:**629-645.

Cashman JR, Perotti BY, Berkman CE, and Lin J (1996) Pharmacokinetics and molecular detoxication. *Environ Health Perspect* **104 Suppl 1:**23-40.

Chalancon G, Ravarani CN, Balaji S, Martinez-Arias A, Aravind L, Jothi R, and Babu MM (2012) Interplay between gene expression noise and regulatory network architecture. *Trends Genet* **28:**221-232.

Chang GW and Kam PC (1999) The physiological and pharmacological role of CYP450 isoenzymes. *Anesthesia* **54:**42-50.

Chen DW, Krstic-Demonacos M, and Schwartz JM (2012) Modeling the Mechanism of GR/c-Jun/Erg Crosstalk in Apoptosis of Acute Lymphoblastic Leukemia. *Front Physiol* **3:**410.

Chen DW, Lynch JT, Demonacos C, Krstic-Demonacos M, and Schwartz JM (2010) Quantitative analysis and modeling of glucocorticoid-controlled gene expression. *Pharmacogenomics* **11:**1545-1560.

Chen J and Raymond K (2006) Roles of rifampicin in drug-drug interactions: underlying molecular mechanisms involving the nuclear pregnane X receptor. *Ann Clin Microbiol Antimicrob* **5:**3.

Chen W, Dang T, Blind RD, Wang Z, Cavasotto CN, Hittelman AB, Rogatsky I, Logan SK, and Garabedian MJ (2008) Glucocorticoid receptor phosphorylation differentially affects target gene expression. *Mol Endocrinol* **22:**1754-1766.

Chen Y, Ferguson SS, Negishi M, and Goldstein JA (2004) Induction of human CYP2C9 by rifampicin, hyperforin, and phenobarbital is mediated by the pregnane X receptor. *J Pharmacol Exp Ther* **308:**495-501.

Chen Y and Goldstein JA (2009) The transcriptional regulation of the human CYP2C genes. *Curr Drug Metab* **10:**567-578.

Chen Y, Kissling G, Negishi M, and Goldstein JA (2005) The nuclear receptors constitutive androstane receptor and pregnane X receptor cross-talk with hepatic nuclear factor 4alpha to synergistically activate the human CYP2C9 promoter. *J Pharmacol Exp Ther* **314:**1125-1133.

Cholerton S, Daly AK, and Idle JR (1992) The role of individual human cytochromes P450 in drug-metabolism and clinical-response. *Trends Pharmacol Sci* **13:**434–439.

Chu V, Einolf HJ, Evers R, Kumar G, Moore D, Ripp S, Silva J, Sinha V, Sinz M, and Skerjanec A (2009) In vitro and in vivo induction of cytochrome p450: a survey of the current practices and recommendations: a pharmaceutical research and manufacturers of america perspective. *Drug Metab Dispos* **37:**1339-1354.

Chutka DS, Takahashi PY, and Hoel RW (2005) Inappropriate medication use in the elderly. *Essent Psychopharmacol* **6:**331–340.

Conway-Campbell BL, George CL, Pooley JR, Knight DM, Norman MR, Hager GL, and Lightman SL (2011) The HSP90 molecular chaperone cycle regulates cyclical transcriptional dynamics of the glucocorticoid receptor and its coregulatory molecules CBP/p300 during ultradian ligand treatment. *Mol Endocrinol* **25:**944-954.

Danhof M, Alvan G, Dahl SG, Kuhlmann J, and Paintaud G (2005) Mechanism-based pharmacokinetic-pharmacodynamic modeling-a new classification of biomarkers. *Pharm Res* **22:**1432-1437.

Danielson PB (2002) The cytochrome P450 superfamily: biochemistry, evolution and drug metabolism in humans. *Curr Drug Metab* **3:**561-597.

De Bosscher K (2010) Selective Glucocorticoid Receptor modulators. *J Steroid Biochem Mol Biol* **120:**96-104.

De Bosscher K, Beck IM, Dejager L, Bougarne N, Gaigneaux A, Chateauvieux S, Ratman D, Bracke M, Tavernier J, Vanden Berghe W, Libert C, Diederich M, and Haegeman G (2014) Selective modulation of the glucocorticoid receptor can distinguish between transrepression of NF-κB and AP-1. *Cell Mol Life Sci* **71:**143-163.

de Groot MJ (2006) Designing better drugs: predicting cytochrome P450 metabolism. *Drug Discov Today* **11:**601-606.

Dickins M (2004) Induction of cytochromes P450. *Curr Top Med Chem* **4:**1745-1766.

Doherty MM and Charman WN (2002) The mucosa of the small intestine: how clinically relevant as an organ of drug metabolism? *Clin Pharmacokinet* **41:**235-253.

Donato MT, Castell JV, and Gómez-Lechón MJ (1995) Effect of model inducers on cytochrome P450 activities of human hepatocytes in primary culture. *Drug Metab Dispos* **23:**553-558.

Donato MT, Hallifax D, Picazo L, Castell JV, Houston JB, Gomez-Lechón MJ, and Lahoz A (2010) Metabolite formation kinetics and intrinsic clearance of phenacetin, tolbutamide, alprazolam, and midazolam in adenoviral cytochrome P450-transfected HepG2 cells and comparison with hepatocytes and in vivo. *Drug Metab Dispos* **38:**1449-1455.

Duma D, Jewell CM, and Cidlowski JA (2006) Multiple glucocorticoid receptor isoforms and mechanisms of post-translational modification. *J Steroid Biochem Mol Biol* **102:**11-21.

Duret C, Daujat-Chavanieu M, Pascussi JM, Pichard-Garcia L, Balaguer P, Fabre JM, Vilarem MJ, Maurel P, and Gerbal-Chaloin S (2006) Ketoconazole and miconazole are antagonists of the human glucocorticoid receptor: consequences on the expression and function of the constitutive androstane receptor and the pregnane X receptor. *Mol Pharmacol* **70:**329-339.

Dvorak Z and Pavek P (2010) Regulation of drug-metabolizing cytochrome P450 enzymes by glucocorticoids. *Drug Metab Rev* **42:**621-635.

Eichelbaum M and Gross AS (1990) The genetic polymorphism of debrisoquine/sparteine metabolism--clinical aspects. *Pharmacol Ther* **46:**377-394.

El-Kadi AO, Bleau AM, Dumont I, Maurice H, and du Souich P (2000) Role of reactive oxygen intermediates in the decrease of hepatic cytochrome P450 activity by serum of humans and rabbits with an acute inflammatory reaction. *Drug Metab Dispos* **28:**1112-1120.

Endres CJ, Hsiao P, Chung FS, and Unadkat JD (2006) The role of transporters in drug interactions. *Eur J Pharm Sci* **27:**501-517.

Evans RM (2005) The nuclear receptor superfamily: a rosetta stone for physiology. *Mol Endocrinol* **19:**1429-1438.

Faucette SR, Sueyoshi T, Smith CM, Negishi M, Lecluyse EL, and Wang H (2006) Differential regulation of hepatic CYP2B6 and CYP3A4 genes by constitutive androstane receptor but not pregnane X receptor. *J Pharmacol Exp Ther* **317:**1200-1209.

FDA (2006) Guidance for industry: Drug interaction studies– Study, design, data analysis, and implication for dosing and labelling, Chemical inhibitors for in vitro experiments, www.fda.gov/downloads/Drugs/GuidanceComplianceRegulatoryInformation/Guidances/ucm072101.pdf. (Accessed: September 2011).

Feierman DE, Melnikov Z, and Zhang J (2002) The paradoxical effect of acetaminophen on CYP3A4 activity and content in transfected HepG2 cells. *Arch Biochem Biophys* **398:**109-117.

Fickett JW and Hatzigeorgiou AG (1997) Eukaryotic promoter recognition. *Genome Res* **7:**861-878.

Fleury I, Primeau M, Doreau A, Costea I, Moghrabi A, Sinnett D, and Krajinovic M (2004) Polymorphisms in genes involved in the corticosteroid response and the

outcome of childhood acute lymphoblastic leukemia. *Am J Pharmacogenomics* **4:**331-341.

Fontana E, Dansette PM, and M. PS (2005) Cytochrome p450 enzymes mechanism based inhibitors: common sub-structures and reactivity. *Curr Drug Met* **6:**413–454.

Foti RS and Wahlstrom JL (2008) Prediction of CYP-mediated drug interactions in vivo using in vitro data. *IDrugs* **11:**900-905.

Fowler S and Zhang H (2008) In vitro evaluation of reversible and irreversible cytochrome P450 inhibition: current status on methodologies and their utility for predicting drug-drug interactions. *AAPS J* **10:**410-424.

Friedman N, Linial M, Nachman I, and Pe'er D (2000) Using Bayesian networks to analyze expression data. *J Comput Biol* **7:**601-620.

Fukuen S, Fukuda T, Matsuda H, Sumida A, Yamamoto I, Inaba T, and Azuma J (2002) Identification of the novel splicing variants for the hPXR in human livers. *Biochem Biophys Res Commun* **298:**433-438.

Galetin A, Burt H, Gibbons L, and Houston JB (2006) Prediction of time-dependent CYP3A4 drug-drug interactions: impact of enzyme degradation, parallel elimination pathways, and intestinal inhibition. *Drug Metab Dispos* **34:**166-175.

Galigniana MD, Scruggs JL, Herrington J, Welsh MJ, Carter-Su C, Housley PR, and Pratt WB (1998) Heat shock protein 90-dependent (geldanamycin-inhibited) movement of the glucocorticoid receptor through the cytoplasm to the nucleus requires intact cytoskeleton. *Mol Endocrinol* **12:**1903-1913.

Galliher-Beckley AJ and Cidlowski JA (2009) Emerging roles of glucocorticoid receptor phosphorylation in modulating glucocorticoid hormone action in health and disease. *IUBMB Life* **61:**979-986.

George J, Byth K, and Farrell GC (1995) Age but not gender selectively affects expression of individual cytochrome P450 proteins in human liver. *Biochem Pharmacol* **50:**727-730.

Gerbal-Chaloin S, Daujat M, Pascussi JM, Pichard-Garcia L, Vilarem MJ, and Maurel P (2002) Transcriptional regulation of CYP2C9 gene. Role of glucocorticoid receptor and constitutive androstane receptor. *J Biol Chem* **277:**209-217.

Gerbal-Chaloin S, Pascussi JM, Pichard-Garcia L, Daujat M, Waechter F, Fabre JM, Carrère N, and Maurel P (2001) Induction of CYP2C genes in human hepatocytes in primary culture. *Drug Metab Dispos* **29:**242-251.

Gerbal-Chaloin S, Pichard-Garcia L, Fabre J-M, Sa-Cunha A, Poellinger L, Maurel P, and Daujat-Chavanieu M (2006) Role of CYP3A4 in the regulation of the aryl hydrocarbon receptor by omeprazole sulphide. *Cellular Signalling* **18:**740-750.

Germain P, Staels B, Dacquet C, Spedding M, and Laudet V (2006) Overview of nomenclature of nuclear receptors. *Pharmacol Rev* **58:**685-704.

Gertz M, Davis JD, Harrison A, Houston JB, and Galetin A (2008) Grapefruit juice-drug interaction studies as a method to assess the extent of intestinal availability: utility and limitations. *Curr Drug Metab* **9:**785-795.

Ghanbari F, Rowland-Yeo K, Bloomer JC, Clarke SE, Lennard MS, Tucker GT, and Rostami-Hodjegan A (2006) A critical evaluation of the experimental design of studies of mechanism based enzyme inhibition, with implications for in vitro-in vivo extrapolation. *Curr Drug Metab* **7:**315-334.

Gibson G, Plant N, Swales K, Ayrton A, and W. E-S (2002) Receptor-dependent transcriptional activation of cytochrome P450 3A genes: induction mechanisms, species differences and inter-individual variation in man. *Xenobiotica***:**165–206.

Givens RC, Lin YS, Dowling AL, Thummel KE, Lamba JK, Schuetz EG, Stewart PW, and Watkins PB (2003) CYP3A5 genotype predicts renal CYP3A activity and blood pressure in healthy adults. *J Appl Physiol (1985)* **95:**1297-1300.

Goodwin B, Hodgson E, and Liddle C (1999) The orphan human pregnane X receptor mediates the transcriptional activation of CYP3A4 by rifampicin through a distal enhancer module. *Mol Pharmacol* **56:**1329–1339.

Goodwin G and Vieta E (2005) Effective maintenance treatment--breaking the cycle of bipolar disorder. *European Psychiatry* **20:**365-371.

Greenblatt DJ, Zhao Y, Venkatakrishnan K, Duan SX, Harmatz JS, Parent SJ, Court MH, and von Moltke LL (2011) Mechanism of cytochrome P450-3A inhibition by ketoconazole. *J Pharm Pharmacol* **63:**214-221.

Gross KL and Cidlowski JA (2008) Tissue-specific glucocorticoid action: a family affair. *Trends Endocrinol Metab* **19:**331-339.

Guengerich FP (1991) Reactions and significance of cytochrome P-450 enzymes. *J Biol Chem* **266:**10019-10022.

Guengerich FP (1999) Cytochrome P-450 3A4: regulation and role in drug metabolism. *Annu Rev Pharmacol Toxicol* **39:**1-17.

Gurley BJ, Gardner SF, Hubbard MA, Williams DK, Gentry WB, Cui Y, and Ang CY (2005) Clinical assessment of effects of botanical supplementation on cytochrome P450 phenotypes in the elderly: St John's wort, garlic oil, Panax ginseng and Ginkgo biloba. *Drugs Aging* **22:**525-539.

Hamman MA, Thompson GA, and Hall SD (1997) Regioselective and stereoselective metabolism of ibuprofen by human cytochrome P450 2C. *Biochem Pharm* **54:**33-41.

Hammerich L and Tacke F (2014) Interleukins in chronic liver disease: lessons learned from experimental mouse models. *Clin Exp Gastroenterol* **7:**297-306.

Handschin C and Meyer UA (2003) Induction of drug metabolism: the role of nuclear receptors. *Pharmacol Rev* **55:**649-673.

Harbuz MS and Jessop DS (1999) Is there a defect in cortisol production in rheumatoid arthritis? *Rheumatology (Oxford)* **38:**298-302.

Hargrove JL and Schmidt FH (1989) The role of mRNA and protein stability in gene expression. *FASEB J* **3:**2360-2370.

Harmsen S, Meijerman I, Beijnen JH, and Schellens JH (2007) The role of nuclear receptors in pharmacokinetic drug-drug interactions in oncology. *Cancer Treat Rev* **33:**369-380.

Hasegawa M, Kapelyukh Y, Tahara H, Seibler J, Rode A, Krueger S, Lee DN, Wolf CR, and Scheer N (2011) Quantitative prediction of human pregnane X receptor and cytochrome P450 3A4 mediated drug-drug interaction in a novel multiple humanized mouse line. *Mol Pharmacol*.

HausserScientific (2015) Haemacytometer, http://hausserscientific.com/products/hausser_bright_line.html (Accessed: September 2015).

Hazra A, DuBois DC, Almon RR, and Jusko WJ (2007a) Assessing the dynamics of nuclear glucocorticoid-receptor complex: adding flexibility to gene expression modeling. *J Pharmacokinet Pharmacodyn* **34:**333-354.

Hazra A, Pyszczynski N, DuBois DC, Almon RR, and Jusko WJ (2007b) Modeling receptor/gene-mediated effects of corticosteroids on hepatic tyrosine aminotransferase dynamics in rats: dual regulation by endogenous and exogenous corticosteroids. *J Pharmacokinet Pharmacodyn* **34:**643-667.

Hewitt NJ, Lecluyse EL, and Ferguson SS (2007) Induction of hepatic cytochrome P450 enzymes: methods, mechanisms, recommendations, and in vitro-in vivo correlations. *Xenobiotica* **37:**1196-1224.

Hong Y, Mager DE, Blum RA, and Jusko WJ (2007) Population pharmacokinetic/pharmacodynamic modeling of systemic corticosteroid inhibition of whole blood lymphocytes: modeling interoccasion pharmacodynamic variability. *Pharm Res* **24:**1088-1097.

Honkakoski P and Negishi M (2000) Regulation of cytochrome P450 (CYP) genes by nuclear receptors. *Biochem J* **347:**321-337.

Houston JB and Galetin A (2008) Methods for predicting in vivo pharmacokinetics using data from in vitro assays. *Curr Drug Metab* **9:**940-951.

Huang SM, Strong JM, Zhang L, Reynolds KS, Nallani S, Temple R, Abraham S, Habet SA, Baweja RK, Burckart GJ, Chung S, Colangelo P, Frucht D, Green MD, Hepp P, Karnaukhova E, Ko HS, Lee JI, Marroum PJ, Norden JM, Qiu W, Rahman A, Sobel S, Stifano T, Thummel K, Wei XX, Yasuda S, Zheng JH, Zhao H, and Lesko LJ (2008) New era in drug interaction evaluation: US Food and Drug Administration update on CYP enzymes, transporters, and the guidance process. *J Clin Pharmacol* **48:**662-670.

Huang SM, Temple R, Throckmorton DC, and Lesko LJ (2007) Drug interaction studies: study design, data analysis, and implications for dosing and labeling. *Clin Pharmacol Ther* **81:**298-304.

Hustert E, Zibat A, Presecan-Siedel E, Eiselt R, Mueller R, Fuss C, Brehm I, Brinkmann U, Eichelbaum M, Wojnowski L, and Burk O (2001) Natural protein variants of pregnane X receptor with altered transactivation activity toward CYP3A4. *Drug Metab Dispos* **29:**1454-1459.

Inaba H and Pui CH (2010) Glucocorticoid use in acute lymphoblastic leukaemia. *Lancet Oncol* **11:**1096-1106.

Ing NH (2005) Steroid hormones regulate gene expression posttranscriptionally by altering the stabilities of messenger RNAs. *Biol Reprod* **72:**1290-1296.

Ingelman-Sundberg M (2001) Pharmacogenetics: an opportunity for a safer and more efficient pharmacotherapy. *J Internal Med* **250:**186-200.

Ioannides C (2008) *Cytochromes P450 Role in the Metabolism and Toxicity of Drugs and other Xenobiotics*. Cambridge : Royal Society of Chemistry, Cambridge.

Ismaili N and Garabedian MJ (2004) Modulation of glucocorticoid receptor function via phosphorylation. *Ann N Y Acad Sci* **1024:**86-101.

Itoh M, Adachi M, Yasui H, Takekawa M, Tanaka H, and Imai K (2002) Nuclear export of glucocorticoid receptor is enhanced by c-Jun N-terminal kinase-mediated phosphorylation. *Mol Endocrinol* **16:**2382-2392.

Jackson JP, Ferguson SS, Negishi M, and Goldstein JA (2006) Phenytoin induction of the cyp2c37 gene is mediated by the constitutive androstane receptor. *Drug Metab Dispos* **34:**2003-2010.

Jessop DS and Harbuz MS (2005) A defect in cortisol production in rheumatoid arthritis: why are we still looking? *Rheumatology (Oxford)* **44:**1097-1100.

Jin JY, Almon RR, DuBois DC, and Jusko WJ (2003) Modeling of corticosteroid pharmacogenomics in rat liver using gene microarrays. *J Pharmacol Exp Ther* **307:**93-109.

Jin M, Shimada T, Yokogawa K, Nomura M, Kato Y, Tsuji A, and Miyamoto K (2006) Contributions of intestinal P-glycoprotein and CYP3A to oral bioavailability of cyclosporin A in mice treated with or without dexamethasone. *Int J Pharm* **309:**81-86.

Jover R, Moya M, and Gómez-Lechón MJ (2009) Transcriptional regulation of cytochrome p450 genes by the nuclear receptor hepatocyte nuclear factor 4-alpha. *Curr Drug Metab* **10:**508-519.

Kalra BS (2007) Cytochrome P450 enzyme isoforms and their therapeutic implications: an update. *Indian J Med Sci* **61:**102-116.

Kanamitsu S-i, Ito K, Green CE, Tyson CA, Shimada N, and Sugiyama Y (2000) Prediction of In Vivo Interaction Between Triazolam and Erythromycin Based on In Vitro Studies Using Human Liver Microsomes and Recombinant Human CYP3A4. *Pharmaceutical Research* **17:**419-426-426.

Kanazu T, Yamaguchi Y, Okamura N, Baba T, and Koike M (2004) Model for the drug–drug interaction responsible for CYP3A enzyme inhibition. II: establishment and evaluation of dexamethasone-pretreated female rats. *Xenobiotica* **34:**403-413.

Kenworthy KE, Bloomer JC, Clarke SE, and Houston JB (1999) CYP3A4 drug interactions: correlation of 10 in vitro probe substrates. *Br J Clin Pharmacol* **48:**716-727.

Khan M, Mohan IK, Kutala VK, Kumbala D, and Kuppusamy P (2007) Cardioprotection by sulfaphenazole, a cytochrome p450 inhibitor: mitigation of ischemia-reperfusion injury by scavenging of reactive oxygen species. *J Pharmacol Exp Ther* **323:**813-821.

Khojasteh SC, Prabhu S, Kenny JR, Halladay JS, and Lu AY (2011) Chemical inhibitors of cytochrome P450 isoforms in human liver microsomes: a re-evaluation of P450 isoform selectivity. *Eur J Drug Metab Pharmacokinet* **36:**1-16.

Kim HR, Lee GH, Cho EY, Chae SW, Ahn T, and Chae HJ (2009) Bax inhibitor 1 regulates ER-stress-induced ROS accumulation through the regulation of cytochrome P450 2E1. *J Cell Sci* **122:**1126-1133.

Kim S, Dinchuk JE, Anthony MN, Orcutt T, Zoeckler ME, Sauer MB, Mosure KW, Vuppugalla R, Grace JE, Simmermacher J, Dulac HA, Pizzano J, and Sinz M (2010) Evaluation of cynomolgus monkey pregnane X receptor, primary hepatocyte, and in vivo pharmacokinetic changes in predicting human CYP3A4 induction. *Drug Metab Dispos* **38:**16-24.

Kirschke E, Goswami D, Southworth D, Griffin PR, and Agard DA (2014) Glucocorticoid receptor function regulated by coordinated action of the Hsp90 and Hsp70 chaperone cycles. *Cell* **157:**1685-1697.

Kitano H (2002) Systems biology: a brief overview. *Science* **295:**1662-1664.

Kivisto KT, Niemi M, and Fromm MF (2004) Functional interaction of intestinal CYP3A4 and P-glycoprotein. *Fundam Clin Pharmacol***:**621-626.

Kliewer SA, Goodwin B, and Willson TM (2002) The nuclear pregnane X receptor: a key regulator of xenobiotic metabolism. *Endocr Rev* **23:**687-702.

Kliewer SA, Moore JT, Wade L, Staudinger JL, Watson MA, Jones SA, McKee DD, Oliver BB, Willson TM, Zetterstrom RH, Perlmann T, and Lehmann JM (1998) An orphan nuclear receptor activated by pregnanes defines a novel steroid signaling pathway. *Cell* **92:**73–82.

Klipp E, Herwig R, Kowald A, Wierling C, and Lehrach H (2005) *Systems biology in practice. Concepts, implementation, and application*. WILEY-VCH Verlag GmbH & Co. KGaA, Berlin.

Korhonova M, Doricakova A, and Dvorak Z (2015) Optical Isomers of Atorvastatin, Rosuvastatin and Fluvastatin Enantiospecifically Activate Pregnane X Receptor PXR and Induce CYP2A6, CYP2B6 and CYP3A4 in Human Hepatocytes. *PLoS One* **10:**e0137720.

Kramer JA, Sagartz JE, and Morris DL (2007) The application of discovery toxicology and pathology towards the design of safer pharmaceutical lead candidates. *Nat Rev Drug Discov* **6:**636-649.

Krishna DR and Klotz U (1994) Extrahepatic metabolism of drugs in humans. *Clin Pharmacokinet* **26:**144-160.

Kuehl P, Zhang J, Lin Y, Lamba J, Assem M, Schuetz J, Watkins PB, Daly A, Wrighton SA, Hall SD, Maurel P, Relling M, Brimer C, Yasuda K, Venkataramanan R, Strom S, Thummel K, Boguski MS, and Schuetz E (2001) Sequence diversity in CYP3A promoters and characterization of the genetic basis of polymorphic CYP3A5 expression. *Nat Genet* **27:**383-391.

Kumar S (2011) Comparative modeling and molecular docking of orphan human CYP4V2 protein with fatty acid substrates: Insights into substrate specificity. *Bioinformation* **7:**360-365.

Lacroix D, Sonnier MA, Moncion A, Cheron G, and Cresteil T (1997) Expression of CYP3A in the human liver — Evidence that the shift between CYP3A7 and CYP3A4 occurs immediately after birth. *Eur J Biochem* **247:**625–634.

Lakhman SS, Ma Q, and Morse GD (2009) Pharmacogenomics of CYP3A: considerations for HIV treatment. *Pharmacogenomics* **10:**1323-1339.

Landaw EM and DiStefano JJ (1984) Multiexponential, multicompartmental, and noncompartmental modeling. II. Data analysis and statistical considerations. *Am J Physiol* **246:**R665-677.

Lee SY, Lee JY, Kim YM, Kim SK, and Oh SJ (2015) Expression of hepatic cytochrome P450s and UDP-glucuronosyltransferases in PXR and CAR double humanized mice treated with rifampicin. *Toxicol Lett* **235:**107-115.

Lehmann JM, McKee DD, Watson MA, Willson TM, Moore JT, and Kliewer SA (1998) The human orphan nuclear receptor PXR is activated by compounds that regulate CYP3A4 gene expression and cause drug interactions. *J Clin Invest* **102:**1016-1023.

Lesko LJ (2007) Personalized medicine: elusive dream or imminent reality? *Clin Pharmacol Ther* **81:**807-816.

Lesovaya E, Yemelyanov A, Swart AC, Swart P, Haegeman G, and Budunova I (2015) Discovery of Compound A--a selective activator of the glucocorticoid receptor with anti-inflammatory and anti-cancer activity. *Oncotarget* **6:**30730-30744.

Lewis DF (2004) 57 varieties: the human cytochromes P450. *Pharmacogenomics* **5:**305-318.

Lewis DF, Ogg MS, Goldfarb PS, and Gibson GG (2002) Molecular modelling of the human glucocorticoid receptor (hGR) ligand-binding domain (LBD) by homology with the human estrogen receptor alpha (hERalpha) LBD: quantitative structure-activity relationships within a series of CYP3A4 inducers where induction is mediated via hGR involvement. *J Steroid Biochem Mol Biol* **82:**195-199.

Lewis DF, Watson E, and Lake BG (1998) Evolution of the cytochrome P450 superfamily: sequence alignments and pharmacogenetics. *Mutat Res* **410:**245-270.

Li H and Wang H (2010) Activation of xenobiotic receptors: driving into the nucleus. *Expert Opin Drug Metab Toxicol* **6:**409-426.

Li L, Li ZQ, Deng CH, Ning MR, Li HQ, Bi SS, Zhou TY, and Lu W (2012) A mechanism-based pharmacokinetic/pharmacodynamic model for CYP3A1/2 induction by dexamethasone in rats. *Acta Pharmacol Sin* **33:**127-136.

Lim YP and Huang JD (2008) Interplay of pregnane X receptor with other nuclear receptors on gene regulation. *Drug Metab Pharmacokinet* **23:**14-21.

Limdi NA and Veenstra DL (2008) Warfarin pharmacogenetics. *Pharmacotherapy* **28:**1084-1097.

Lin JH and Yamazaki M (2003) Clinical relevance of P-glycoprotein in drug therapy. *Drug Metab Rev* **35:**417-454.

Lind AB, Wadelius M, Darj E, Finnström N, Lundgren S, and Rane A (2003) Gene expression of cytochrome P450 1B1 and 2D6 in leukocytes in human pregnancy. *Pharmacol Toxicol* **92:**295-299.

Lind U, Greenidge P, Gillner M, Koehler KF, Wright A, and Carlstedt-Duke J (2000) Functional probing of the human glucocorticoid receptor steroid-interacting surface by site-directed mutagenesis. Gln-642 plays an important role in steroid recognition and binding. *J Biol Chem* **275:**19041-19049.

Lobo ED and Balthasar JP (2002) Pharmacodynamic modeling of chemotherapeutic effects: application of a transit compartment model to characterize methotrexate effects in vitro. *AAPS PharmSci* **4:**E42.

Longui CA (2007) Glucocorticoid therapy: minimizing side effects. *Jornal de Pediatria* **83:**S163-171.

Luo G, Cunningham M, Kim S, Burn T, Lin J, Sinz M, Hamilton G, Rizzo C, Jolley S, Gilbert D, Downey A, Mudra D, Graham R, Carroll K, Xie J, Madan A, Parkinson A, Christ D, Selling B, LeCluyse E, and Gan LS (2002) CYP3A4 induction by drugs: correlation between a pregnane X receptor reporter gene assay and CYP3A4 expression in human hepatocytes. *Drug Metab Dispos* **30:**795-804.

Lynch JT, Rajendran R, Xenaki G, Berrou I, Demonacos C, and Krstic-Demonacos M (2010) The role of glucocorticoid receptor phosphorylation in Mcl-1 and NOXA gene expression. *Mol Cancer* **9:**38.

Ma X, Cheung C, Krausz KW, Shah YM, Wang T, Idle JR, and Gonzalez FJ (2008) A double transgenic mouse model expressing human pregnane X receptor and cytochrome P450 3A4. *Drug Metab Dispos* **36:**2506-2512.

Macey MGe (2007) *Flow Cytometry Principles and Applications / edited by Marion G. Macey*. Totowa, NJ : Humana Press.

Mager DE and Jusko WJ (2001) Pharmacodynamic modeling of time-dependent transduction systems. *Clin Pharmacol Ther* **70:**210-216.

Mager DE and Jusko WJ (2008) Development of translational pharmacokinetic-pharmacodynamic models. *Clin Pharmacol Ther* **83:**909-912.

Mager DE, Woo S, and Jusko WJ (2009) Scaling pharmacodynamics from in vitro and preclinical animal studies to humans. *Drug Metab Pharmacokinet* **24:**16-24.

Mager DE, Wyska E, and Jusko WJ (2003) Diversity of mechanism-based pharmacodynamic models. *Drug Metab Dispos* **31:**510-518.

Maglich JM, Parks DJ, Moore LB, Collins JL, Goodwin B, Billin AN, Stoltz CA, Kliewer SA, Lambert MH, Willson TM, and Moore JT (2003) Identification of a novel human constitutive androstane receptor (CAR) agonist and its use in the identification of CAR target genes. *J Biol Chem* **278:**17277-17283.

Maier T, Güell M, and Serrano L (2009) Correlation of mRNA and protein in complex biological samples. *FEBS Lett* **583:**3966-3973.

Martiny VY and Miteva MA (2013) Advances in molecular modeling of human cytochrome P450 polymorphism. *J Mol Biol* **425:**3978-3992.

Marí M and Cederbaum AI (2001) Induction of catalase, alpha, and microsomal glutathione S-transferase in CYP2E1 overexpressing HepG2 cells and protection against short-term oxidative stress. *Hepatology* **33:**652-661.

McArthur AG, Hegelund T, Cox RL, Stegeman JJ, Liljenberg M, Olsson U, Sundberg P, and Celander MC (2003) Phylogenetic analysis of the cytochrome P450 3 (CYP3) gene family. *J Mol Evol* **57:**200-211.

McGinnity DF and Riley RJ (2001) Predicting drug pharmacokinetics in humans from in vitro metabolism studies. *Biochem Soc Trans* **29:**135-139.

Meijer OC, Karssen AM, and de Kloet ER (2003) Cell- and tIssue-specific effects of corticosteroids in relation to glucocorticoid resistance: examples from the brain. *J Endocrinol* **178:**13-18.

Meyer UA (2000) Pharmacogenetics and adverse drug reactions. *Lancet* **356:**1667-1671.

Mizutani T (2003) PM frequencies of major CYPs in Asians and Caucasians. *Drug Met Rev* **35:**99–106.

Moore JT, Moore LB, Maglich JM, and Kliewer SA (2003) Functional and structural comparison of PXR and CAR. *Biochim Biophys Acta* **1619:**235-238.

Mueller SC, Majcher-Peszynska J, Uehleke B, Klammt S, Mundkowski RG, Miekisch W, Sievers H, Bauer S, Frank B, Kundt G, and Drewelow B (2006) The extent of induction of CYP3A by St. John's wort varies among products and is linked to hyperforin dose. *Eur J Clin Pharmacol* **62:**29-36.

Muller P (2007) Drug-Induced Idiosyncratic Liver Injury, in: *Researcher*, pp 18-20, RCC Ltd, Switzerland.

Murray GI, Taylor MC, McFadyen MC, McKay JA, Greenlee WF, Burke MD, and Melvin WT (1997) Tumor-specific expression of cytochrome P450 CYP1B1. *Cancer Res* **57:**3026-3031.

Musante CJ, Lewis AK, and Hall K (2002) Small- and large-scale biosimulation applied to drug discovery and development. *Drug Discov Today* **7:**S192-196.

Myhr KM and Mellgren SI (2009) Corticosteroids in the treatment of multiple sclerosis. *Acta Neurol Scand Suppl***:**73-80.

Nebert DW and Russell DW (2002) Clinical importance of the cytochromes P450. *Lancet* **360:**1155-1162.

Nebert DW, Wikvall K, and Miller WL (2013) Human cytochromes P450 in health and disease. *Philos Trans R Soc Lond B Biol Sci* **368:**20120431.

Nelson DR, Koymans L, Kamataki T, Stegeman JJ, Feyereisen R, Waxman DJ, Waterman MR, Gotoh O, Coon MJ, Estabrook RW, Gunsalus IC, and Neber DW (1996) P450 superfamily: update on new sequences, gene mapping, accession numbers and nomenclature. *Pharmacogenetics* **6:**1-42.

Nem D, Baranyai D, Qiu H, Gödtel-Armbrust U, Nestler S, and Wojnowski L (2012) Pregnane X receptor and yin yang 1 contribute to the differential tissue expression and induction of CYP3A5 and CYP3A4. *PLoS One* **7:**e30895.

Neve EP and Ingelman-Sundberg M (2008) Intracellular transport and localization of microsomal cytochrome P450. *Anal Bioanal Chem* **392:**1075-1084.

Ng HW, Perkins R, Tong W, and Hong H (2014) Versatility or promiscuity: the estrogen receptors, control of ligand selectivity and an update on subtype selective ligands. *Int J Environ Res Public Health* **11:**8709-8742.

Nicolaides NC, Galata Z, Kino T, Chrousos GP, and Charmandari E (2010) The human glucocorticoid receptor: molecular basis of biologic function. *Steroids* **75:**1-12.

Nishi M, Takenaka N, Morita N, Ito T, Ozawa H, and Kawata M (1999) Real-time imaging of glucocorticoid receptor dynamics in living neurons and glial cells in comparison with non-neural cells. *Eur J Neurosci* **11:**1927-1936.

Nixon M, Andrew R, and Chapman KE (2013) It takes two to tango: dimerisation of glucocorticoid receptor and its anti-inflammatory functions. *Steroids* **78:**59-68.

Nordeen SK, Suh BJ, Kühnel B, and Hutchison CA (1990) Structural determinants of a glucocorticoid receptor recognition element. *Mol Endocrinol* **4:**1866-1873.

Oakley RH and Cidlowski JA (2011) Cellular processing of the glucocorticoid receptor gene and protein: new mechanisms for generating tissue-specific actions of glucocorticoids. *J Biol Chem* **286:**3177-3184.

Oakley RH and Cidlowski JA (2013) The biology of the glucocorticoid receptor: new signaling mechanisms in health and disease. *J Allergy Clin Immunol* **132:**1033-1044.

Obach RS (2000) Inhibition of human cytochrome P450 enzymes by constituents of St. John's Wort, an herbal preparation used in the treatment of depression. *J Pharmacol Exp Ther* **294:**88-95.

Okada Y, Murayama N, Yanagida C, Shimizu M, Guengerich FP, and Yamazaki H (2009) Drug interactions of thalidomide with midazolam and cyclosporine A: heterotropic cooperativity of human cytochrome P450 3A5. *Drug Metab Dispos* **37:**18-23.

Over RS and Michaels SD (2014) Open and closed: the roles of linker histones in plants and animals. *Mol Plant* **7:**481-491.

Paine MF, Hart HL, Ludington SS, Haining RL, Rettie AE, and Zeldin DC (2006) The human intestinal cytochrome P450 "pie". *Drug Metab Dispos* **34:**880-886.

Park JY, Kim KA, Kang MH, Kim SL, and Shin JG (2004) Effect of rifampin on the pharmacokinetics of rosiglitazone in healthy subjects. *Clin Pharmacol Ther* **75:**157-162.

Pascussi JM, Drocourt L, Gerbal-Chaloin S, Fabre JM, Maurel P, and Vilarem MJ (2001) Dual effect of dexamethasone on CYP3A4 gene expression in human hepatocytes. Sequential role of glucocorticoid receptor and pregnane X receptor. *Eur J Biochem* **268:**6346-6358.

Pascussi JM, Gerbal-Chaloin S, Drocourt L, Maurel P, and Vilarem MJ (2003) The expression of CYP2B6, CYP2C9 and CYP3A4 genes: a tangle of networks of nuclear and steroid receptors. *Biochim Biophys Acta* **1619:**243-253.

Pavek P, Cerveny L, Svecova L, Brysch M, Libra A, Vrzal R, Nachtigal P, Staud F, Ulrichova J, Fendrich Z, and Dvorak Z (2007) Examination of Glucocorticoid receptor alpha-mediated transcriptional regulation of P-glycoprotein, CYP3A4, and CYP2C9 genes in placental trophoblast cell lines. *Placenta* **28:**1004-1011.

Pavek P and Dvorak Z (2008) Xenobiotic-induced transcriptional regulation of xenobiotic metabolizing enzymes of the cytochrome P450 superfamily in human extrahepatic tissues. *Curr Drug Metab* **9:**129-143.

Perloff MD, von Moltke LL, Störmer E, Shader RI, and Greenblatt DJ (2001) Saint John's wort: an in vitro analysis of P-glycoprotein induction due to extended exposure. *Br J Pharmacol* **134:**1601-1608.

Phillips KA, Veenstra DL, Oren E, Lee JK, and Sadee W (2001) Potential role of pharmacogenomics in reducing adverse drug reactions: a systematic review. *JAMA* **286:**2270-2279.

Pichard L, Fabre I, Daujat M, Domergue J, Joyeux H, and Maurel P (1992) Effect of corticosteroids on the expression of cytochromes P450 and on cyclosporin A oxidase activity in primary cultures of human hepatocytes. *Mol Pharmacol* **41:**1047-1055.

Pinsonneault J and Sadée W (2003) Pharmacogenomics of multigenic diseases: sex-specific differences in disease and treatment outcome. *AAPS PharmSci* **5:**E29.

Plant N (2004) Interaction networks: coordinating responses to xenobiotic exposure. *Toxicology* **202:**21-32.

Plant N (2007) The human cytochrome P450 sub-family: Transcriptional regulation, inter-individual variation and interaction networks. *Biochimica et Biophysica Acta (BBA) - General Subjects* **1770:**478-488.

Preissner SC, Hoffmann MF, Preissner R, Dunkel M, Gewiess A, and Preissner S (2013) Polymorphic cytochrome P450 enzymes (CYPs) and their role in personalized therapy. *PLoS One* **8:**e82562.

Proulx M and du Souich P (1995) Inflammation-induced decrease in hepatic cytochrome P450 in conscious rabbits is accompanied by an increase in hepatic oxidative stress. *Res Commun Mol Pathol Pharmacol* **87:**221-236.

Pui CH and Evans WE (2006) Treatment of acute lymphoblastic leukemia. *N Engl J Med* **354:**166-178.

Puntarulo S and Cederbaum AI (1998) Production of reactive oxygen species by microsomes enriched in specific human cytochrome P450 enzymes. *Free Radic Biol Med* **24:**1324-1330.

Qatanani M and Moore DD (2005) CAR, the continuously advancing receptor, in drug metabolism and disease. *Curr Drug Metab* **6:**329-339.

Qin LX and Tang ZY (2004) Recent progress in predictive biomarkers for metastatic recurrence of human hepatocellular carcinoma: a review of the literature. *J Cancer Res Clin Oncol* **130:**497-513.

Quax RA, Koper JW, Huisman AM, Weel A, Hazes JM, Lamberts SW, and Feelders RA (2015) Polymorphisms in the glucocorticoid receptor gene and in the glucocorticoid-induced transcript 1 gene are associated with disease activity and response to glucocorticoid bridging therapy in rheumatoid arthritis. *Rheumatol Int* **35:**1325-1333.

Rashba-Step J and Cederbaum AI (1994) Generation of reactive oxygen intermediates by human liver microsomes in the presence of NADPH or NADH. *Mol Pharmacol* **45:**150-157.

Raucy JL, Mueller L, Duan K, Allen SW, Strom S, and Lasker JM (2002) Expression and induction of CYP2C P450 enzymes in primary cultures of human hepatocytes. *J Pharmacol Exp Ther* **302:**475-482.

Rettie AE, Korzekwa KR, Kunze KL, Lawrence RF, Eddy AC, Aoyama T, Gelboin HV, Gonzalez FJ, and Trager WF (1992) Hydroxylation of warfarin by human cDNA-expressed cytochrome P-450: a role for P-4502C9 in the etiology of (S)-warfarin-drug interactions. *Chem Res Toxicol* **5:**54-59.

Rivory LP, Slaviero KA, and Clarke SJ (2002) Hepatic cytochrome P450 3A drug metabolism is reduced in cancer patients who have an acute-phase response. *Br J Cancer* **87:**277-280.

Rizzo N, Hispard E, Dolbeault S, Dally S, Leverge R, and Girre C (1997) Impact of long-term ethanol consumption on CYP1A2 activity. *Clin Pharmacol Ther* **62:**505-509.

Robert J, Vekris A, Pourquier P, and Bonnet J (2004) Predicting drug response based on gene expression. *Crit Rev Oncol Hematol* **51:**205-227.

Robertson GR, Field J, Goodwin B, Bierach S, Tran M, Lehnert A, and Liddle C (2003) Transgenic mouse models of human CYP3A4 gene regulation. *Mol Pharmacol* **64:**42-50.

Rogatsky I, Logan SK, and Garabedian MJ (1998) Antagonism of glucocorticoid receptor transcriptional activation by the c-Jun N-terminal kinase. *Proc Natl Acad Sci U S A* **95:**2050-2055.

Rogers JF, Nafziger AN, and Bertino JSJ (2002) Pharmacogenetics affects dosing, efficacy, and toxicity of cytochrome P450-metabolized drugs. *Am J Med* **113:**746-750.

Rostami-Hodjegan A and Tucker GT (2007) Simulation and prediction of in vivo drug metabolism in human populations from in vitro data. *Nat Rev Drug Discov* **6:**140-148.

Roy B and Jacobson A (2013) The intimate relationships of mRNA decay and translation. *Trends Genet* **29:**691-699.

Roy JN, Lajoie J, Zijenah LS, Barama A, Poirier C, Ward BJ, and Roger M (2005) CYP3A5 genetic polymorphisms in different ethnic populations. *Drug Metab Dispos* **33:**884-887.

Rubin K, Janefeldt A, Andersson L, Berke Z, Grime K, and Andersson TB (2015) HepaRG cells as human-relevant in vitro model to study the effects of inflammatory stimuli on cytochrome P450 isoenzymes. *Drug Metab Dispos* **43:**119-125.

Rushmore TH and Kong AN (2002) Pharmacogenomics, regulation and signaling pathways of phase I and II drug metabolizing enzymes. *Curr Drug Metab* **3:**481-490.

Sahi J, Shord SS, Lindley C, Ferguson S, and LeCluyse EL (2009) Regulation of cytochrome P450 2C9 expression in primary cultures of human hepatocytes. *J Biochem Mol Toxicol* **23:**43-58.

Savic RM, Jonker DM, Kerbusch T, and Karlsson MO (2007) Implementation of a transit compartment model for describing drug absorption in pharmacokinetic studies. *J Pharmacokinet Pharmacodyn* **34:**711-726.

Savkur RS, Wu Y, Bramlett KS, Wang M, Yao S, Perkins D, Totten M, Searfoss G, Ryan TP, Su EW, and Burris TP (2003) Alternative splicing within the ligand binding domain of the human constitutive androstane receptor. *Mol Genet Metab* **80:**216-226.

Sax PE (2006) Therapeutic options for treatment experienced patients: a focus on resistance testing and optimizing background therapy. *AIDS Reader* **16:**265–275.

Schaaf MJ and Cidlowski JA (2002) Molecular mechanisms of glucocorticoid action and resistance. *J Steroid Biochem Mol Biol* **83:**37-48.

Schmitt P, Splettstösser W, Porsch-Ozcürümez M, Finke EJ, and Grunow R (2005) A novel screening ELISA and a confirmatory Western blot useful for diagnosis and epidemiological studies of tularemia. *Epidemiol Infect* **133:**759-766.

Schneider CA, Rasband WS, and Eliceiri KW (2012) NIH Image to ImageJ: 25 years of image analysis. *Nat Methods* **9:**671-675.

Schuetz EG (2004) Lessons from the CYP3A4 promoter. *Mol Pharmacol* **65:**279-281.

Schuetz EG, Schuetz JD, Strom SC, Thompson MT, Fisher RA, Molowa DT, Li D, and Guzelian PS (1993) Regulation of human liver cytochromes P-450 in family 3A in primary and continuous culture of human hepatocytes. *Hepatology* **18:**1254-1262.

Schuetz EG, Wrighton SA, Barwick JL, and Guzelian PS (1984) Induction of cytochrome P-450 by glucocorticoids in rat liver. I. Evidence that glucocorticoids and pregnenolone 16 alpha-carbonitrile regulate de novo synthesis of a common form of cytochrome P-450 in cultures of adult rat hepatocytes and in the liver in vivo. *J Biol Chem* **259:**1999-2006.

Schuetz JD, Beach DL, and Guzelian PS (1994) Selective expression of cytochrome P450 CYP3A mRNAs in embryonic and adult human liver. *Pharmacogenetics* **4:**11-20.

Schwanhäusser B, Busse D, Li N, Dittmar G, Schuchhardt J, Wolf J, Chen W, and Selbach M (2011) Global quantification of mammalian gene expression control. *Nature* **473:**337-342.

Schwartz JB (2003) The influence of sex on pharmacokinetics. *Clin Pharmacokinet* **42:**107-121.

Schäcke H, Berger M, Rehwinkel H, and Asadullah K (2007) Selective glucocorticoid receptor agonists (SEGRAs): novel ligands with an improved therapeutic index. *Mol Cell Endocrinol* **275:**109-117.

Sezutsu H, Le Goff G, and Feyereisen R (2013) Origins of P450 diversity. *Philos Trans R Soc Lond B Biol Sci* **368:**20120428.

Shen DD, Kunze KL, and Thummel KE (1997) Enzyme-catalyzed processes of first-pass hepatic and intestinal drug extraction. *Adv Drug Deliv Rev* **27:**99-127.

Shimada T, Yamazaki H, Mimura M, Inui Y, and Guengerich FP (1994) Interindividual variations in human liver cytochrome P-450 enzymes involved in the oxidation of drugs, carcinogens and toxic chemicals: studies with liver microsomes of 30 Japanese and 30 Caucasians. *J Pharmacol Exp Ther* **270:**414-423.

Simonsson US, Jansson B, Hai TN, Huong DX, Tybring G, and Ashton M (2003) Artemisinin autoinduction is caused by involvement of cytochrome P450 2B6 but not 2C9. *Clin Pharmacol Ther* **74:**32-43.

Singh H, Singh JR, Dhillon VS, Bali D, and Paul H (1994) In vitro and in vivo genotoxicity evaluation of hormonal drugs. II. Dexamethasone. *Mutat Res* **308:**89-97.

So AY, Chaivorapol C, Bolton EC, Li H, and Yamamoto KR (2007) Determinants of cell- and gene-specific transcriptional regulation by the glucocorticoid receptor. *PLoS Genet* **3:**e94.

Solus JF, Arietta BJ, Harris JR, Sexton DP, Steward JQ, McMunn C, Ihrie P, Mehall JM, Edwards TL, and Dawson EP (2004) Genetic variation in eleven phase I drug metabolism genes in an ethnically diverse population. *Pharmacogenomics* **5:**895-931.

Sommer P, Le Rouzic P, Gillingham H, Berry A, Kayahara M, Huynh T, White A, and Ray DW (2007) Glucocorticoid receptor overexpression exerts an antisurvival effect on human small cell lung cancer cells. *Oncogene* **26:**7111-7121.

Song X, Xie M, Zhang H, Li Y, Sachdeva K, and Yan B (2004) The pregnane X receptor binds to response elements in a genomic context-dependent manner, and PXR activator rifampicin selectively alters the binding among target genes. *Drug Metab Dispos* **32:**35-42.

Sparfel L, Payen L, Gilot D, Sidaway J, Morel F, Guillouzo A, and Fardel O (2003) Pregnane X receptor-dependent and -independent effects of 2-acetylaminofluorene on cytochrome P450 3A23 expression and liver cell proliferation. *Biochem Biophys Res Commun* **300:**278-284.

Stavreva DA, Müller WG, Hager GL, Smith CL, and McNally JG (2004) Rapid glucocorticoid receptor exchange at a promoter is coupled to transcription and regulated by chaperones and proteasomes. *Mol Cell Biol* **24:**2682-2697.

Sukumaran S, Jusko WJ, DuBois DC, and Almon RR (2011) Mechanistic modeling of the effects of glucocorticoids and circadian rhythms on adipokine expression. *J Pharmacol Exp Ther* **337:**734-746.

Tanaka E (1999) Clinically significant pharmacokinetic drug interactions with benzodiazepines. *J Clin Pharm Ther* **24:**347-355.

Tandon VR, Kapoor B, Bano G, Gupta S, Gillani Z, Gupta S, and Kour D (2006) P-glycoprotein: Pharmacological relevance. *Indian J Pharmacol* **38:**13-24.

Terstriep S and Grothey A (2006) First- and second-line therapy of metastatic colorectal cancer. *Expert Rev Anticancer Ther* **6:**921-930.

Thummel KE and Wilkinson GR (1998) In vitro and in vivo drug interactions involving human CYP3A. *Annu Rev Pharmacol Toxicol* **38:**389-430.

Tindall M (2012) Teaching Modelling using Simulation Tools: Examples using Copasi and Matlab, https://bio***math***ed.files.wordpress.com/2012/07/bio***m***aths-2012-*tindall*.pdf, Accessed June 2016.

Tirona RG and Kim RB (2005) Nuclear receptors and drug disposition gene regulation. *J Pharm Sci* **94:**1169-1186.

Trebble PJ, Woolven JM, Saunders KA, Simpson KD, Farrow SN, Matthews LC, and Ray DW (2013) A ligand-specific kinetic switch regulates glucocorticoid receptor trafficking and function. *J Cell Sci* **126:**3159-3169.

Udvardi MK, Czechowski T, and Scheible WR (2008) Eleven golden rules of quantitative RT-PCR. *Plant Cell* **20:**1736-1737.

Urquhart BL, Tirona RG, and Kim RB (2007) Nuclear receptors and the regulation of drug-metabolizing enzymes and drug transporters: implications for interindividual variability in response to drugs. *J Clin Pharmacol* **47:**566-578.

Van Bogaert T, De Bosscher K, and Libert C (2010) Crosstalk between TNF and glucocorticoid receptor signaling pathways. *Cytokine Growth Factor Rev* **21:**275-286.

van de Waterbeemd H and Gifford E (2003) ADMET in silico modelling: towards prediction paradise? *Nat Rev Drug Discov* **2:**192-204.

van Waterschoot RA and Schinkel AH (2011) A critical analysis of the interplay between cytochrome P450 3A and P-glycoprotein: recent insights from knockout and transgenic mice. *Pharmacol Rev* **63:**390-410.

van Winsen LM, Muris DF, Polman CH, Dijkstra CD, van den Berg TK, and Uitdehaag BM (2005) Sensitivity to glucocorticoids is decreased in relapsing remitting multiple sclerosis. *J Clin Endocrinol Metab* **90:**734-740.

VandenBrink BM and Isoherranen N (2010) The role of metabolites in predicting drug-drug interactions: focus on irreversible cytochrome P450 inhibition. *Curr Opin Drug Discov Devel* **13:**66-77.

Vandevyver S, Dejager L, Tuckermann J, and Libert C (2013) New insights into the anti-inflammatory mechanisms of glucocorticoids: an emerging role for glucocorticoid-receptor-mediated transactivation. *Endocrinology* **154:**993-1007.

Vermeir M, Annaert P, Mamidi RN, Roymans D, Meuldermans W, and Mannens G (2005) Cell-based models to study hepatic drug metabolism and enzyme induction in humans. *Expert Opin Drug Metab Toxicol* **1:**75-90.

Vermeulen NPE (1996) *Cytochromes P450, Role in the Metabolism and Toxicity of Drugs and Other Xenobiotics ed. , CRC Press, Boca Raton, FL, 1996, 29.*

Villeneuve JP and Pichette V (2004) Cytochrome P450 and liver diseases. *Curr Drug Metab* **5:**273-282.

Vogel C and Marcotte EM (2012) Insights into the regulation of protein abundance from proteomic and transcriptomic analyses. *Nat Rev Genet* **13:**227-232.

Wadelius M, Darj E, Frenne G, and Rane A (1997) Induction of CYP2D6 in pregnancy. *Clin Pharmacol Ther* **62:**400-407.

Wang H and LeCluyse EL (2003) Role of orphan nuclear receptors in the regulation of drug-metabolising enzymes. *Clin Pharmacokinet* **42:**1331-1357.

Wang Y, Liao M, Hoe N, Acharya P, Deng C, Krutchinsky AN, and Correia MA (2009) A role for protein phosphorylation in cytochrome P450 3A4 ubiquitin-dependent proteasomal degradation. *J Biol Chem* **284:**5671-5684.

Wang Z, Frederick J, and Garabedian MJ (2002) Deciphering the Phosphorylation Code of the Glucocorticoid Receptor in Vivo. *J Biol Chem* **277:**26573-26580.

Watkins PB, Wrighton SA, Maurel P, Schuetz EG, Mendez-Picon G, Parker GA, and Guzelian PS (1985) Identification of an inducible form of cytochrome P-450 in human liver. *Proc Natl Acad Sci U S A* **82:**6310-6314.

Wauthier V, Verbeeck RK, and Calderon PB (2007) The effect of ageing on cytochrome p450 enzymes: consequences for drug biotransformation in the elderly. *Curr Med Chem* **14:**745-757.

Waxman DJ (1999) P450 gene induction by structurally diverse xenochemicals: central role of nuclear receptors CAR, PXR, and PPAR. *Arch Biochem Biophys* **369:**11-23.

Wei P, Zhang J, Egan-Hafley M, Liang S, and Moore DD (2000) The nuclear receptor CAR mediates specific xenobiotic induction of drug metabolism. *Nature* **407:**920-923.

Weitzman ED, Fukushima D, Nogeire C, Roffwarg H, Gallagher TF, and Hellman L (1971) Twenty-four hour pattern of the episodic secretion of cortisol in normal subjects. *J Clin Endocrinol Metab* **33:**14-22.

Westerink WM and Schoonen WG (2007) Cytochrome P450 enzyme levels in HepG2 cells and cryopreserved primary human hepatocytes and their induction in HepG2 cells. *Toxicol In Vitro* **21:**1581-1591.

Wienkers LC and Heath TG (2005) Predicting in vivo drug interactions from in vitro drug discovery data. *Nat Rev Drug Discov* **4:**825-833.

Wilkening S, Stahl F, and Bader A (2003) Comparison of primary human hepatocytes and hepatoma cell line Hepg2 with regard to their biotransformation properties. *Drug Metab Dispos* **31:**1035-1042.

Williams JA, Hyland R, Jones BC, Smith DA, Hurst S, Goosen TC, Peterkin V, Koup JR, and Ball SE (2004) Drug-drug Interactions for UDP-glucuronosyltransferase substrates: A pharmacokinetic explanation for typically observed low exposure (AUCI/AUC) ratios. *Drug Metab Dispos* **32:**1201-1208.

Williams JA, Ring BJ, Cantrell VE, Jones DR, Eckstein J, Ruterbories K, Hamman MA, Hall SD, and Wrighton SA (2002) Comparative metabolic capabilities of CYP3A4, CYP3A5, and CYP3A7. *Drug Metab Dispos* **30:**883-891.

Wilusz CJ, Wormington M, and Peltz SW (2001) The cap-to-tail guide to mRNA turnover. *Nat Rev Mol Cell Biol* **2:**237-246.

Xie H, Griskevicius L, Ståhle L, Hassan Z, Yasar U, Rane A, Broberg U, Kimby E, and Hassan M (2006) Pharmacogenetics of cyclophosphamide in patients with hematological malignancies. *Eur J Pharm Sci* **27:**54-61.

Xie HG, Wood AJ, Kim RB, Stein CM, and Wilkinson GR (2004) Genetic variability in CYP3A5 and its possible consequences. *Pharmacogenomics* **5:**243-272.

Xie W, Barwick JL, Simmon CM, Pierce AM, Safe S, Blumberg B, Guzelian PS, and Evans RM (2000) Reciprocal activation of xenobiotic response genes by nuclear receptors SXR/PXR and CAR. *Genes Dev* **14:**3014–3023.

Yan Z and Caldwell GW (2001) Metabolism profiling, and cytochrome P450 inhibition & induction in drug discovery. *Curr Top Med Chem* **1:**403-425.

Zak DE, Vadigepalli R, Gonye GE, Doyle Iii FJ, Schwaber JS, and Ogunnaike BA (2005) Unconventional systems analysis problems in molecular biology: a case study in gene regulatory network modeling. *Comp Chemic Eng* **29:**547-563.

Zangar RC, Bollinger N, Verma S, Karin NJ, and Lu Y (2008) The nuclear factor-kappa B pathway regulates cytochrome P450 3A4 protein stability. *Mol Pharmacol* **73:**1652-1658.

Zangar RC, Bollinger N, Weber TJ, Tan RM, Markillie LM, and Karin NJ (2011) Reactive oxygen species alter autocrine and paracrine signaling. *Free Radic Biol Med* **51:**2041-2047.

Zangar RC, Davydov DR, and Verma S (2004) Mechanisms that regulate production of reactive oxygen species by cytochrome P450. *Toxicol Appl Pharmacol* **199:**316-331.

Zanger UM and Schwab M (2013) Cytochrome P450 enzymes in drug metabolism: regulation of gene expression, enzyme activities, and impact of genetic variation. *Pharmacol Ther* **138:**103-141.

Zelko I, Sueyoshi T, Kawamoto T, Moore R, and Negishi M (2001) The Peptide Near the C Terminus Regulates Receptor CAR Nuclear Translocation Induced by Xenochemicals in Mouse Liver. *Molecular and Cellular Biology* **21:**2838-2846.

Zhang Z, Burch PE, Cooney AJ, Lanz RB, Pereira FA, Wu J, Gibbs RA, Weinstock G, and Wheeler DA (2004) Genomic analysis of the nuclear receptor family: new insights into structure, regulation, and evolution from the rat genome. *Genome Res* **14:**580–590.

Zhao JY, Ikeguchi M, Eckersberg T, and Kuo MT (1993) Modulation of multidrug resistance gene expression by dexamethasone in cultured hepatoma cells. *Endocrinology* **133:**521-528.

Zhou SF (2008) Potential strategies for minimizing mechanism-based inhibition of cytochrome P450 3A4. *Curr Pharm Des* **14:**990-1000.

Zhou SF (2009) Polymorphism of human cytochrome P450 2D6 and its clinical significance: Part I. *Clin Pharmacokinet* **48:**689-723.

Zhukov A and Ingelman-Sundberg M (1999) Relationship between cytochrome P450 catalytic cycling and stability: fast degradation of ethanol-inducible cytochrome P450 2E1 (CYP2E1) in hepatoma cells is abolished by inactivation of its electron donor NADPH-cytochrome P450 reductase. *Biochem J* **340 (Pt 2):**453-458.